



NRC - CNRC

Final Report from Task 7 of MEWS Project at the Institute for Research in Construction : Long-Term Performance: Predict the Moisture Management Performance of Wall Systems as a Function of Climate, Material Properties, etc. Through Mathematical Modelling

Mukhopadhyaya, P.; Kumaran, K.; Tariku, F.; van Reenen, D.

IRC-RR-132

www.nrc.ca/irc/irepubs



IMPORTANT NOTICE TO READERS

The main emphasis of the MEWS project was to predict the hygrothermal responses of several wall assemblies that are exposed to North American climate loads, and a range of water leakage loads. Researchers used a method based on both laboratory experimentation and 2-D modeling with IRC's benchmarked model, hygIRC. This method introduced built-in detailing deficiencies that allowed water leakage into the stud cavity - both in the laboratory test specimens and in the virtual (modeling) "specimens"- for the purpose of investigating water entry rates into the stud cavity and the drying potential of the wall assemblies under different climate loads. Since the project was a first step in investigating a range of wall hygrothermal responses in a parametric analysis, no field study of building characteristics was performed to confirm inputs such as water entry rates and outputs such as wall response in a given climate. Rather, ranges from 'no water entry and no response' to 'too much water entry and too wet for too long' were investigated.

Also, for the sake of convenience, the project used the generic cladding systems (e.g., stucco, masonry, EIFS, and wood and vinyl siding) for labeling and reporting the results on all wall assemblies examined in the study. However, when reading the MEWS publications, the reader must bear in mind that the reported results are more closely related to the nature of the deliberately introduced deficiencies (allowing wetting of the stud cavity) and the construction details of the wall systems investigated (allowing wetting/drying of the assembly) than to the generic cladding systems themselves. As a general rule, the reader must assume, unless told otherwise, that the nature of the deficiencies and the water entry rates into the stud cavity were different for each of the seventeen wall specimens tested as well as for each of the four types of wall assemblies investigated in the modeling study. For this reason, simply comparing the order of magnitude of results between different cladding systems would take the results out of context and likely lead to erroneous conclusions.

**FINAL REPORT FROM TASK 7 OF MEWS PROJECT AT THE
INSTITUTE FOR RESEARCH IN CONSTRUCTION**

**Long-term Performance: Predict the Moisture Management Performance of
Wall Systems as a Function of Climate, Material Properties, etc. Through
Mathematical Modelling**

Phalguni Mukhopadhyaya

Kumar Kumaran

Fitsum Tariku

David van Reenen

February 2003

IMPORTANT NOTICE TO READERS

The main emphasis of the MEWS project was to predict the hygrothermal responses of several wall assemblies that are exposed to North American climate loads, and a range of water leakage loads. Researchers used a method based on both laboratory experimentation and 2-D modeling with IRC's benchmarked model, hygIRC. This method introduced built-in detailing deficiencies that allowed water leakage into the stud cavity - both in the laboratory test specimens and in the virtual (modeling) "specimens"- for the purpose of investigating water entry rates into the stud cavity and the drying potential of the wall assemblies under different climate loads. Since the project was a first step in investigating a range of wall hygrothermal responses in a parametric analysis, no field study of building characteristics was performed to confirm inputs such as water entry rates and outputs such as wall response in a given climate. Rather, ranges from 'no water entry and no response' to 'too much water entry and too wet for too long' were investigated.

Also, for the sake of convenience, the project used the generic cladding systems (e.g., stucco, masonry, EIFS, and wood and vinyl siding) for labeling and reporting the results on all wall assemblies examined in the study. However, when reading the MEWS publications, the reader must bear in mind that the reported results are more closely related to the nature of the deliberately introduced deficiencies (allowing wetting of the stud cavity) and the construction details of the wall systems investigated (allowing wetting/drying of the assembly) than to the generic cladding systems themselves. As a general rule, the reader must assume, unless told otherwise, that the nature of the deficiencies and the water entry rates into the stud cavity were different for each of the seventeen wall specimens tested as well as for each of the four types of wall assemblies investigated in the modeling study. For this reason, simply comparing the order of magnitude of results between different cladding systems would take the results out of context and likely lead to erroneous conclusions.

MEWS PROJECT REPORT - TASK 7: FEBRUARY 2003

**FINAL REPORT FROM TASK 7 OF MEWS PROJECT AT THE INSTITUTE FOR
RESEARCH IN CONSTRUCTION**

**Long-term Performance: Predict the Moisture Management Performance of Wall
Systems as a Function of Climate, Material Properties, etc. Through Mathematical
Modelling**

IRC Research Team

Peter Beaulieu
Mark Bomberg
Steve Cornick
Alan Dalgliesh
Guylaine Desmarais
Reda Djebbar
Kumar Kumaran
Michael Lacasse
John Lackey
Wahid Maref
Phalguni Mukhopadhyaya

Mostafa Nofal
Nicole Normandin
Mike Nicholls
Tim O'Connor
David Quirt
Madeleine Rousseau
Nady Said
Mike Swinton
Fitsum Tariku
David van Reenen

MEWS Steering Committee

David Ritter, Louisiana Pacific Corporation
Fred Baker, Fortifiber Corporation
Michael Bryner, El DuPont de Nemours & Co
Gilles Landry, Fiberboard Manufacturers
Association of Canada
Stephane Baffier, CPIA
Paul Morris, Forintek Canada Corporation
Greg McManus, Marriott International Inc.
Stephan Klamke, EIMA

Eric Jones, Canadian Wood Council
Gary Sturgeon, Masonry Canada
Sylvio Plescia, CMHC
Fadi Nabhan, IRC, NRC Canada

David Quirt, IRC, NRC Canada
Kumar Kumaran, IRC NRC Canada
Michael Lacasse, IRC NRC Canada

List of Contents

	Page
Summary	8
CHAPTER A - Stucco Walls	11
1.0 Parameters under consideration	12
2.0 <i>hygIRC</i> and Input for Simulation	12
2.1 Basic Wall Construction Details	13
2.2 Material Properties	15
2.2.1 Air permeability	15
2.2.2 Thermal conductivity	16
2.2.3 Dry density	16
2.2.4 Heat capacity	17
2.2.5 Sorption isotherm	17
2.2.6 Suction curve	17
2.2.7 Water vapour permeability	17
2.2.8 Liquid diffusivity	17
2.3 Boundary Conditions	38
2.3.1 Indoor Environment	38
2.3.2 Outdoor Environment	38
2.4 Exposure Duration	39
2.5 Initial Moisture Content and Temperature	39
2.6 Accidental Moisture Entry - Quantity and Location	39
3.0 Results from <i>hygIRC</i> Simulation	40
3.1 Results from Parametric Studies	43
3.1.1 Exterior cladding (3 types of stucco)	43
3.1.2. Sheathing membrane (3 types)	48
3.1.3. Sheathing board (3 types of oriented strand board (OSB), fibre board (FB), Plywood)	48
3.1.4. Vapour barrier (3 types)	48
3.1.5. Locations with seven different Moisture Indices (MI)	49
3.1.6. Yearly climate variation (Wet-Wet-Average (WWA) and Wet-Wet-Dry (WWD))	50
3.1.7. Accidental moisture entry inside the wall	50
3.1.8. Quantity of accidental moisture entry	50
3.1.9. Presence of a ventilation cavity inside the wall (i.e. behind the exterior cladding)	51
3.1.10. Interior RH	51
3.1.11. Air leakage	52
3.1.12. Elimination of 1mm air gap between sheathing board and sheathing membrane	53
3.1.13. Optimization of stucco properties	53
3.1.14. Best & Worst combination of materials	53
3.1.15. Removal of vapour barrier	53
3.1.16. Use of coated gypsum board with no vapour barrier	54
3.1.17. Alternate Wet and Average years	54
4.0 Concluding Remarks	54
References	54

	Page
CHAPTER B - EIFS Walls	56
1.0 Parameters under consideration	57
2.0 <i>hygIRC</i> and Input for Simulation	57
2.1 Basic Wall Construction Details	57
2.2 Material Properties	59
2.2.1 Air permeability	59
2.2.2 Thermal conductivity	59
2.2.3 Dry density	60
2.2.4 Heat capacity	60
2.2.5 Sorption isotherm	60
2.2.6 Suction curve	60
2.2.7 Water vapour permeability	60
2.2.8 Liquid diffusivity	60
2.3 Boundary Conditions	69
2.4 Exposure Duration	69
2.5 Initial Moisture Content and Temperature	69
2.6 Accidental Moisture Entry - Quantity and Location	69
3.0 Results from <i>hygIRC</i> Simulation	70
3.1 Results from Parametric Studies	72
3.1.1 Base and finish coat thickness of EIFS cladding	72
3.1.2 Sheathing Membrane	76
3.1.3 Sheathing Board	76
3.1.4 Vapour Barrier	76
3.1.5 Insulation	77
3.1.6 Moisture Entry Location	78
3.1.7 Quantity of Moisture Entry	78
3.1.8 Yearly climate variation (Wet-Wet-Average (WWA) and Wet-Wet-Dry (WWD))	78
3.1.9 Interior RH	80
3.1.10 Use of coated gypsum board with no vapour barrier	80
3.1.11 Locations with seven different Moisture Indices (MI)	81
3.1.12 Air leakage	81
4.0 Concluding Remarks	83
References	83

	Page
CHAPTER C - Masonry Walls	84
1.0 Parameters under consideration	85
2.0 <i>hygIRC</i> and Input for Simulation	85
2.1 Basic Wall Construction Details	85
2.2 Material Properties	85
2.2.1 Air permeability	87
2.2.2 Thermal conductivity	87
2.2.3 Dry density	88
2.2.4 Heat capacity	88
2.2.5 Sorption isotherm	88
2.2.6 Suction curve	88
2.2.7 Water vapour permeability	88
2.2.8 Liquid diffusivity	88
2.3 Boundary Conditions	91
2.4 Exposure Duration	91
2.5 Initial Moisture Content and Temperature	91
2.6 Accidental Moisture Entry - Quantity and Location	91
3.0 Results from <i>hygIRC</i> Simulation	91
3.1 Results from Parametric Studies	98
3.1.1 Brick cladding (3 types: Clay brick, Concrete brick and Calcium silicate brick)	98
3.1.2 Two sheathing membranes (2 types: 30 minute building paper and SBPO polymeric membrane)	98
3.1.3 Three sheathing boards (OSB, Asphalt coated fibreboard and XPS foam sheathing board)	99
3.1.4 Three vapour barriers	100
3.1.5 Width of drainage cavity behind exterior cladding (25mm and 50mm)	101
3.1.6 Quantity of accidental moisture entry	101
3.1.7 Locations with seven different Moisture Indices (MI)	102
4.0 Concluding Remarks	103
References	103

	Page
CHAPTER D - Siding Walls (Hardboard & Vinyl)	104
1.0 Parameters under consideration	105
2.0 <i>hygIRC</i> and Input for Simulation	105
2.1 Basic Wall Construction Details	106
2.2 Material Properties	106
2.2.1 Air permeability	106
2.2.2 Thermal conductivity	110
2.2.3 Dry density	110
2.2.4 Heat capacity	111
2.2.5 Sorption isotherm	111
2.2.6 Suction curve	111
2.2.7 Water vapour permeability	111
2.2.8 Liquid diffusivity	111
2.3 Boundary Conditions	124
2.4 Exposure Duration	124
2.5 Initial Moisture Content and Temperature	124
2.6 Accidental Moisture Entry - Quantity and Location	124
3.0 Results from <i>hygIRC</i> Simulation	124
3.1 Results from Parametric Studies	135
<u>Hardboard Siding:</u>	135
3.1.1 Sheathing board (4 types: OSB, Plywood, Uncoated fibre board, Asphalt coated fibre board)	
3.1.2 Sheathing membrane (2 types: SBPO polymeric membrane and 60 minute building paper)	136
3.1.3 Vapour barrier (2 types: Type I, Variable)	136
3.1.4 Locations with seven different Moisture Indices (MI)	136
3.1.5 Accidental moisture entry inside the wall	137
3.1.6 Quantity of accidental moisture entry	137
3.1.7 Use of coated gypsum board with no vapour barrier	137
3.1.8 Presence of a19mm ventilation cavity inside the wall (i.e. behind the exterior cladding)	140
<u>Vinyl Siding:</u>	140
3.1.9 Accidental moisture entry inside the wall	
3.1.10 Quantity of accidental moisture entry	140
3.1.11 Locations with seven different Moisture Indices (MI)	141
3.1.12 Sheathing board (2 types: OSB and Extruded Polystyrene (XPS) foam board)	141
3.1.13 Sheathing membrane (2 types: SBPO polymeric membrane and 30 minute building paper)	141
3.1.14 Vapour barrier (2 types: Type I and Type II)	142
3.1.15 Use of coated gypsum board with no vapour barrier	142
3.1.16 Presence of a19mm ventilation cavity inside the wall (i.e. behind the exterior cladding)	142
4.0 Concluding Remarks	142
References	142

APPENDICES

Page

Appendix A1	Drying Curves - Stucco Wall	143
Appendix A2	RHT Indices - Stucco Wall	206
Appendix B1	Drying Curves - EIFS Wall	209
Appendix C1	Drying Curves - Masonry Walls	264
Appendix D1	Drying Curves - Siding Walls	304
Appendix E1	Comments and Responses	384

Summary

This document is one of the major outcomes from the consortium project called MEWS (Moisture Management in Exterior Wall Systems), carried out at the Institute for Research in Construction (IRC) of National Research Council (NRC), Canada. This report deals with the parametric analyses of four different types of wall assemblies in a building envelope. The four types of walls considered are (1) Stucco walls, (2) EIFS walls, (3) Masonry walls, and (4) Siding walls. The parametric analysis was done using IRC's hygrothermal modelling tool *hygIRC*. *hygIRC* is a 2-dimensional numerical modelling tool specifically developed for research purposes and it is continuously evolving at the IRC/NRC. The utility and reliability of *hygIRC* outputs have been established through laboratory measurements and benchmarking exercises.

This report has all the necessary information for *hygIRC* input (*e.g.* material properties, construction details, assumptions made for indoor and outdoor boundary conditions etc.) and the outputs obtained from the *hygIRC* simulations. A total of around 450 *hygIRC* simulations were done. The parameters studied here involve a wide range of options that represent the variation in material properties, construction details, boundary (indoor and outdoor) conditions, geographical location of the construction and many others. The basic output data are presented in the form of drying curves over a time period of two years. Drying curves present the change in moisture content with time in the wall and in each of its major components. These drying curves indicate the overall moisture response of the wall assembly. However, most of the moisture related problems in building envelopes or wall systems manifest initially in a concentrated localised area of the wall. In the MEWS project this localised area for moisture related problems is termed as the 'region of focus'. In other words, a small area of the wall cross section has been selected, based on the relative humidity (RH) and temperature (T) distribution pattern, and the hygrothermal conditions of this selected area was closely monitored over a period of two years. In order to quantify the hygrothermal response of the 'region of focus', a novel hygrothermal performance indicator, aptly named the 'RHT index', has been introduced in this study. The RHT index captures the duration of the coexistence of moisture and thermal conditions above a set of threshold values (see Chapter A for more details). This RHT index was used as a measure to do parametric analyses. In fact a methodology, the MEWS methodology, to compare the long-term hygrothermal performance of various wall systems, and its components, at various geographical locations has been evolved from the results of the parametric analyses. The RHT index introduced in task 7 and Moisture index (MI) developed in Task 4 are the two fundamental building blocks of the MEWS methodology.

There are four chapters in this document and each of them exclusively deals with one of the four types of wall systems considered in MEWS. These four chapters are:

Chapter A: *Parametric Studies - Stucco Walls*

Chapter B: *Parametric Studies - EIFS Walls*

Chapter C: *Parametric Studies - Masonry Walls*

Chapter D: *Parametric Studies - Siding Walls (Hardboard & Vinyl)*

In *Chapter A*, seventeen (17) parameters have been investigated for wood-frame stucco-walls. These parameters are:

- (i) Exterior cladding,
- (ii) Sheathing membrane,
- (iii) Sheathing board,
- (iv) Vapour barrier,
- (v) Geographic locations with seven different Moisture Indices (MI),
- (vi) Yearly climate variation,
- (vii) Accidental moisture entry inside the wall,
- (viii) Quantity of accidental moisture entry,
- (ix) Presence of a ventilation cavity behind the stucco cladding,
- (x) Interior relative humidity (RH),
- (xi) Air leakage,
- (xii) Elimination of 1 mm air gap between sheathing board and sheathing membrane,
- (xiii) Optimization of stucco properties,
- (xiv) Best and worst combination of materials,
- (xv) Removal of vapour barrier,
- (xvi) Use of coated gypsum board with no vapour barrier, and
- (xvii) Alternate, wet and average years.

In *Chapter B*, twelve (12) parameters have been investigated for EIFS-walls. These parameters are:

- (i) Base and finish coat thickness of EIFS cladding,
- (ii) Sheathing membrane,
- (iii) Sheathing board,
- (iv) Vapour barrier,
- (v) Insulation,
- (vi) Moisture entry location,
- (vii) Quantity of moisture entry,
- (viii) Yearly climate variation,
- (ix) Interior RH,
- (x) Use of coated gypsum board with no vapour barrier,
- (xi) Geographic locations with seven different Moisture Indices (MI), and
- (xii) Air leakage.

In *Chapter C*, seven (7) parameters have been investigated for masonry-walls. These parameters are:

- (i) Brick cladding,
- (ii) Two sheathing membranes,
- (iii) Three sheathing boards,
- (iv) Three vapour barriers,
- (v) Width of drainage cavity behind exterior cladding,
- (vi) Quantity of accidental moisture entry, and
- (vii) Geographic locations with seven different Moisture Indices (MI).

In *Chapter D*, a total of sixteen (16) parameters have been investigated for siding-walls. Hardboard siding and vinyl siding are the two types of walls considered in this study. Each wall type has eight (8) parameters and these parameters are:

Hardboard Siding-

- (i) Sheathing board,
- (ii) Sheathing membrane,
- (iii) Vapour barrier,
- (iv) Geographic locations with seven different Moisture Indices (MI),
- (v) Accidental moisture entry inside the wall,
- (vi) Quantity of accidental moisture entry,
- (vii) Use of coated gypsum board with no vapour barrier, and
- (viii) Presence of a 19mm ventilation cavity.

Vinyl Siding-

- (i) Accidental moisture entry inside the wall,
- (ii) Quantity of accidental moisture entry,
- (iii) Geographic locations with seven different Moisture Indices (MI),
- (iv) Sheathing board,
- (v) Sheathing membrane,
- (vi) Vapour barrier,
- (i) Use of coated gypsum board with no vapour barrier, and
- (ii) Presence of a 19mm ventilation cavity.

It is to be noted that parametric analyses results, depicted in a concise fashion, in the aforementioned four chapters are the basis for a major part of the MEWS Task 8 reports on various wall systems. This report contains all the information relevant to parametric studies and the analysis of outcome from the *hygIRC* simulations. For further and detailed analysis of the results, in global MEWS context, readers should refer the relevant chapters in MEWS Task 8 report.

Chapter A

Parametric Studies - Stucco Walls

Chapter A

Parametric Studies - Stucco Walls

1.0 Parameters under Consideration

Following are the major parameters considered in this study and presented in the MEWS task group meetings.

1. Exterior cladding (3 types of stucco)
2. Sheathing membrane (3 types)
3. Sheathing board (3 types of oriented strand board (OSB), fibre board (FB), Plywood)
4. Vapour barrier (3 types)
5. Locations with seven different Moisture Indices (MI) (Wilmington: 1.13, Seattle: 0.99, Ottawa: 0.93, Winnipeg: 0.86, San Diego: 0.74, Fresno: 0.49 & Phoenix: 0.13)
6. Yearly climate variation (Wet-Wet-Average (WWA) and Wet-Wet-Dry (WWD))
7. Accidental moisture entry inside the wall
8. Quantity of accidental moisture entry
9. Presence of a ventilation cavity inside the wall (i.e. behind the exterior cladding)
10. Interior RH
11. Air leakage
12. Elimination of 1mm air gap between sheathing board and sheathing membrane
13. Optimization of stucco properties
14. Best & Worst combination of materials
15. Removal of vapour barrier
16. Use of coated gypsum board with no vapour barrier
17. Alternate Wet and Average years

These parameters were chosen by MEWS research team to investigate various moisture management issues related to stucco-walls. These chosen parameters also encompass the suggestions and comments obtained from the representatives of the MEWS partners.

2.0 *hygIRC* and Input for Simulation

hygIRC is IRC's modelling tool for hygrothermal simulation. Interested readers are referred to Karagiozis, 1993,1997; Karagiozis et al., 1996; and Djebbar et al., 2002a,b which document, in detail, the formulation of the combined heat, air and moisture transport equations used in *hygIRC* and the techniques used to solve them numerically.

hygIRC accommodates many advanced features, such as transient heat, air and moisture (liquid and vapour) transport, 2 -dimensional spatial formulation, variable material properties with moisture content and temperature, air flow through building materials, effect of solar radiation, presence of moisture source inside the material, freezing-thawing effect, as well as other useful features.

hygIRC also has the capability to define accidental moisture entry of any quantity as a function of time at any location of the wall. This accidental moisture entry feature of *hygIRC* has been widely used in this study.

hygIRC has a pre-processor that allows the user to divide a wall into a number of layers, both in the horizontal and vertical directions. Using this tool a wall-section can be divided in several layers to accommodate its material and geometrical specifications and specific construction details. Each of these layers is 'meshed' into rectangular elements by dividing each layer horizontally and vertically. The pre-processor allows the division of each layer into a number of elements that can be each of equal size or either expanded or contracted towards the boundary or centre, as specified by the user, according to designated stretching factor. This provision helps to obtain more efficient solutions derived from numerical modelling, by selecting an optimum number of elements for the model. Several preliminary simulations have been carried out to determine the optimum mesh size required for this study.

However, the effective use of such type of advanced numerical tools to analyse and obtain meaningful results demands both the proper physical understanding of the problem, appropriate definition of input parameters and the ability to judiciously interpret the results.

There are a number of major input parameters required for *hygIRC* simulation and they are:

1. Basic wall construction details,
2. Material properties,
3. Boundary conditions,
4. Exposure duration,
5. Initial moisture content and temperature, and
6. Accidental moisture entry - quantity and location

These major input parameters are described in the following paragraphs.

2.1 Basic Wall Construction Details

The basic stucco-wall construction details are shown in Figure A1. This wall did not have a drainage/ventilation cavity behind the exterior cladding. This wall was used for all the parametric studies, except where specific parametric analyses were conducted for the introduction of cavity behind the stucco cladding. The stucco-wall with a cavity behind the exterior cladding is shown in Figure A2.

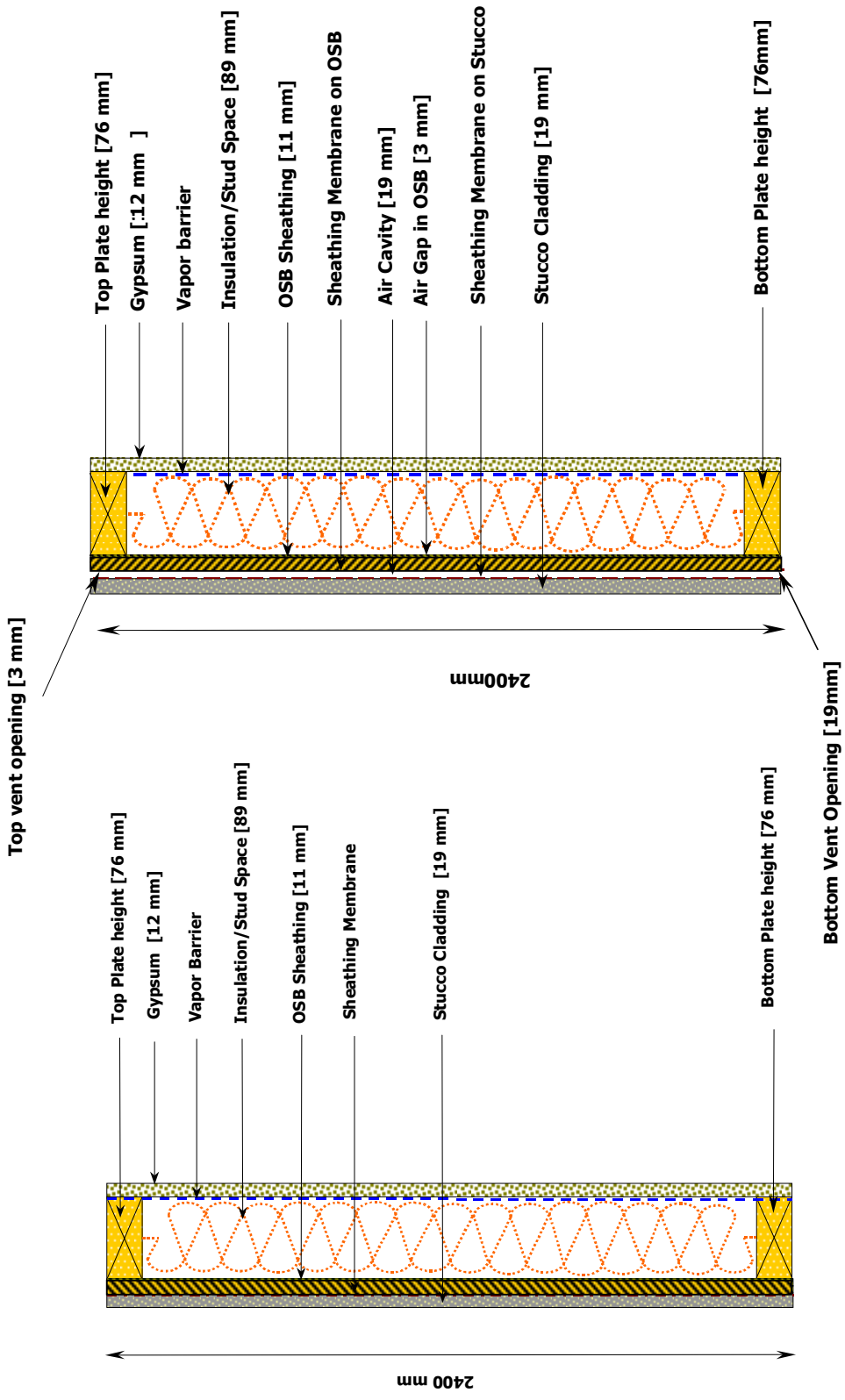


Figure A1: Stucco-wall without a cavity

Figure A2: Stucco-wall with a cavity behind the cladding

2.2 Material Properties

The basic materials used for the wall construction are:

1. Stucco
2. Sheathing membrane
3. Oriented strand board
4. Glass fibre
5. Spruce
6. Vapour barrier
7. Gypsum board
8. Natural fibre board (Uncoated)
9. Plywood
10. Coated gypsum board

In addition, another material, appropriately named as 'modified stucco', has also been used to demonstrate how modifying specific material properties can optimize the hygrothermal response of the wall. The changes that are to be made in the properties of 'Modified stucco' will be discussed in section 3.0.

The material properties used for simulations were taken from the MEWS material property database (*Kumaran et al. 2002*). These properties were carefully determined in the IRC's Thermal and Moisture Performance Laboratory following the standard test procedures (*Kumaran et al. 2002*). The materials considered are also representative of currently available building materials commonly used in North America.

The eight distinct sets of material properties required for *hygIRC* simulation are:

- (i) Air permeability (m^2) in the X and Y-direction ($kg_{water} kg^{-1}_{dry\ weight}$)
- (ii) Thermal conductivity ($W m^{-1} K^{-1}$) in the X and Y-direction
- (iii) Dry density ($kg m^{-3}$)
- (iv) Heat capacity ($J K^{-1} kg^{-1}$)
- (v) Sorption characteristics (i.e. change of moisture content with relative humidity)
- (vi) Suction pressure (Pa)
- (vii) Water vapour permeability ($kg m^{-1} s^{-1} Pa^{-1}$) in the X and Y-direction
- (viii) Liquid diffusivity ($m^2 s^{-1}$) in the X and Y-direction

The aforementioned material properties are documented in the following sections.

2.2.1 Air permeability

The air permeability properties of the materials, as used for simulations, are shown in Table A1. The values shown in the Table A1 are the product of air permeability and dynamic viscosity of air.

Table A1: Air permeability of materials

Material	Air permeability (m ²)
Stucco I,II,III	6.87x10 ⁻¹⁷ , 1.67x10 ⁻¹⁶ , 4.19x10 ⁻¹⁶
Sheathing Membrane I,II,III	2.22x10 ⁻¹⁴ , 1.18x10 ⁻¹⁴ , 1.69x10 ⁻¹⁴
Vapour Barrier I, II, III	1.00x10 ⁻²⁰ , 1.00x10 ⁻²⁰ , 1.00x10 ⁻²⁰
OSB I,II,III	7.89x10 ⁻¹⁵ , 1.65x10 ⁻¹⁵ , 4.28x10 ⁻¹⁵
Gypsum Board	6.78x10 ⁻¹⁴
Spruce	1.00x10 ⁻¹³
Glass Fibre	1.10x10 ⁻⁰⁹
Natural Fibre Board (Uncoated)	4.67x10 ⁻¹²
Plywood	8.50x10 ⁻¹⁵
Coated Gypsum Board	6.78x10 ⁻¹⁴

2.2.2 Thermal conductivity

Measurements were made on dry materials alone. The thermal conductivity of the material changes in relation to the moisture content of the material. Approximate combining rules are used to account for the effect of moisture on thermal conductivity. The thermal conductivity of the dry materials is shown in Table A2.

Table A2: Thermal conductivity of materials (dry)

Material	Thermal Conductivity (W m ⁻¹ K ⁻¹)
Stucco I,II,III	3.52x10 ⁻⁰¹ , 4.07x10 ⁻⁰¹ , 3.81x10 ⁻⁰¹
Sheathing Membrane I,II,III	1.09x10 ⁻⁰¹ , 1.09x10 ⁻⁰¹ , 2.00x10 ⁻⁰¹
Vapour Barrier I, II, III	1.59x10 ⁻⁰¹ , 1.59x10 ⁻⁰¹ , 1.59x10 ⁻⁰¹
OSB I,II,III	9.42x10 ⁻⁰² , 9.34x10 ⁻⁰² , 9.78x10 ⁻⁰²
Gypsum Board	1.60x10 ⁻⁰¹
Spruce	9.01x10 ⁻⁰²
Glass Fibre	4.33x10 ⁻⁰²
Natural Fibre Board (Uncoated)	4.60x10 ⁻⁰²
Plywood	9.05x10 ⁻⁰²
Coated Gypsum Board	1.60x10 ⁻⁰¹

2.2.3 Dry density

The measured dry density of all the materials are provided in the Table A3.

Table A3: Dry density of materials

Material	Dry density (kgm ⁻³)
Stucco I,II,III	1.86x10 ³ , 2.01x10 ³ , 1.81x10 ³
Sheathing Membrane I,II,III	8.10x10 ² , 8.70x10 ² , 8.40x10 ²
Vapour Barrier I, II, III	8.40x10 ² , 8.40x10 ² , 8.40x10 ²
OSB I,II,III	5.94x10 ² , 6.28x10 ² , 6.71x10 ²
Gypsum Board	7.00x10 ²
Spruce	4.25x10 ²
Glass Fibre	1.10x10 ²
Natural Fibre Board (Uncoated)	2.42x10 ²
Plywood	5.00x10 ²
Coated Gypsum Board	7.00x10 ²

2.2.4 Heat capacity

The heat capacity of all the materials are given in the Table A4.

Table A4: Heat capacity of materials

Material	Heat Capacity ($\text{J K}^{-1} \text{kg}^{-1}$)
Stucco 1,2,3	8.40×10^2 , 8.40×10^2 , 8.40×10^2
Sheathing Membrane 4,5,6	1.88×10^3 , 1.88×10^3 , 1.47×10^3
Vapour Barrier 7, 8, 9	1.26×10^3 , 1.26×10^3 , 1.26×10^3
OSB 10,11,12	1.88×10^3 , 1.88×10^3 , 1.88×10^3
Gypsum Board	8.70×10^2
Spruce	2.39×10^3
Glass Fibre	1.26×10^3
Natural Fibre Board (Uncoated)	2.10×10^3
Plywood	1.88×10^3
Coated Gypsum Board	8.70×10^2

2.2.5 Sorption isotherm

The relation between relative humidity and moisture content of all the materials are shown in Figures A3a to A3j.

2.2.6 Suction curve

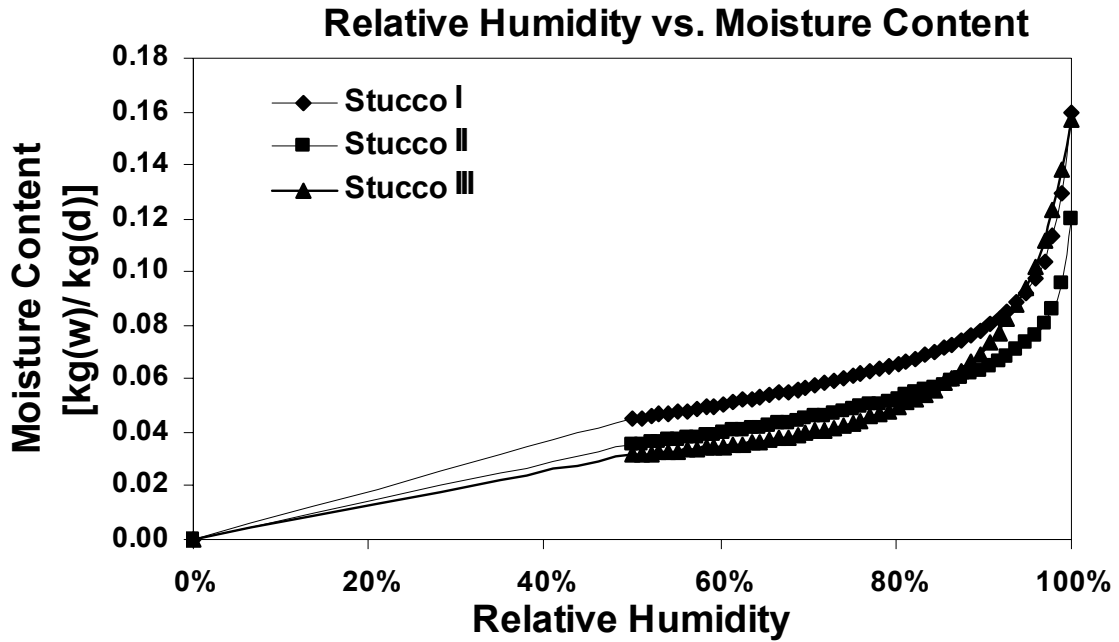
The plots of moisture content as a function of suction pressure are shown in Figures A4a to A4j.

2.2.7 Water vapour permeability

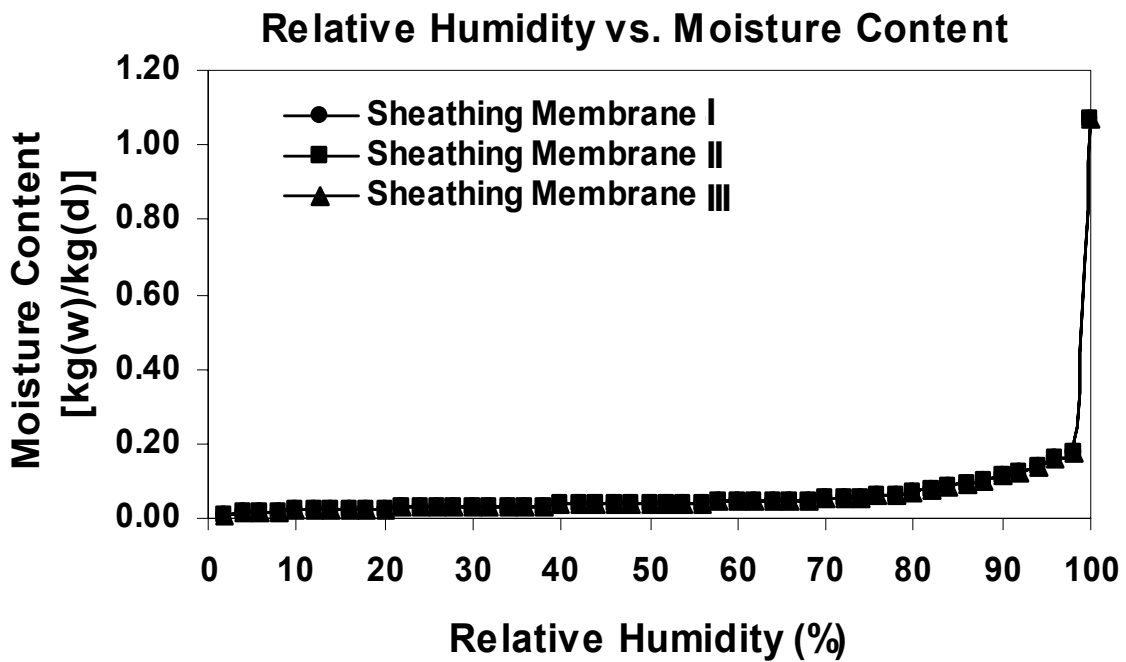
Water vapour permeability of the building material is one of the most critical properties influencing the overall drying characteristics of the wall. In fact, in this study, the selection of materials for the parametric study was done on the basis of its water vapour permeability characteristics. The variations of water vapour permeability in relation to relative humidity for all the materials are shown in Figures A5a to A5j. Three specimens of Stucco, Sheathing Membrane, Vapour Barrier and OSB have been chosen to represent the upper limit, average and lower limit of the water vapour permeability, as provided by the MEWS database (*Kumaran et al. 2002*). The influence of this selection criterion will be discussed in section 3.0.

2.2.8 Liquid diffusivity

The plots of liquid diffusivity vs. moisture content, for all materials used in this study, are shown in Figures A6a to A6j. The diffusion of liquid through the material takes place when moisture content of the material is close to the corresponding relative humidity of 100% (refer to the sorption isotherm plots).

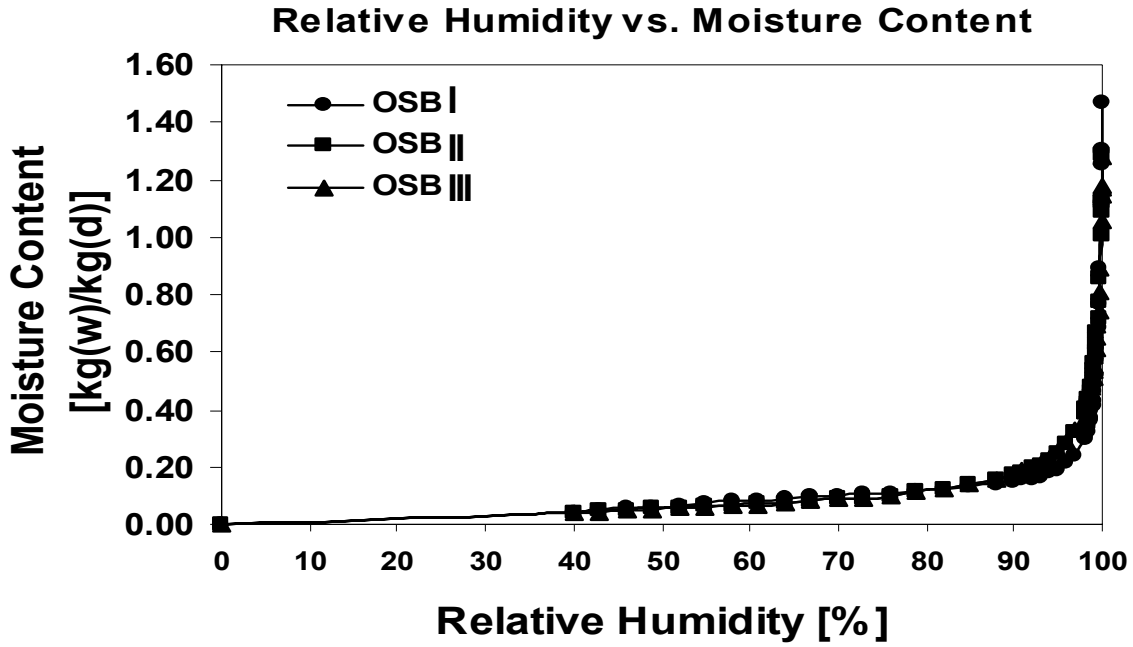


(a) Stucco

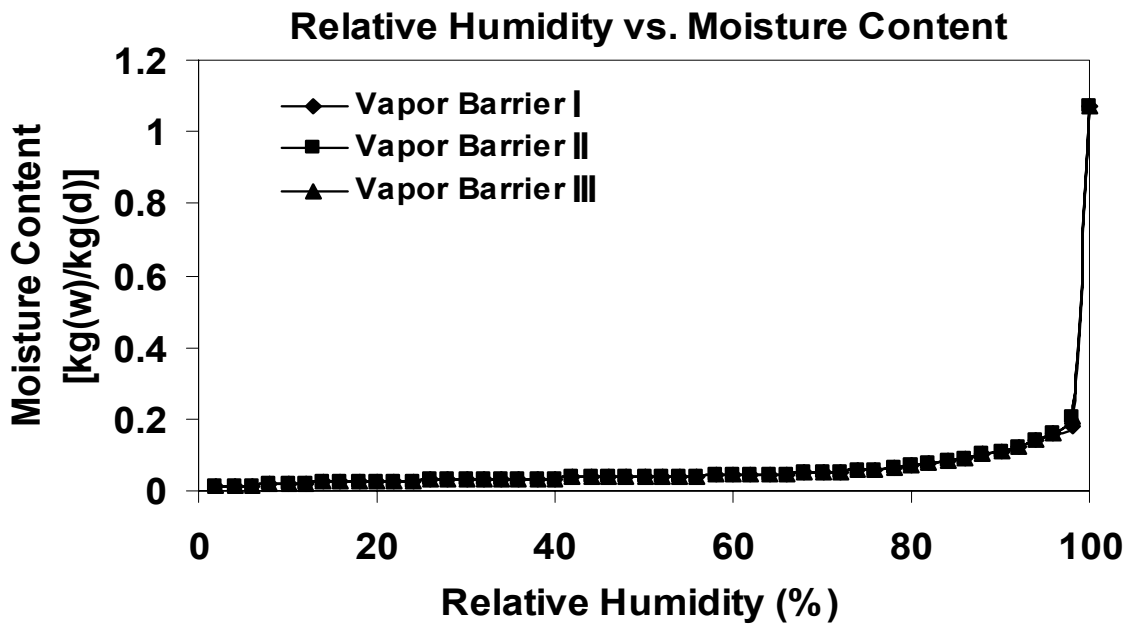


(b) Sheathing membrane

Figure A3: Sorption Isotherm

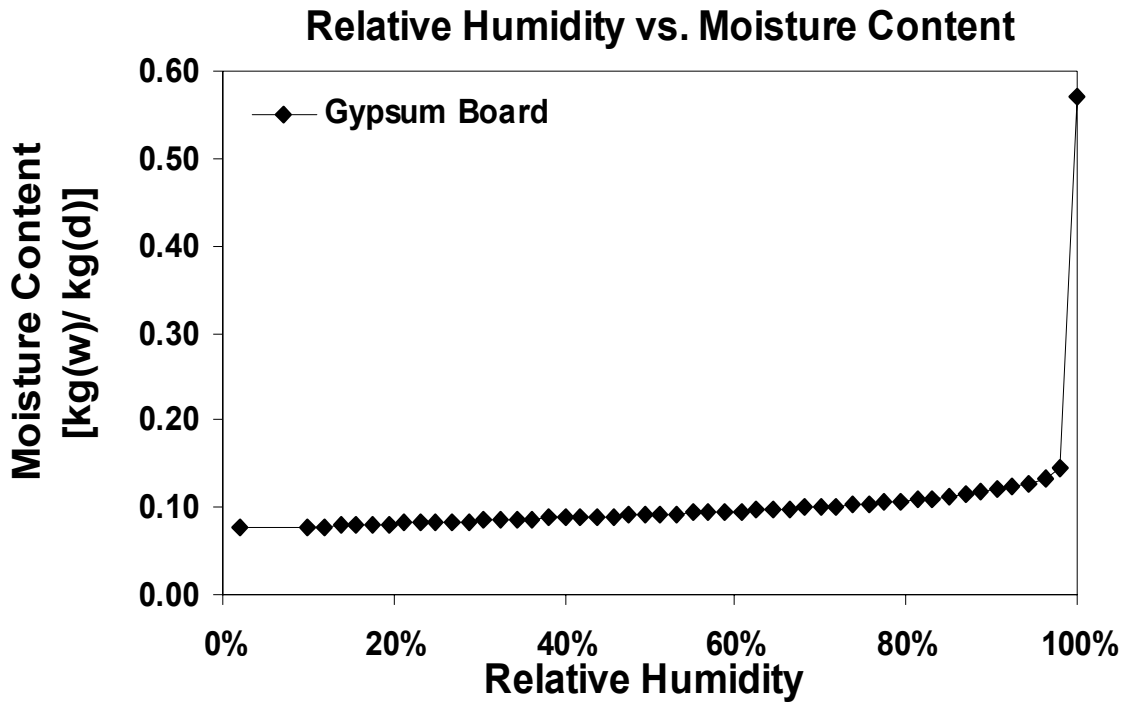


(c) OSB

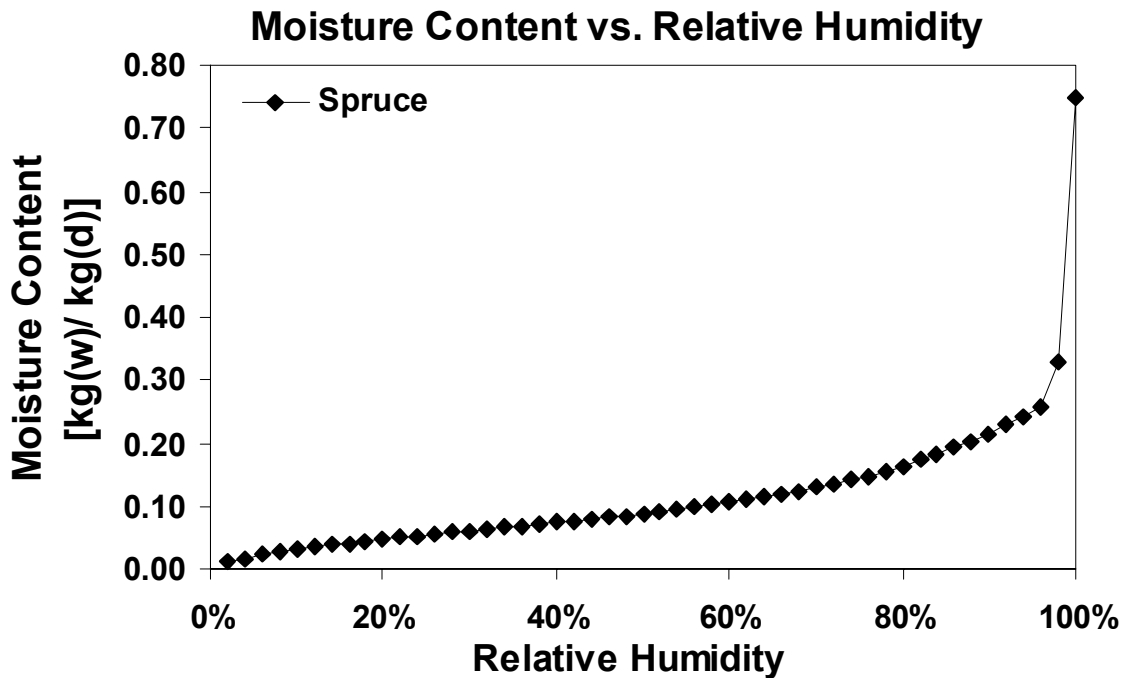


(d) Vapour barrier

Figure A3: Sorption Isotherm

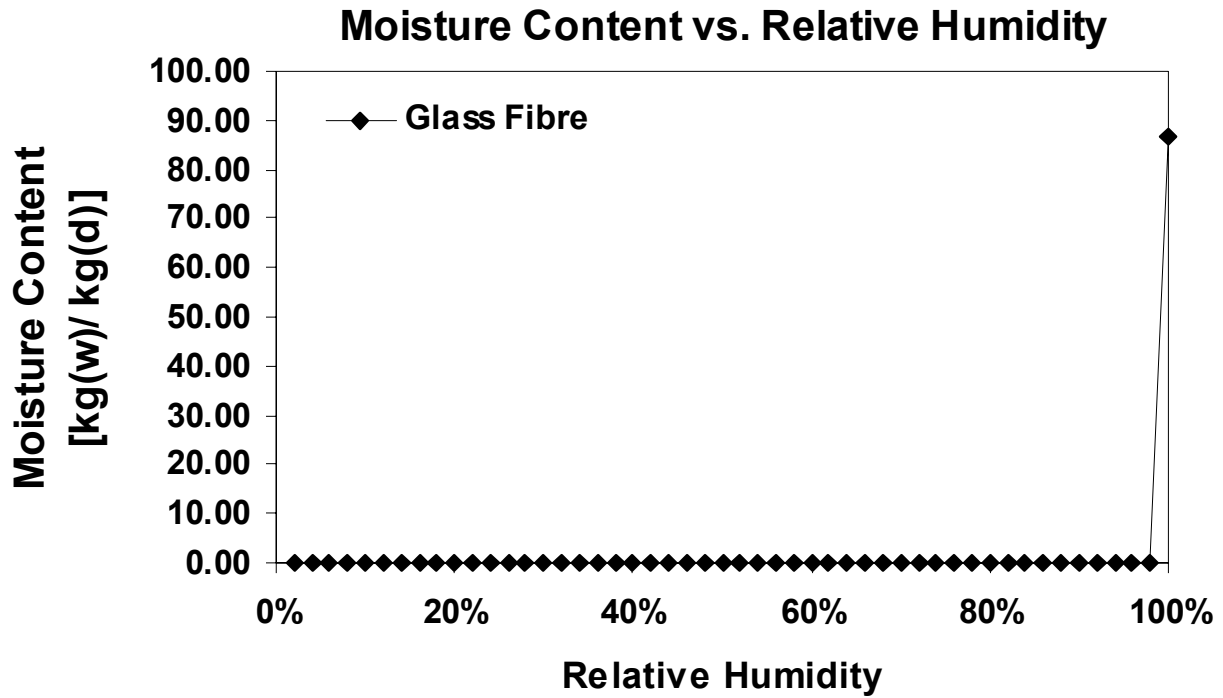


(e) Gypsum board

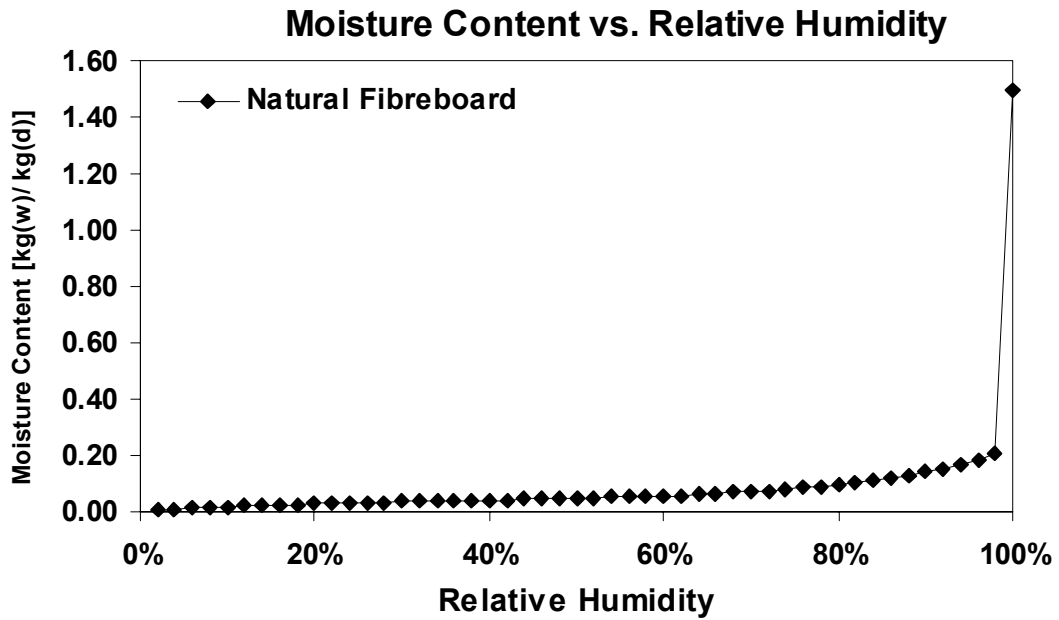


(f) Spruce

Figure A3: Sorption Isotherm

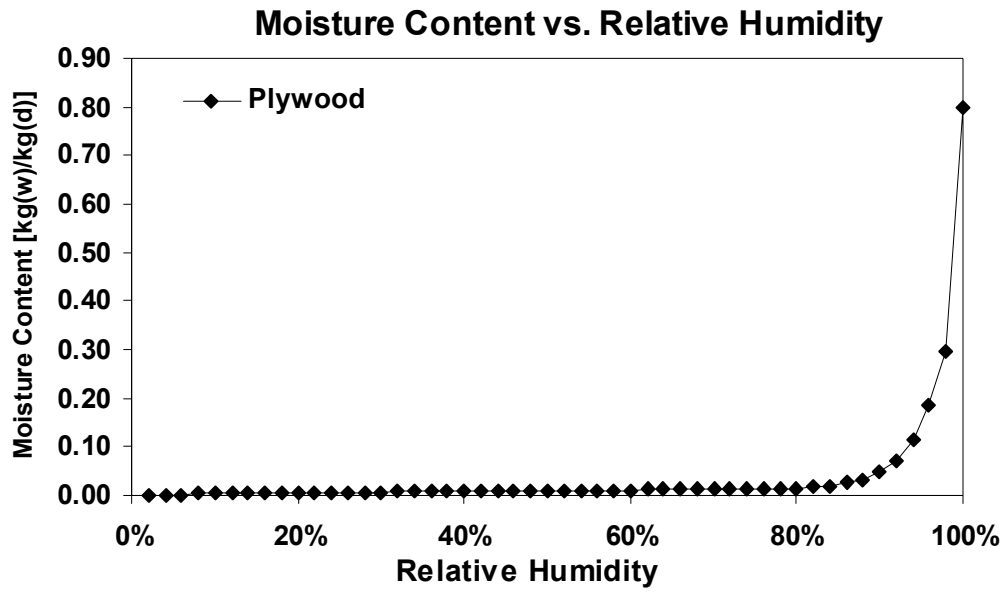


(g) Glass fibre

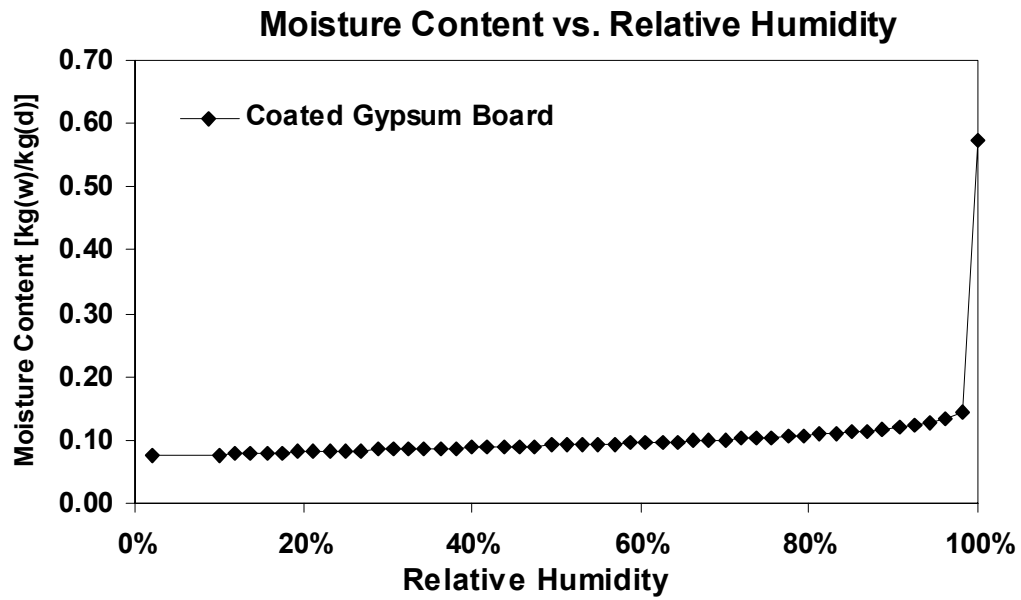


(h) Natural fibreboard (Uncoated)

Figure A3: Sorption Isotherm

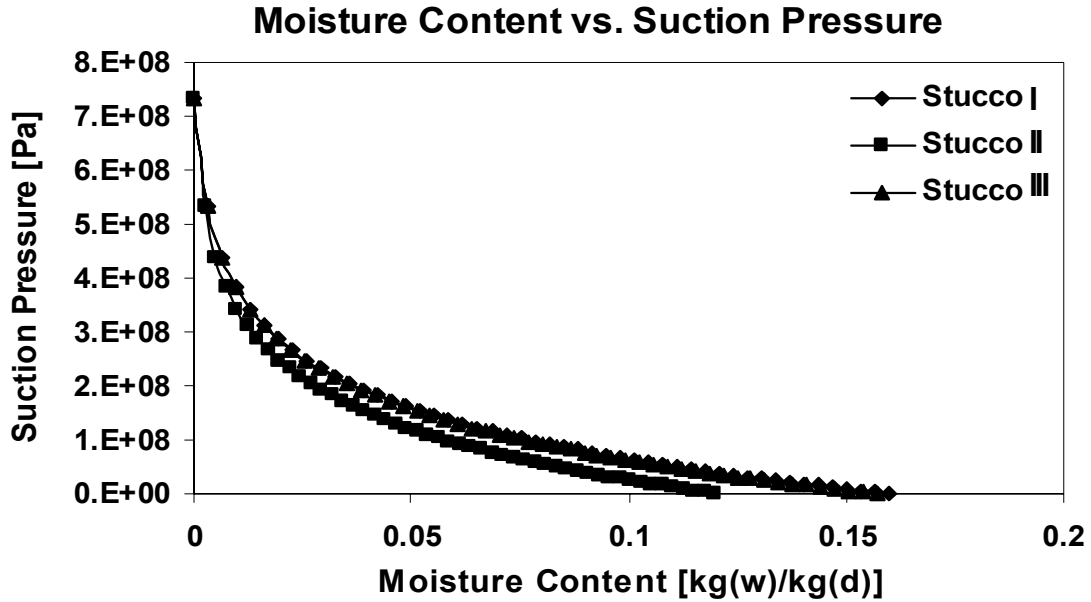


(i) Plywood

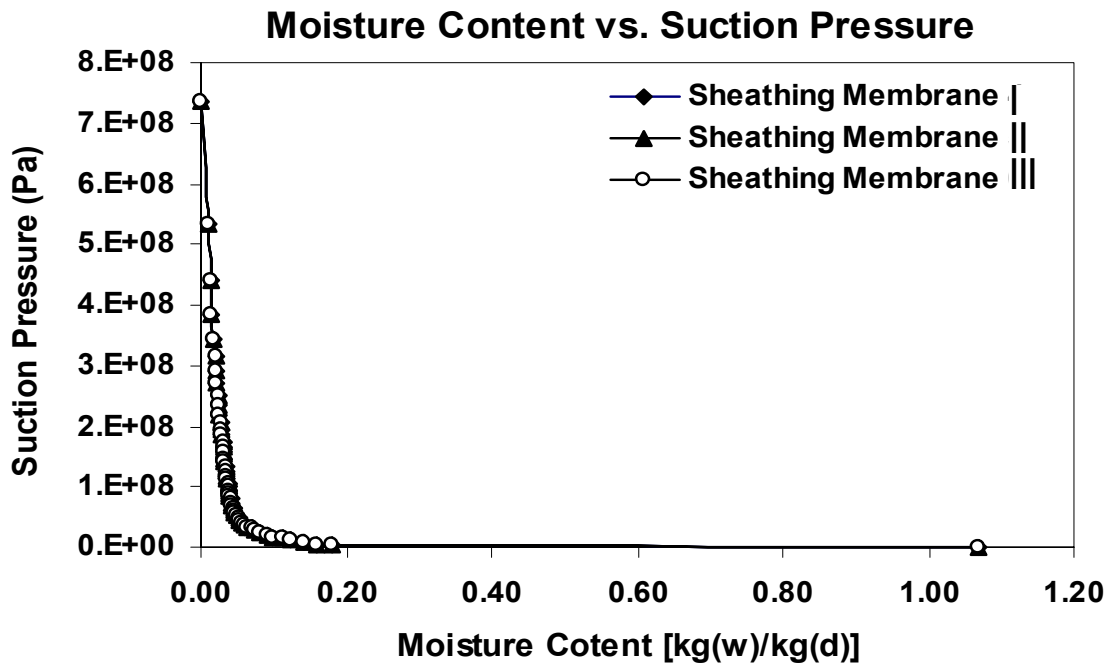


(j) Coated gypsum board

Figure A3: Sorption Isotherm



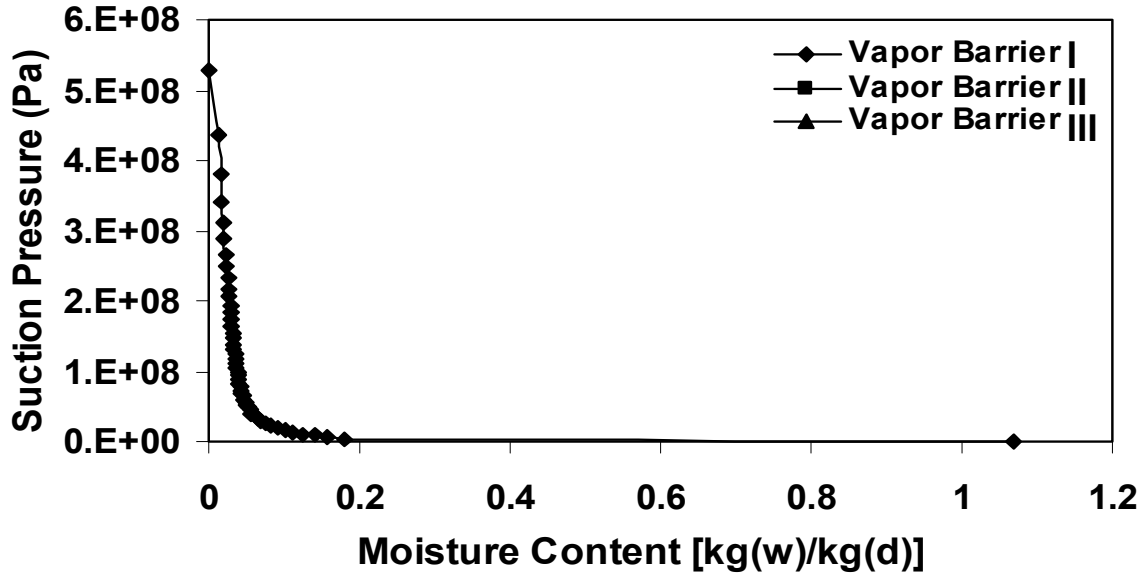
(a) Stucco



(b) Sheathing membrane

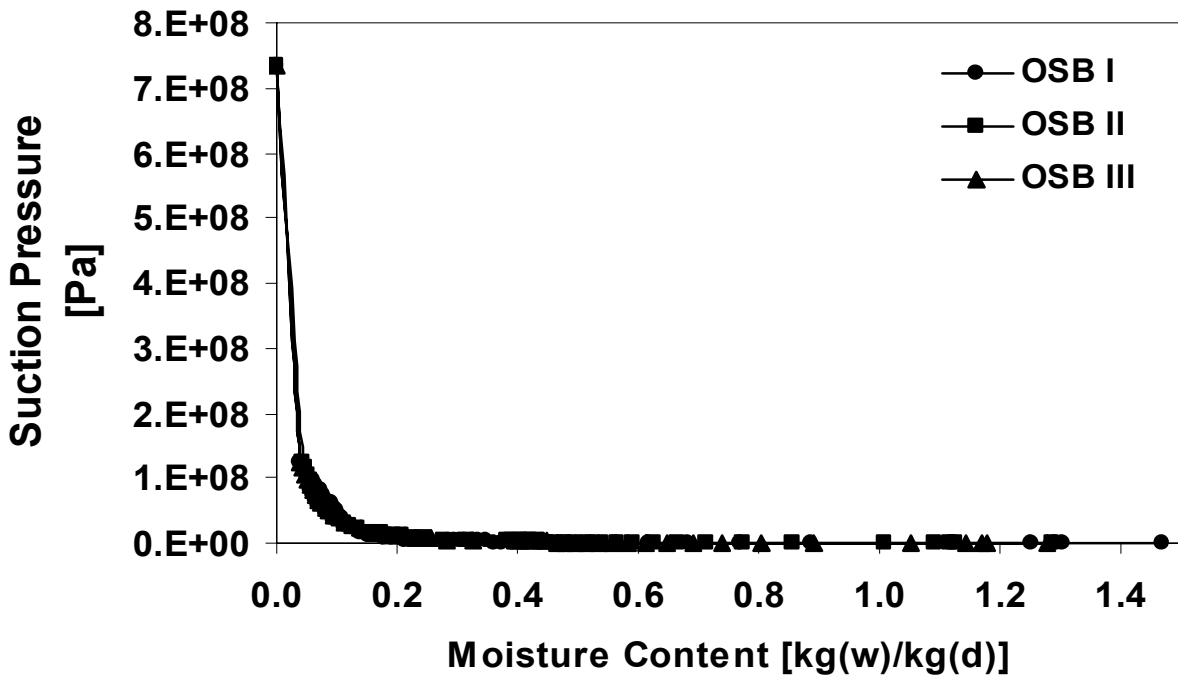
Figure A4: Suction Curve

Moisture Content vs. Suction Pressure



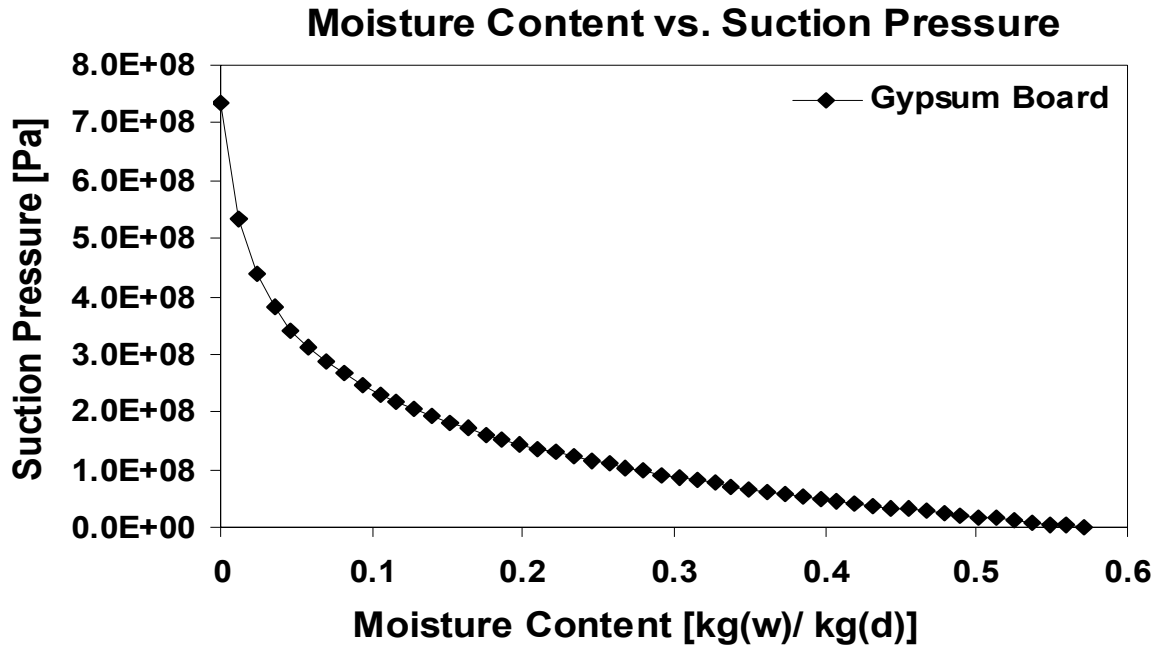
(c) Vapour barrier

Moisture Content vs. Suction Pressure

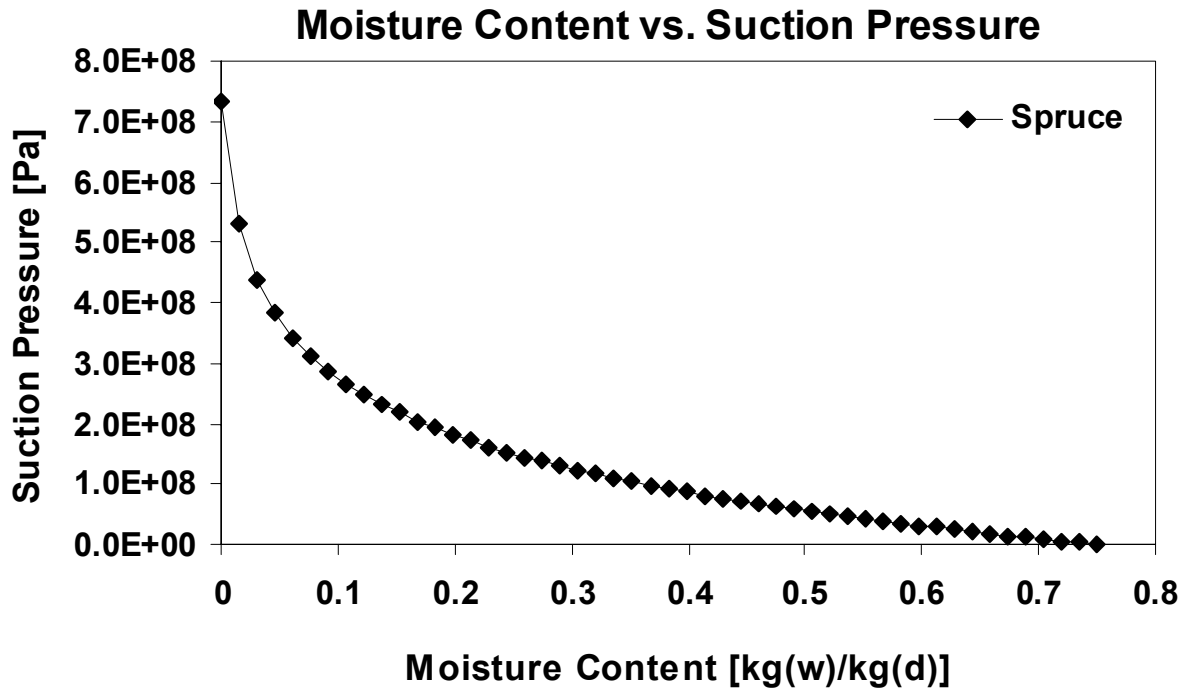


(d) OSB

Figure A4: Suction Curve

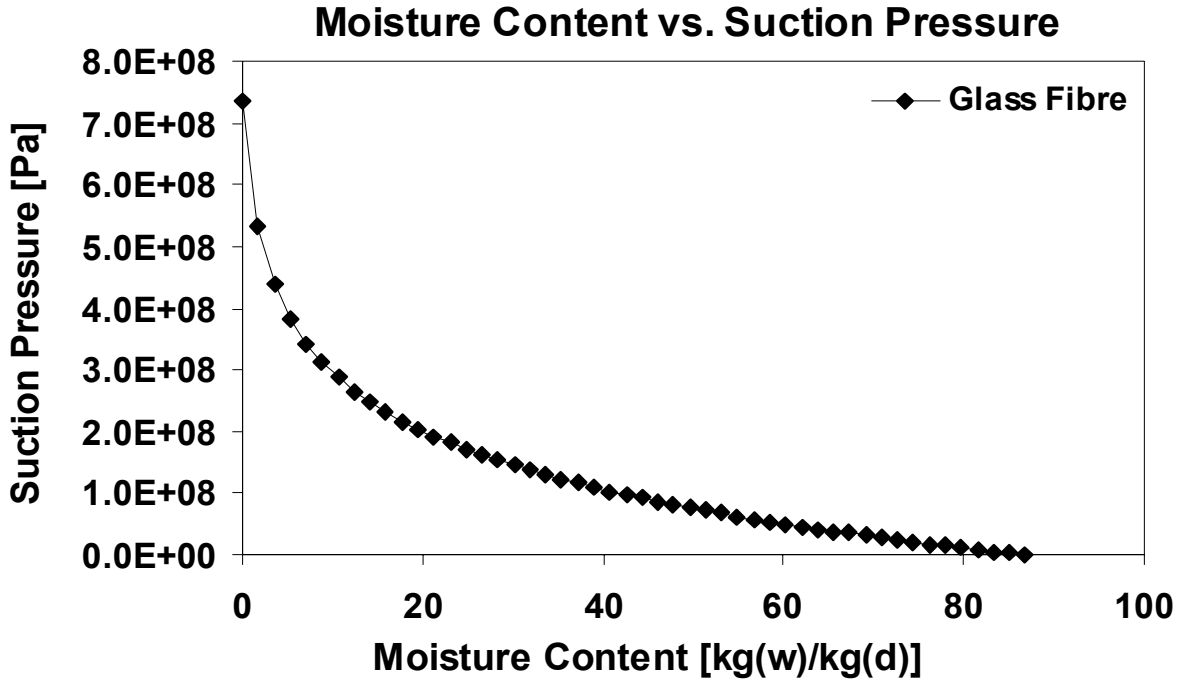


(e) Gypsum board

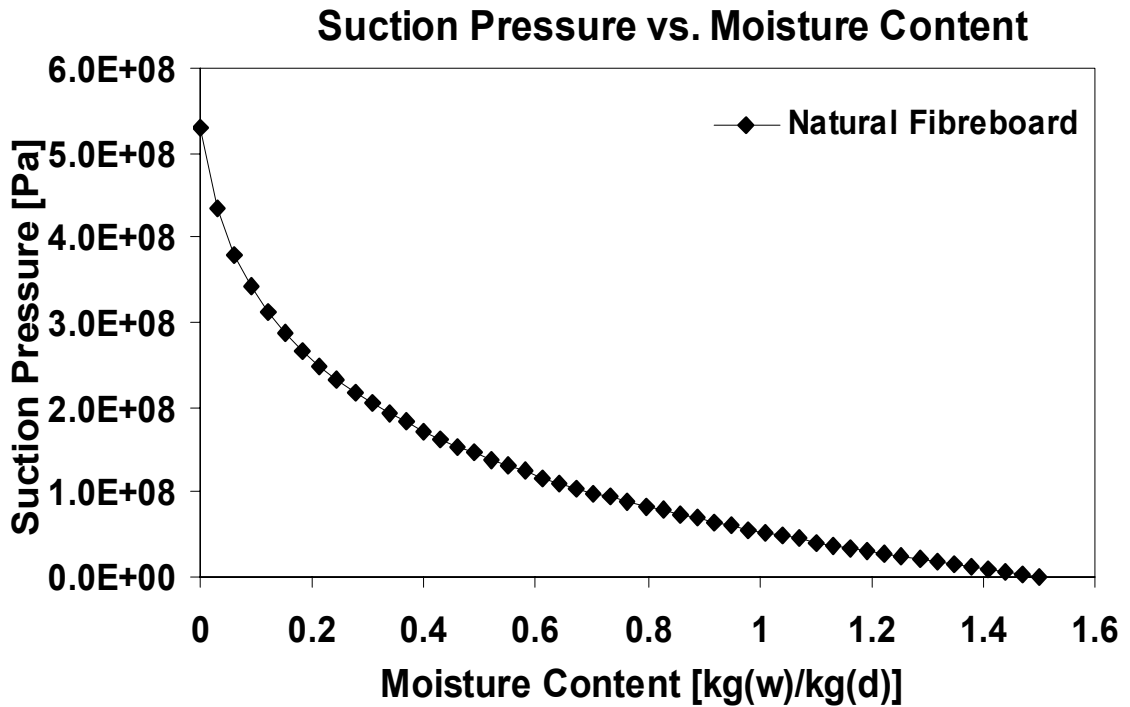


(f) Spruce

Figure A4: Suction Curve

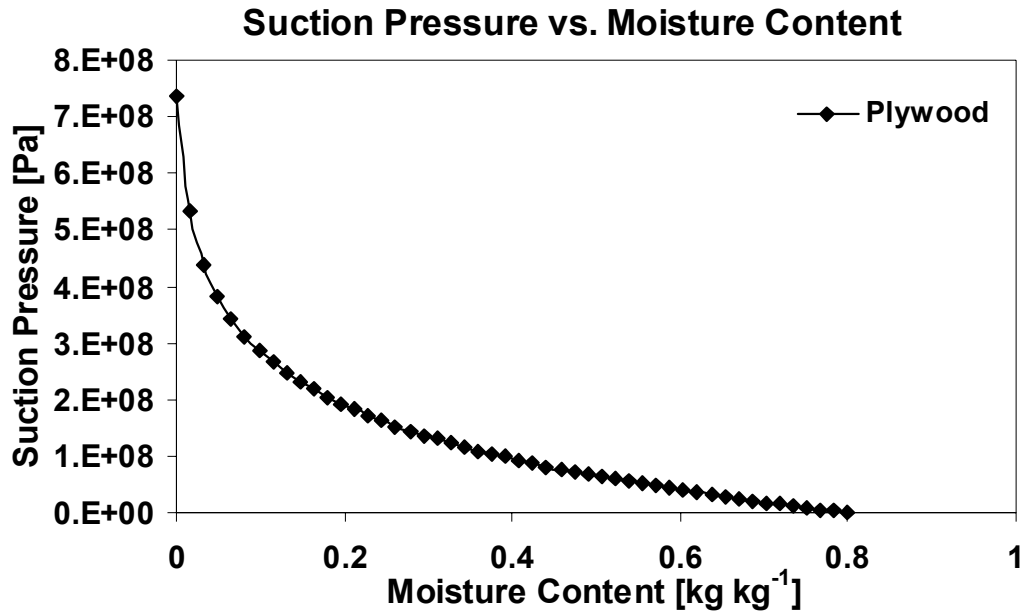


(g) Glass fibre

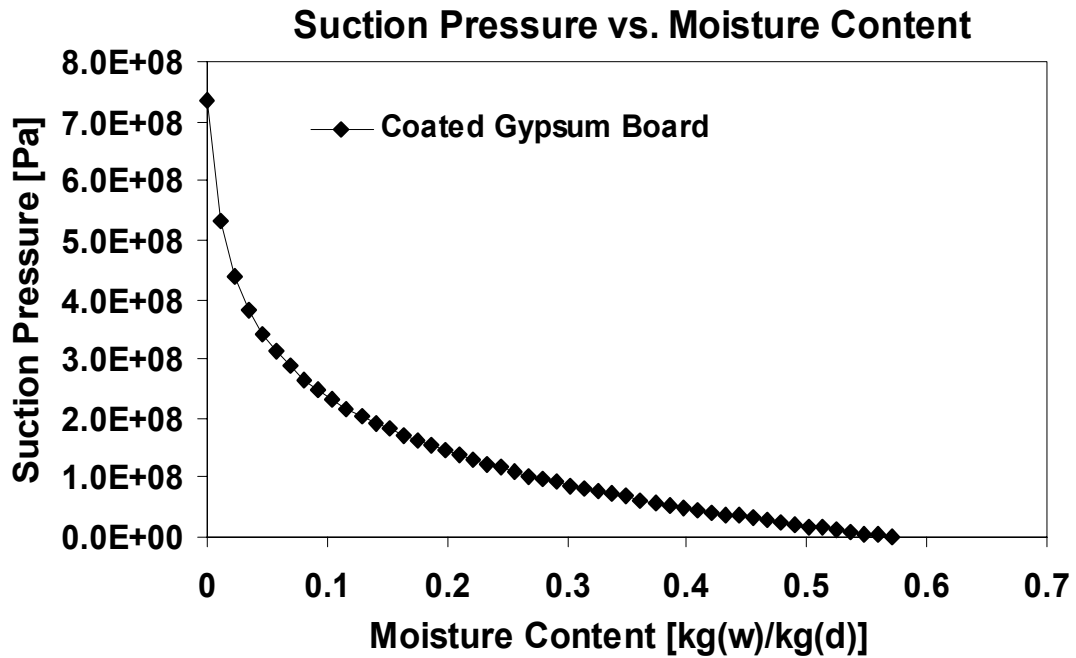


(h) Natural fibreboard (Uncoated)

Figure A4: Suction Curve

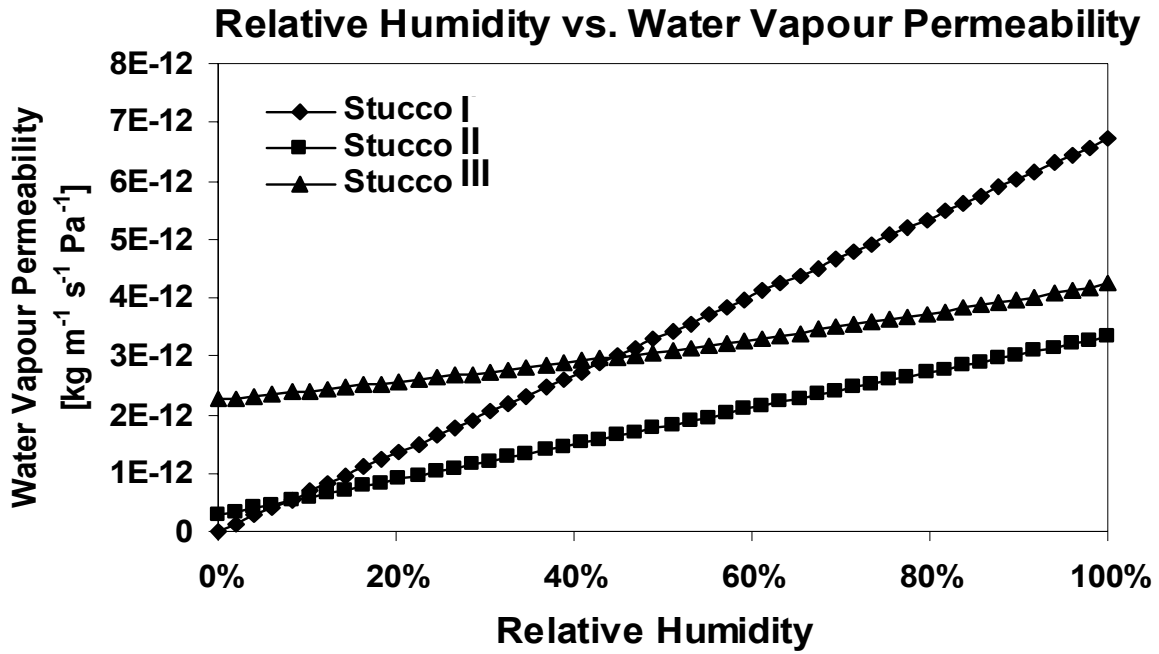


(i) Plywood

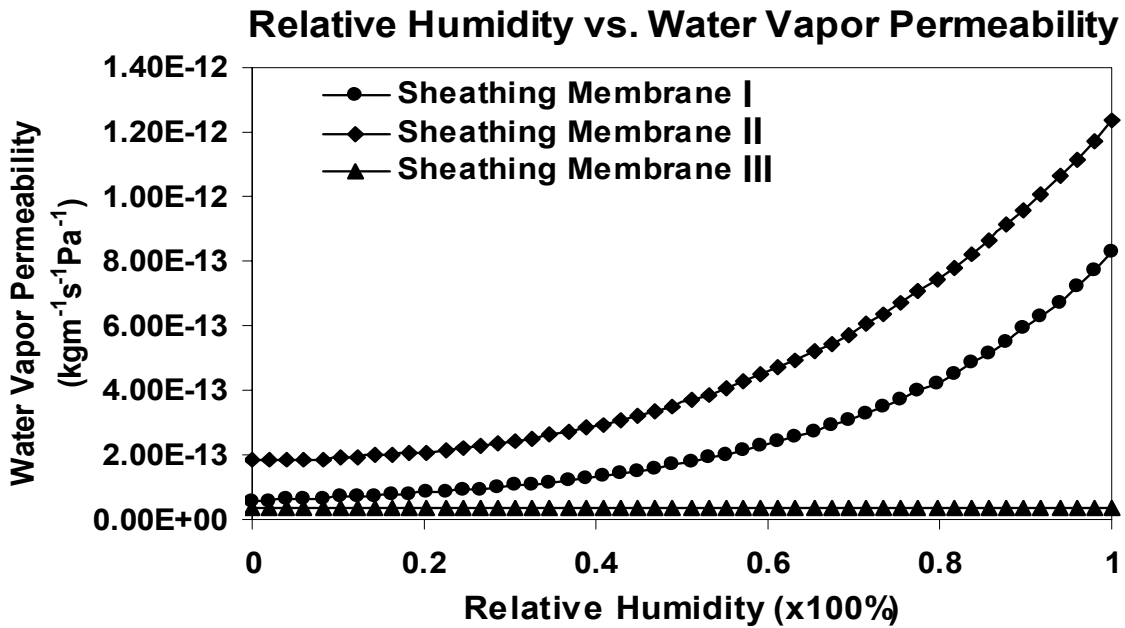


(j) Coated gypsum board

Figure A4: Suction Curve

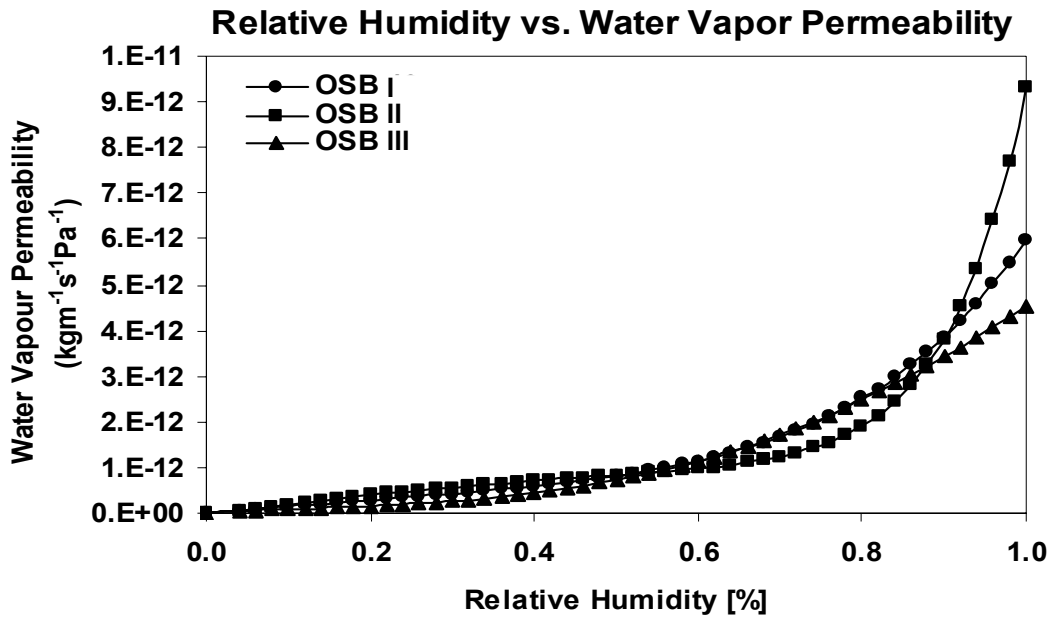


(a) Stucco

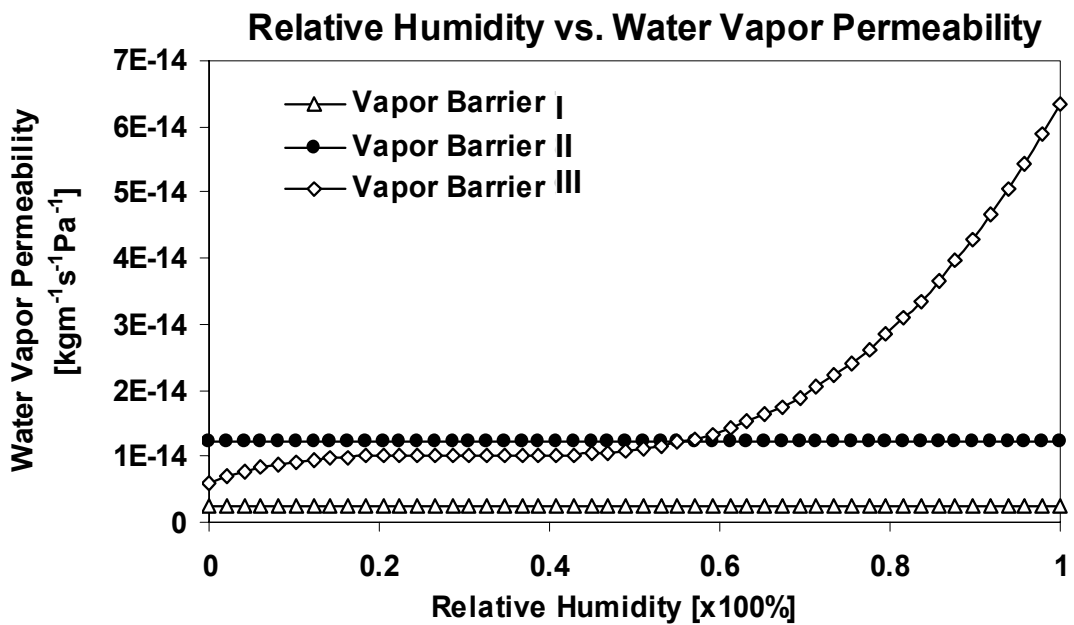


(b) Sheathing membrane

Figure A5: Water Vapour Permeability

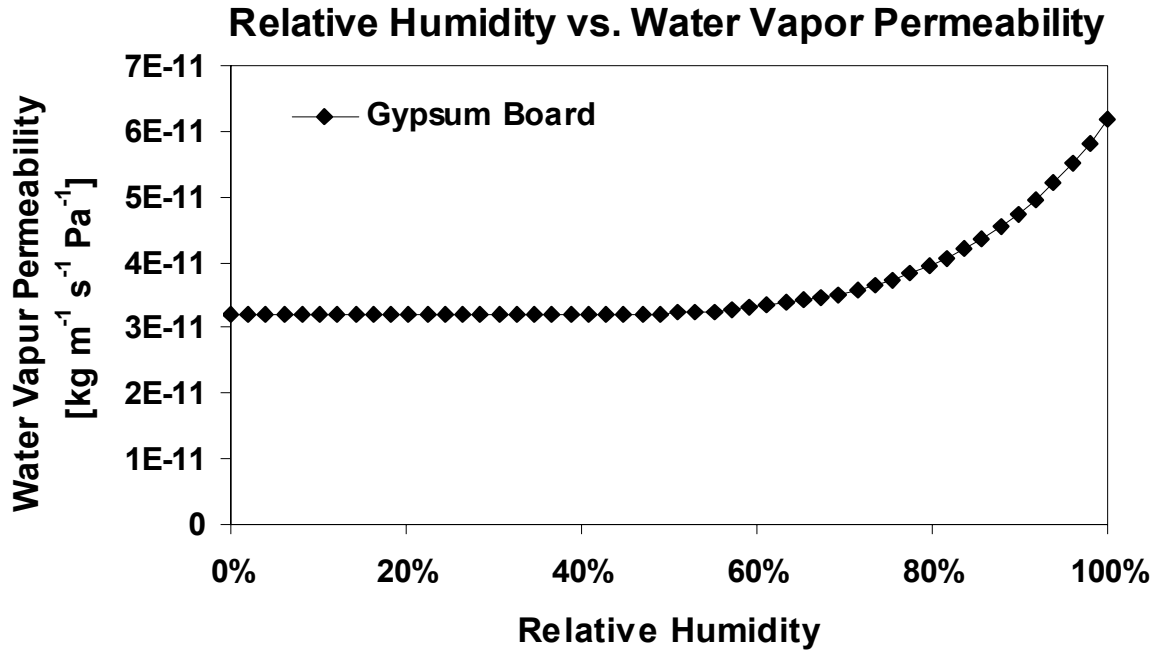


(c) OSB

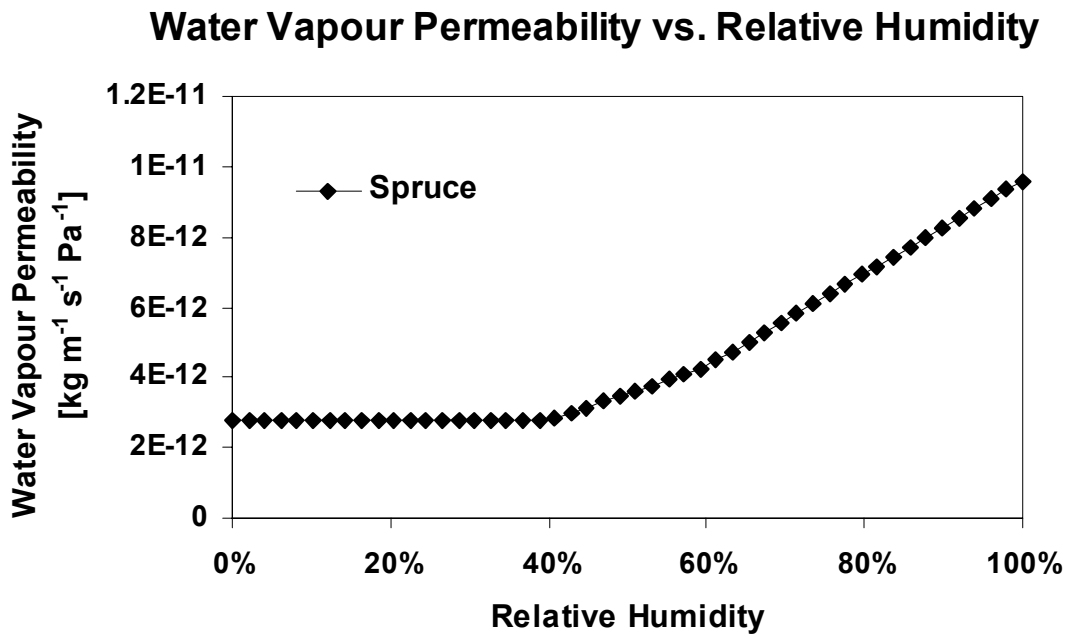


(d) Vapour barrier

Figure A5: Water Vapour Permeability

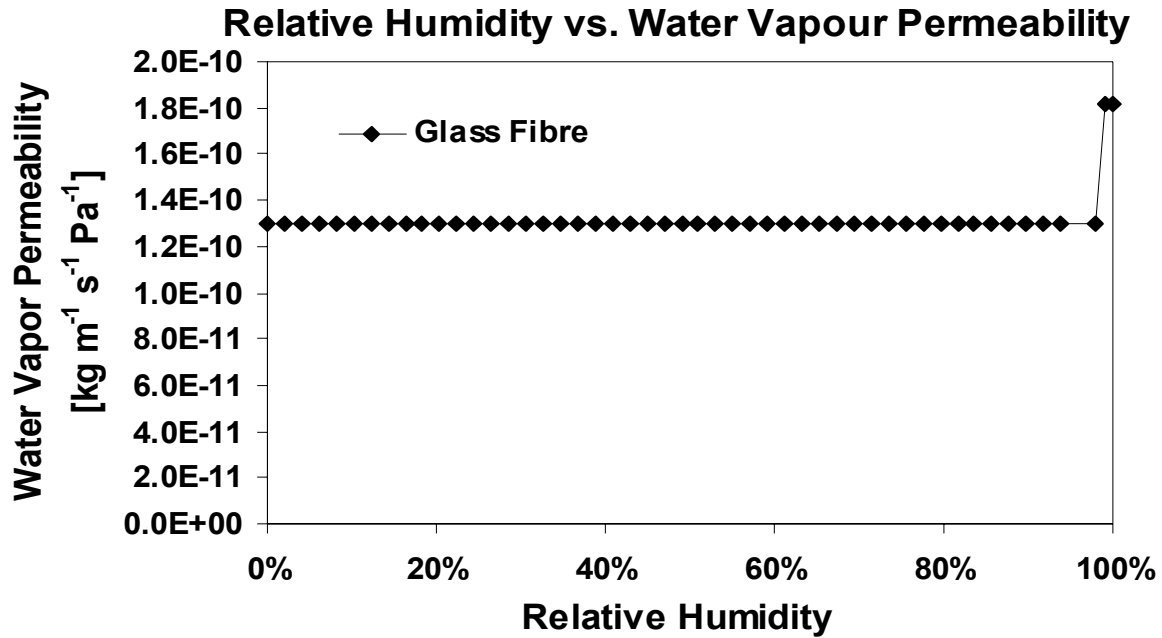


(e) Gypsum board

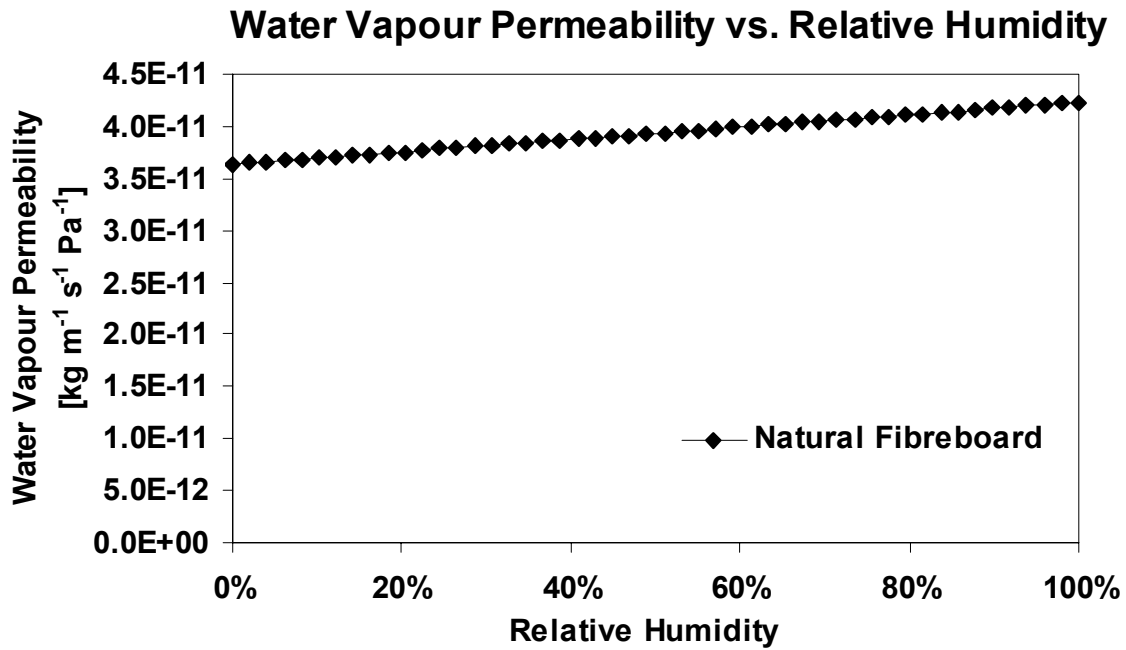


(f) Spruce

Figure A5: Water Vapour Permeability

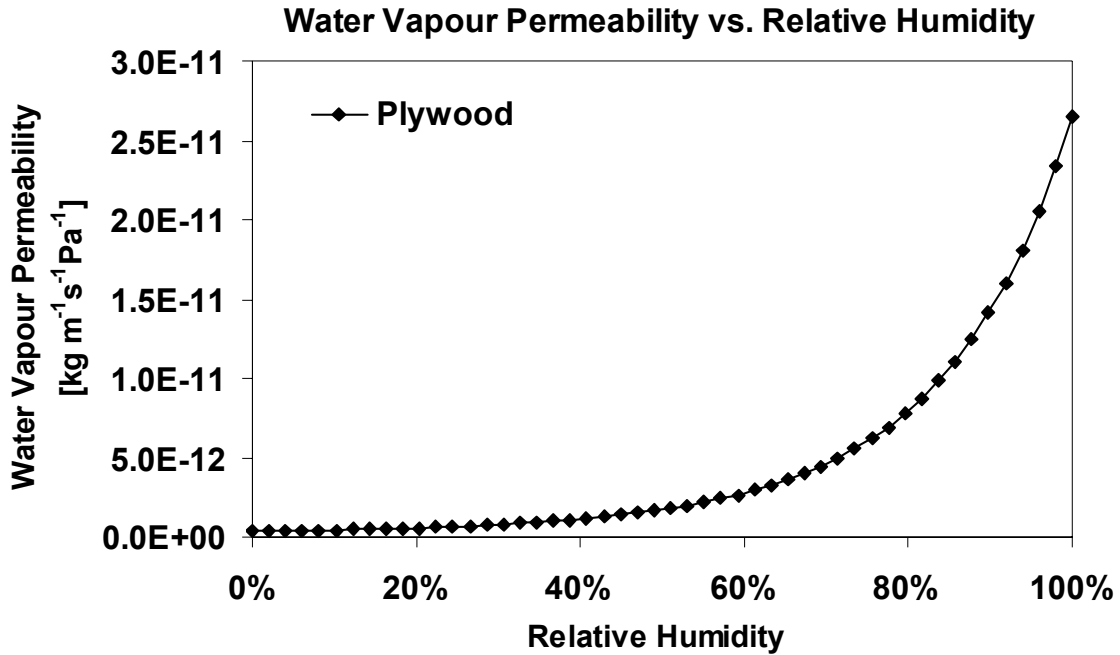


(g) Glass fibre

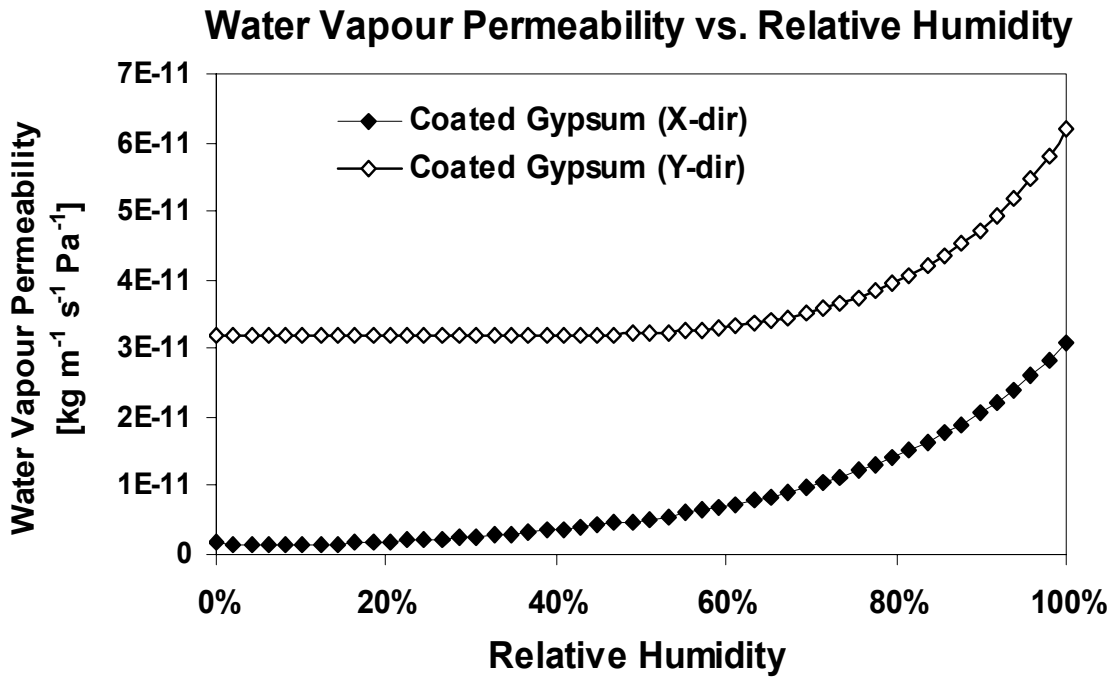


(h) Natural fibreboard

Figure A5: Water Vapour Permeability

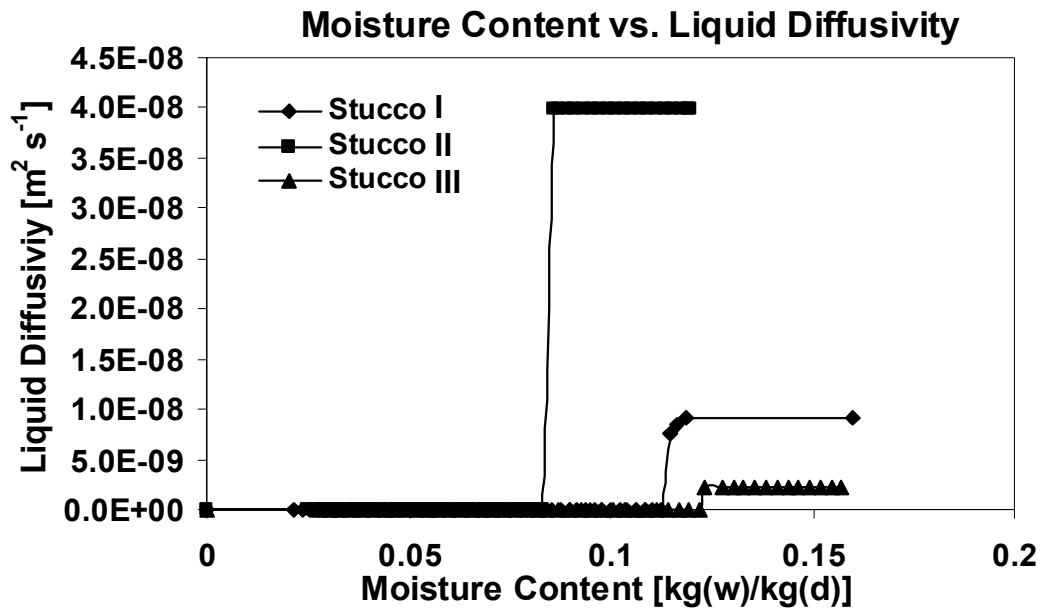


(i) Plywood

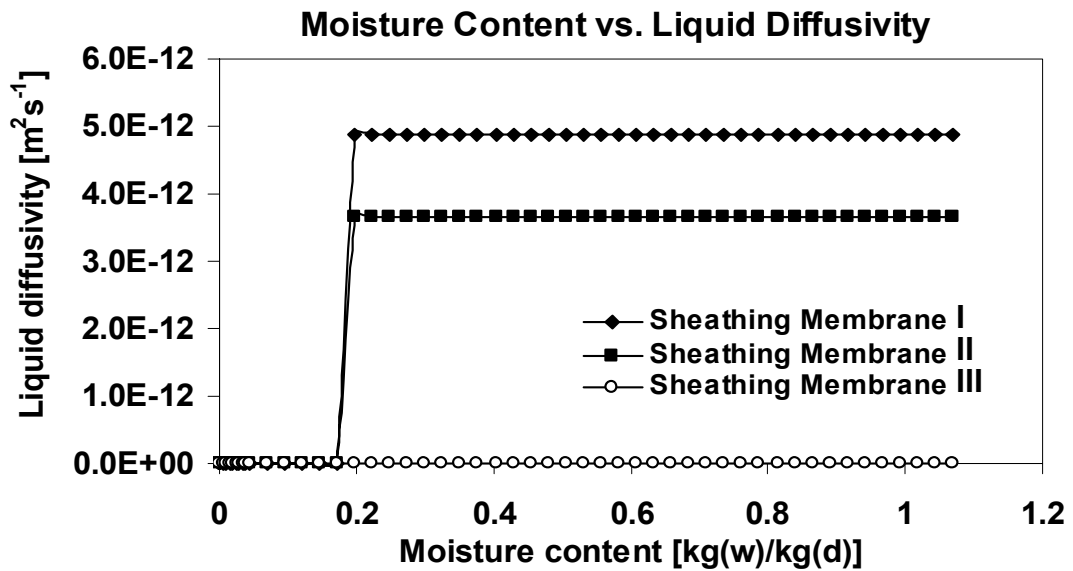


(j) Coated gypsum board

Figure A5: Water Vapour Permeability

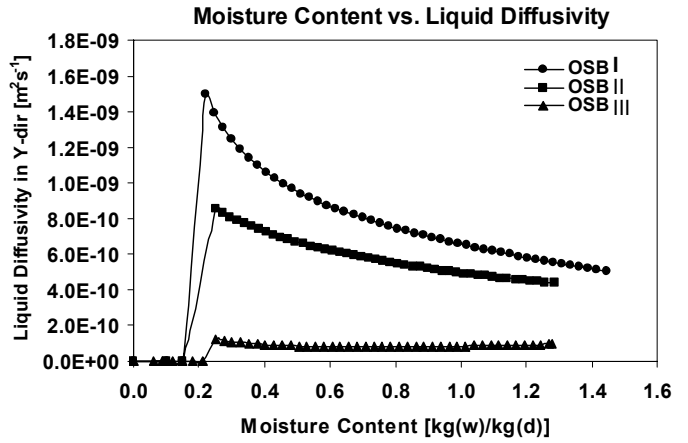
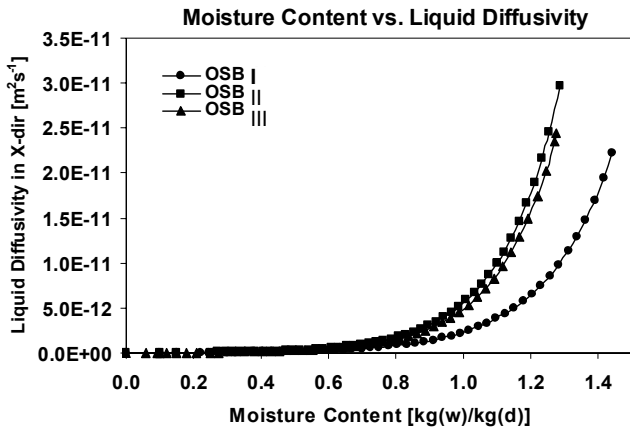


(a) Stucco

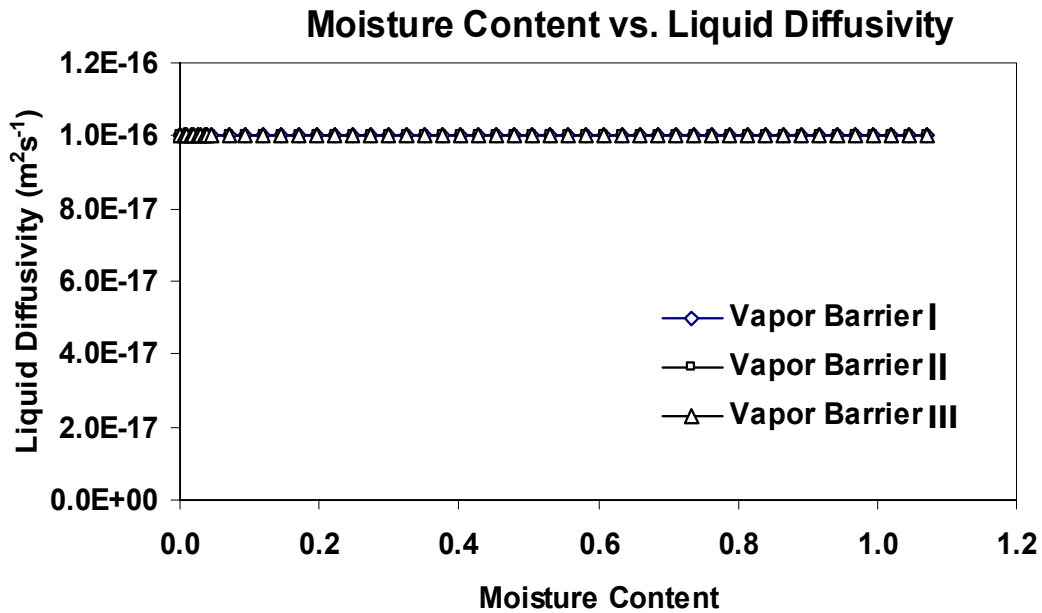


(b) Sheathing membrane

Figure A6: Liquid Diffusivity

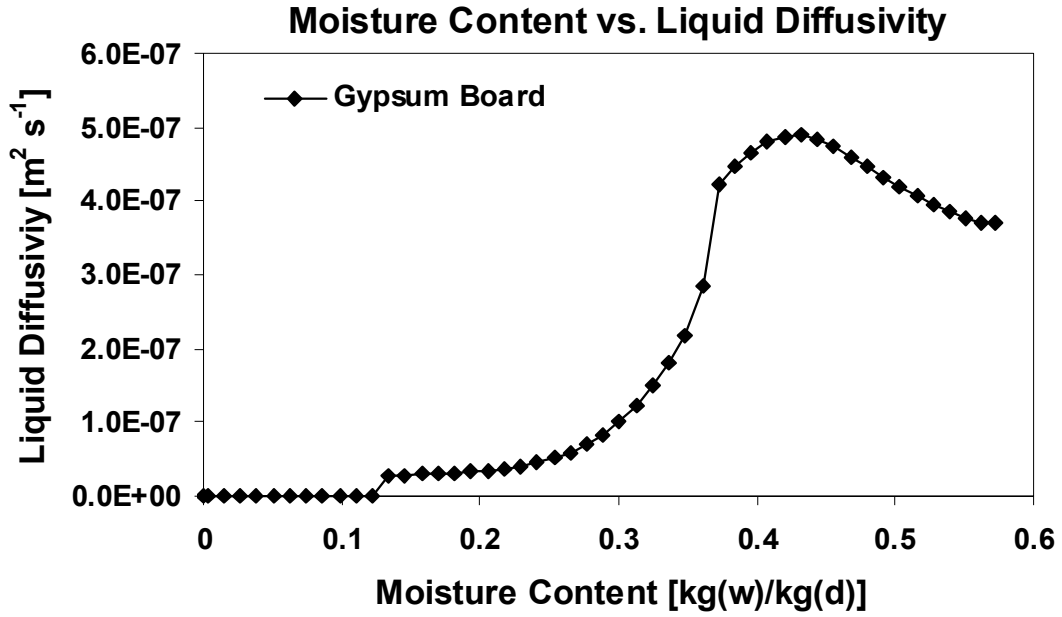


(c) OSB

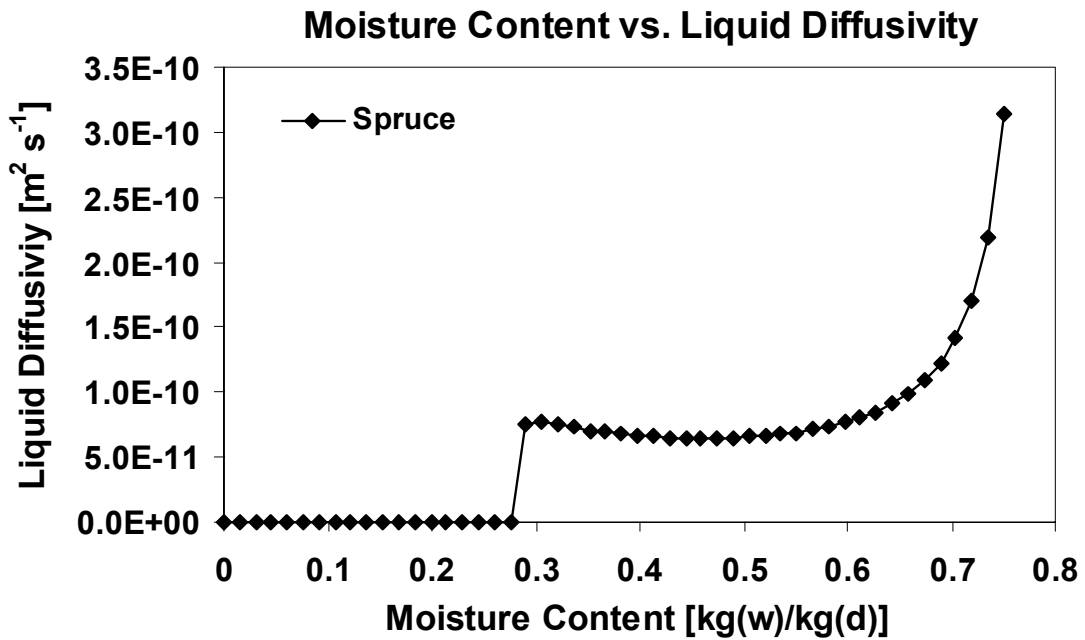


(d) Vapour barrier

Figure A6: Liquid Diffusivity

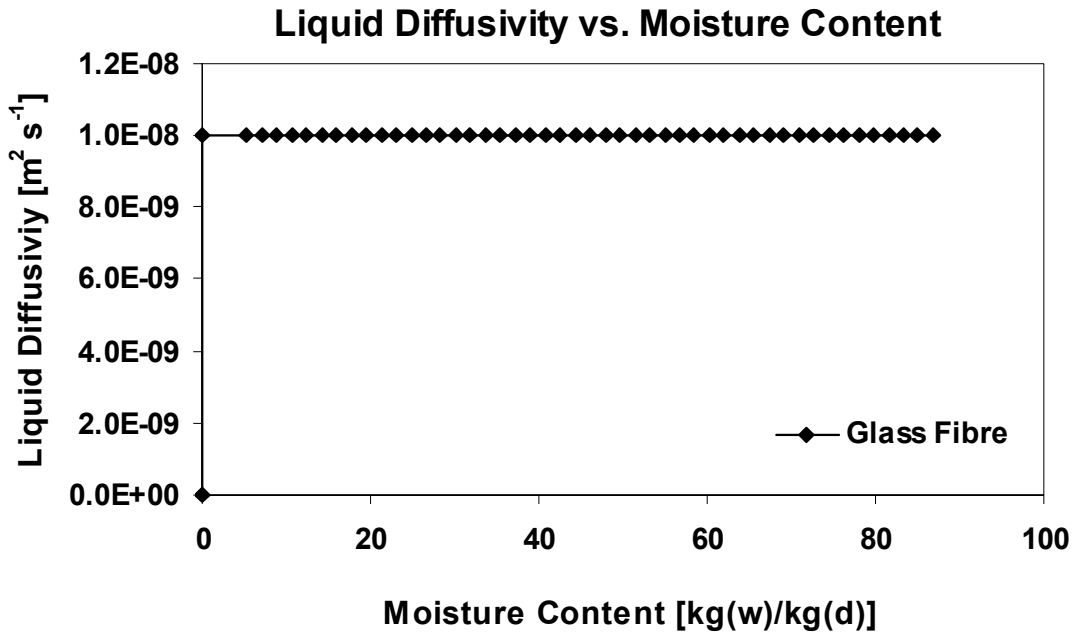


(e) Gypsum board

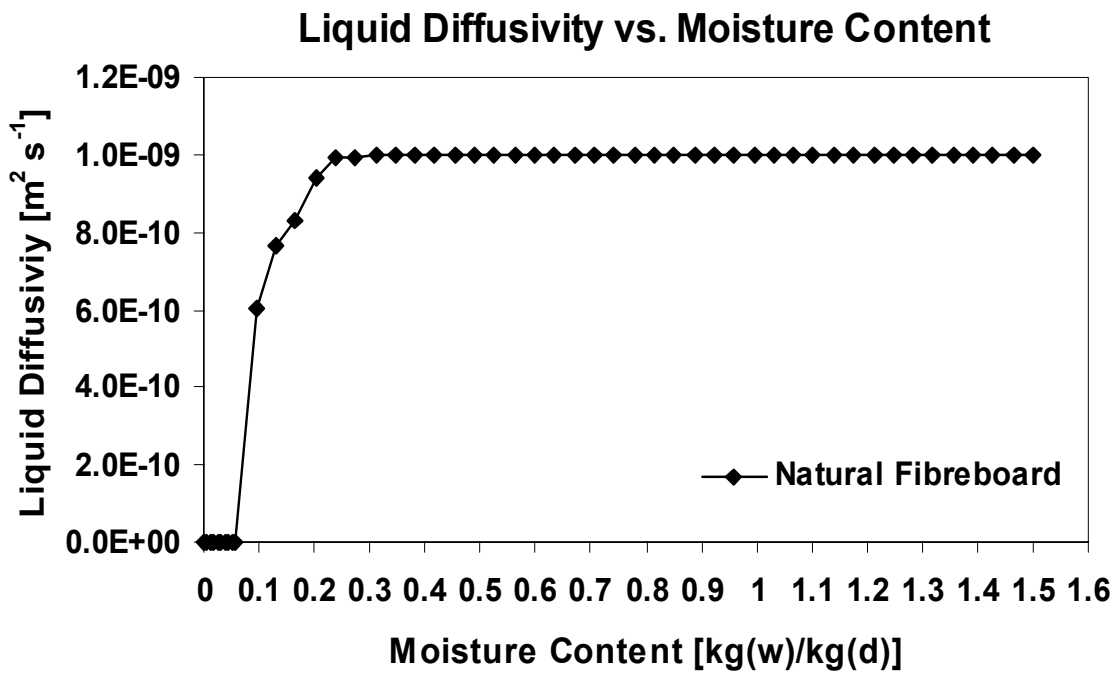


(f) Spruce

Figure A6: Liquid Diffusivity

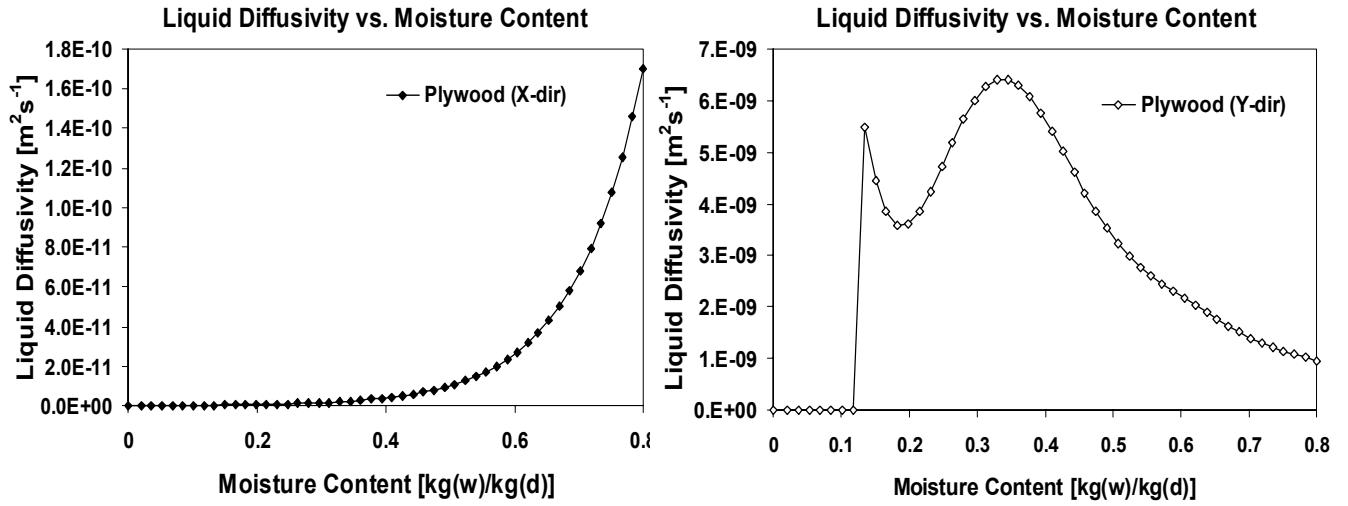


(g) Glass Fibre

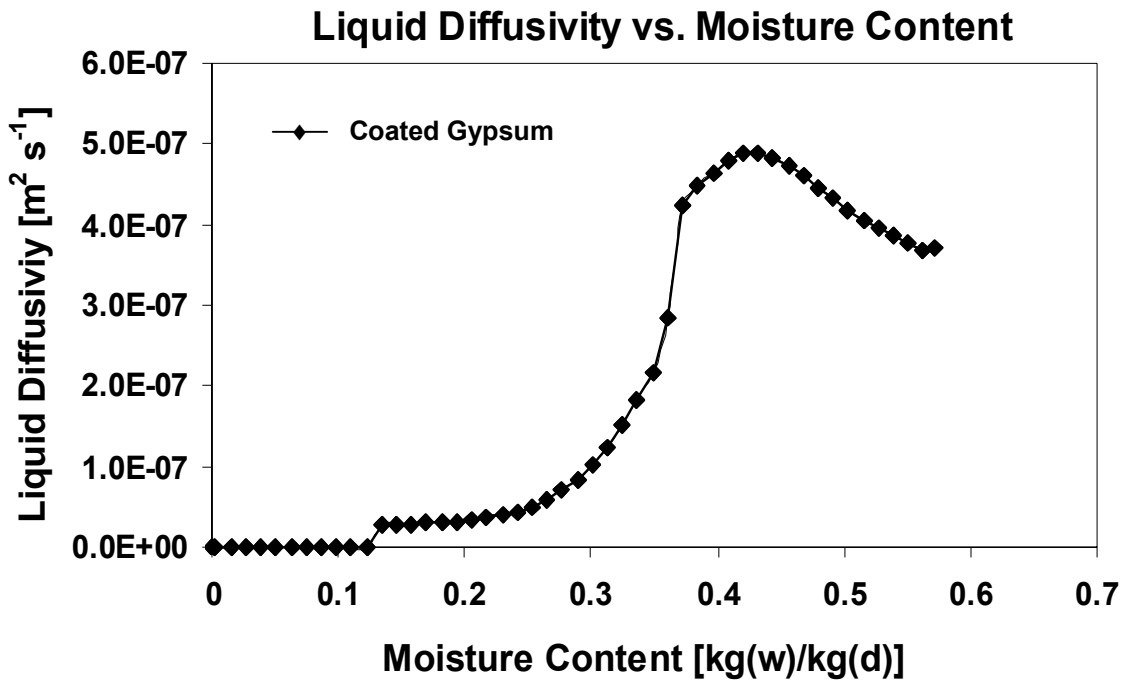


(h) Natural fibre board (Uncoated)

Figure A6: Liquid Diffusivity



(i) Plywood



(j) Coated gypsum board

Figure A6: Liquid Diffusivity

2.3 Boundary Conditions

The two main boundary conditions are the indoor/Interior condition, and the Outdoor/Exterior condition.

2.3.1 Indoor Environment

The interior boundary conditions considered are the indoor temperature (T) and the indoor relative humidity (RH). A summer and winter setting of RH and T are simulated in accordance with ASHRAE recommendations (*ASHRAE Handbook of Fundamentals, Chapter 3*). The summer and winter seasons, identified according to the criteria specified in the 'Specifications to National (Canada) Energy Code for Houses, (*Swinton and Sander, 1994*)', as follows:

Winter: Mean monthly outdoor temperature < 11°C

Summer: Mean monthly outdoor temperature > 11°C

A typical variation of indoor RH and T at Ottawa in a calendar year is shown in Figure A7.

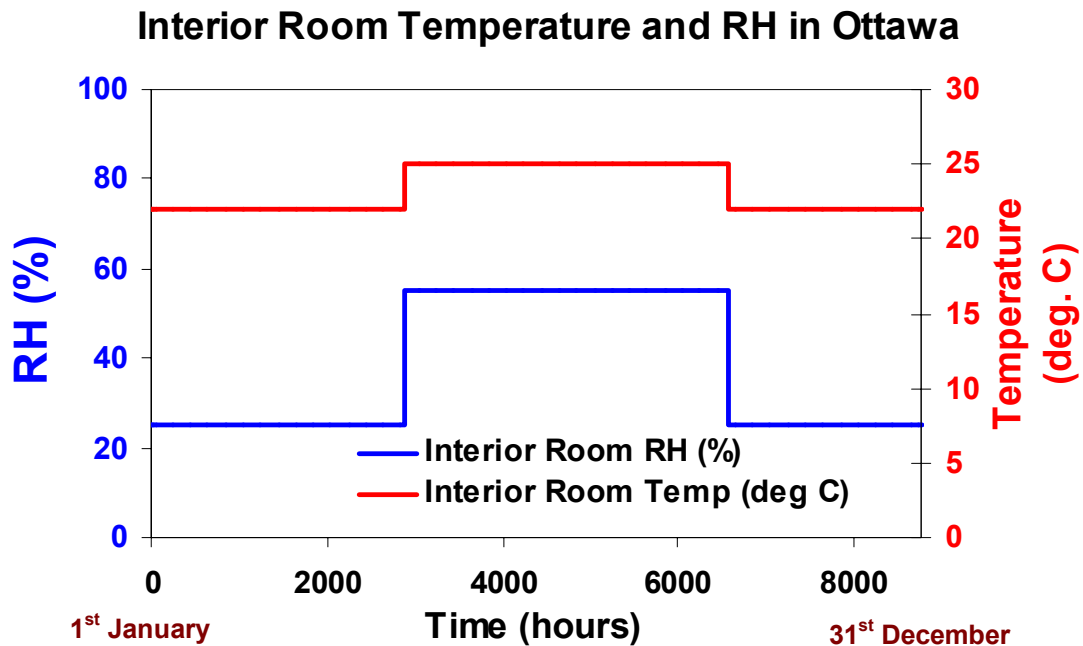


Figure A7: Typical Interior Room Temperature and Relative Humidity at Ottawa

2.3.2 Outdoor Environment

The external weather data as necessary for *hygIRC* modelling has seven components. They are:

- (1) Temperature
- (2) Relative Humidity
- (3) Wind Velocity
- (4) Wind Direction
- (5) Radiation (Direct, Diffused and Reflective components)
- (6) Horizontal rainfall
- (7) Cloud index

A typical format of exterior weather hourly-recorded data file is shown in the Table A5 below.

Table A5: Typical exterior weather data format

Time (hr)	Temperature (°C)	Relative humidity (%)	Wind velocity (km/hr)	Wind direction (°)	Radiation (W/m ²)			Rain (mm/hr)	Cloud Index
					Direct	Diffused	Reflexive		
1	-10.6	74.19	19.08	68	241.39	180.39	0	0	8
2	-5	86.45	8.90	126.39	126.39	125.45	0	5	6
.....					

Three typical years, representing the *Wet*, *Average* and *Dry* year respectively, have been selected for this study. The selection methodology for the *Wet*, *Average* and *Dry* years is described in the MEWS Task 4 report (*Cornick et al. 2002*).

2.4 Exposure Duration

A total of three years of exposure duration is considered in this study. In all cases, except one, the first two years are *Wet* years (same year repeated) and the third year is an *Average* year. In one case for parametric study the third *Average* year is replaced by a *Dry* year.

2.5 Initial Moisture Content and Temperature

In any hygrothermal simulation, the user defines the initial moisture content of each wall component at the beginning of the first year. It is assumed in this study that the initial moisture content of each wall component is equivalent to the corresponding relative humidity of 50 percent, derived from the sorption isotherm of the respective materials. The first year of the simulation is considered to be an initial conditioning period, and all the observations are made on the basis of the hygrothermal response of the wall assembly during the second and third years. Similarly, the initial temperature across the entire wall cross section is assumed to be 20°C.

2.6 Accidental Moisture Entry - Quantity and Location

hygIRC has the capability to inject any quantity of accidentally entered moisture at any location of the wall and at any time (hourly). The quantity of accidentally entered moisture inside the wall and its location were determined from the output of full-scale and small-scale laboratory tests done in MEWS Task 6 (*Lacasse et al. 2002*).

Quantity

An equation was derived from the full-scale lab results to estimate the moisture entry rate (Q). This equation depends on the pressure difference across the wall assembly (ΔP) as well as the rate of water dR_p striking the wall, as given below:

$$dQ/dR_p = 0.0314 + 7.74 \times 10^{-5} \Delta P - 8.14 \times 10^{-8} \Delta P^2 \quad [\text{Eqn. A1}]$$

In real-life ΔP is a function of wind pressure and dR_p is representative of wind driven rain.

However, for the stucco-wall, initially, the aforementioned equation A1 was slightly modified to reduce the quantity of moisture entry inside the wall. *It was felt at that time*

that quantity of water derived from equation A1 might be too much for the parametric analysis. The modified equation is defined as:

$$dQ/dR_p = 0.00314 + 7.74 \times 10^{-5} \Delta P - 8.14 \times 10^{-8} \Delta P^2 \quad [\text{Eqn. A2}]$$

All the parametric studies reported in this report are based on the quantity of moisture entry determined with the use of equation A2. However, similar studies for a selected number of parameters have also been done with the use of equation A1 and a different 'region of focus'. The results are shown in Appendix A2.

Location

As observed in the full and small-scale tests of MEWS Task 6, the worst-case scenario location of accidentally entered moisture is found to be at the bottom of the insulated stud cavity. Hence, the quantity of accidentally entered moisture determined from either equation A1 or A2 was injected at the bottom of the stud cavity, on the top of the bottom plate, at every hour.

3.0 Results from *hygIRC* Simulation

More than one hundred simulations were done for the parametric study on stucco-wall. An enormous amount of data was generated from *hygIRC* and subsequently post-processed for overall and critical evaluation of the simulated hygrothermal response of the wall. However, only selected amount of data are presented in this report that are pertinent to the discussion. If required and requested for a stated purpose then any particular aspect of the remaining data could be made available exclusively to the MEWS partners.

The following are the important points about the simulations that the authors feel should be clearly and unambiguously disclosed to the readers before presenting the results and the related discussions:

1. The main objective of this study is to determine the drying potential and characteristics of the wall assembly in the case of accidentally entered moisture inside the insulation cavity of the stucco-clad wood-frame wall assembly.
2. The materials used in the simulations are described in section 2.2.
3. Each simulation done in this study has a unique identification code and in order to make it clear to the readers the identification codes are explained at the end of Table A6, where *hygIRC* simulation results have been summarised.
4. A three-year simulation was done for each of the cases considered in this study. However, all the simulation results were analysed based on the results of second and third year. Hence, all the discussions presented in this chapter are based on the second and third year simulation results and all the graphs represent the data for that period only.
5. It is to be noted that all simulations done in this study have the first conditioning year (a wet year) without any accidental moisture entry. This was done to generate a realistic moisture distribution inside the wall at the end of first year and prior to accidental moisture entry in the subsequent two years.
6. All the simulations done in this study have accidental moisture entry inside the stud/insulation, except one simulation (with the letters BC at the end of the simulation ID) for each location which did not have any accidental moisture entry. The

accidental moisture enters inside the cavity from the beginning of second year till the end of 3rd year.

7. The wall with accidental moisture entry represents the real wall with deficiency. The wall without accidental moisture entry can be considered as an ideal wall.
8. Drying curves obtained from the simulations, after first year, are shown in Appendix A1. The moisture content in these graphs is expressed with the unit of mass of moisture per unit length (kg/m) of wall or its components entire cross section. These drying curves provide the overall drying characteristics of the whole wall and its major components.
9. More detailed study (microanalysis) of the hygrothermal response of the wall assembly was done by analysing the relative humidity(RH) and temperature (T) contour plots (Figure A8)
10. A novel concept called the RHT Index was introduced by the researchers at IRC/NRC that was used in the parametric study to quantify and compare the localized hygrothermal response of any part of the wall and its component. The RHT index is derived from the RH and T distribution pattern (Figure A8) over a period of time for any specific area of the wall cross-section. Hence, the RHT index as defined in this study:

$$\text{Cumulative 2 year (2}^{nd} \text{ and 3}^{rd} \text{ year) RHT} = \sum (RH - RH_x) \times (T - T_x),$$

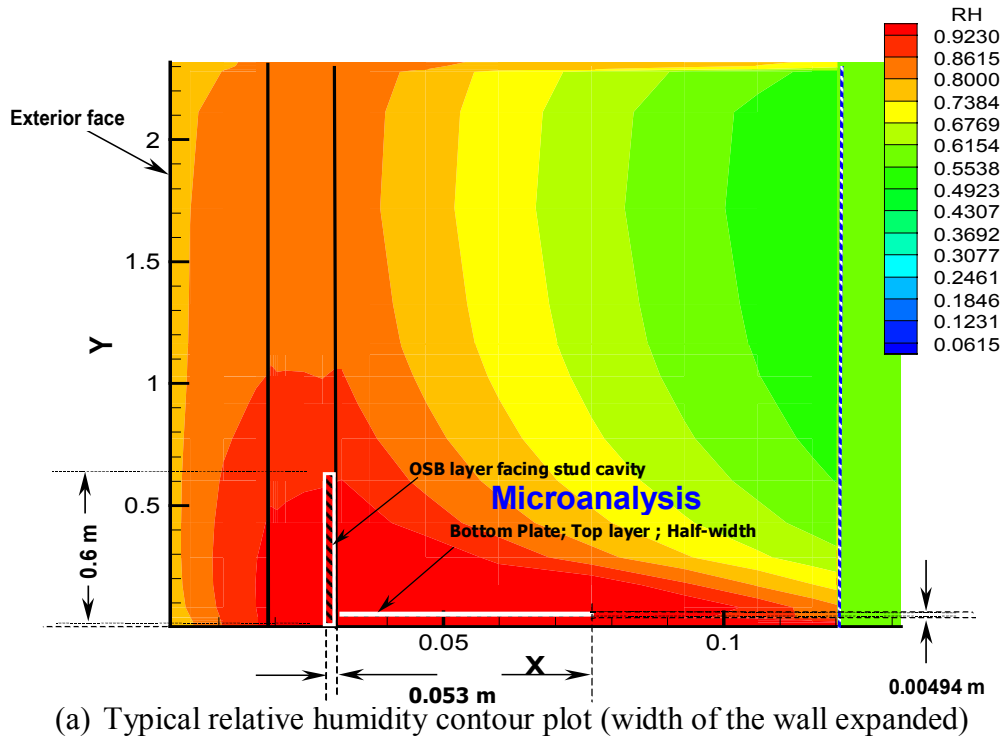
[Eqn. A3]

for $RH > RH_x\%$ and $T > T_x^\circ\text{C}$ at every 10 days interval

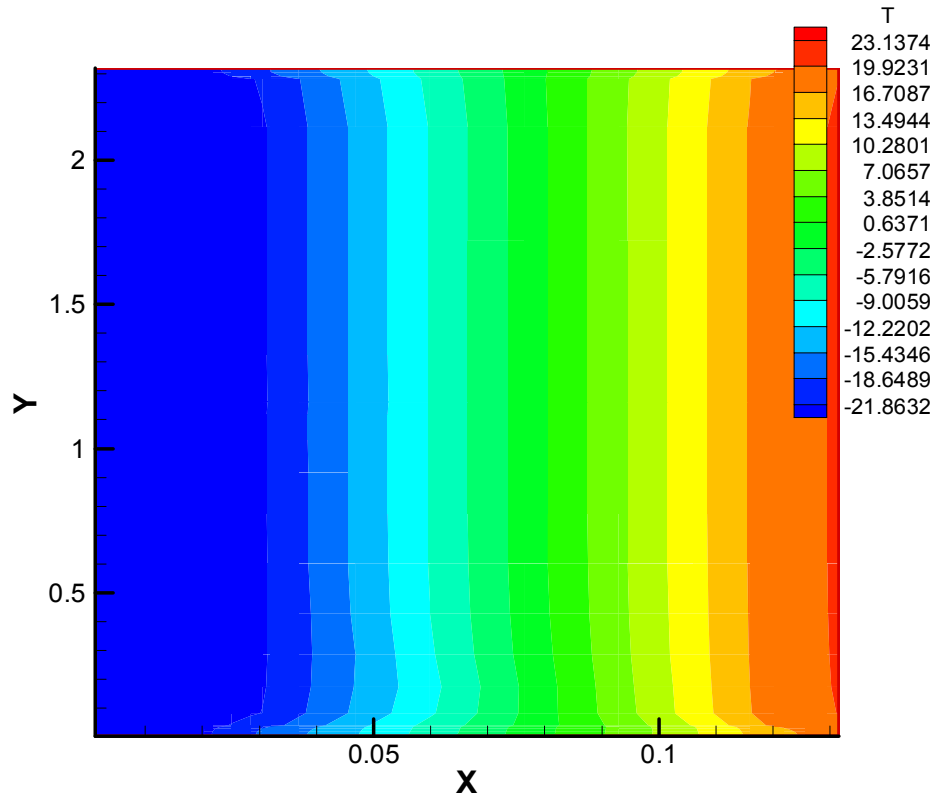
(During any time step when either or both $RH \leq RH_x\%$ and $T \leq T_x^\circ\text{C}$, the RHT value for that time step is zero.)

Where user-defined threshold values for $RH_x = 95\%$ and $T_x = 5^\circ\text{C}$ have been chosen for this parametric study. For general interest, RHT values for $RH_x=90\%$ and 80% have also been derived and reported. The RHT values are referred to as RHT(95), RHT(90) or RHT(80) index according to the threshold RH (i.e. RH_x) level.

11. 'Region of focus' is the area for which the RHT index is calculated and this area should be the wettest portion of the wall assembly most of the time (see Figure A8a). For all stucco-wall simulations, where quantity of moisture entry inside the wall was calculated from equation A2, the 'region of focus' is a thin slice (1.4 mm) of the OSB sheathing board, 600mm height from the bottom of the stud cavity, facing the insulation layer. However, when equation A1 was used the 'region of focus' was shifted to a thin slice (5 mm) of the top surface of the bottom plate, extending 53 mm from the sheathing board (see Figure A8a).
12. As can be seen from the description of RHT index, it brings out the overall localized combined moisture and temperature response of the selected area of the material or wall assembly. For overall drying and wetting pattern of the stucco-wall assembly, at any point of time, the readers should look at the drying curves shown in Appendix A1.



(a) Typical relative humidity contour plot (width of the wall expanded)



(b) Typical temperature contour plot (width of the wall expanded)

Figure A8: RH and T Contour

3.1 Results from Parametric Studies

Results from the parametric studies are to be discussed here primarily with the RHT(95) values shown in Table A6 calculated for a thin layer of OSB using equation A2. However, in qualitative sense, the observations would be same if RHT(80) or RHT(90) is to be used instead of RHT(95).

It is to be mentioned here that the 'region of focus' for the stucco-wall results discussed here is the thin OSB layer (Figure A8a). Changing the 'region of focus' from the OSB to the bottom plate can and will change the results. The conclusions regarding the effects of specific parameters may also vary. Readers interested in the results for the bottom-plate as the 'region of focus' should refer Task group 8 report (*Beaulieu et al. 2002*).

3.1.1 Exterior cladding (3 types of stucco)

Stucco cladding is the first component of the wall assembly, in the line of defence, to protect the living indoor climate from the outdoor or external climate. Three stucco materials (Stucco I, II and III) were chosen for this parametric study. All the material properties of these three stucco materials, determined in the laboratory, are shown in section 2.2. The simulation identification code for these three types of stucco (I, II and III) are **S1M2O1V1, **S2M2O1V1 and **S3M2O1V1 (Table A6).

It can be seen from Table A6 that variation of stucco properties can have significant influence on RHT(95) values at every location, except in very dry location (e.g. Phoenix) where it becomes insignificant. Stucco III with the lowest liquid diffusivity has caused the lowest RHT(95) values (i.e. the least severe hygrothermal response) in all locations.

Table A6: Simulation Results - RHT (95) Indices
(OSB layer: Region of focus; Equation A2)

Simulation ID	RHT (95) Index	Simulation ID	RHT (95) Index	Simulation ID	RHT (95) Index	Simulation ID	RHT (95) Index
(A) OTTAWA		(B) PHOENIX		(D) WILMINGTON		(E) WINNIPEG	
OTS2M2O1V1BC	0	PHS2M2O1V1BC	0	WIS2M2O1V1BC	149	WIS2M2O1VN2575	337
OTS2M2O1V1	652	PHS2M2O1V1	0	WIS2M2O1V1	2270	WIS2M2O1VN5075	500
OTS2M2O2V1	480	PHS2M2O2V1	0	WIS2M2O2V1	2127	WIS2M2O1VN2565	133
OTS2M2O3V1	390	PHS2M2O3V1	0	WIS2M2O3V1	2034	WIS2M2O1NV4065	186
OTS1M2O1V1	110	PHS1M2O1V1	0	WIS1M2O1V1	1766	WIS2M2O1V1BC_VD	8
OTS3M2O1V1	110	PHS3M2O1V1	0	WIS3M2O1V1	1604	WIS2M2O1V1NRBC	9
OTS2M1O1V1	657	PHS2M1O1V1	0	WIS2M1O1V1	2271	WIS2M2O1V0CG	10
OTS2M3O1V1	773	PHS2M3O1V1	0	WIS2M3O1V1	2342	(E) WINNIPEG	
OTS2M2O1V2	264	PHS2M2O1V2	0	WIS2M2O1V2	1928	WPS2M2O1V1BC	0
OTS2M2O1V3	135	PHS2M2O1V3	0	WIS2M2O1V3	964	WPS2M2O1V1	533
OTS2M2O1V1W2	113	PHS2M2O1V1W2	0	WIS2M2O1V1W2	1846	WPS2M2O2V1	475
OTS2M2O1V1W4	0.2	PHS2M2O1V1W4	89	WIS2M2O1V1W4	1456	WPS2M2O3V1	431
OTS2M2O1V1WD	692	(C) SEATTLE		WIS2M2O1V1WD	2464	WPS1M2O1V1	281
OTS2M2O3V1CB	4	SES2M2O1V1BC	0	WIS2M2F*V3	484	WPS3M2O1V1	334
OTS2M2O3V1CL	108	SES2M2O1V1	1322	WIS2M3F*V1	2427	WPS2M1O1V1	536
OTS2M2F*V3	11	SES2M2O2V1	1228	WIS2M2F*VIBC	212	WPS2M3O1V1	600
OTS2M3F*V1	971	SES2M2O3V1	1212	WIS2M2F*V1	1342	WPS2M2O1V2	383
OTS2M2F*V1BC	0	SES1M2O1V1	1006	WIS3M1O1V3BP	441	WPS2M2O1V3	157
OTS2M2F*V1	56	SES3M2O1V1	712	WIS3M1O3V3BR	319	WPS2M2O1V1W2	69
OTS3M1O1V3BP	26	SES2M1O1V1	1323	WIS2M3O1V1WR	2369	WPS2M2O1V1W4	0
OTS1M1O3V3BR	6	SES2M3O1V1	1394	WIS2M2P*V3	1075	WPS2M2O3V1CB	23
OTS2M3O1V1WR	807	SES2M2O1V2	768	WIS2M3P*V1	2400	WPS2M2O3V1CL	232
OTS2M2P*V3	126	SES2M2O1V3	450	WIS2M2P*VIBC	252	(F) FRESNO	
OTS2M3P*V1	684	SES2M2O1V1W2	809	WIS2M2P*V1	1753	FRS2M3O1V1	10
OTS2M2P*V1BC	0	SES2M2O1V1W4	324	WIS2M2O1V0NV	2	FRS2M2O1V3	0
OTS2M2P*V1	441	SES2M2O3V1CB	146	WIS2M2O1V0NV	1	FRS2M2O1V1BC	0
OTS2M2O1V0NV	0	SES2M2O3V1CBB	0	WIS2M3O1V0NV	1	FRS2M2O1V1	112
OYS2M3O1V0NV	0	SES2M2O1V1AL	337	WIS2M2O1V32575	1719	(G) SAN DIEGO	
OTS2M2O1V1AL	80			WIS2M2O1V35075	1812	SDS2M3O1V1	0
OTS2M2O1V1NAG	619			WIS2M2O1V32565	1320	SDS2M2O1V3	0
OTS2M2O1V1LT	1133			WIS2M2O1V34075	1776	SDS2M2O1V1BC	0
		Grey = Second series		WIS2M2O1V34065	1398	SDS2M2O1V1	0

Table A7: Simulation Results - RHT (80) Indices
(OSB layer - Region of focus; Equation A2)

Simulation ID	RHT (80) Index	Simulation ID	RHT (80) Index	Simulation ID	RHT (80) Index	Simulation ID	RHT (80) Index
(A) OTTAWA		(B) PHOENIX		(D) WILMINGTON		WIS2M2O1VN2575	6269
OTS2M2O1V1BC	948	PHS2M2O1V1BC	0	WIS2M2O1V1BC	10179	WIS2M2O1VN5075	7250
OTS2M2O1V1	6071	PHS2M2O1V1	0	WIS2M2O1V1	14920	WIS2M2O1NV2565	4409
OTS2M2O2V1	5812	PHS2M2O2V1	2	WIS2M2O2V1	14646	WIS2M2O1VN4065	5049
OTS2M2O3V1	5711	PHS2M2O3V1	0	WIS2M2O3V1	14577	WIS2M2O1V1BC_VD	480
OTS1M2O1V1	4527	PHS1M2O1V1	0	WIS1M2O1V1	14381	WIS2M2O1V1NRBC	3191
OTS3M2O1V1	4687	PHS3M2O1V1	0	WIS3M2O1V1	14115	WIS2M2O1V0CG	3835
OTS2M1O1V1	6070	PHS2M1O1V1	0	WIS2M1O1V1	14924	(E) WINNIPEG	
OTS2M3O1V1	6186	PHS2M3O1V1	8	WIS2M3O1V1	14981	WPS2M2O1V1BC	0
OTS2M2O1V2	5487	PHS2M2O1V2	0	WIS2M2O1V2	14451	WPS2M2O1V1	4870
OTS2M2O1V3	4532	PHS2M2O1V3	0	WIS2M2O1V3	12412	WPS2M2O2V1	4730
OTS2M2O1V1W2	4934	PHS2M2O1V1W2	1598	WIS2M2O1V1W2	14304	WPS2M2O3V1	4628
OTS2M2O1V1W4	3335	PHS2M2O1V1W4	4943	WIS2M2O1V1W4	13417	WPS1M2O1V1	4432
OTS2M2O1V1WD	6368	(C) SEATTLE		WIS2M2O1V1WD	16198	WPS3M2O1V1	4612
OTS2M2O3V1CB	2308	SES2M2O1V1BC	5266	WIS2M2F*V3	10757	WPS2M1O1V1	4880
OTS2M2O3V1CL	5479	SES2M2O1V1	8841	WIS2M3F*V1	15395	WPS2M3O1V1	4992
OTS2M2F*V3	2961	SES2M2O2V1	8580	WIS2M2F*V1BC	9388	WPS2M2O1V2	4679
OTS2M3F*V1	6702	SES2M2O3V1	8621	WIS2M2F*V1	13805	WPS2M2O1V3	4240
OTS2M2F*V1BC	1033	SES1M2O1V1	8371	WIS3M1O1V3BP	7382	WPS2M2O1V1W2	3761
OTS2M2F*V1	4870	SES3M2O1V1	7844	WIS3M1O3V3BR	7594	WPS2M2O1V1W4	1904
OTS3M1O1V3BP	2422	SES2M1O1V1	8837	WIS2M3O1V1WR	15010	WPS2M2O3V1CB	4110
OTS1M1O3V3BR	2451	SES2M3O1V1	8901	WIS2M2P*V3	12973	WPS2M2O3V1CL	4949
OTS2M3O1V1WR	6227	SES2M2O1V2	8059	WIS2M3P*V1	14806	(F) FRESNO	
OTS2M2P*V3	4634	SES2M2O1V3	6941	WIS2M2P*V1BC	11528	FRS2M3O1V1	4033
OTS2M3P*V1	5928	SES2M2O1V1W2	8115	WIS2M2P*V1	13935	FRS2M2O1V3	1878
OTS2M2P*V1BC	1322	SES2M2O1V1W4	7290	WIS2M2O1V0NV	2570	FRS2M2O1V1BC	1552
OTS2M2P*V1	5677	SES2M2O3V1CB	4958	WIS2M3O1V0NV	2157	FRS2M2O1V1	4111
OTS2M2O1V0NV	861	SES2M2O3V1CBBC	0	WIS2M2O1V32575	13937	(G) SAN DIEGO	
OYS2M3O1V0NV	850	SES2M2O1V1AL	4378	WIS2M2O1V35075	14125	SDS2M3O1V1	5769
OTS2M2O1V1AL	2819			WIS2M2O1V32565	13178	SDS2M2O1V3	1947
OTS2M2O1V1NAG	6060			WIS2M2O1V34075	14057	SDS2M2O1V1BC	23
OTS2M2O1V1LT	7262	Grey = Second series		WIS2M2O1V34065	13303	SDS2M2O1V1	4440

Table A8: Simulation Results - RHT (90) Indices
(OSB layer - Region of focus; Equation A2)

Simulation ID	RHT (90) Index	Simulation ID	RHT (90) Index	Simulation ID	RHT (90) Index	Simulation ID	RHT (90) Index
(A) OTTAWA		(B) PHOENIX		(D) WILMINGTON			
OTS2M2O1V1BC	0	PHS2M2O1V1BC	0	WIS2M2O1V1BC	2471	WIS2M2O1VN2575	1818
OTS2M2O1V1	2450	PHS2M2O1V1	0	WIS2M2O1V1	6486	WIS2M2O1VN5075	2259
OTS2M2O2V1	2240	PHS2M2O2V1	0	WIS2M2O2V1	6283	WIS2M2O1nv2565	1010
OTS2M2O3V1	2120	PHS2M2O3V1	0	WIS2M2O3V1	6196	WIS2M2O1VN4065	1228
OTS1M2O1V1	952	PHS1M2O1V1	0	WIS1M2O1V1	5908	WIS2M2O1V1BC_VD	123
OTS3M2O1V1	1171	PHS3M2O1V1	0	WIS3M2O1V1	5672	WIS2M2O1V1NRBC	397
OTS2M1O1V1	2454	PHS2M1O1V1	0	WIS2M1O1V1	6488	WIS2M2O1V0CG	610
OTS2M3O1V1	2568	PHS2M3O1V1	0	WIS2M3O1V1	6554	(E) WINNIPEG	
OTS2M2O1V2	1900	PHS2M2O1V2	0	WIS2M2O1V2	6059	WPS2M2O1V1BC	0
OTS2M2O1V3	1031	PHS2M2O1V3	0	WIS2M2O1V3	4351	WPS2M2O1V1	1819
OTS2M2O1V1W2	1388	PHS2M2O1V1W2	43	WIS2M2O1V1W2	5954	WPS2M2O2V1	1723
OTS2M2O1V1W4	321	PHS2M2O1V1W4	947	WIS2M2O1V1W4	5152	WPS2M2O3V1	1641
OTS2M2O1V1WD	2576	(C) SEATTLE		WIS2M2O1V1WD	7041	WPS1M2O1V1	1486
OTS2M2O3V1CB	237	SES2M2O1V1BC	692	WIS2M2F*V3	3111	WPS3M2O1V1	1572
OTS2M2O3V1CL	1199	SES2M2O1V1	3827	WIS2M3F*V1	6849	WPS2M1O1V1	1827
OTS2M2F*V3	502	SES2M2O2V1	3674	WIS2M2F*V1BC	2330	WPS2M3O1V1	1931
OTS2M3F*V1	2881	SES2M2O3V1	3674	WIS2M2F*V1	5326	WPS2M2O1V2	1636
OTS2M2F*V1BC	0	SES1M2O1V1	3343	WIS3M1O1V3BP	2057	WPS2M2O1V3	1264
OTS2M2F*V1	1158	SES3M2O1V1	2841	WIS3M1O3V3BR	1920	WPS2M2O1V1W2	1023
OTS3M1O1V3BP	429	SES2M1O1V1	3826	WIS2M3O1V1WR	6582	WPS2M2O1V1W4	61
OTS1M1O3V3BR	306	SES2M3O1V1	3896	WIS2M2P*V3	4824	WPS2M2O3V1CB	787
OTS2M3O1V1WR	2604	SES2M2O1V2	3143	WIS2M3P*V1	6535	WPS2M2O3V1CL	1549
OTS2M2P*V3	1157	SES2M2O1V3	2191	WIS2M2P*V1BC	3440	(F) FRESNO	
OTS2M3P*V1	2432	SES2M2O1V1W2	3242	WIS2M2P*V1	5814	FRS2M3O1VI	673
OTS2M2P*V1BC	0	SES2M2O1V1W4	2501	WIS2M2O1V0NV	326	FRS2M2O1V3	158
OTS2M2P*V1	2180	SES2M2O3V1CB	1261	WIS2M3O1V0NV	248	FRS2M2O1V1BC	7
OTS2M2O1V0NV	66	SES2M2O3V1CBBC	0	WIS2M2O1V32575	5586	FRS2M2O1V1	1009
OYS2M3O1V0NV	60	SES2M2O1V1AL	1411	WIS2M2O1V35075	5759	(G) SAN DIEGO	
OTS2M2O1V1AL	707			WIS2M2O1V32565	4919	SDS2M3O1V1	581
OTS2M2O1V1NAG	2422			WIS2M2O1V34075	5694	SDS2M2O1V3	28
OTS2M2O1V1LT	3176			WIS2M2O1V34065	5029	SDS2M2O1V1BC	0
		Grey = Second series				SDS2M2O1V1	489

Explanations for the symbols used in the simulation ID in the tables

Simulation ID are similar in formatting to this example: OTS2M2F*V1BC

- The first two letters define the location. Example, OT for Ottawa, etc
- The next letter and number define the stucco cladding. Ex: S2 is stucco No.2
- The next letter and number define the type of water resistive membrane. Ex. M2 is membrane No.2
- The next letter and symbol define the sheathing board. O means OSB, P for plywood and F for natural fibreboard. The star is replaced by a number when more than one product had been characterized in laboratory.
- The next letter and number define the vapour barrier. V1 is vapour barrier No.1. V0 means no vapour barrier

There may be additional letters at the end of the code to give more information on the simulation case. Ex. BC means base case i.e. the wall has no deficiency for water leakage into the stud cavity.

When a simulation ID has following letters, it means:

- BC: No water entry into the stud cavity
- CB: Cavity behind the stucco has opening both at top and bottom
- CL: Cavity behind the stucco has opening at the bottom only
- WD: Simulation done with Wet-Dry weather years instead of Wet-Average
- F*: Presence of natural fibreboard in place of OSB
- P*: Presence of plywood in place of OSB
- BP: Simulation done with the best material combination derived from parametric analysis
- BR: Simulation done with the best material combination derived from RHT indices
- WR: Simulation done with the worst material combination derived from RHT indices
- NV: No vapour barrier
- AL: Air leakage included
- NAG: No air-gap between sheathing membrane and sheathing board
- LT: Alternate Wet-Avg years
- _VD: Vapour permeability and liquid Diffusivity of the stucco have been altered

3.1.2. Sheathing membrane (3 types)

The sheathing membrane in the wall, behind the stucco cladding, is the second in the line to defence against the outdoor climate. Three sheathing membranes are considered for the parametric study, named as sheathing membrane I, II and III. The simulation identification codes for these three types of sheathing membranes (I, II and III) are **S2M1O1V1, **S2M2O1V1 and **S2M3O1V1 (Table A6). It is to be noted that the water vapour permeability of sheathing membrane I and II increases in a non-linear continuous pattern with the increase of relative humidity. However, the water vapour permeability of sheathing membrane III remains always constant and it has the lowest value of water vapour permeability (Figure A5) among the three selected sheathing membranes. The water vapour permeances of three sheathing membranes are:

Sheathing membrane I - between 290 ng/Pa.s.m² and 4150 ng/Pa.s.m²;
 Sheathing membrane II - between 920 ng/Pa.s.m² and 6180 ng/Pa.s.m²; and
 Sheathing membrane III - 280 ng/Pa.s.m² (constant).

It can be seen from the summarised RHT(95) values in Table A6 that the effects of using different types of sheathing membranes on the overall moisture response of the wall and its components are minimal. However, the use of sheathing membrane III resulted in slightly higher RHT(95) values. This observation is believed to be due to the lower water vapour permeability of sheathing membrane III that allows smaller amount of accidentally entered moisture to be transferred to outside of the insulation cavity

3.1.3. Sheathing board (3 types of oriented strand board (OSB), fibre board (FB), Plywood)

Three OSBs (OSB I, II and III), uncoated natural fibreboard and plywood are taken into consideration in this study and their hygrothermal properties are shown in Figure A5. For simulation identification, **S2M2O1V1, ** S2M2O2V1 and ** S2M2O3V1 refer to OSB I, II and III respectively (see Table A6). Simulations identifications with F* and P* in it indicate fibreboard and plywood respectively.

It is evident from the results provided in Table A6 that of the three OSB products, OSB III produced the lowest RHT(95) indices. It is important to note that OSB III has the lowest water vapour permeability. The results from plywood and uncoated fibreboard as sheathing board remained mixed. In case of plywood, maximum reduction of RHT(95) index (Table A6), compared to OSB sheathing board, occurred when vapour barrier I was used in the wall construction. On the other hand, when uncoated fibreboard was used as sheathing board, the maximum reduction of RHT(95) index (Table A6) occurred when vapour barrier III was used in the wall construction.

3.1.4. Vapour barrier (3 types)

The vapour barrier is the last effective component of the wall to protect the indoor room environment from the influence and fluctuation of moisture content in outdoor climate. Three vapour barriers (I, II and III) are considered in this study. They represent three different water vapour diffusion control levels.

Vapour barrier I has a constant water vapour permeance of 15 ng/Pa.s.m²
 Vapour barrier II has a constant water vapour permeance of 60 ng/Pa.s.m², and

Vapour barrier III has water vapour permeance value as a function of relative humidity and varying between 30 and 320 ng/Pa.s.m².

The simulation identification code for these three vapour barriers (I, II and III) are **S2M2O1V1, **S2M2O1V2 and **S2M2O1V3, respectively.

The RHT(95) results from the simulations (Table A6) clearly indicate that the change of vapour barrier type has a distinct influence on the overall moisture response of the wall and its components. Vapour barrier III, with the highest value of water vapour permeance, facilitated the lowest RHT(95) index values.

3.1.5. Locations with seven different Moisture Indices (MI)

Moisture Index (MI)- Moisture Index (MI) describes the climatic moisture load. MI allows a better comparison of potential moisture loads than the traditional simple distribution of rainfall amounts. The Moisture Index is a function of two terms, the potential for wetting, the Wetting Index (WI) and the potential for drying, the Drying Index (DI). The higher the value of the MI, the more severe is the moisture loading. The WI is based on annual rainfall while the DI is based on annual potential evaporation. MI is independent of wall characteristics and design strategies that might be used to manage moisture loading. To assign rankings on the basis of climate analysis for several locations in North America, the following definition was used (see Task 4 final report for details):

$$MI = \sqrt{WI_{\text{normalized}}^2 + (1 - DI_{\text{normalized}})^2} \quad [\text{Eqn. A3}]$$

Table A9 lists the MI for 41 North American locations, calculated with hourly historical weather records, using equation [A3].

Table A9: Moisture Index for 41 North American locations

Location	MI	Location	MI
Mobile AB	1.22	Tampa FL	0.95
New Orleans LA	1.21	Madison WI	0.95
St Johns NF	1.17	Windsor ON	0.94
Shearwater NS	1.15	Montreal QC	0.94
Wilmington NC	1.13	Ottawa ON	0.93
Vancouver BC	1.09	Kansas City MO	0.93
Miami FL	1.08	St. Louis MO	0.92
Atlanta GA	1.06	Toronto ON	0.92
Orlando FL	1.03	Minneapolis MN	0.90
Boston MA	1.01	Edmonton AB	0.89
Houston TX	1.01	Winnipeg MB	0.86
Victoria BC	1.00	San Francisco CA	0.86
Fredericton NB	0.99	Fargo ND	0.85
Seattle WA	0.99	Calgary AB	0.81
Wilmington DE	0.98	Fort Worth TX	0.79
Raleigh NC	0.97	San Diego CA	0.74
Iqaluit NU	0.97	Colorado Springs CO	0.70
Charlotte NC	0.96	Fresno CA	0.49
Baltimore MD	0.96	Phoenix AZ	0.13
Chicago IL	0.95	Las Vegas NV	0.11
Pittsburgh PA	0.95		

Out of these forty-one locations, seven locations (bold and highlighted in Table A9) were chosen for parametric study.

The variation of RHT(95) values with the change in MI indicates a general regular pattern of increasing order as shown in Figure A9. Similar trends have been observed for

RHT(80) and RHT(90) values too. RHT(95) values become greater than zero when MI of a location is greater than a certain value. The stucco-wall with accidentally entered moisture shows higher RHT index at a location with lower MI than the stucco-wall without accidental moisture entry in the same location. The relationship between RHT index and MI is the basis for MEWS methodology and further discussion on this can be found in MEWS reports from Task 8 (*Beaulieu et al. 2002*).

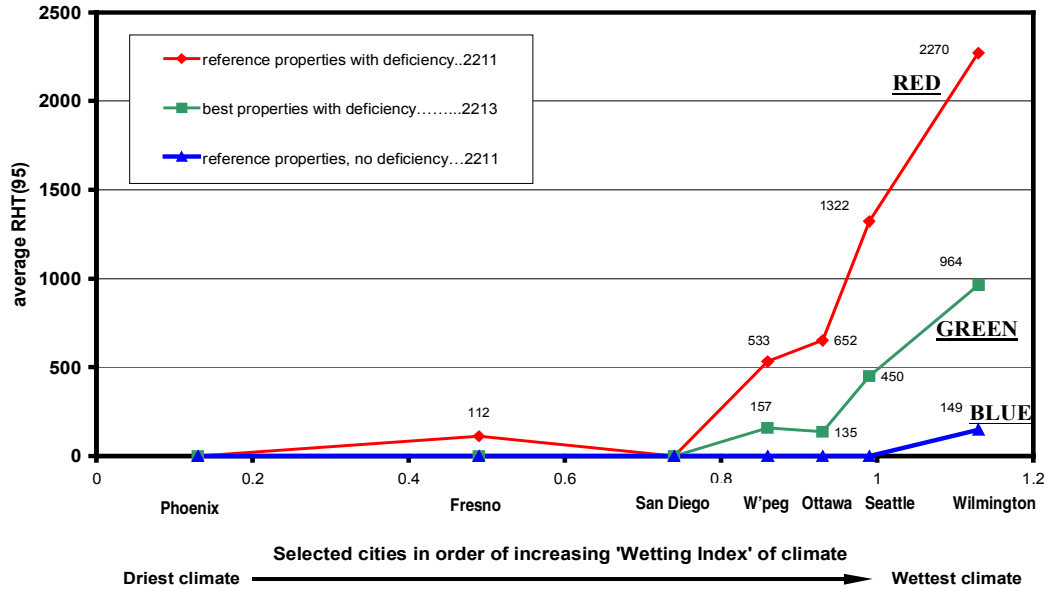


Figure A9: RHT(95) varies with MI

3.1.6. Yearly climate variation (Wet-Wet-Average (WWA) and Wet-Wet-Dry (WWD))

Two cases (one each in Ottawa and Wilmington) were done where the *Average* year (3rd year) was replaced by a *Dry* year. The selection process of *Dry*, *Average* and *Wet* year can be found in MEWS Task 4 report. It is found from RHT(95) values shown in Table A6 that yearly climate variation due to *Average* or *Dry* year has very little significance in Ottawa and Wilmington

3.1.7. Accidental moisture entry inside the wall

Walls are not designed to have accidental water entry. However, in real life, it does happen in some cases. As it can be seen in Figure A9 the bottom (blue) line shows the RHT(95) values when there is no accidental moisture entry (this wall is called as reference wall without deficiency), and uppermost (red) line indicates the performance of the same wall (i.e. reference wall with deficiency) when there is accidental moisture entry into the bottom of the stud cavity. Accidental moisture entry inside the wall can cause severe hygrothermal response in all locations.

3.1.8. Quantity of accidental moisture entry

The amount of moisture intruded inside the insulation cavity wall in this study was based on experimental observations in the laboratory (Task A6). It is imperative to note that the quantity of accidentally entered moisture can vary widely. In order to investigate the effect of such variation, simulations were done for five locations (Phoenix, Winnipeg, Ottawa, Seattle and Wilmington). Except for Phoenix, the quantities of moisture considered are full or Q (as from the equation A2), 1/2 and 1/4. In case of Phoenix,

because of its dry nature, the moisture quantities are doubled (2 times) and quadrupled (4 times).

The results from the simulations (Table A6) show that the effects of variation of the quantity of accidentally entered moisture on the change of RHT(95) index can be interpreted as linearly variable with the quantity of accidentally entered moisture (Figure A10).

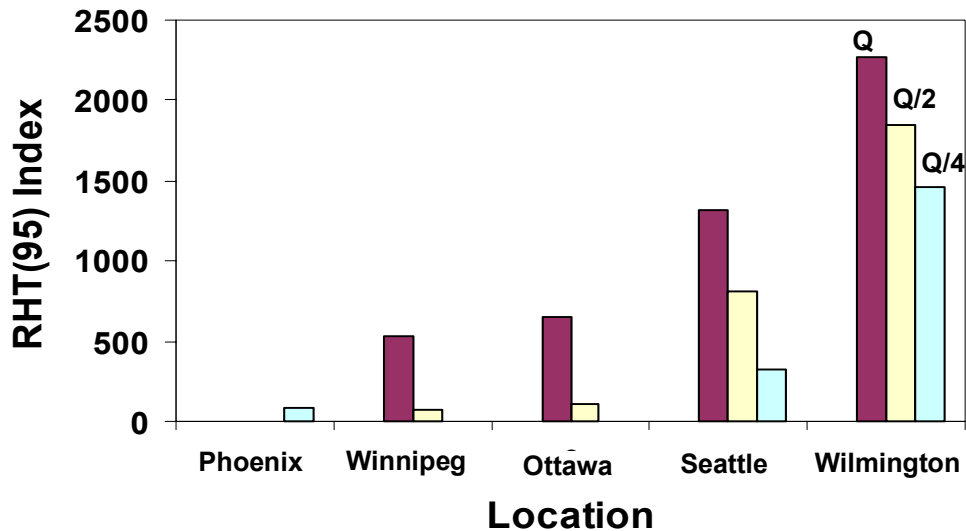


Figure A10: RHT(95) varies linearly with quantity of moisture entry

3.1.9. Presence of a ventilation cavity inside the wall (i.e. behind the exterior cladding)

It was expected that the introduction of an air ventilation cavity behind the stucco cladding would improve the drying characteristics of the wall assembly. Typically a 19-mm wide cavity (Figure A2) was considered in this investigation. In one case the cavity had only a bottom opening (entire 19-mm width) and in the other case it has both bottom (19-mm) and top (3-mm) opening. The simulations were done with the weather data of Ottawa, Seattle and Winnipeg. The general identification for simulations with cavity opening at the bottom (i.e. at the lower end of the cavity only) is **S2M2O3V1CL and for simulations with both end of the cavity the identifier is **S2M2O3V1CB.

The RHT(95) results in Table 6 show that introduction of cavity behind the stucco helps to reduce the RHT(95) index significantly for the amount of moisture entry given by equation A2. It is also evident that cavity opening at both ends (top and bottom) has reduced the RHT(95) index more significantly than the case when only bottom end of the cavity is ventilated. In general, it can be said that a stucco-wall with a ventilated cavity behind the cladding has better moisture management potential.

3.1.10. Interior RH

The variation of RH inside the room can be controlled. In this study, so far, the winter RH inside the room was taken as 25% and for summer 55% (see Figure A7). To further investigate on the effects of interior RH on the moisture response of the wall the following simulations were carried out at Wilmington only.

Simulation ID

WISM2O1V3
 WIS2M2O1V32575
 WIS2M2O1V35075
 WIS2M2O1V32565
 WIS2M2O1V34075
 WIS2M2O1V34065

Interior RH

Winter: 25%, Summer: 55%
 Winter: 25%, Summer: 75%
 Winter: 50%, Summer: 75%
 Winter: 25%, Summer: 65%
 Winter: 40%, Summer: 75%
 Winter: 40%, Summer: 65%

The results from these simulations in Table 6 show that there is a slight increase in RHT(95) index with the higher room RH but that variation is not very significant at Wilmington.

3.1.11. Air leakage

The air leakage path chosen in this study is depicted schematically in Figure A11. It should be pointed out that the air-leakage path shown has the maximum path length possible inside the wall. The simulations were done for Ottawa and Seattle and the general simulation identification for air leakage is **S2M2O1V1AL. The amount of accidental moisture entry was determined by equation A2 (i.e. 1Q).

From the drying curves (Figures AP29 and 58 in Appendix A1), it is clear that the introduction of air-leakage helped to dry out the wall during the drying period but it also contributed to higher wetting during the wetting spell of the weather. However, the drying of the entire wall and its individual components at the end of 3rd year improved due to the introduction of air-leakage across the wall.

The RHT(95) results in Table A6 show that there is a trend to reduce the RHT values when air leakage is introduced into the wall model. However, further investigation of the positive and negative effects of various rates of air leakage on the moisture deposition and moisture removal capacity of airflow through a wall assembly exposed to a range of climate loads is required prior to making general statement.

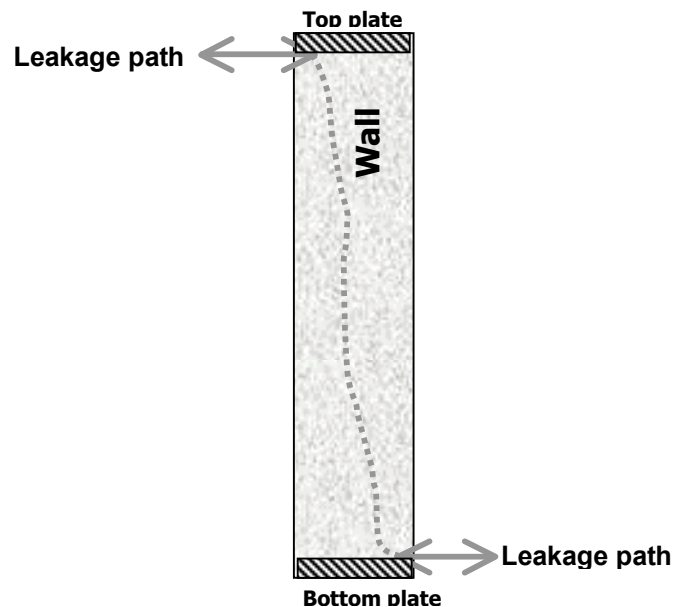


Figure A11: Schematic air flow or leakage path

3.1.12. Elimination of the 1mm air gap between the sheathing board and sheathing membrane

It has been assumed in all the simulations done in this study that there exists a small air gap (1mm) between the sheathing membrane and sheathing board. One simulation is done at Ottawa (OTS2M2O1V1NAG) that has no air gap between the sheathing membrane and sheathing board. The result presented in Table A6 clearly indicates that the presence of air gap between the sheathing membrane and sheathing board has a negligible effect on the RHT(95) index.

3.1.13. Optimisation of stucco properties

The exterior cladding is the first line of defence against rain penetration and hence, its hygrothermal properties can influence the moisture management of the wall in a very significant way. Simulations were done on a wall with no accidentally entered moisture and using a 'hypothetical' stucco that was exposed to the climate loading at Wilmington (simulation ID:WIS2M2O1V1BC_VD). This 'hypothetical' stucco was designed to exhibit a reduced potential for wetting but likewise allow an enhanced drying potential compared to the 'normal' stucco characterized in this study. It has a vapour permeability 6 to 8 times higher and liquid diffusivity 10 times lower than the normal stucco that ranked 'best' in the previous simulations. Results in Table A6 indicate a drop of RHT (95) from about 149 to near zero. The development of such 'hypothetical' stuccos is a job for which researchers at IRC will be working in near future.

3.1.14. Best & Worst combination of materials

It would not be practical to run simulations for all the possible combinations of material components of the wall. In this study three additional combinations of materials were chosen to investigate the effects of the best and the worst combination of materials on the overall drying pattern of the wall. These three material combinations were:

- (i) The best material combination derived from parametric studies conducted based on the change in moisture content (Simulation IDs: OTS3M1O1V3BP, WIS3M1O1V3BP).
- (ii) The best material combination chosen from the parametric studies conducted based on the RHT index (Simulation IDs: OTS1M1O3V3BR, WIS3M1O3V3BR).
- (iii) The worst material combination chosen from the parametric studies conducted based on the RHT index (Simulation IDs: OTS2M3O1V1WR, WIS2M3O1V1WR).

It can be easily seen from Table A6 that the best and the worst material combinations produce the best and the worst drying rate. The trend in Ottawa is very much similar to that in Wilmington. The middle (green) line in Figure A9 shows that use of a certain combination of materials can bring down the RHT(95) values.

3.1.15. Removal of the vapour barrier

Simulations were done at Ottawa at Wilmington with no vapour barrier in the wall. Simulation IDs with 'NV' or 'V0' in it indicate that there is no vapour barrier. It should be mentioned here that the effect of this vapour barrier removal on the interior boundary condition (room RH) was not taken into account in this study. The effects of removing

vapour barrier from the wall assembly can be seen Table A6 in terms of RHT(95) index. The results clearly indicate that in both locations (Ottawa & Wilmington) the absence of vapour barrier results in better drying (i.e. lower RHT index) of the whole wall and its individual major components (see respective drying curves in Appendix A1). However, further investigation of the positive and negative effects of the indoor climate and the water vapour permeance of the interior layers of the walls on the drying ability of a wet stud cavity is necessary prior to making general statements.

3.1.16. Use of coated gypsum board with no vapour barrier

One simulation was done where gypsum board coated with a primer and latex paint was considered as the vapour control element. The hygrothermal properties of such coated gypsum board are given in section 2.2. The permeance of this coated gypsum board is about 8 times higher than that of the vapour barrier no. III (at 100%RH). The simulation was done for Wilmington and the simulation ID is WIS2M2O1V0CG. The resulting RHT value obtained for that situation is 10. This was not much higher than the value obtained for an unpainted gypsum board with no vapour barrier (simulation ID is WIS2M2O1V0).

3.1.17. Alternate Wet and Average years

In this study two different *Wet* and *Average* years were compared in terms of moisture response of the wall. The alternate wet and average years were selected according to MI and they represent the second ranking years for wet and average classifications. Simulation was done for Ottawa (Simulation ID OTS2M2O1V1LT).

Results in Table 6 indicate that there is a considerable increase in RHT(95) values for alternate *Wet* and *Average* years. However, results in Appendix A2 would show that that this change is not that significant for RHT(80) or RHT(90).

4.0 Concluding Remarks

The results presented discussed the effect of various environmental and material parameters on the overall moisture response of the wall and its components by primarily examining the local hygrothermal conditions in the wall assembly. A novel concept called RHT index was successfully developed and used for this purpose. This report has got only the limited scope to discuss the utility and effectiveness of RHT index concept for assessing relative hygrothermal performance of the building envelope and its components. Further discussion and interpretation of the results can be found in MEWS Task 8 reports (*Beaulieu et al. 2002*).

Further investigation of the positive and negative effects of some parameters such as the removal of the vapour barrier membrane and the air leakage through the assembly is required prior to making general statements.

References

1. ASHRAE Applications Handbook, 1999, Chapter 3 - Commercial and Public Buildings.
2. Beaulieu, P.; Cornick, S.M.; Dalglish, W.A.; Djebbar, R.; Kumaran, M.K.; Lacasse, M.A.; Lackey, J.; Maref, W.; Mukhopadhyaya, P.; Nofal, M.; Normandin, N.; Nicholis, M.; O'Connor, T.; Quirt, J.D.; Rousseau, M.Z.; Said, M.N.; Swinton, M.C.; Tariku, F.; van Reenen, D. 2002 "MEWS Task 8 Report", Institute for Research in Construction, National Research Council, Ottawa, Canada.

3. Cornick, S. M., Dalgliesh, W. A., Said, N. M., Djebbar, R., Tariku, F. and Kumaran, M. K. 2002, "Task 4- Environmental Conditions", Institute for Research in Construction, National Research Council, Ottawa, Canada, (NRCC-45222), pp. 1-106.
4. Djebbar, R., Kumaran, M.K., Van Reenen, D. and Tariku, F. 2002a. "Hygrothermal Modelling of Building Envelope Retrofit Measures in Multi-Unit Residential and Commercial Office Buildings", Client Final Report B-1110.3, pp. 187, IRC/NRC.
5. Djebbar, R.; Kumaran, M.K.; Van Reenen, D.; Tariku, F. 2002b. "Use of hygrothermal numerical modelling to identify optimal retrofit options for high-rise buildings," in press: 12th International Heat Transfer Conference (Grenoble, France, Aug, 2002), pp. 1-6, (NRCC-45215)
6. Karagiozis, A. 1993. "Overview of the 2-D Hygrothermal Heat-Moisture Transport Model LATENITE", Internal IRC/BPL Report.
7. Karagiozis, A. 1997 "Analysis of the Hygrothermal Behavior of Residential High-Rise Building Components", Client Report A-3052.4, IRC/NRC.
8. Karagiozis, A., Salonvaara, M. and Kumaran, M. K. 1996 "Numerical Simulation of Experimental Freeze Conditions in Glass Fibre Insulation", Building Physics in The Nordic Countries, Finland, August.
9. Kumaran, K., Lackey, J., Normandin, N., van Reenen, D., and Tariku, F. 2002. "Summary Report from Task 3 of MEWS Project at the Institute for Research in Construction", Institute for Research in Construction, National Research Council, Ottawa, Canada, (NRCC-45369), pp. 1-68.
10. Lacasse, M. A., Beaulieu, P., O'Connor, T. and Nicholls, M., 2002. "MEWS Task 6 Final Report - Experimental Assessment of Water Entry into Wood-frame Wall Assemblies", Institute for Research in Construction, National Research Council, Ottawa, Canada.
11. Swinton, M.C.; Sander, D.M., 1994. "Trade-off Compliance for Houses: Specifications for Calculation Procedures for Demonstrating Compliance to the National Energy Code for Houses using Trade-offs, pp. 46, March 01,(NRCC-39861).

Chapter - B

Parametric Studies - EIFS Walls

Chapter - B

Parametric Studies - EIFS Walls

1.0 Parameters under Consideration

The followings the parameters were considered for EIFS-wall systems.

1. Base and finish coat thickness of the EIFS cladding
2. Sheathing Membrane
3. Sheathing Board
4. Vapour Barrier
5. Insulation
6. Moisture Entry Location
7. Quantity of Moisture Entry
8. Yearly climate variation (Wet-Wet-Average (WWA) and Wet-Wet-Dry (WWD))
9. Interior RH
10. Use of coated gypsum board with no vapour barrier
11. Locations with seven different Moisture Indices (MI)
12. Air leakage

These parameters were chosen by the MEWS research team to investigate various moisture management issues related to stucco-walls. These choices also encompass the suggestions and comments obtained from the representatives of the MEWS partners.

2.0 *hygIRC* and Input for Simulation

The details of *hygIRC* and the input required are as those discussed Chapter A, dealing with stucco walls. EIFS walls use different construction details and materials. The following sections describe the additional information that was used for EIFS walls.

2.1 Basic Wall Construction Details

The basic EIFS-wall construction details are shown in Figure B1. This wall uses oriented strand board (OSB) as a sheathing board. The wall shown in Figure B1 was the reference wall and was used for all parametric studies, except where specific parametric analyses were conducted to replace OSB sheathing with glass mat gypsum board sheathing. The EIFS-wall with glass mat gypsum board sheathing is shown in Figure B2.

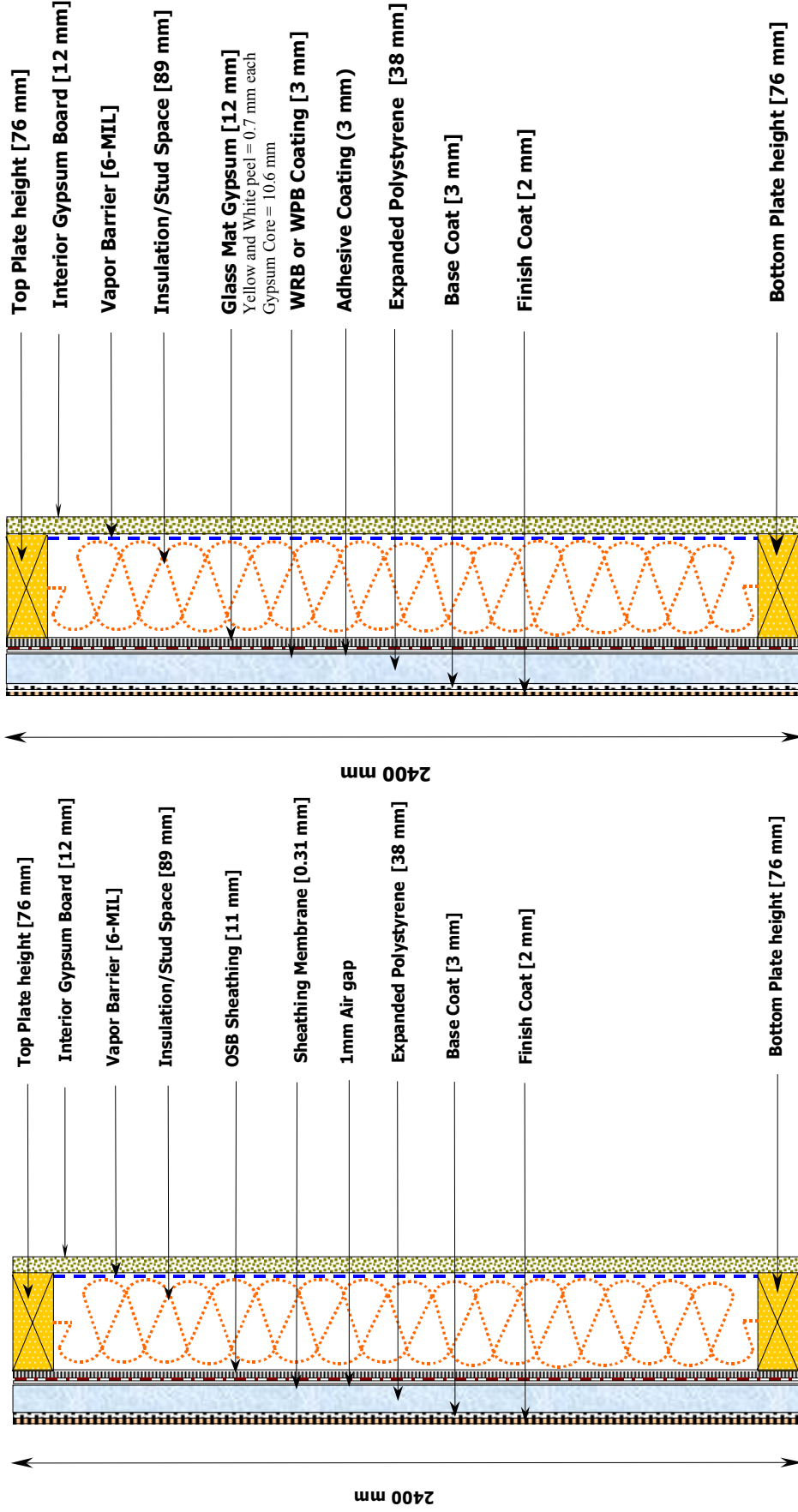


Figure B1: EIFS-wall with OSB sheathing

Figure B2: EIFS-wall with exterior grade gypsum board sheathing

2.2 Material Properties

Apart from the materials used for stucco-wall (Chapter A), the following additional wall components were used for EIFS-walls.

1. Base and finish coat
2. Expanded Polystyrene (EPS)
3. Glass mat gypsum board (exterior grade gypsum board)
4. Water penetration barrier

As mentioned in Chapter A, eight distinct sets of material properties were required for *hygIRC*. The material properties for the four additional EIFS wall components are described in the following sections. Detailed information about material properties and the determination of same are provided by *Kumaran et al. 2002* (Task 3 report).

2.2.1 Air permeability

The air permeability properties of the four materials, used for simulations, are shown in Table B1. The values shown in the Table B1 are the product of air permeability and dynamic viscosity of air.

Table B1: Air permeability of materials

Material	Air permeability (m^2)
Base and finish coat	1.00×10^{-16}
Expanded Polystyrene (EPS)	3.70×10^{-11}
Glass mat gypsum board (exterior grade gypsum board)	5.70×10^{-14} (core), 1.10×10^{-09} (glass matt)
Water penetration barrier	3.58×10^{-14}

2.2.2 Thermal conductivity

Measurements were made on dry materials alone. The thermal conductivity of materials changes in relation to the moisture content. Approximate combining rules were used to account for the effect of moisture on thermal conductivity. The thermal conductivity of dry materials is shown in Table B2.

Table B2: Thermal conductivity of materials (dry)

Material	Thermal Conductivity ($\text{W m}^{-1}\text{K}^{-1}$)
Base and finish coat	5.88×10^{-01}
Expanded Polystyrene (EPS)	3.43×10^{-02}
Glass mat gypsum board (exterior grade gypsum board)	1.74×10^{-01} (core), 4.33×10^{-02} (mat)
Water penetration barrier	1.086×10^{-01}

2.2.3 Dry density

The measured dry density of all the materials are provided in the Table B3.

Table B3: Dry density of materials

Material	Dry density (kgm^{-3})
Base and finish coat	1.15×10^{03}
Expanded Polystyrene (EPS)	1.97×10^{01}
Glass mat gypsum board (exterior grade gypsum board)	7.07×10^{02} (core), 1.10×10^{01} (mat)
Water penetration barrier	8.09×10^{02}

2.2.4 Heat capacity

The heat capacity of all the materials are given in the Table B4.

Table B4: Heat capacity of materials

Material	Heat Capacity ($\text{J K}^{-1} \text{kg}^{-1}$)
Base and finish coat	8.40×10^{02}
Expanded Polystyrene (EPS)	1.47×10^{03}
Glass mat gypsum board (exterior grade gypsum board)	8.70×10^{02} (core), 1.26×10^{03}
Water penetration barrier	1.88×10^{03}

2.2.5 Sorption isotherm

The relationship between relative humidity and moisture content of all the four materials are shown in Figures B3a to B3d.

2.2.6 Suction curve

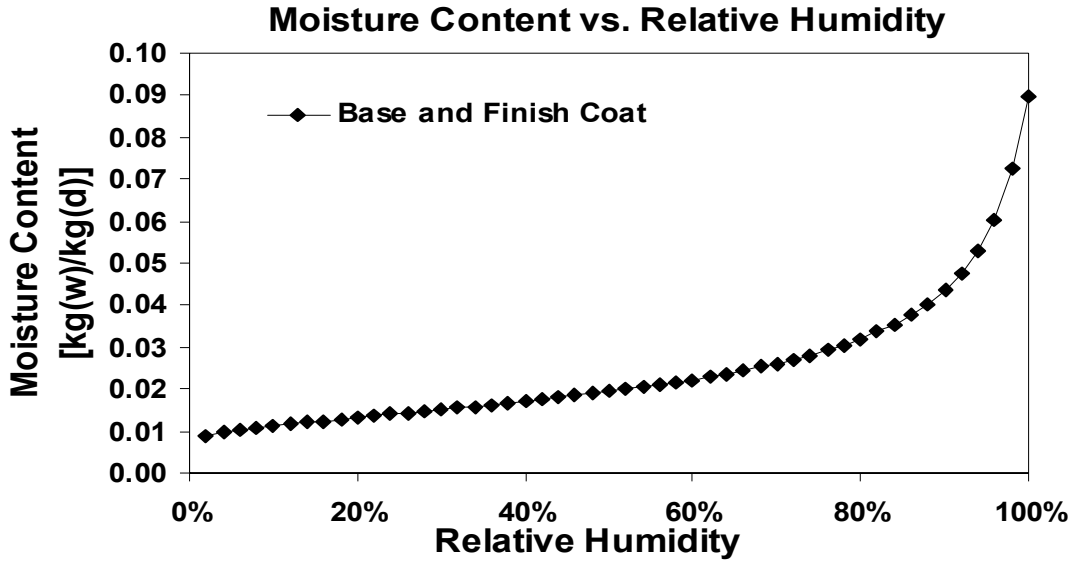
The plots of moisture content as a function of suction pressure are shown in Figures B4a to B4d.

2.2.7 Water vapour permeability

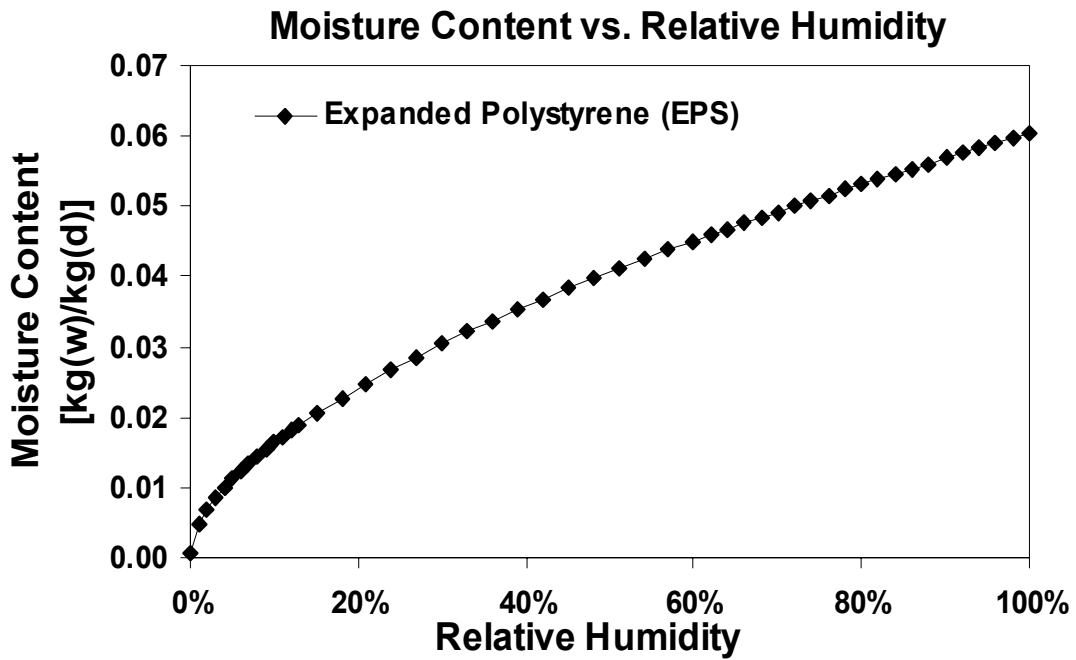
Water vapour permeability of the building material is one of the most critical properties influencing the overall drying characteristics of the wall. The variations of water vapour permeability in relation to relative humidity for all the four materials are shown in Figures B5a to B5d.

2.2.8 Liquid diffusivity

The plots of liquid diffusivity vs. moisture content, for all the four materials are shown in Figures B6a to B6d. The diffusion of liquid through the material takes place when moisture content of the material is close to the corresponding relative humidity of 100% (refer to the sorption isotherm plots).

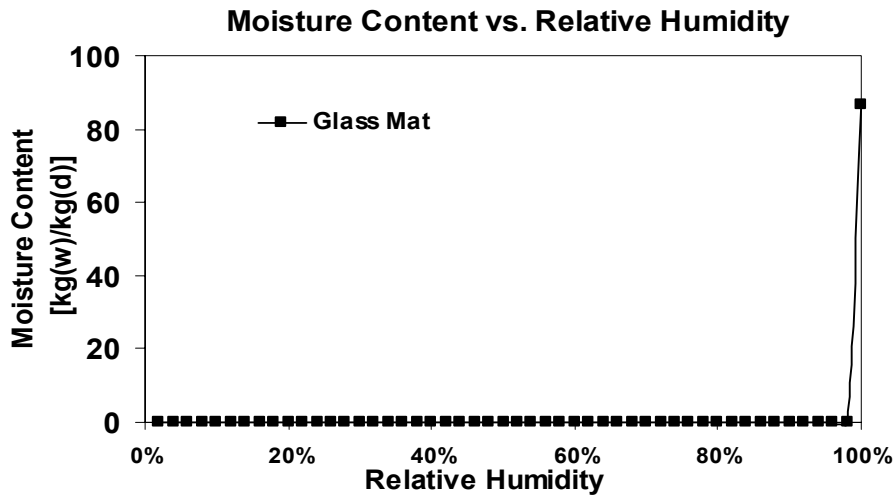
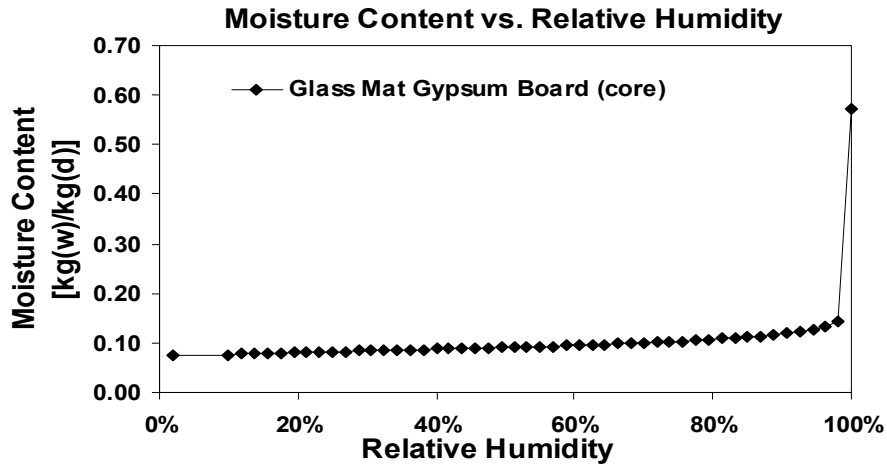


(a) Base and finish coat

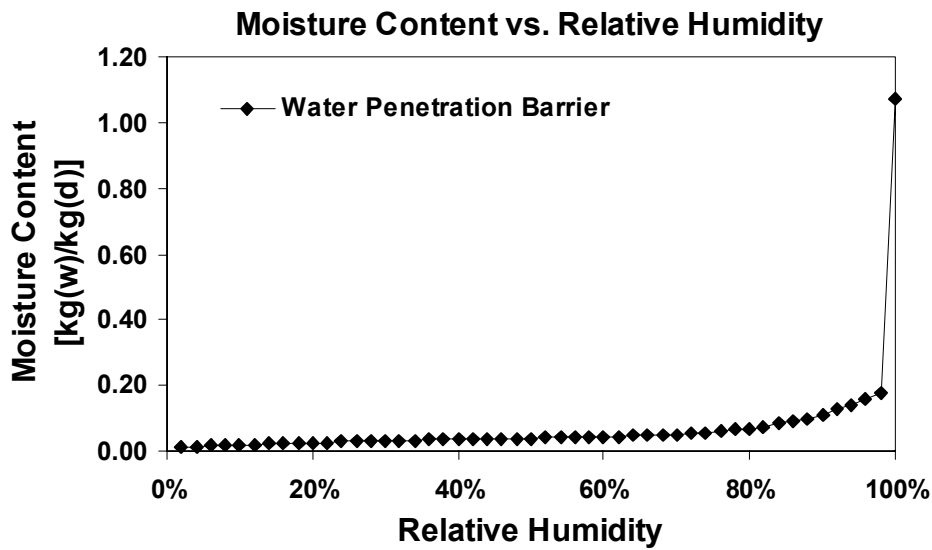


(b) Expanded polystyrene

Figure B3: Sorption Isotherm

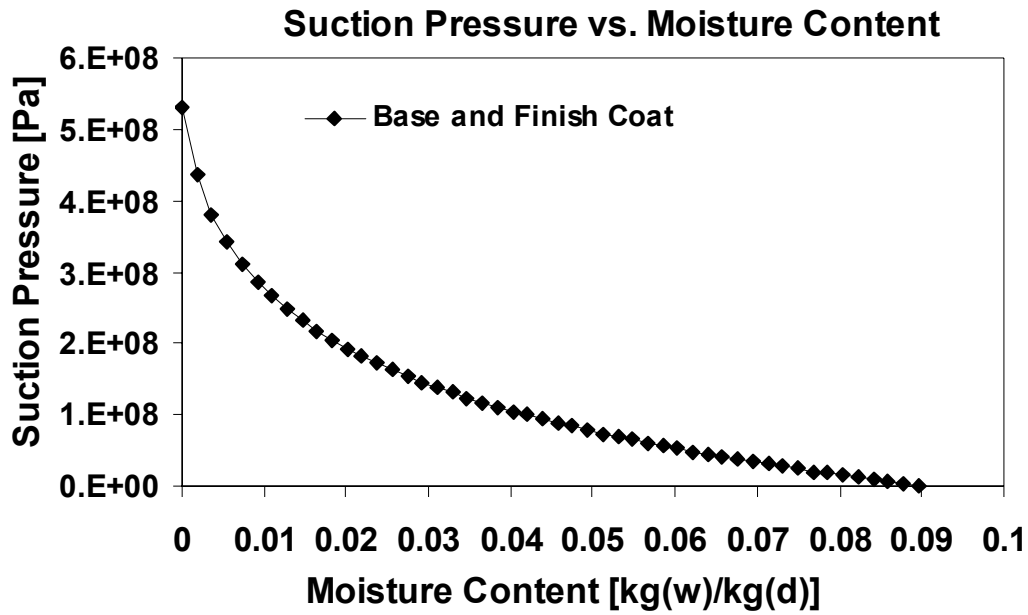


(c) Glass mat gypsum board

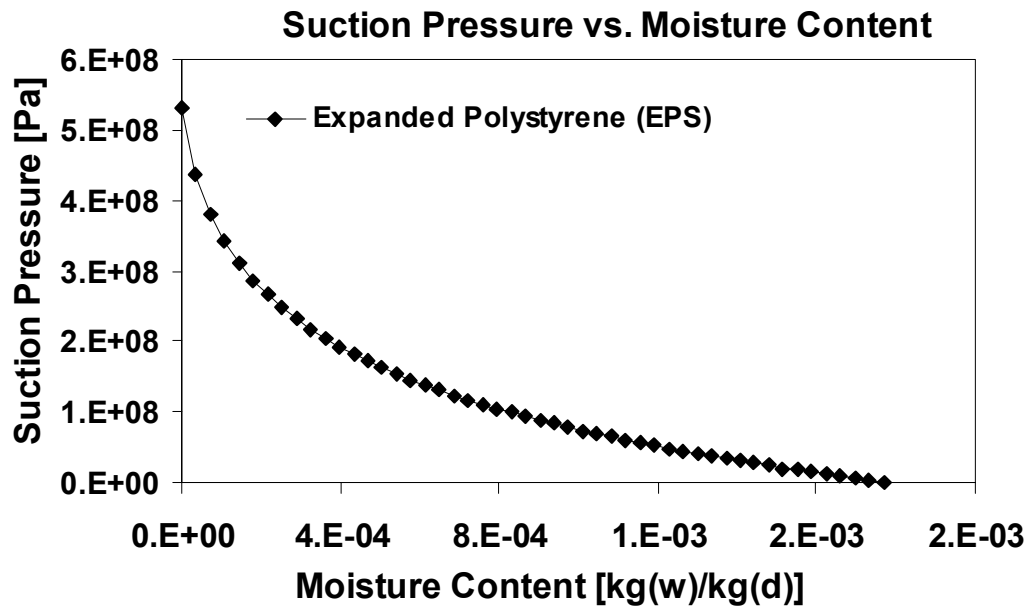


(d) Water penetration barrier

Figure B3: Sorption Isotherm

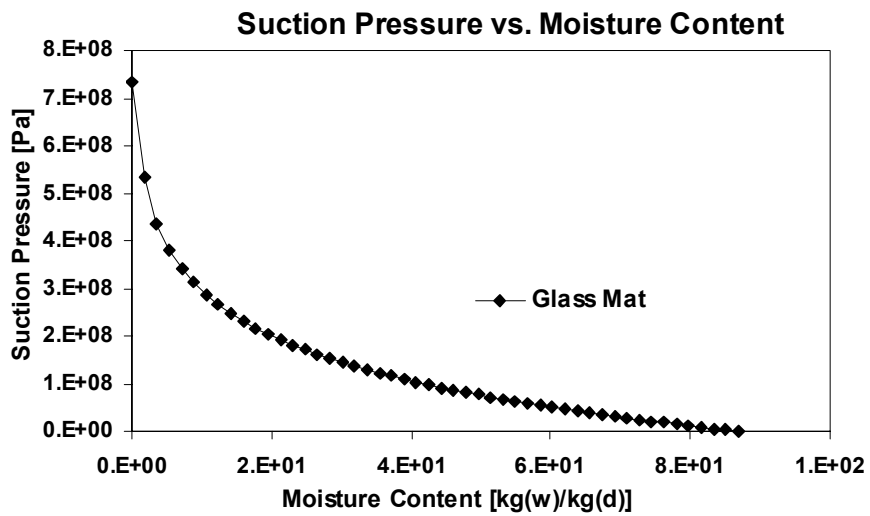
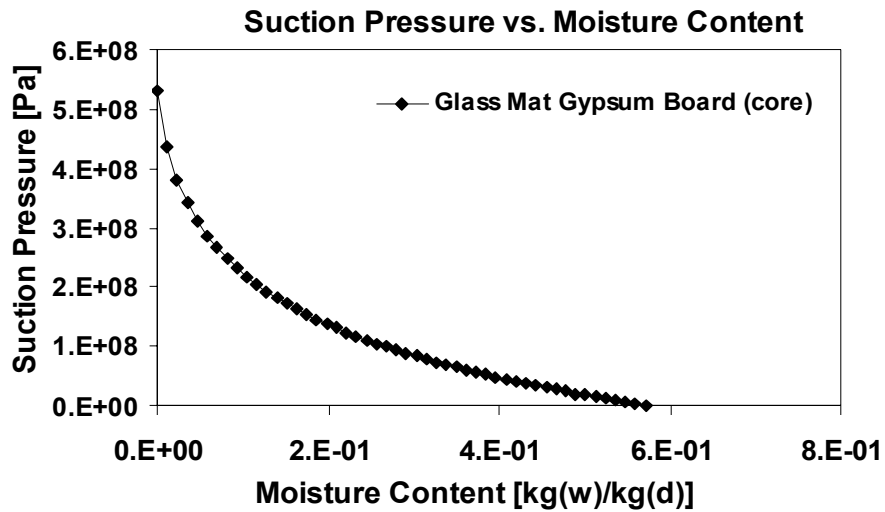


(a) Base and finish coat

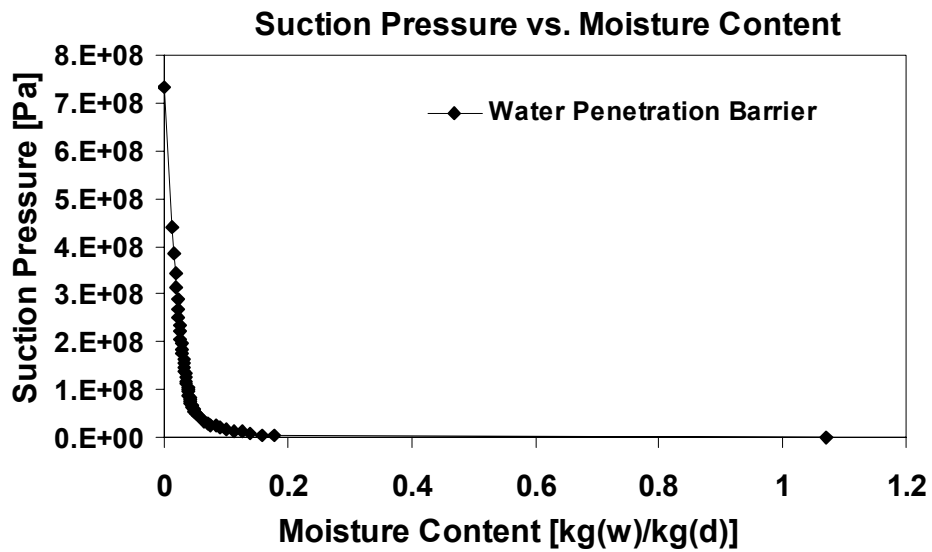


(b) Expanded polystyrene (EPS)

Figure B4: Suction Curve

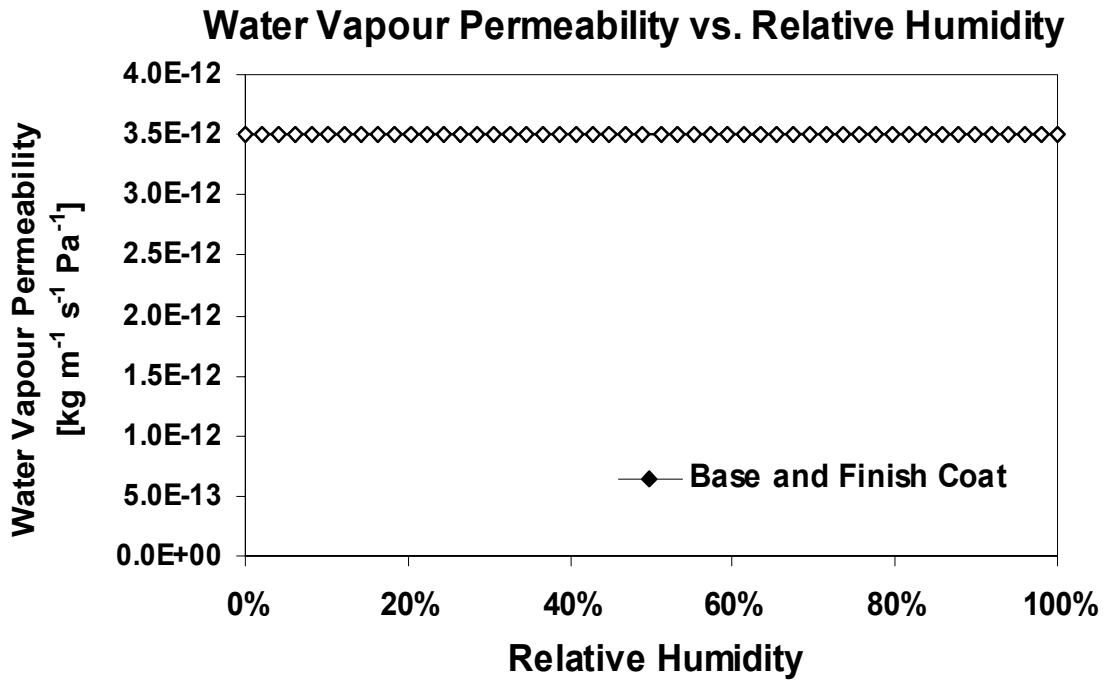


(c) Glass mat gypsum board

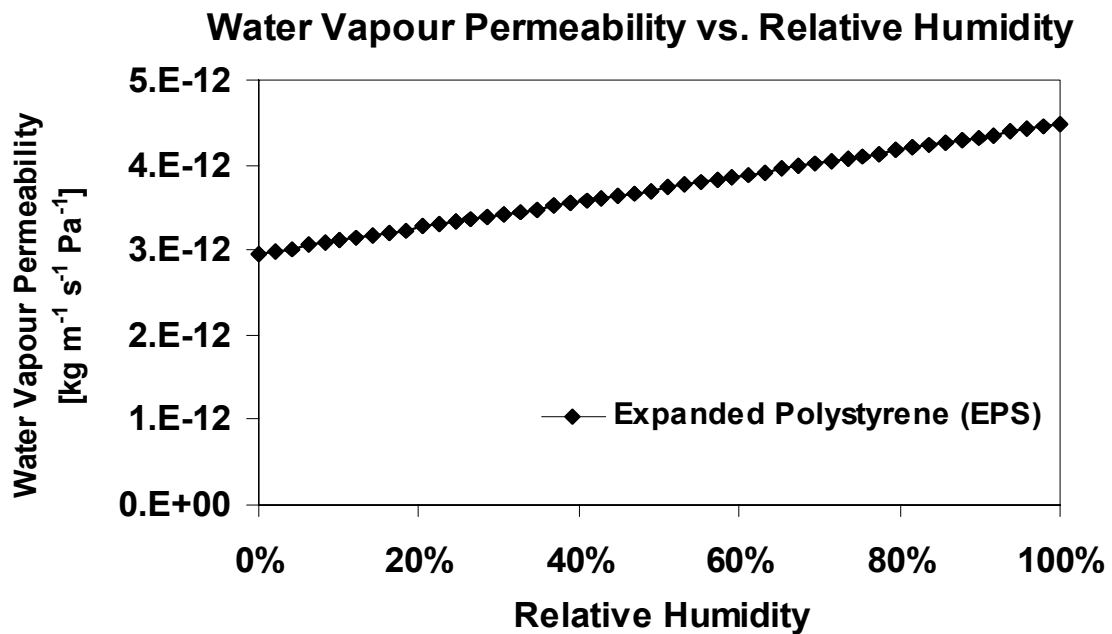


(d) Water penetration barrier

Figure B4: Suction Curve

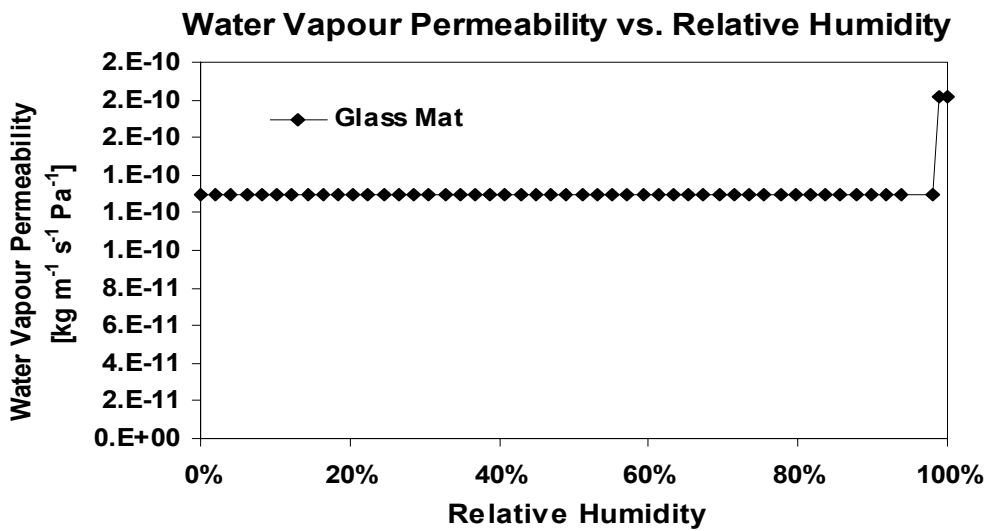
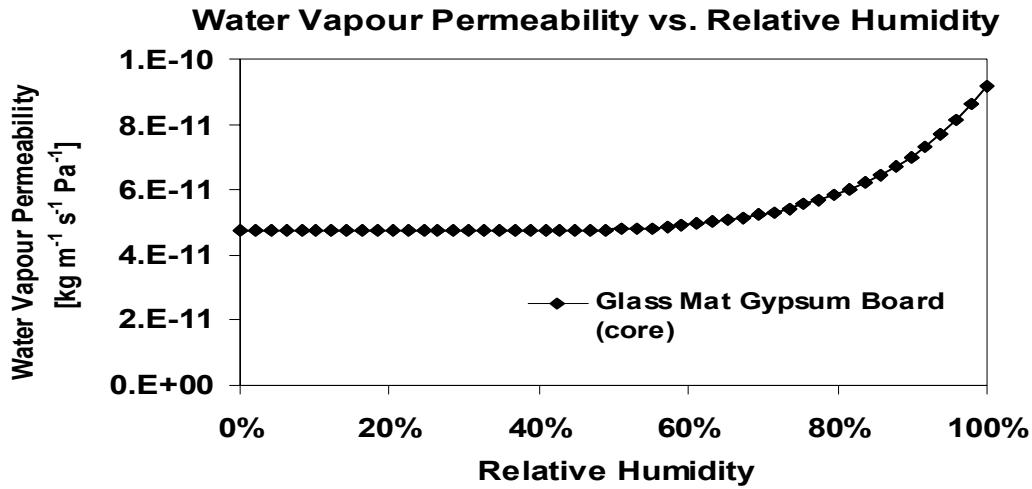


(a) Base and finish coat

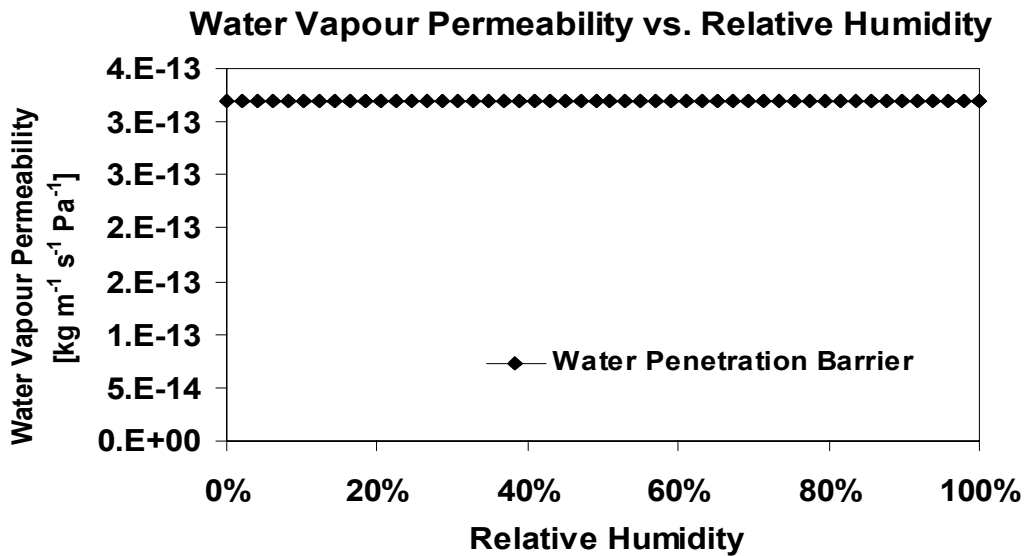


(b) Expanded polystyrene

Figure B5: Water Vapour Permeability

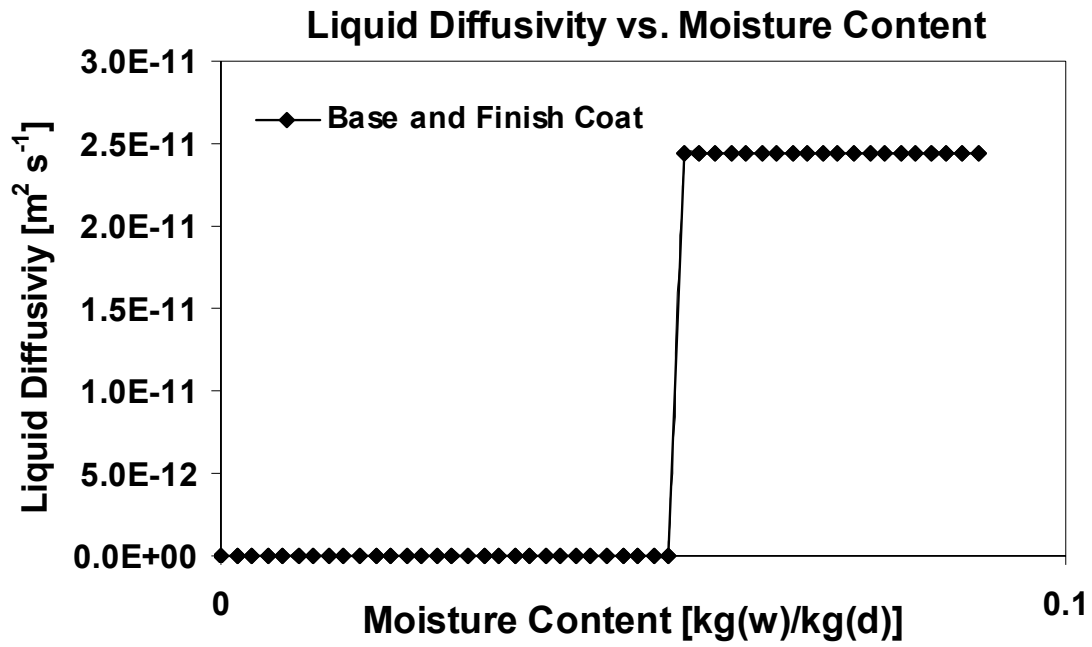


(c) Glass mat gypsum board

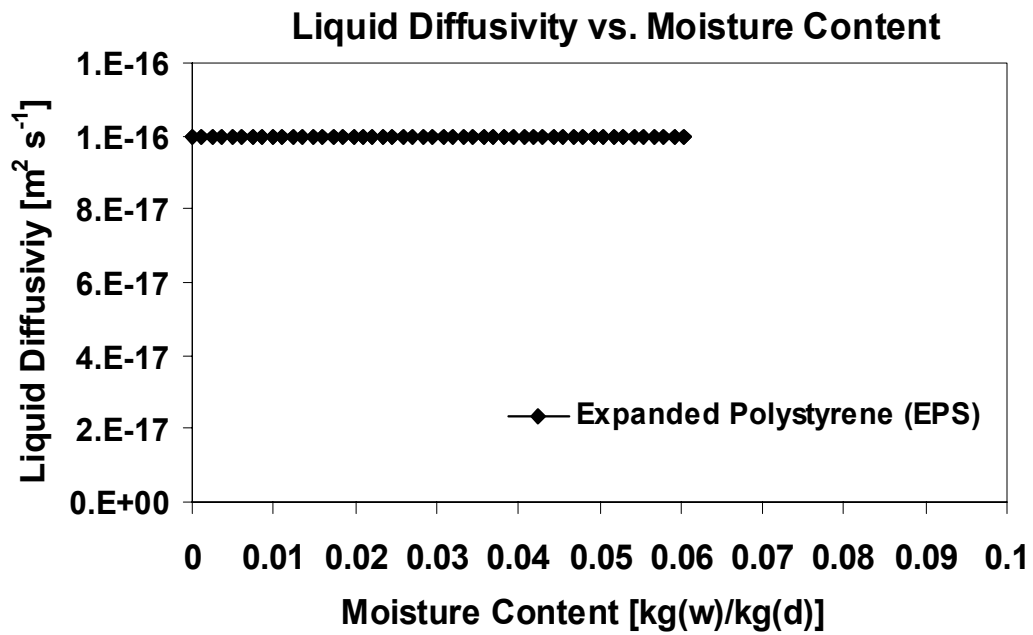


(d) Water penetration barrier

Figure B5: Water Vapour Permeability

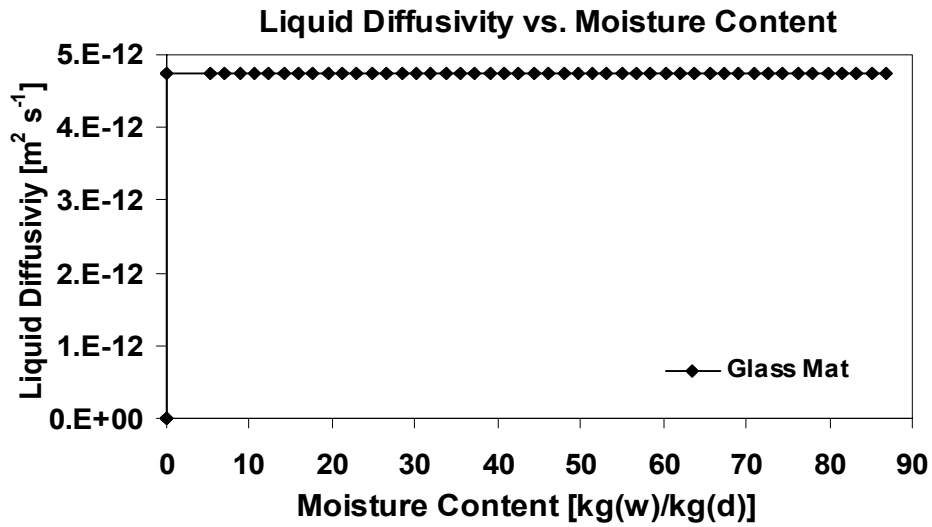
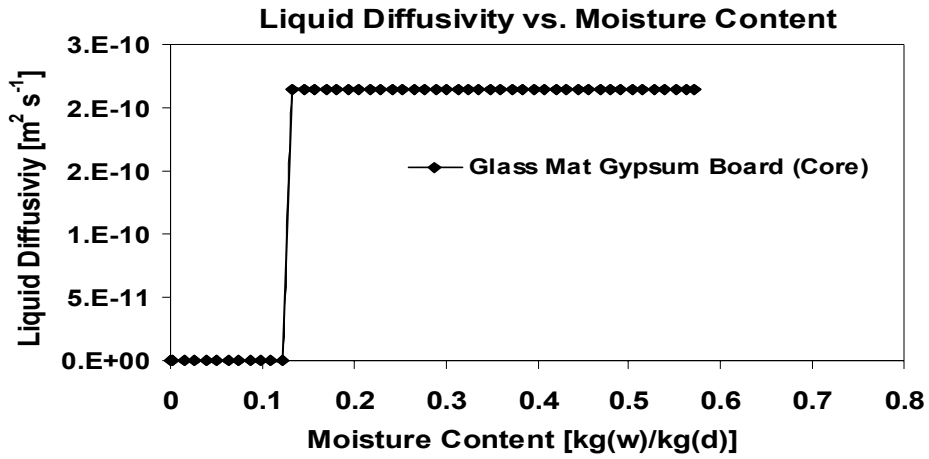


(a) Base and finish coat

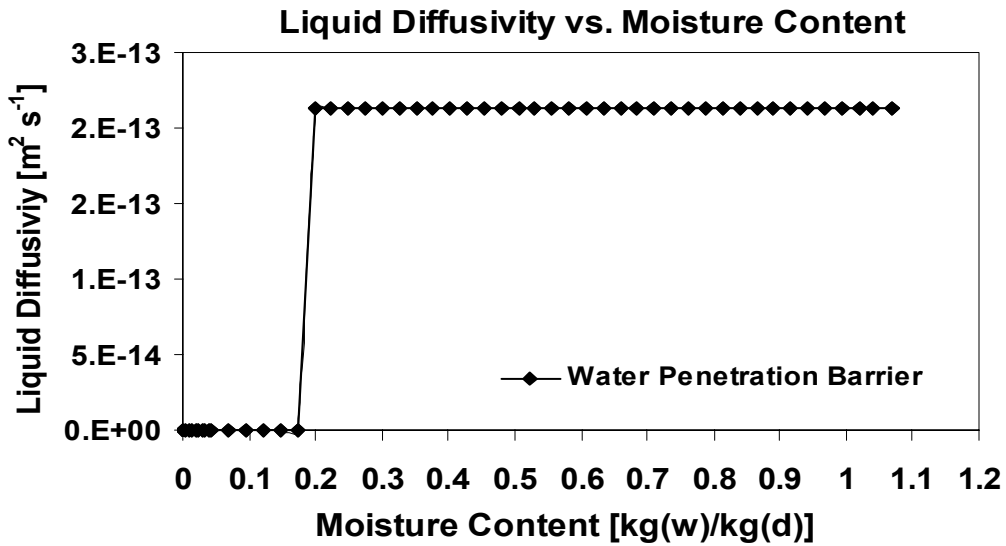


(b) Expanded polystyrene

Figure B6: Liquid Diffusivity



(c) Glass mat gypsum board



(d) Water penetration barrier

Figure B6: Liquid Diffusivity

2.3 Boundary Conditions

The indoor and outdoor boundary conditions for EIFS-walls are same as those for stucco-clad-walls and are described in Chapter A.

2.4 Exposure Duration

The exposure duration for EIFS-wall is exactly the same as the exposure duration for stucco-walls. Readers should refer Chapter A for details.

2.5 Initial Moisture Content and Temperature

Initial conditions (RH and T) for EIFS-walls defined in this study were based on the same principles as those for stucco-walls. The principles are described in Chapter A.

2.6 Accidental Moisture Entry - Quantity and Location

hygIRC has the capability to inject accidentally entered moisture at any location of the wall and at any time (hourly interval). The quantity of accidentally entered moisture inside the wall and its location were determined from the output of full-scale and small-scale laboratory tests done in MEWS Task 6 (*Lacasse et al. 2002*). Each wall has a unique moisture entry function. The function used to determine the quantity of accidental moisture entry inside the EIFS-walls is described below.

Quantity

An equation was derived from the full-scale lab results to estimate the moisture entry rate (Q). This equation depends on the pressure difference across the wall assembly (ΔP) as well as the rate of water dR_p striking the wall, and is given below:

$$dQ/dR_p = 0.0418 + 0.0243 \cdot \Delta P / (110.3359 + \Delta P) \quad [\text{Eqn. B1}]$$

ΔP is a function of wind pressure and dR_p is representative of wind driven rain.

All the parametric studies reported in this report were based on quantities of moisture entry determined using equation B1.

Location

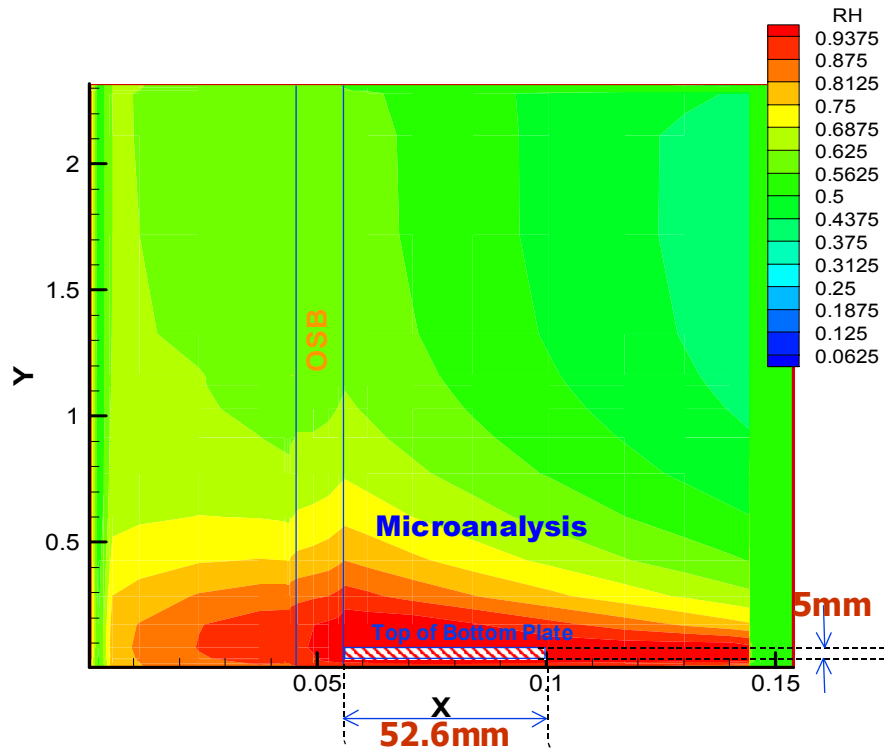
The location of moisture entry for EIFS-walls is same as it was for stucco-walls. The quantity of accidentally entered moisture, determined from equation B1, was injected at the bottom of the stud cavity, on the top of the bottom plate at hourly intervals when applicable.

3.0 Results from *hygIRC* Simulation

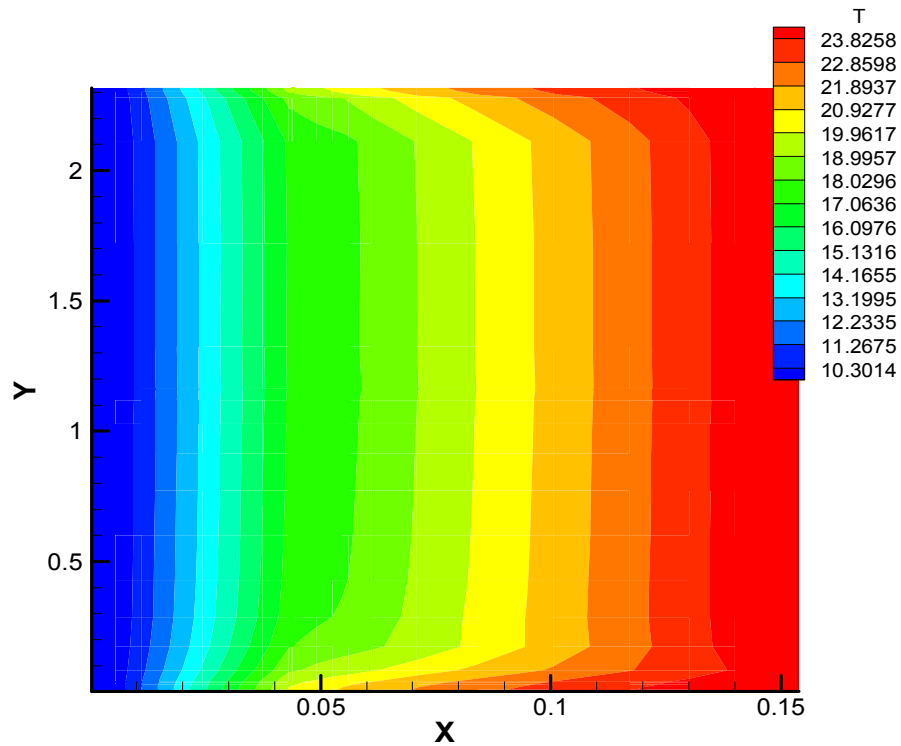
More than one hundred simulations were done in this study. An enormous amount of data was been generated using the *hygIRC* simulation tool and subsequently post-processed for overall and critical evaluation of the hygrothermal response of the wall. Only a selected amount of data is presented in this report. If required and requested for a stated purpose then any particular aspect of the remaining data could be made available exclusively to the MEWS partners.

The following are the important points about the simulations that the authors feel should be clearly and unambiguously disclosed to the readers before presenting the results and the related discussions:

1. The main objective of this study was to determine the drying characteristics of the wall assembly in case of accidentally entered moisture inside the stud/insulation cavity of the EIFS-wall.
2. The materials used in the simulations are described in section 2.2 of this Chapter and section 2.2 of Chapter A.
3. Each simulation done has a unique identification code and in order to make it clear to the readers. The identification codes are explained at the end of Table B6.
4. All the simulations done in this study have accidental moisture entry inside the stud/insulation cavity, save those with the letters BC appended to the end of the identifier. This case did not have any accidental moisture entry. Accidental moisture enters the stud cavity from the beginning of second year until the end of 3rd year.
5. It is to be noted that all simulations done in this study have the first year (a wet year) without any accidental moisture entry. This has been done to generate a realistic moisture distribution inside the wall at the end of first year and prior to accidental moisture entry in the subsequent two years.
6. The wall with accidental moisture entry represents the real wall with a deficiency. The wall without accidental moisture entry can be considered as an ideal wall.
7. A total of three years simulation was done for each of the cases considered in this study. However, all the simulation results were analysed based on the results of second and third year. Hence, all the discussions presented in this chapter are based on the second and third year simulation results and all the graphs represent the data for that period only.
8. Drying curves obtained from the simulations, after first year, are shown in Appendix B1. The moisture content in these graphs is expressed with the unit of mass of moisture per unit length (kg/m) of wall or its components entire cross section. These drying curves provide the overall dry characteristics of the whole wall and its major components.
9. A detailed small scale study (microanalysis) of the hygrothermal response of the wall assembly was done by analysing the relative humidity (RH) and temperature (T) contour plots (Figure B7)



(a) Typical relative humidity contour plot (width of the wall expanded)



(b) Typical temperature contour plot (width of the wall expanded)

Figure B7: (a) RH and (b) T profiles inside the EIFS wall

10. A novel concept called the RHT Index has been introduced by the researchers at IRC/NRC and was used in the parametric study to quantify and compare the localized hygrothermal response of any part of the wall and its component. The RHT index is derived from the RH and T distribution pattern (Figure B7) over a period of time for any specific area of the wall cross-section. The RHT index as defined in this study is:

$$\text{Cumulative 2 year (2}^{nd} \text{ and 3}^{rd} \text{ year) RHT} = \sum (RH - RH_X) \times (T - T_X),$$

[Eqn. B2]

for $RH > RH_X\%$ and $T > T_X^\circ\text{C}$ at every 10 days interval

(During any time step when either or both $RH \leq RH_X\%$ and $T \leq T_X^\circ\text{C}$, the RHT value for that time step is zero.)

Where user-defined threshold values for $RH_X = 95\%$ and $T_X = 5^\circ\text{C}$ have been chosen for this parametric study. RHT values for $RH_X=80\%$ have also been derived and presented in this report. For convenience the RHT values will be referred to as RHT(95) or RHT(80) index according to the threshold RH (i.e. RH_X) level.

11. 'Region of focus' is the area for which the RHT index is calculated. This area is the wettest portion of the wall assembly most of the time (see Figure B7a). For EIFS-wall simulations, presented in this report for parametric study, the 'region of focus' is a thin slice (5 mm) of the top surface of the bottom plate, extending 53 mm from the sheathing board (see Figure B7a).
12. The RHT index brings out the overall localized combined moisture and temperature response of the selected area of the material or wall assembly. For overall drying and wetting pattern of the EIFS-wall assembly, at any point of time, interested readers should look at the drying curves given in Appendix B1.

3.1 Results from Parametric Studies

Results from the parametric studies are to be discussed here primarily with the RHT(95) values from Table B5. However, in qualitative sense, the observations would be same if RHT(80) is to be used instead of RHT(95).

3.1.1 Base and finish coat thickness of EIFS cladding

Three different base and finish coat thickness combinations were chosen in this study. These combinations were:

- (1) BF0 : Base Coat - 3.0mm; Finish Coat - 2.0mm (*Simulation ID - **O11EF*)
- (2) BF1 : Base Coat - 2.5mm; Finish Coat - 1.5mm (*Simulation ID - **CO1EF*)
- (3) BF2 : Base Coat - 1.5mm; Finish Coat - 1.0mm (*Simulation ID - **CO2EF*)

As can be seen in Table B5, the effect of base and finish coat thickness on the overall moisture response of the EIFS-wall assembly, in terms of RHT(95) index, was small to negligible. For all other simulations, base and finish coat thickness are assumed to be 3.0mm and 2.0mm respectively (i.e. BF0).

Table B5: RHT (95) indices for EIFS wall
 (Top of the bottom plate - Region of focus; Equation B1)

Simulation ID	RHT (95)	Simulation ID	RHT (95)	Simulation ID	RHT (95)	Simulation ID	RHT (95)
(A) OTTAWA					3861	FRCO2EF	1403
OTO11EFBC	0	(C) SEATTLE		WIVB10EF4065RH		FRO11EFW2	451
OTO11EF	2529	SEO11EFBC	0	WIVB10EF4075RH	3887	FRO11EFW4	58
OTP20EF	2479	SEO11EF	3345	WIVB10EF5075RH	3893	FRNOIEFMI	2010
OTG22EFBC	0	SEP20EF	3304				
OTG22EF	2272	SESM5EF	3345			(G) SAN DIEGO	
OTSM5EF	2529	SESM7EF	3370			SDO11EFBC	0
OTSM7EF	2545	SEVB9EF	3281			SDO11EF	3343
OTVB9EF	2474	SEVB10EF	3007			SDP20EF	3072
OTVB10EF	2354	SECO1EF	3341	(E) WINNIPEG		SDG22EF	3497
OTCO1EF	2526	SECO2EF	3336	WPO11EFBC	0	SDSM5EF	3364
OTCO2EF	2522	SEO11EFW2	2884	WPO11EF	2134	SDSM7EF	3692
OTO11EFW2	2176	SEO11EFW4	1242	WPP20EF	2059	SDVB9EF	2347
OTO11EFW4	278	SEO11EFAL	2984	WPG22EF	1982	SDVB10EF	1677
OTO11EFAL	2322	SENOIEFMI	5413	WPSM5EF	2134	SDCO1EF	3306
OTNOIEFMI	3907	SEO11EFWD	3336	WPSM7EF	2144	SDCO2EF	3238
OTNOIEFALW4	256	SEG22EF	3215	WPVB9EF	2092	SDO11EFW2	1140
OTO11EFWD	2547	SEO11EFALW4	906	WPVB10EF	2012	SDO11EFW4	195
OTO11EFLV1	2686	(D) WILMINGTON		WPCO1EF	2131	SDNOIEFMI	4948
		WIO11EFBC	0	WPCO2EF	2127		
(B) PHOENIX		WIO11EF	3990	WPO11EFW2	1841		
PHO11EFBC	0	WIP20EF	3923	WPO11EFW4	768		
PHO11EF	1196	WISM5EF	3991	WPNOIEFMI	3288		
PHP20EF	976	WISM7EF	4014	WPO11EFWD	2105		
PHG22EF	902	WIVB9EF	3926				
PHSM5EF	1227	WIVB10EF	3827	(F) FRESNO			
PHSM7EF	1378	WICO1EF	3987	FRO11EFBC	0		
PHVB9EF	733	WICO2EF	3984	FRO11EF	1435		
PHVB10EF	505	WIO11EFW2	3622	FRP20EF	1264		
PHCO1EF	1187	WIO11EFW4	2885	FRG22EF	1578		
PHCO2EF	1157	WIO11EFWD	3947	FRSM5EF	1448		
PHO11EFW2	3196	WINOIEFMI	5907	FRSM7EF	1595		
PHO11EFW4	4394	WIO11EFV0CG	1363	FRVB9EF	1094		
PHNOIEFMI	1426		3846	FRVB10EF	868		
		WIVB10EF2565RH		FRCO1EF	1423		
		WIVB10EF2575RH	3872				

Table B6: RHT (80) indices for EIFS wall
 (Top of the bottom plate - Region of focus; Equation B1)

Simulation ID	RHT (80)	Simulation ID	RHT (80)	Simulation ID	RHT (80)	Simulation ID	RHT (80)
(A) OTTAWA							
OTO11EFBC	0	(C) SEATTLE		WIVB10EF4065RH	22400	FRCO2EF	11921
OTO11EF	15300	SEO11EFBC	0	WIVB10EF4075RH	22453	FRO11EFW2	5452
OTP20EF	14969	SEO11EF	19511	WIVB10EF5075RH	22465	FRO11EFW4	1280
OTG22EFBC	0	SEP20EF	19346			FRNOIEFMI	14155
OTG22EF	14887	SESM5EF	19508			(G) SAN DIEGO	
OTSM5EF	15296	SESM7EF	19562			SDO11EFBC	0
OTSM7EF	15331	SEVB9EF	19359			SDO11EF	22567
OTVB9EF	15120	SEVB10EF	18796			SDP20EF	22100
OTVB10EF	14763	SECO1EF	19498	(E) WINNIPEG		SDG22EF	23699
OTCO1EF	15288	SECO2EF	19481	WPO11EFBC	0	SDSM5EF	22569
OTCO2EF	15270	SEO11EFW2	18682	WPO11EF	12719	SDSM7EF	23045
OTO11EFW2	14175	SEO11EFW4	12254	WPP20EF	12487	SDVB9EF	18292
OTO11EFW4	6791	SEO11EFAL	18110	WPG22EF	12405	SDVB10EF	14166
OTO11EFAL	14293	SENOIEFMI	22453	WPSM5EF	12717	SDCO1EF	22482
OTNOIEFMI	17389	SEO11EFWD	19492	WPSM7EF	12732	SDCO2EF	22358
OTO11EFALW4	4066	SEG22EF	19152	WPVB9EF	12582	SDO11EFW2	12569
OTO11EFWD	15337	SEO11EFALW4	8267	WPVB10EF	12239	SDO11EFW4	4424
		(D) WILMINGTON		WPCO1EF	12708	SDNOIEFMI	24518
		WIO11EFBC	0	WPCO2EF	12691		
(B) PHOENIX		WIO11EF	22660	WPO11EFW2	11748		
PHO11EFBC	0	WIP20EF	22473	WPO11EFW4	8011		
PHO11EF	11897	WISM5EF	22653	WPNOIEFMI	15041		
PHP20EF	11317	WISM7EF	22704	WPO11EFWD	12645		
PHG22EF	13158	WIVB9EF	22535				
PHSM5EF	12065	WIVB10EF	22337	(F) FRESNO			
PHSM7EF	13144	WICO1EF	22651	FRO11EFBC	0		
PHVB9EF	8805	WICO2EF	22641	FRO11EF	12143		
PHVB10EF	7505	WIO11EFW2	21877	FRP20EF	11586		
PHCO1EF	11830	WIO11EFW4	20374	FRG22EF	16300		
PHCO2EF	11689	WIO11EFWD	22594	FRSM5EF	12252		
PHO11EFW2	22319	WINOIEFMI	24961	FRSM7EF	13564		
PHO11EFW4	26081	WIO11EFV0CG	16485	FRVB9EF	9701		
PHNOIEFMI	11491		22376	FRVB10EF	8136		
		WIVB10EF2565RH	22430	FRCO1EF	12058		
		WIVB10EF2575RH					

Notation

**O11EFBC	Base case: 5 mm EIFS lamina, 11 mm OSB sheathing, sheathing membrane #27, VB #8 (type 1), no accidental water entry into the stud cavity
**O11EF	Same as **O11EFBC but with moisture entry
**P20EF	Same as **O11EF but with plywood board
**G22EFBC	Same as **O11EFBC but with exterior grade gypsum board
**G22EF	Same as **O11EF but with exterior grade gypsum board
**SM5EF	Same as **O11EF but with sheathing membrane #5
**SM7EF	Same as **O11EF but with sheathing membrane #7
**VB9EF	Same as **O11EF but with vapour barrier #9
**VB10EF	Same as **O11EF but with vapour barrier #10
**CO1EF	Same as **O11EF but with different base coat and finish coat thickness
**CO2EF	Same as **O11EF but with different base coat and finish coat thickness
**O11EFW2	Same as **O11EF but with ½ the reference water entry rate (only exception is Phoenix with twice the reference water entry rate)
**O11EFW4	Same as **O11EF but with quarter of the normal moisture entry (only exception is Phoenix with quadruple moisture entry)
**O11EFAL	Same as **O11EF but with air leakage
**NOIEFMI	Same as **O11EF but with no insulation in stud cavity
**O11EFALW4	Same as **O11EFW4 but with air leakage
**O11EFWD	Same as **O11EF but average weather year is replaced dry weather year
**O11EFLV1	Same as **O11EF but with moisture entry location is at the window level between sheathing membrane and sheathing board (note : in all other cases moisture entry location is at the bottom of the stud cavity).
**O11EFV0CG	Same as **O11EF but no vapour barrier and with painted/coated interior gypsum board.
**VB10EF2565RH	Same as **VB10EF but interior room RH variation (Winter 25%; Summer 65%). Std./Reference case : Winter 25%; Summer 55%
**VB10EF2575RH	Same as **VB10EF but interior room RH variation (Winter 25%; Summer 75%). Std./Reference case : Winter 25%; Summer 55%
**VB10EF4065RH	Same as **VB10EF but interior room RH variation (Winter 40%; Summer 65%). Std./Reference case : Winter 25%; Summer 55%
**VB10EF4075RH	Same as **VB10EF but interior room RH variation (Winter 40%; Summer 75%). Std./Reference case : Winter 25%; Summer 55%
**VB10EF5075RH	Same as **VB10EF but interior room RH variation (Winter 50%; Summer 75%). Std./Reference case : Winter 25%; Summer 55%

** : PH - Phoenix; FR - Fresno; SD - San Diego; WP - Winnipeg; OT - Ottawa; SE - Seattle;
 WI : Wilmington

3.1.2. Sheathing Membrane

Three sheathing membranes considered in this study have the following water vapour permeance characteristics:

- (1) SM I - between 290 and 4150 ng/Pa.s.m²; (*Simulation ID - **SM5EF*)
- (2) SM II - between 1647 and 5494 ng/Pa.s.m²; (*Simulation ID - **O11EF*)
- (3) SM III - 280 ng/Pa.s.m² (constant) (*Simulation ID - **OSM7EF*)

The effect of water vapour transmission properties of sheathing membrane on the overall moisture response of the EIFS wall, in terms of RHT(95) index, can be seen in Table B5. The simulation outputs show that the effect of changing sheathing membranes was not significant. There was a slight increase in RHT values due to increased water vapour tightness of the sheathing membrane.

3.1.3. Sheathing Board

Three sheathing board types considered here are OSB, Plywood and Exterior grade gypsum board (Glass mat gypsum board). It should be mentioned that the construction details of the walls with OSB and plywood sheathing board are the same (Figure B1) but when exterior grade gypsum was used as sheathing board the construction details were slightly modified (Figure B2).

The water vapour transmission and liquid diffusivity properties of these three sheathing boards are summarised below.

OSB Sheathing:

Water vapour permeability @ 100% RH (kgm⁻¹s⁻¹Pa⁻¹): 5.9×10^{-12}

Liquid diffusivity (m²s⁻¹): 2.2×10^{-11} (x) and 5.07×10^{-10} (y)

Exterior grade gypsum (Glass mat gypsum board):

Water vapour permeability @ 100% RH (kgm⁻¹s⁻¹Pa⁻¹): 1.8×10^{-10} (exterior) & 9.2×10^{-11} (core)

Liquid diffusivity (m²s⁻¹): 4.8×10^{-12} (x) & 2.14×10^{-10} (y)

Plywood:

Water vapour permeability @ 100% RH (kgm⁻¹s⁻¹Pa⁻¹): 2.65×10^{-11}

Liquid diffusivity (m²s⁻¹): 1.70×10^{-10} (x) & 9.40×10^{-10} (y)

The influence of these differences in material properties on the RHT(95) index values can be seen in Table B5. It is evident that the moisture response of the wall is influenced by the sheathing board properties. However, the influence was small and does not show a consistent pattern at various locations.

3.1.4. Vapour Barrier

The vapour barrier is the last effective component of the wall to protect the interior from the influence and fluctuation of moisture content in interior and ambient conditions. Three vapour barriers (I, II and III) were considered in this study. They represent three different water vapour diffusion control levels.

Vapour barrier I has a constant water vapour permeance of 15 ng/Pa.s.m²

Vapour barrier II has a constant water vapour permeance of 60 ng/Pa.s.m², and

Vapour barrier III has water vapour permeance value as a function of relative humidity and varying between 30 and 320 ng/Pa.s.m².

The simulation identification code for these three vapour barriers (I, II and III) are **O11EF, **VB9EF and **VB10EF, respectively.

The RHT(95) results from the simulations (Table B5) and Figure B8 clearly indicate that the change of vapour barrier type has a distinct influence on the overall moisture response

of the wall and its components. Vapour barrier III, with the highest value of water vapour permeance, facilitated the lowest RHT(95) index values. The effect is more pronounced for hotter drier climates.

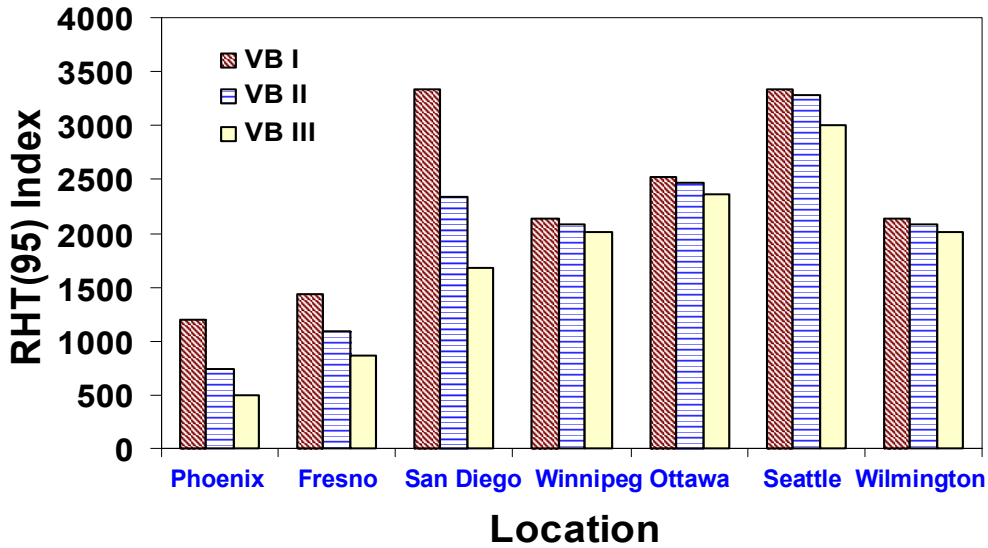


Figure B8: Effect of changing vapour barriers

3.1.5 Insulation

Generally simulations were done with insulation placed within the stud cavity. Some simulations were done without insulation in the stud cavity (simulation ID: **NOIEFMI). Simulation results indicate that the EIFS-wall with insulation in the stud cavity obtains a lower RHT(95) value than the same wall without insulation (Table B5 and Figure B9). The effect is less pronounced in locations with lower moisture loads. There are primarily two reasons for such a change, (1) absence of insulation alters the temperature (T) regime in the region of focus', and (2) insulation present in the stud cavity draws away the accidentally entered moisture from the 'region of focus', thus altering the RH profile. Further detailed discussion on these issues can be found in the report from Task 8.

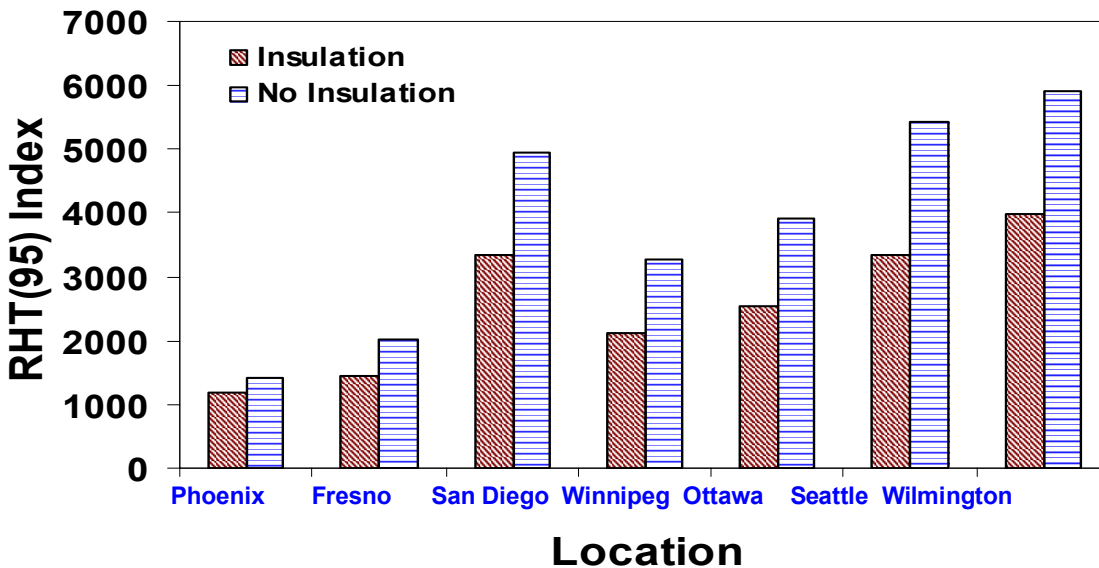


Figure B9: Effect of insulation in the stud cavity

3.1.6 Moisture Entry Location

This case was done only for Ottawa to find out if a change in accidental moisture entry location had any significant effect on RHT index or any visible change in the moisture distribution pattern inside the wall. For this purpose, the location of moisture entry was changed (simulation ID: OTO11EFLV1) from the bottom of the stud cavity to the mid-height of the wall, between the sheathing membrane and sheathing board. The simulation results show (Figure B10 and Table B5) that neither the RHT(95) index nor the moisture distribution pattern changes significantly due to change in accidental moisture entry location.

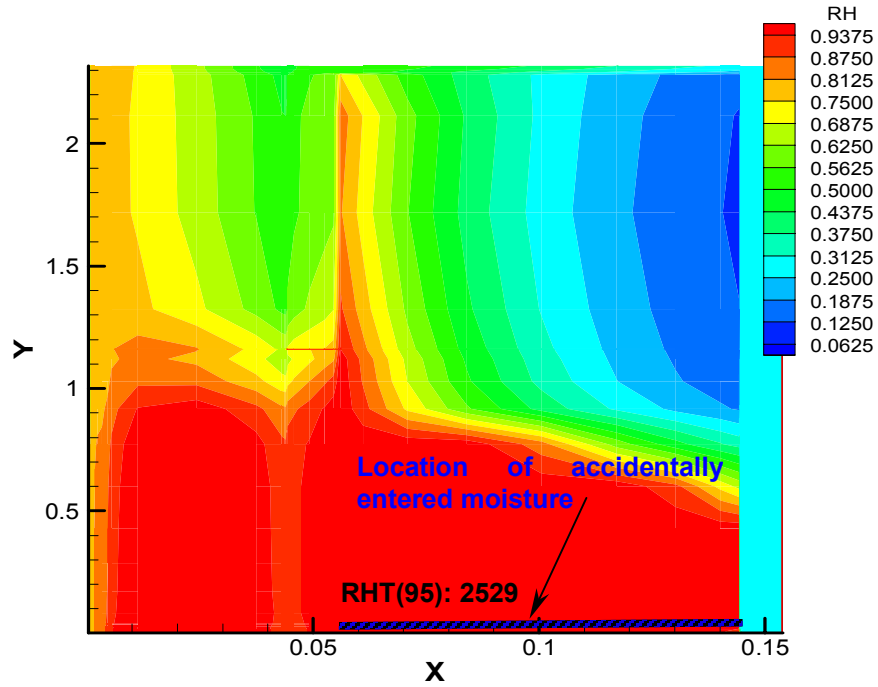
3.1.7 Quantity of Moisture Entry

The amount accidentally entered moisture inside the stud cavity wall in this study was based on experimental observations in the laboratory (Task 6). It is imperative to note that the quantity of accidentally entered moisture can vary widely. In order to investigate the possibility of such variation simulations were done for five locations (Phoenix, Winnipeg, Ottawa, Seattle and Wilmington). Except for Phoenix, the quantities of moisture considered are full, or 1Q as from the equation B1, and 1/2 and 1/4 of the full amount. In case of Phoenix, because of its dry nature, the moisture quantities are doubled (2 times) and quadrupled (4 times).

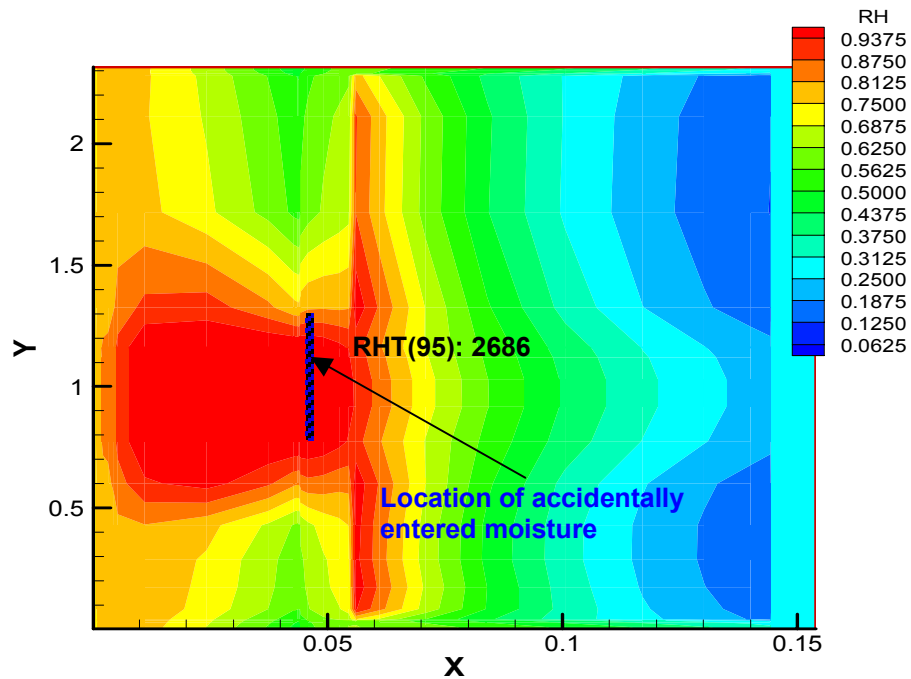
The results from the simulations (see Table B5 and Figure B11) show that the effect of varying the quantity of accidentally entered moisture on the change of RHT(95) index can be interpreted as a function of quantity of accidentally entered moisture. Further analysis of the results showed that this relationship remains linear up to a certain quantity of accidentally entered moisture and thereafter the increment of RHT(95) index with the increase in quantity of accidentally entered moisture becomes less significant to a nearly constant value. Further discussion on this issue can be found in Task 8 report (*Beaulieu et al. 2002*).

3.1.8. Yearly climate variation (Wet-Wet-Average (WWA) and Wet-Wet-Dry (WWD))

Four cases, one each for Ottawa, Seattle, Winnipeg and Wilmington of simulation were done where *Average* year (3rd year) was replaced by *Dry* year. The selection process of *Dry*, *Average* and *Wet* year can be found in MEWS Task 4 report (*Cornick et al 2002*). It was found from RHT(95) values shown in Table B5 that yearly climate variation due to *Average* or *Dry* year had little significance in all the four locations.



(a) Accidental moisture entry at the bottom of the stud cavity (Ottawa)



(b) Accidental moisture entry at the mid height of the wall between the sheathing membrane and sheathing board (Ottawa)

Figure B10: Accidentally entered moisture at different locations

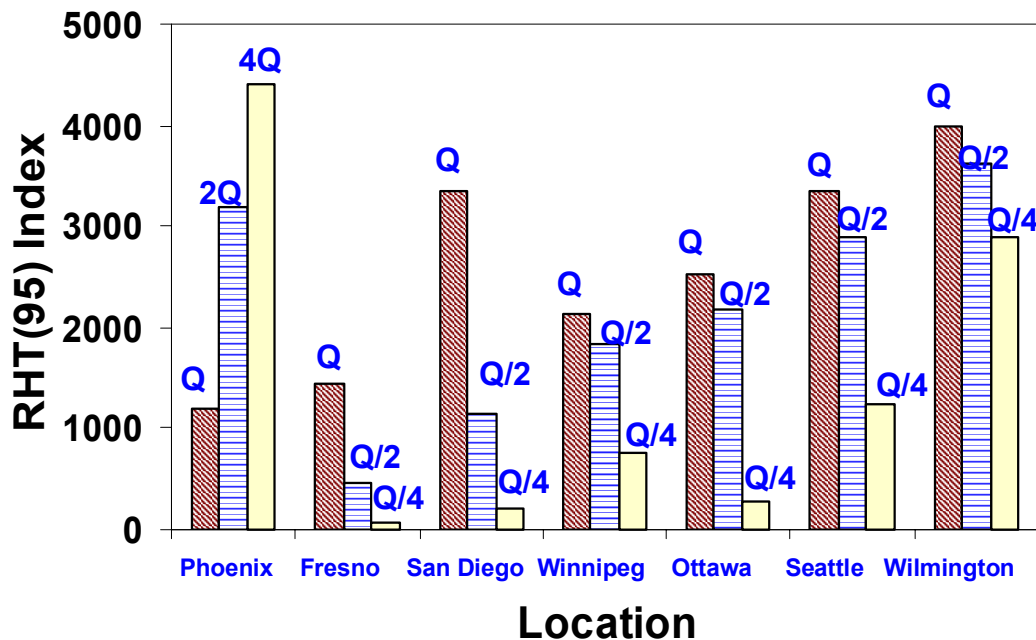


Figure B11: Quantity of moisture entry (Q = full, i.e. estimated quantity from equation B1)

3.1.9. Interior RH

Different interior RH profiles were also investigated. In this study the winter interior RH was 25% and for summer it was 55% (see Figure A7 of Chapter A). To investigate the effects of interior RH on the moisture response of the wall, following simulations were carried out for Wilmington only.

<u>Simulation ID</u>	<u>Interior RH</u>
WIVB10EF	Winter: 25%, Summer: 55%
WIVB10EF2575RH	Winter: 25%, Summer: 75%
WIVB10EF5075RH	Winter: 50%, Summer: 75%
WIVB10EF2565RH	Winter: 25%, Summer: 65%
WIVB10EF4075RH	Winter: 40%, Summer: 75%
WIVB10EF4065RH	Winter: 40%, Summer: 65%

The results from these simulations in Table B5 show that there was a slight increase in RHT(95) index with the higher room RH but that variation was not very significant at Wilmington.

3.1.10 Use of coated gypsum board with no vapour barrier

One simulation was done where vapour control was provided by only one sheet of gypsum board coated with a primer and latex paint. The hygrothermal properties of such coated gypsum board are given in section 2.2 of Chapter A. The permeance of this coated gypsum board is about 8 times higher than that of the vapour barrier III (at 100%RH). The simulation was done for Wilmington and the simulation ID is WIO11EFV0CG. The simulation result shows that there is a noticeable drop (3990 to 1363) in the RHT(95) value due to the use of coated gypsum board with no vapour barrier when the EIFS-wall

was exposed to Wilmington climate data. This case however represents only one point on continuum. The interior RH conditions, 55% summer and 25% winter, might be too conservative for Wilmington.

3.1.11. Locations with seven different Moisture Indices (MI)

The fundamentals behind the moisture index (MI) (see section 3.1.5 of Chapter A) and its values for most of the major locations in North America are given in the report from MEWS Task 4 (*Cornick et al. 2002*). Seven locations were chosen for parametric study and the MI values for these cities vary over a wide range as shown below:

<u>Location:</u>	<u>Moisture Index (MI)</u>
Wilmington:	1.13
Seattle:	0.99
Ottawa:	0.93
Winnipeg:	0.86
San Diego:	0.74
Fresno:	0.49
Phoenix:	0.13

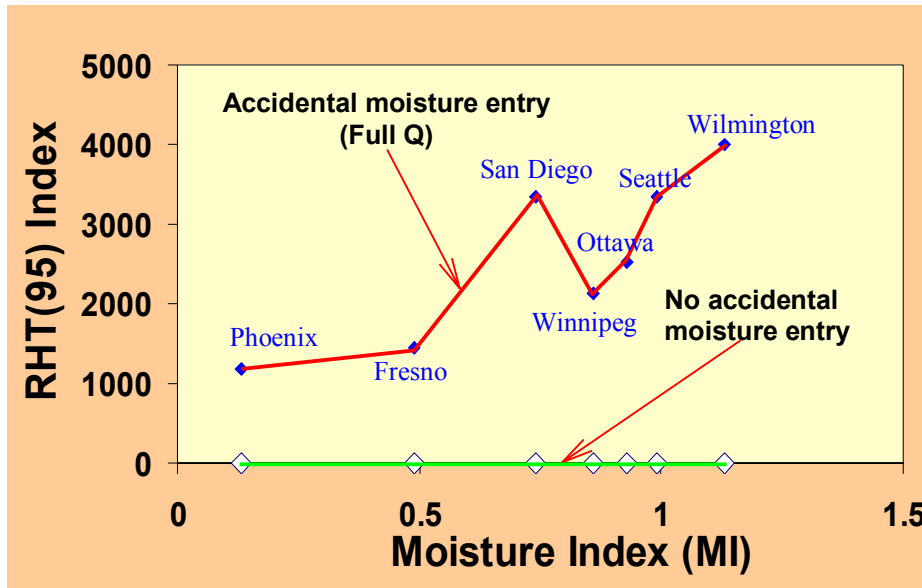
The variation of RHT(95) values with the change in MI for two different quantities (full-Q, and half-Q/2) of accidental moisture entry inside the stud cavity and also without accidental moisture entry (i.e. wall without any deficiency) are shown in Figures B12a and B12b. It is interesting to note that with the full quantity (Q) of accidental moisture entry the relationship between RHT(95) and MI does follow a general trend of gradual increase, except the RHT(95) index value for San Diego (Figure B12a). However, if the quantity of accidental moisture entry is halved (i.e. Q/2) then the familiar relationship of gradual increase of RHT(95) index with the MI becomes very clear. Further analysis of the RH and T profile over the entire time span reveals that there is an upper and lower limit of the quantity of moisture load for which the gradual increment relationship between RHT index and MI is valid. The full quantity of accidental moisture entry load (Q) crosses that limit and hence, the region of focus' becomes 'too wet' to reflect the RH and T variation effect together on the RHT index. In such a situation RHT index shows only the temperature variation effect and the RHT value will deviate to a higher value. On the other hand if the quantity of accidental moisture entry is too small then also it fails to reflect the RH variation effect and the RHT value will deviate to a lower value. It appears that Q/2 falls in the range of accidental moisture entry that can reflect effects of RH and T together (Figure B12b). Further discussion on this issue can be found in the report from Task 8.

3.1.12. Air leakage

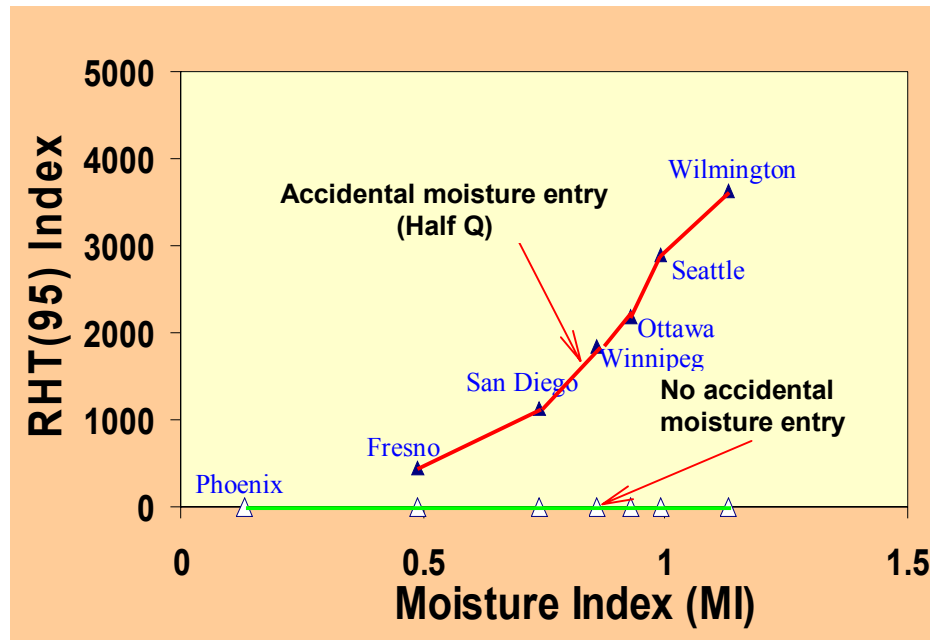
The air leakage path chosen in this study is depicted schematically in Figure B13. It should be pointed out that the air-leakage path shown has the maximum path length possible inside the wall. The simulations were done for Ottawa and Seattle and the general simulation identification for air leakage is **O11EFAL.

The RHT(95) results in Table B5 show that there was a small but insignificant reduction of RHT values due to the air leakage in EIFS-wall, unlike stucco-wall. Two more simulations were done with 1/4th accidental moisture entry (Q/4) load (simulation ID:

**O11EFALW4). The simulation results (Table B5) show a significant reduction of RHT(95) index due to air leakage, like stucco-wall.



(a) RHT(95) vs. MI plot for full quantity (Q) of accidental moisture entry



(b) RHT(95) vs. MI plot for half of the full quantity (Q/2) of accidental moisture entry

Figure B12: RHT(95) varies with MI

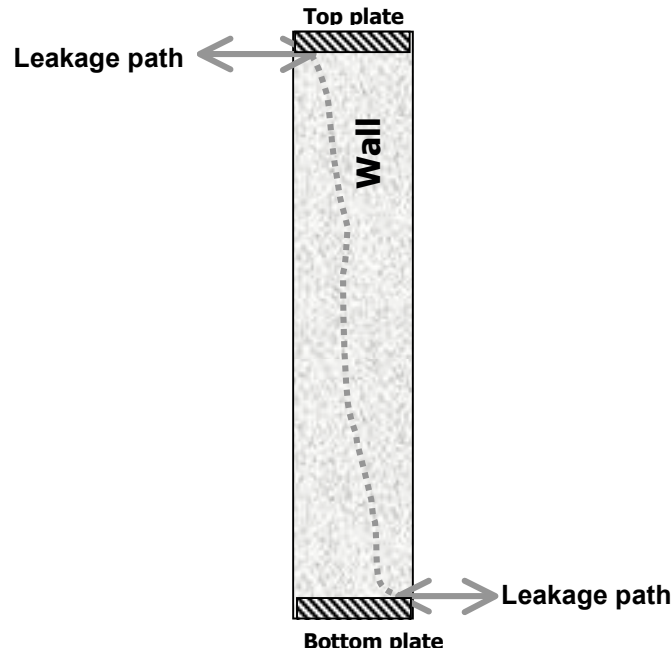


Figure B13: Schematic air flow or leakage path

4.0 Concluding Remarks

The results presented discussed the effect of various environmental and material parameters on the overall moisture response of the EIFS-wall and its components by primarily examining the local hygrothermal conditions in the wall assembly. A novel concept called RHT index has been successfully developed and used for this purpose. Further discussion and interpretation of the results can be found in MEWS Task 8 reports (*Beaulieu et al. 2002*).

References

1. Beaulieu, P.; Cornick, S.M.; Dalgliesh, W.A.; Djebbar, R.; Kumaran, M.K.; Lacasse, M.A.; Lackey, J.; Maref, W.; Mukhopadhyaya, P.; Nofal, M.; Normandin, N.; Nicholis, M.; O'Connor, T.; Quirt, J.D.; Rousseau, M.Z.; Said, M.N.; Swinton, M.C.; Tariku, F.; van Reenen, D. 2002 "MEWS Task 8 Report", Institute for Research in Construction, National Research Council, Ottawa, Canada.
2. Cornick, S. M., Dalgliesh, W. A., Said, N. M., Djebbar, R., Tariku, F. and Kumaran, M. K. 2002, "Task 4- Environmental Conditions", Institute for Research in Construction, National Research Council, Ottawa, Canada, (NRCC-45222), pp. 1-106.
3. Kumaran, K., Lackey, J., Normandin, N., van Reenen, D., and Tariku, F. 2002. "Summary Report from Task 3 of MEWS Project at the Institute for Research in Construction", Institute for Research in Construction, National Research Council, Ottawa, Canada, (NRCC-45369), pp. 1-68.
4. Lacasse, M. A., Beaulieu, P., O'Connor, T. and Nicholls, M., 2002. "MEWS Task 6 Report - Experimental Assessment of Water Entry into Wood-frame Wall Assemblies", Institute for Research in Construction, National Research Council, Ottawa, Canada.

Chapter C

Parametric Studies - Masonry Walls

Chapter C

Parametric Studies - Masonry Walls

1.0 Parameters under Consideration

The major parameters considered in this study and presented in the MEWS task group meetings are:

1. Brick cladding (3 types: Clay brick, Concrete brick and Calcium Silicate brick)
2. Two sheathing membranes; 30 minute building paper and SBPO polymeric membrane
3. Three sheathing boards; OSB, Asphalt coated fibreboard and XPS foam sheathing board
4. Three vapour barriers
5. Two widths of drainage cavity behind exterior cladding, 25mm and 50mm
6. Quantity of accidental moisture entry
7. Locations with seven different Moisture Indices (MI)

These parameters were chosen by the MEWS research team to investigate various moisture management issues related to masonry-walls. These chosen parameters also encompass the suggestions and comments obtained from the representatives of the MEWS partners.

2.0 *hygIRC* and Input for Simulation

The details of *hygIRC* and input required are the same, as those stucco-walls and are presented in Chapter A and EIFS-walls in Chapter B or siding-walls in Chapter D. Masonry walls have different construction details and there are a number of new materials that were used in the construction. The following sections describe the additional information that were used for masonry-walls.

2.1 Basic Wall Construction Details

The typical masonry wall construction detail is shown in Figure C1. Figure C1 shows a masonry wall with OSB sheathing and a 25mm width drainage cavity behind the masonry cladding. Masonry walls are always constructed with cavity behind the brick cladding. The cavity is vented at both top and bottom.

2.2 Material Properties

Apart from the materials that have been documented in Chapters A, B and D (next chapter), two additional materials were used for masonry walls. These two additional materials were brick and mortar.

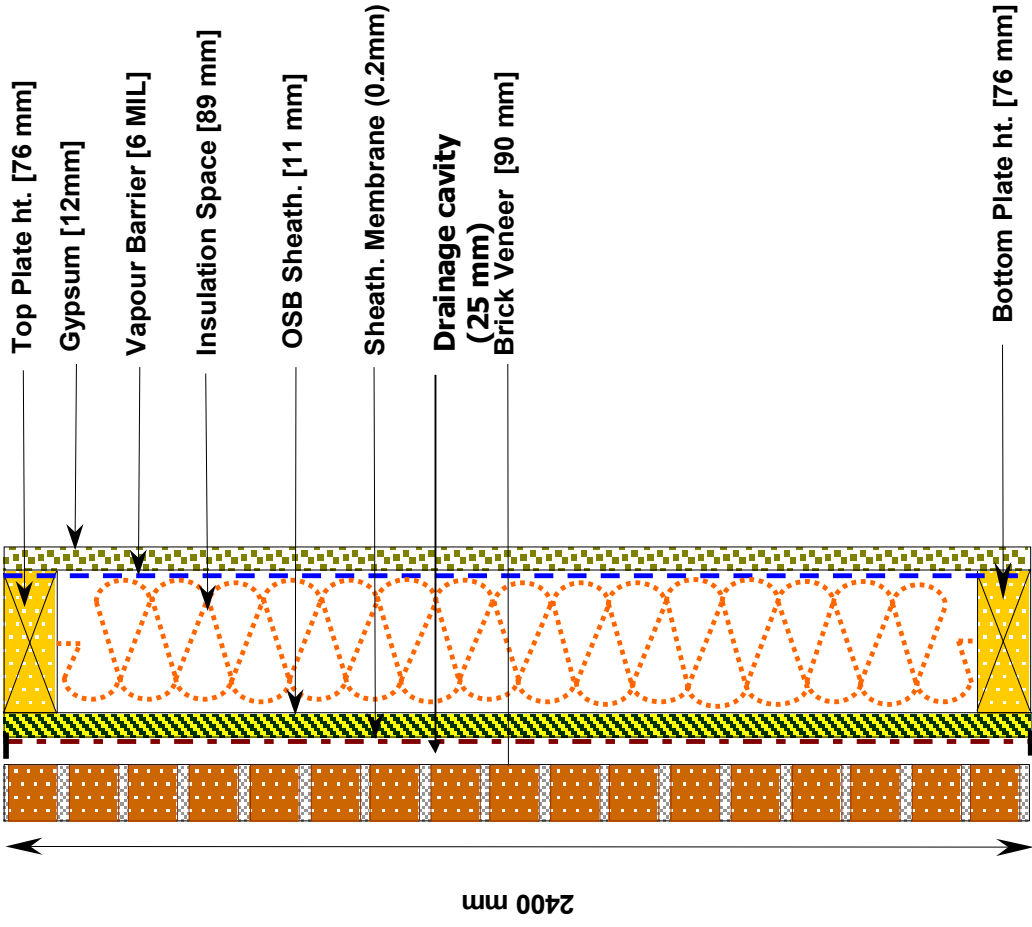


Figure C1: Masonry-wall construction detail

It should be noted here that theoretically *hygIRC* allows the user to model each brick unit and mortar layers separately. However, for computational purposes this was not practical. Therefore a bulk material property approach was adopted. This implies that the masonry cladding consists of one material having one set of bulk material properties. The bulk material properties of the masonry-clad wall system are calculated from area-weighted average of the material properties of the masonry unit and the material properties of the bonding mortar. Figure C2 depicts how the area-weighted average is calculated.

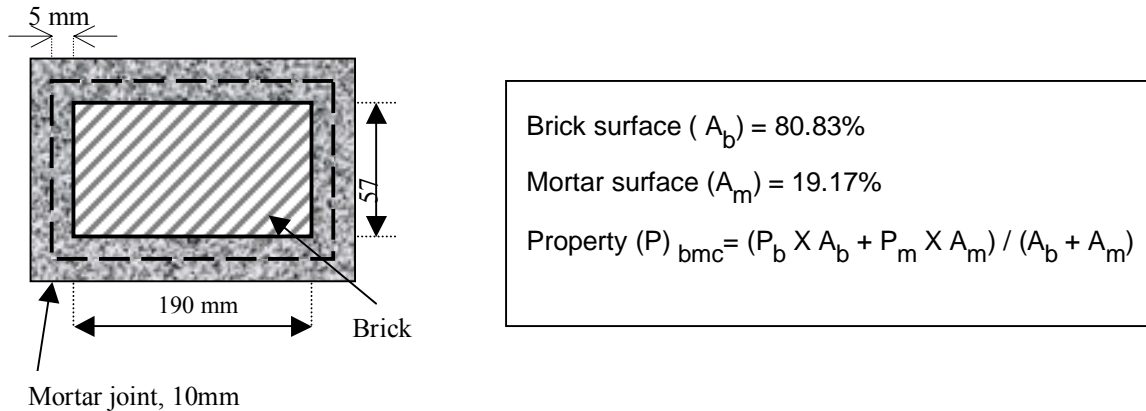


Figure C2: Bulk material properties of a brick-mortar composite

As mentioned in Chapter A, eight distinct sets of material properties are required for *hygIRC* and these material properties for bricks and mortar are described in the following sections.

2.2.1 Air permeability

The air permeability properties of the bricks and mortar, used for simulations, are shown in Table C1. The values shown in the Table C1 are the product of air permeability and dynamic viscosity of air.

Table C1: Air permeability of materials

Material	Air permeability (m^2)
Clay brick	2.10×10^{-15}
Concrete brick	7.10×10^{-15}
Calcium silicate brick	1.00×10^{-14}
Mortar	2.20×10^{-14}

2.2.2 Thermal conductivity

Measurements were made on dry materials alone. The thermal conductivity of some materials change in relation to the moisture content of the material. Approximate combining rules are used to account for the effect of moisture on thermal conductivity. The thermal conductivity of dry materials is shown in Table C2.

Table C2: Thermal conductivity of materials (dry)

Material	Thermal Conductivity ($\text{W m}^{-1}\text{K}^{-1}$)
Clay brick	5.00×10^{-01}
Concrete brick	7.80×10^{-01}
Calcium silicate brick	6.23×10^{-01}
Mortar	4.68×10^{-01}

2.2.3 Dry density

The measured dry density of all the materials are provided in the Table C3.

Table C3: Dry density of materials

Material	Dry Density (kgm^{-3})
Clay brick	1.90×10^{03}
Concrete brick	2.30×10^{03}
Calcium silicate brick	1.90×10^{03}
Mortar	1.63×10^{03}

2.2.4 Heat capacity

The heat capacities of all materials are given in the Table C4.

Table C4: Heat capacity of materials

Material	Heat Capacity ($\text{J K}^{-1} \text{kg}^{-1}$)
Clay brick	8.00×10^{02}
Concrete brick	8.00×10^{02}
Calcium silicate brick	8.00×10^{02}
Mortar	9.00×10^{02}

2.2.5 Sorption isotherm

The relation between relative humidity and moisture content of the three bricks and one mortar used in this study are shown in Figure C3.

2.2.6 Suction curve

The plots of moisture content as a function of suction pressure are shown in Figure C4.

2.2.7 Water vapour permeability

Water vapour permeability of the building material is one of the most critical properties to influence the overall drying characteristics of the wall. The variations of water vapour permeability in relation to relative humidity for all the four materials are shown in Figure C5.

2.2.8 Liquid diffusivity

The plots of liquid diffusivity vs. moisture content, for all the four materials are shown in Figure C6. The diffusion of liquid through the material takes place when moisture content of the material is close to the corresponding relative humidity of 100% (refer to the sorption isotherm plots).

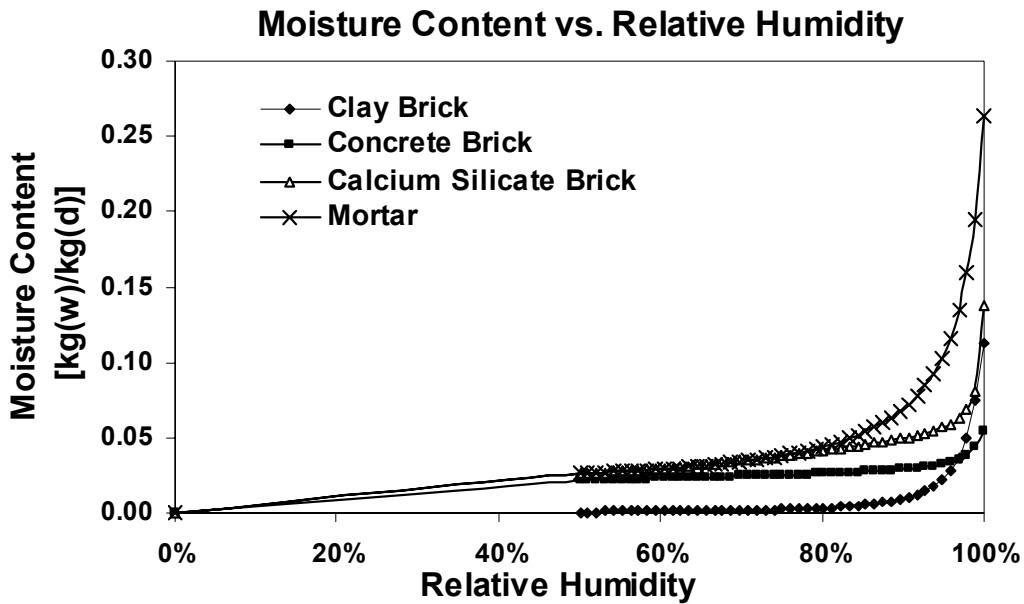


Figure C3: Sorption Isotherm

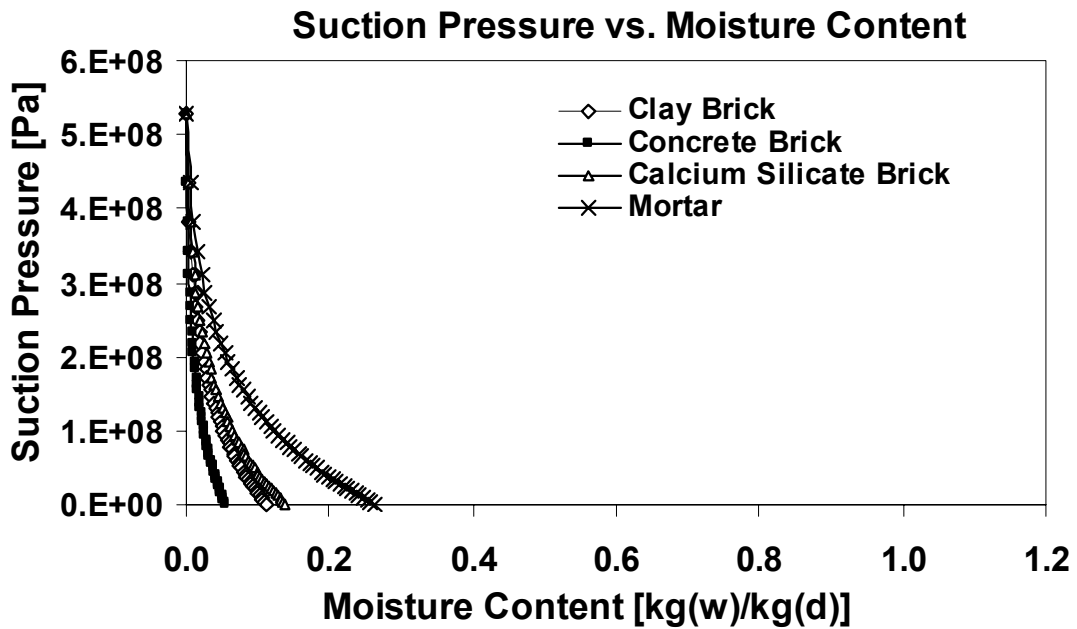


Figure C4: Suction Curve

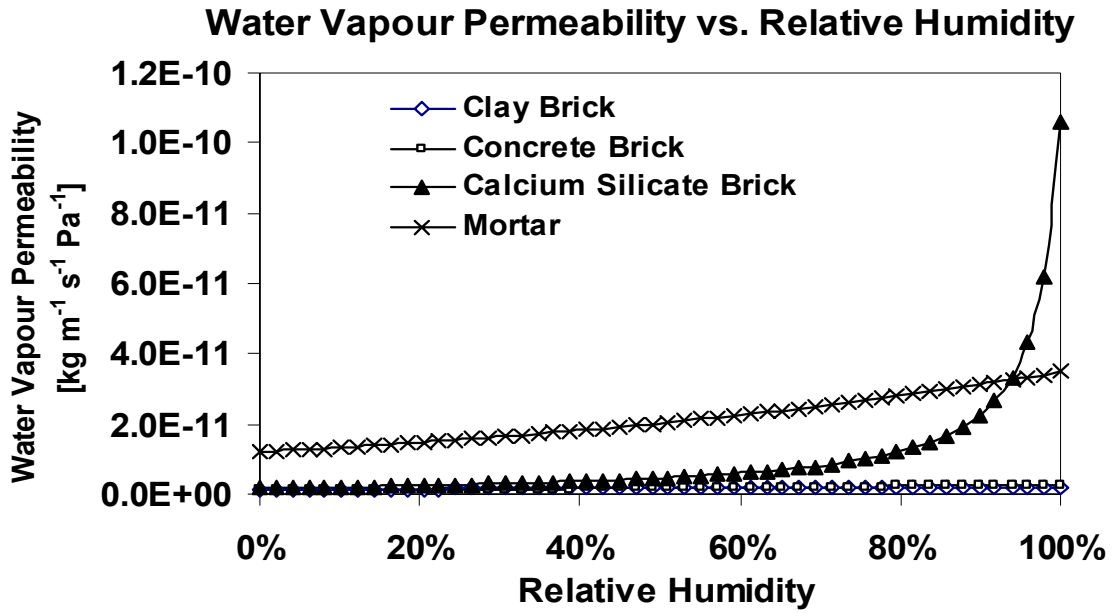


Figure C5: Water Vapour Permeability

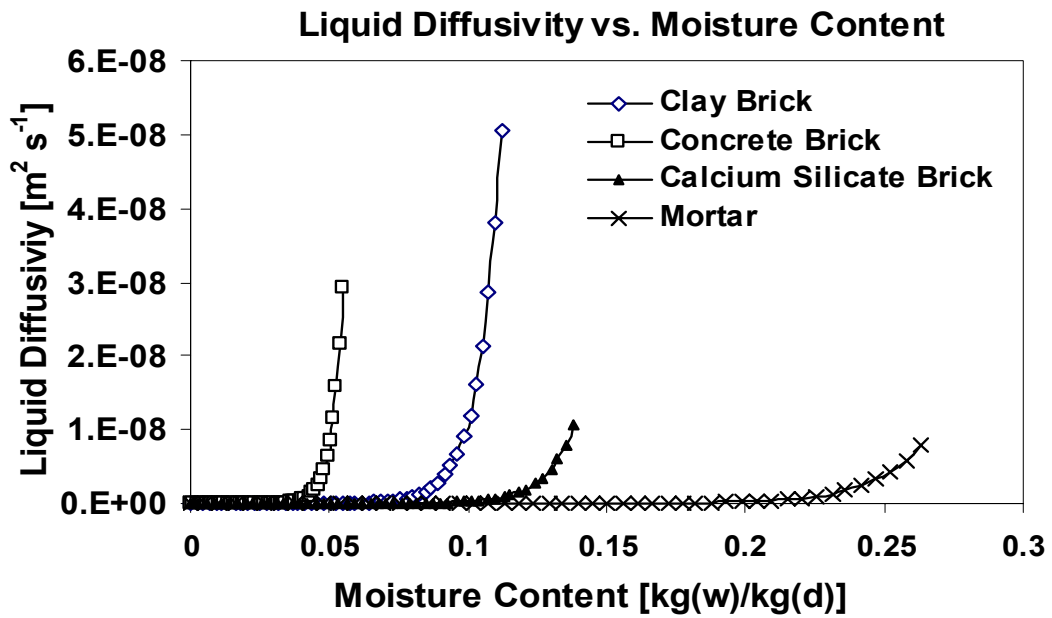


Figure C6: Liquid Diffusivity

2.3 Boundary Conditions

The indoor and outdoor boundary conditions for EIFS-walls are same as those for stucco-clad walls and are described in Chapter A.

2.4 Exposure Duration

The exposure duration for EIFS-wall is exactly the same as the exposure duration for stucco walls. Readers should refer Chapter A for details.

2.5 Initial Moisture Content and Temperature

Initial conditions (RH and T) for EIFS-walls defined in this study were based on the same principles as those for stucco walls. The principles are described in Chapter A.

2.6 Accidental Moisture Entry - Quantity and Location

hygIRC has the capability to inject accidentally entered moisture at any location of the wall and at any time (hourly interval). The quantity of accidentally entered moisture inside the wall and its location were determined from the output of full-scale and small-scale laboratory tests done in MEWS Task 6 (*Lacasse et al. 2002*). Each wall has a unique moisture entry function. The function used to determine the quantity of accidental moisture entry inside the EIFS-walls is described below.

Quantity

An equation was derived from the full-scale lab results to estimate the moisture entry rate (Q). This equation depends on the pressure difference across the wall assembly (ΔP) as well as the rate of water dR_p striking the wall, and is given below:

$$dQ/dR_p = 0.0115 + 1.722 \times 10^{-4} \cdot \Delta P - 1.47 \times 10^{-7} \cdot (\Delta P)^2 \quad (\text{Eqn. C1})$$

ΔP is a function of wind pressure and dR_p is representative of wind driven rain. All the parametric studies reported in this report are based on the amount of moisture entry determined from the use of equation C1.

Location

The locations of moisture entry for siding-walls are same as those for stucco-walls or EIFS-walls or Siding-walls. The quantity of accidentally entered moisture determined from equation C1 was injected at the bottom of the stud cavity, on the top of the bottom plate, at hourly intervals, when applicable.

3.0 Results from *hygIRC* Simulation

More than seventy simulations were done in this study. An enormous amount of data was generated by *hygIRC* and subsequently post-processed for overall and critical evaluation of the hygrothermal response of the wall. Only selected amounts of data are presented in this report for discussion. If required and requested for a stated purpose then any particular aspect of the remaining data could be made available exclusively to the MEWS partners.

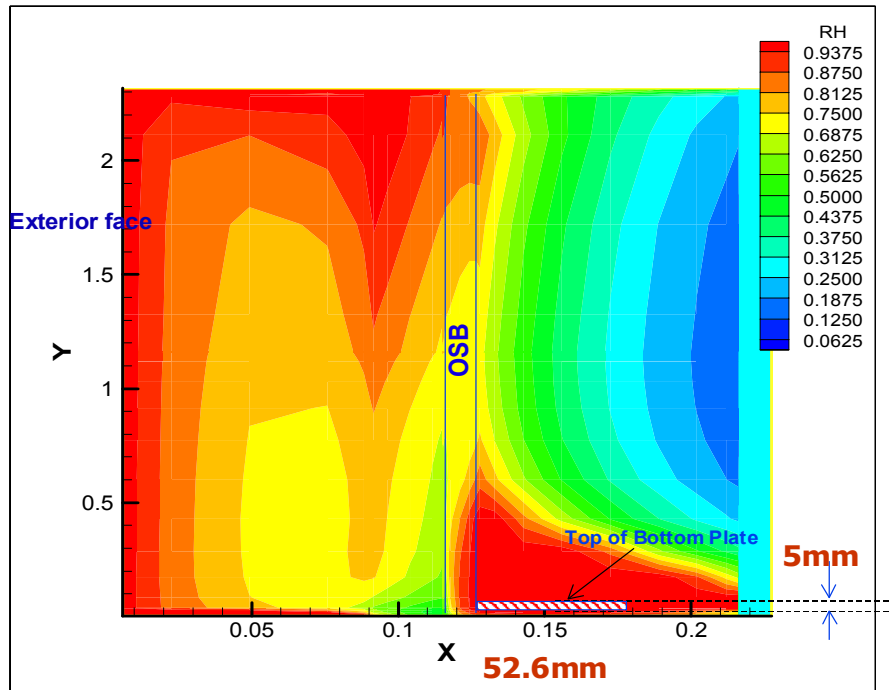
The authors feel that following points about the simulations should be clearly and unambiguously stated before presenting the results and the related discussions:

- (1) The main objective of this study is to determine the drying potential and characteristics of the wall assembly in case of accidentally entered moisture inside the stud/insulation cavity of the masonry-wall.
- (2) The materials used in the simulations are described in section 2.2. of this chapter and the corresponding sections in Chapters A, B, and D.
- (3) Each simulation done in this study has a unique identification, the identification codes are explained at the end of Table C6.
- (4) All the simulations done in this study have accidental moisture entry inside the stud/insulation. One simulation however, with the letters BC appended to the end of the identifier for each location has no accidental moisture entry. The accidental moisture was introduced into the inside of the stud cavity from the beginning of second year until the end of 3rd year.
- (5) It should be noted that all simulations done in this study have the first year (a wet year) without any accidental moisture entry. This was done to generate a realistic moisture distribution inside the wall at the end of first year.
- (6) The wall with accidental moisture entry represents a real wall with a deficiency. The wall without accidental moisture entry can be considered as an ideal wall.
- (7) A total of three years simulation was done for each case considered in this study. All the simulation results were analysed based on the results of second and third year. All the discussions presented in this chapter are based on the second and third year simulation results and all the graphs represent the data for that period only.
- (8) Drying curves obtained from the simulations, after first year, are shown in Appendix C1. The moisture content in these graphs is expressed with the unit of mass of moisture per unit length (kg/m) of wall or its components entire cross section. These drying curves provide the overall dry characteristics of the whole wall and its major components.
- (9) A detailed study (microanalysis) of the hygrothermal response of the wall assembly was done by analysing the relative humidity (RH) and temperature (T) contour plots shown in Figure C7.
- (10) A novel concept called the RHT Index has been introduced by the researchers at IRC/NRC and was used in the parametric study to quantify and compare the localized hygrothermal response of any part of the wall and its component. The RHT index is derived from the RH and T distribution pattern (Figure C7) over a period of time for any specific area of the wall cross-section. The RHT index as defined in this study is:

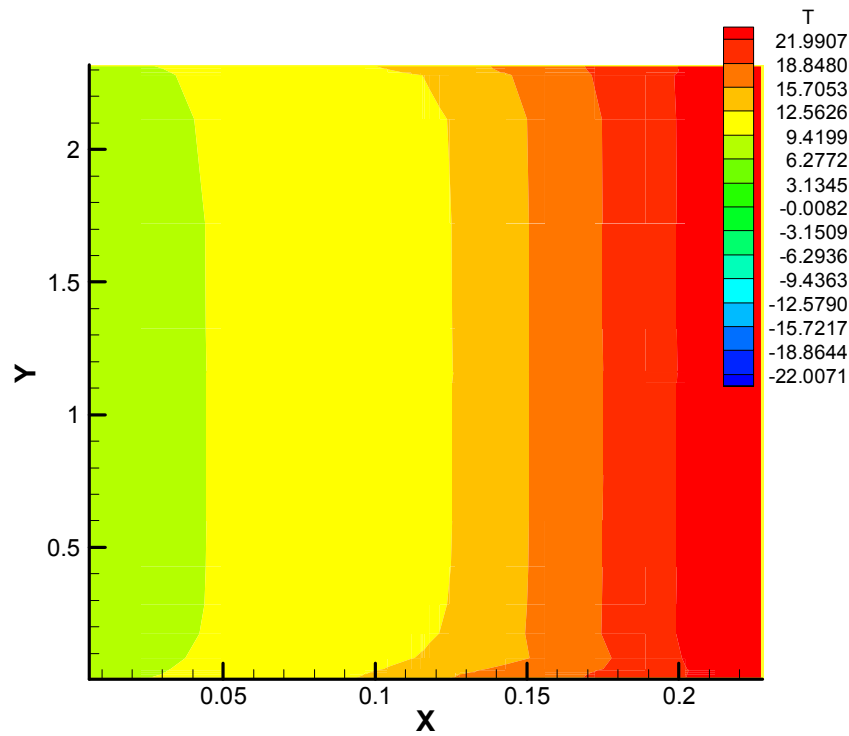
$$\text{Cumulative 2 year (2}^{nd} \text{ and 3}^{rd} \text{ year) RHT} = \sum (RH - RH_X) \times (T - T_X),$$
 for $RH > RH_X\%$ and $T > T_X^\circ\text{C}$ at every 10 days interval [Eqn. C2]
 (During any time step when either or both $RH \leq RH_X\%$ and $T \leq T_X^\circ\text{C}$, the RHT value for that time step is zero.)
 Where user-defined threshold values for $RH_X = 95\%$ and $T_X = 5^\circ\text{C}$ have been chosen for this parametric study. RHT values for $RH_X=80\%$ have also been derived and presented in this report. For convenience the RHT values will be referred to as RHT(95) or RHT(80) index according to the threshold RH (i.e. RH_X) level.
- (11) 'Region of focus' is the area for which the RHT index is calculated. This area is the wettest portion of the wall assembly most of the time (see Figure C7a). For masonry-wall simulations, presented in this report for parametric study, the 'region of

focus' is a thin slice (5 mm) of the top surface of the bottom plate, extending 53 mm from the sheathing board (see Figure C7a).

- (12) The RHT index brings out the overall localized combined moisture and temperature response of the selected area of the material or wall assembly. For overall drying and wetting pattern of the masonry-wall, at any point of time, interested readers should look at the drying curves given in Appendix C1.



(a) Typical relative humidity contour plot - masonry wall (width of the wall expanded)



(b) Typical temperature contour plot - masonry wall (width of the wall expanded)

Figure C7: RH and T Contour

Table C5: RHT (95) Results for Masonry-clad Walls
 (Top of the bottom plate - Region of focus; Equation C1)

Simulation ID	RHT (95) Index	Simulation ID	RHT (95) Index	Simulation ID	RHT (95) Index	Simulation ID	RHT (95) Index
(A) OTTAWA							
OTO9BRBC	0	(C) SEATTLE					
OT O9BR	745	SEO9BRBC	0				
OTVB7BR	534	SEO9BR	1560				
OTVB8BR	434	SEVB7BR	1192				
OTSM21BR	784	SEVB8BR	1043			(G) SAN DIEGO	
OTCE24BR	587	SESM21BR	1625			SDO9BRBC	0
OTCS26BR	589	SECE24BR	1362			SDO9BR	375
OTX22BR	2179	SECS26B4	1349			SDVB7BR	350
OTO9BR50C	591	SEX22BR	2497	(E) WINNIPEG		SDVB8BR	313
OTF27BR	83	SEO9BR50C	1451	WPO9BRBC	0	SDSM21BR	378
OTO9BRW2	72	SEF27BR	362	WPO9BR	1283	SDO9BRW2	0
OTO9BRW4	0	SEO9BRW2	356	WPVB7BR	1053	SDO9BRW4	0
		SEO9BRW4	8	WPVB8BR	925		
		(D) WILMINGTON		WPSM21BR	1319		
		WIO9BRBC	0	WPCE24BR	1137		
(B) PHOENIX		WIO9BR	2715	WPCS26B4	1139		
PHO9BRBC	0	WIVB7BR	2293	WPX22BR	2145		
PHO9BR	39	WIVB8BR	1937	WPO9BR50C	1117		
PHVB7BR	40	WISM21BR	2744	WPF27BR	325		
PHVB8BR	37	WICE24BR	2560	WPO9BRW2	428		
PHSM21BR	39	WICS26B4	2589	WPO9BRW4	39		
PHCE24BR	38	WIX22BR	3557	(F) FRESNO			
PHCS26B4	38	WIO9BR50C	2600	FRO9BRBC	0		
PHX22BR	191	WIF27BR	625	FRO9BR	95		
PHO9BR50C	38	WIO9BRW2	1137	FRVB7BR	92		
PHF27BR	0	WIO9BRW4	240	FRVB8BR	90		
PHO9BRW2	432			FRSM21BR	95		
PHO9BRW4	1987			FRX22BR	437		
				FRO9BR50C	96		
				FRO9BRW2	0		
				FRO9BRW4	0		

Table C6: RHT (80) Results for Masonry-clad Walls
(Top of the bottom plate - Region of focus; Equation C1)

Simulation ID	RHT (80) Index	Simulation ID	RHT (80) Index	Simulation ID	RHT (80) Index	Simulation ID	RHT (80) Index
(A) OTTAWA							
OTO9BRBC	0	(C) SEATTLE					
OT O9BR	9031	SEO9BRBC	0				
OTVB7BR	7700	SEO9BR	13077				
OTVB8BR	7067	SEVB7BR	11054				
OTSM21BR	9214	SEVB8BR	10267			(G) SAN DIEGO	
OTCE24BR	8141	SESM21BR	13379			SDO9BRBC	0
OTCS26B4	8441	SECE24BR	11865			SDO9BR	5335
OTX22BR	14893	SECS26B4	11839			SDVB7BR	5354
OTO9BR50C	8238	SEX22BR	18930	(E) WINNIPEG		SDVB8BR	5001
OTF27BR	2047	SEO9BR50C	12403	WPO9BRBC	0	SDSM21BR	5356
OTO9BRW2	2352	SEF27BR	6228	WPO9BR	9495	SDO9BRW2	1128
OTO9BRW4	226	SEO9BRW2	6110	WPVB7BR	8791	SDO9BRW4	0
		SEO9BRW4	890	WPVB8BR	8169		
		(D) WILMINGTON		WPSM21BR	9565		
		WIO9BRBC	0	WPCE24BR	9040		
		WIO9BR	18697	WPCS26B4	9060		
		WIVB7BR	17531	WPX22BR	13186		
		WIVB8BR	16049	WPO9BR50C	9386		
		WISM21BR	18750	WPF27BR	4861		
		WICE24BR	18251	WPO9BRW2	5368		
		WICS26B4	18331	WPO9BRW4	1488		
		WIX22BR	21418	(F) FRESNO			
		WIO9BR50C	18736	FRO9BRBC	0		
		WIF27BR	8002	FRO9BR	1909		
		WIO9BRW2	11334	FRVB7BR	1669		
		WIO9BRW4	3181	FRVB8BR	1605		
				FRSM21BR	1933		
				FRX22BR	4914		
				FRO9BR50C	1739		
				FRO9BRW2	182		
				FRO9BRW4	0		
(B) PHOENIX							
PHO9BRBC	0						
PHO9BR	1112						
PHVB7BR	1068						
PHVB8BR	900						
PHSM21BR	1111						
PHCE24BR	964						
PHCS26B4	996						
PHX22BR	3060						
PHO9BR50C	1142						
PHF27BR	0						
PHO9BRW2	7286						
PHO9BRW4	15271						

Notation

**O9BRBC	Base case; No moisture entry; OSB sheathing Board
**O9BR	Same as **O9BRBC but with moisture entry
**VB7BR	Same as **O9BR but Type I (15ng) vapour barrier is replaced by a Type II (60ng) vapour barrier
**VB8BR	Same as **O9BR but Type I (15ng) vapour barrier is replaced by a vapour barrier that has vapour permeance variable with relative humidity
**SM21BR	Same as **O9BR but 30 minute building paper water resistive barrier is replaced by SBPO polymeric sheathing
**CE24BR	Same as **O9BR but clay brick is replaced by concrete brick
**CS26BR	Same as **O9BR but clay brick is replaced by calcium silicate brick
**X22BR	Same as **O9BR but with OSB sheathing board is replaced by XPS foam sheathing
**O9BR50C	Same as **O9BR but with 25 mm drainage cavity is replaced by 50 mm drainage cavity
**F27BR	Same as **O9BR but with OSB sheathing board is replaced by asphalt-coated fibreboard sheathing
**O9BRW2 :	Same as **O9BR but with half of the normal moisture entry (only exception is Phoenix with double moisture entry)
**O9BRW4 :	Same as **O9BR but with quarter of the normal moisture entry (only exception is Phoenix with quadruple moisture entry)

** : PH - Phoenix; FR - Fresno; SD - San Diego; WP - Winnipeg; OT - Ottawa; SE - Seattle; WI: Wilmington NC

3.1 Results from Parametric Studies

Results from the parametric studies are to be discussed here primarily with the RHT(95) values from Table C5. However, in qualitative sense, the observations would be same if RHT(80) is to be used instead of RHT(95).

3.1.1 Brick cladding

Clay brick, Concrete brick and Calcium silicate brick were the three types of bricks considered in this study. The simulation identifiers are **O9BR (clay brick), **CE24BR (concrete brick) and **CS26BR (calcium silicate brick). The hygrothermal properties of these three bricks are given in section 2.2. The water vapour permeability and liquid diffusivity properties are as shown below.

Clay Brick :

WVP @ 100% RH ($\text{kgm}^{-1}\text{s}^{-1}\text{Pa}^{-1}$) : 8.43×10^{-12} (x & y)

Liquid diffusivity (m^2s^{-1}) : 4.24×10^{-08} (x & y)

Concrete Brick :

WVP @ 100% RH ($\text{kgm}^{-1}\text{s}^{-1}\text{Pa}^{-1}$) : 8.89×10^{-12} (x) & 8.43×10^{-12} (y)

Liquid diffusivity (m^2s^{-1}) : 2.51×10^{-08} (x) & 4.24×10^{-08} (y)

Calcium Silicate :

WVP @ 100% RH ($\text{kgm}^{-1}\text{s}^{-1}\text{Pa}^{-1}$) : 9.22×10^{-11} (x) & 8.43×10^{-12} (y)

Liquid diffusivity (m^2s^{-1}) : 1.01×10^{-08} (x) & 4.24×10^{-08} (y)

The results from *hygIRC* simulations, in Table C5 and Figure C8, indicate that clay brick shows consistently higher RHT(95) index in all locations. However, the difference in RHT(95) index due to different types of brick unit is small.

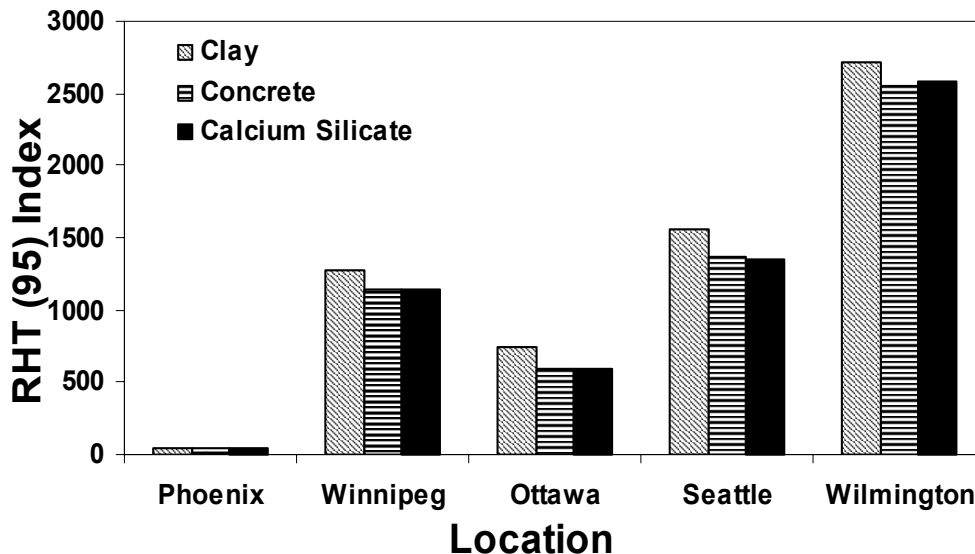


Figure C8: Different bricks in masonry-wall

3.1.2 Two sheathing membranes

The two types of sheathing membranes considered were 30 minute building paper and SBPO polymeric membrane. The simulation IDs are **O9BR and **SM21BR. The material properties of these two sheathing membranes are given in section 2.2. The results, in terms of RHT(95) index, in Table C5 and Figure C9 show that there is little or no difference in the moisture response due to these two different sheathing membranes.

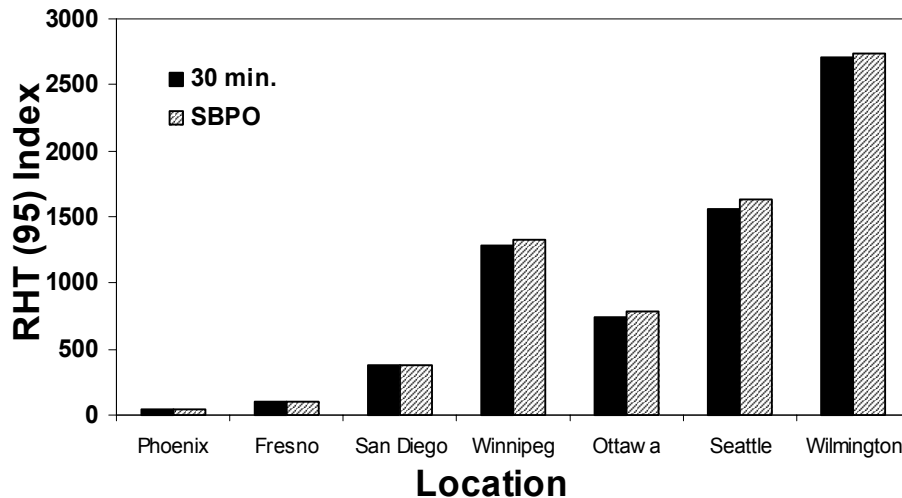


Figure C9: Different sheathing membranes in masonry-wall

3.1.3 Three sheathing boards

The three sheathing boards considered in this study were OSB, asphalt coated fibreboard, and XPS foam sheathing board. The OSB (OSB I, see section 2.2 in Chapter A) that was chosen has the water vapour permeability value at 100% relative humidity that represents approximately the mean of the other two OSBs (II and III). The detailed hygrothermal properties of sheathing boards are given in section 2.2 of Chapters A and D. The water vapour permeability and liquid diffusivity of the three sheathing boards are summarised below.

OSB Sheathing:

WVP @ 100% RH ($\text{kgm}^{-1}\text{s}^{-1}\text{Pa}^{-1}$): 5.9×10^{-12}

Liquid diffusivity (m^2s^{-1}): 2.2×10^{-11} (x) & 5.07×10^{-10} (y)

Asphalt Coated Fibreboard:

WVP @ 100% RH ($\text{kgm}^{-1}\text{s}^{-1}\text{Pa}^{-1}$): 2.3×10^{-11}

Liquid diffusivity (m^2s^{-1}): 1.36×10^{-12} (x) & 1.36×10^{-12} (y)

XPS Foam:

WVP @ 100% RH ($\text{kgm}^{-1}\text{s}^{-1}\text{Pa}^{-1}$): 1.36×10^{-12}

Liquid diffusivity (m^2s^{-1}): 1.00×10^{-16} (x) & 1.00×10^{-16} (y)

The simulation IDs for three sheathing boards are: **O9BR - OSB, **F27B4 - asphalt coated fibreboard, and **X22BR - XPS foam sheathing board respectively.

As can be seen in Table C5 and Figure C10 there was a difference in the moisture response of the masonry-wall, in terms of RHT(95) index, due to the variation in the type of sheathing board used in the masonry-wall. Asphalt coated sheathing board gives the lowest RHT(95) index (i.e. less severe moisture response) when compared to OSB or XPS foam sheathing board. XPS sheathing board generated the highest RHT(95) index. The possible reasons for such response are related to the basic hygrothermal properties of the materials involved. This is discussed in MEWS Task 8 report in the section on masonry (Beaulieu et al. 2002).

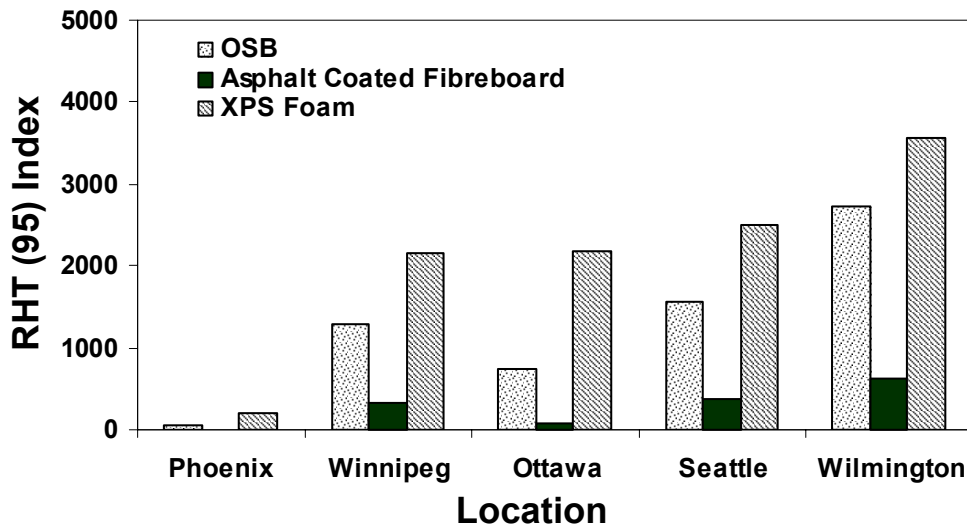


Figure C10: Different sheathing boards in masonry-wall

3.1.4 Three vapour barriers

The vapour barrier is the last effective component of the wall to protect the wall from the influence and fluctuation of temperature and moisture content in interior and ambient climate. Three vapour barriers (I, II and III) were considered in this study. They represent three different water vapour diffusion control levels.

Vapour barrier I has a constant water vapour permeance of 15 ng/Pa.s.m²

Vapour barrier II has a constant water vapour permeance of 60 ng/Pa.s.m², and

Vapour barrier III has water vapour permeance value as a function of relative humidity and varying between 30 and 320 ng/Pa.s.m².

The simulation identification code for these three vapour barriers (I, II and III) are **O9BR, **VB7BR and **VB8BR, respectively.

The RHT(95) results from the simulations (Table C5 and Figure C11) clearly indicate that the changing the vapour barrier type has a distinct influence on the overall moisture response of the wall and its components. Vapour barrier III, with the highest value of water vapour permeance, facilitated the lowest RHT(95) index values. The effect seems to be more pronounced in more severe climate; i.e. higher values of MI.

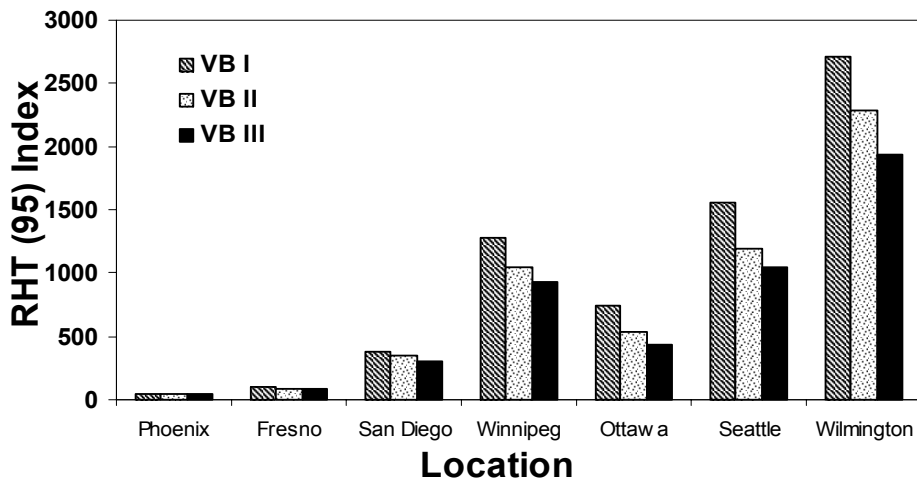


Figure C11: Different vapour barriers in masonry-wall

3.1.5 Width of drainage cavity behind exterior cladding (25mm and 50mm)

All simulations in this parametric study were done with a 25mm width of the vented (both top and bottom) drainage cavity behind the brick cladding. However, one simulation was done for five locations (Table C5) with a 50mm wide vented (both top and bottom) drainage cavity behind the brick cladding. The simulation results (Table C5 and Figure C12) indicate that there is a small reduction in the RHT(95) index due to the increased (50mm) width of the vented drainage cavity.

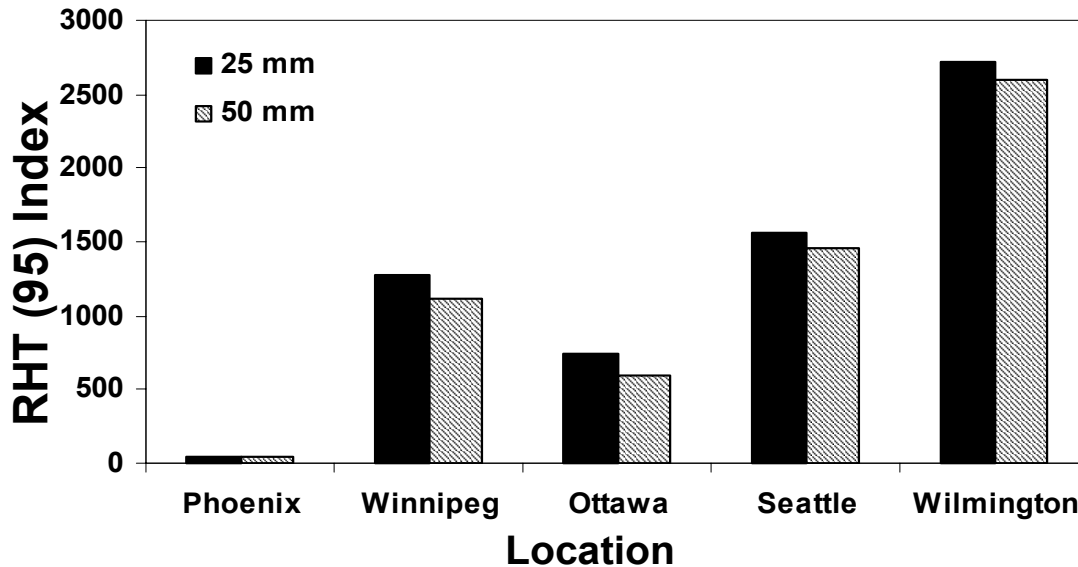


Figure C12: Increased width of drainage cavity in masonry-wall

3.1.6 Quantity of accidental moisture entry

The amount of accidentally entered moisture inside the insulation cavity wall in this study is based on experimental observations in the laboratory (Task 6). It is imperative to note that the quantity of accidentally entered moisture can vary widely. In order to investigate the possibility of such variation simulations are done for five locations (Phoenix, Winnipeg, Ottawa, Seattle and Wilmington). Except for Phoenix, the quantities of moisture considered are full, or 1Q as from the equation C1), 1/2 and 1/4. In case of Phoenix, because of its dry nature, the moisture quantities are doubled (2 times) and quadrupled (4 times).

The results from the simulations (Table C5 and Figure C13) show that the effect of varying the quantity of accidentally entered moisture on the change of RHT(95) index can be interpreted as linearly variable with the quantity of accidentally entered moisture within the range of 0 to 1Q (4 Q for desert climates).

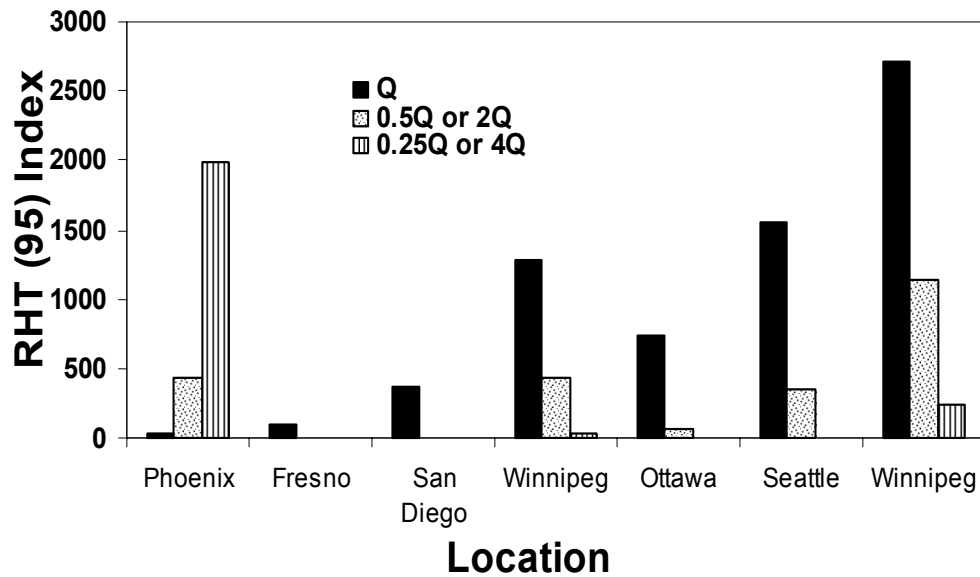


Figure C13: Different quantities of accidental moisture entry in masonry-wall

3.1.7 Locations with seven different Moisture Indices (MI)

The fundamentals behind the moisture index (MI) (see section 3.1.5 of Chapter A) and its values for most of the major locations in North America are given in the report from MEWS Task 4 (*Cornick et al. 2002*). Seven locations were chosen for parametric study and the MI values for these cities vary over a wide range.

<u>Location:</u>	<u>Moisture Index (MI)</u>
Wilmington:	1.13
Seattle:	0.99
Ottawa:	0.93
Winnipeg:	0.86
San Diego:	0.74
Fresno:	0.49
Phoenix:	0.13

The simulations were done with the full quantity (Q) of accidental moisture entry and no accidental moisture entry inside the wall (Table C5). The variation of RHT(95) values with the change in MI indicates a general regular pattern of increasing order as shown in Figure C14. The trend and character of this relationship is very much similar to that has been typically observed in the case of stucco, EIFS and siding-walls (see Chapters A, B, and D respectively). This relationship between RHT index and MI is the cornerstone for the MEWS methodology and further discussion on this can be found in MEWS reports from Task 8 (*Beaulieu et al. 2002*).

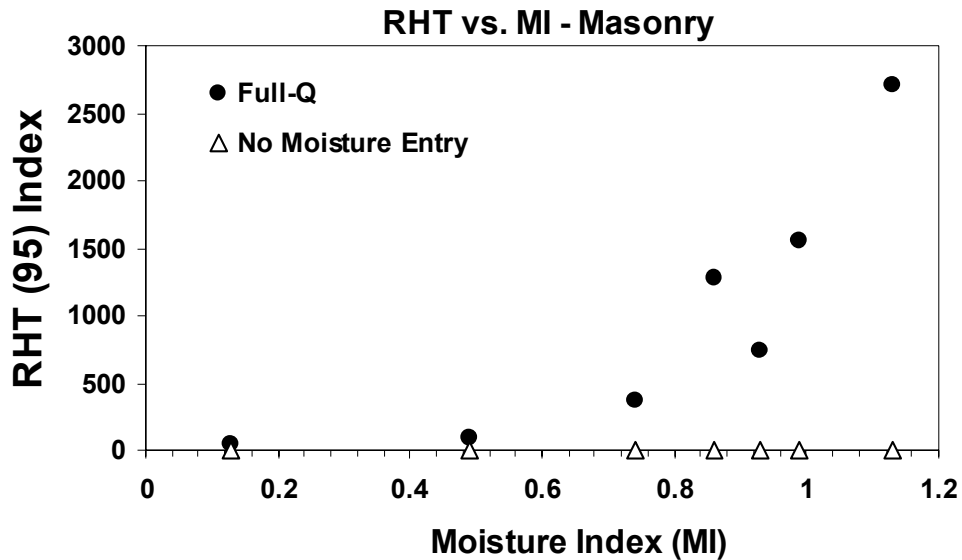


Figure C14: RHT(95) variation with MI

4.0 Concluding Remarks

The results presented discussed the effect of various environmental and material parameters on the overall moisture response of the masonry-wall and its components by primarily examining the local hygrothermal conditions in the wall assembly. A novel concept called RHT index has been successfully developed and used for this purpose. Further discussion and interpretation of the results can be found in MEWS Task 8 report (*Beaulieu et al. 2002*).

References

1. Beaulieu, P.; Cornick, S.M.; Dalglish, W.A.; Djebbar, R.; Kumaran, M.K.; Lacasse, M.A.; Lackey, J.; Maref, W.; Mukhopadhyaya, P.; Nofal, M.; Normandin, N.; Nicholis, M.; O'Connor, T.; Quirt, J.D.; Rousseau, M.Z.; Said, M.N.; Swinton, M.C.; Tariku, F.; van Reenen, D. 2002 "MEWS Task 8 Report", Institute for Research in Construction, National Research Council, Ottawa, Canada.
2. Cornick, S. M., Dalglish, W. A., Said, N. M., Djebbar, R., Tariku, F. and Kumaran, M. K. 2002, "Task 4- Environmental Conditions", Institute for Research in Construction, National Research Council, Ottawa, Canada, (NRCC-45222), pp. 1-106.
3. Kumaran, K., Lackey, J., Normandin, N., van Reenen, D., and Tariku, F. 2002. "Summary Report from Task 3 of MEWS Project at the Institute for Research in Construction", Institute for Research in Construction, National Research Council, Ottawa, Canada, (NRCC-45369), pp. 1-68.
4. Lacasse, M. A., Beaulieu, P., O'Connor, T. and Nicholls, M., 2002. "Task 6 Final Report - Experimental Assessment of Water Entry into Wood-frame Wall Assemblies", Institute for Research in Construction, National Research Council, Ottawa, Canada.

Chapter D

Parametric Studies - Siding Walls (Hardboard & Vinyl)

Chapter D

Parametric Studies - Siding Walls (Hardboard & Vinyl)

1.0 Parameters under Consideration

The major parameters considered in this study and presented in the MEWS task group meetings are:

Hardboard Siding:

1. Sheathing board (4 types: OSB, Plywood, Uncoated fibre board, Asphalt coated fibre board)
2. Sheathing membrane (2 types: SBPO polymeric membrane and 60 minute building paper)
3. Vapour barrier (2 types: Type I, Variable)
4. Locations with seven different Moisture Indices (MI)
5. Accidental moisture entry inside the wall
6. Quantity of accidental moisture entry
7. Use of coated gypsum board with no vapour barrier
8. Presence of a 19mm ventilation cavity inside the wall (i.e. behind the exterior cladding)

Vinyl Siding:

1. Accidental moisture entry inside the wall
2. Quantity of accidental moisture entry
3. Locations with seven different Moisture Indices (MI)
4. Sheathing board (2 types: OSB and Extruded Polystyrene (XPS) foam board)
5. Sheathing membrane (2 types: SBPO polymeric membrane and 30 minute building paper)
6. Vapour barrier (2 types: Type I and Type II)
7. Use of coated gypsum board with no vapour barrier
8. Presence of a 19mm ventilation cavity inside the wall (i.e. behind the exterior cladding)

These parameters were chosen by the MEWS research team to investigate various moisture management issues related to stucco-walls. These chosen parameters also encompass the suggestions and comments obtained from the representatives of the MEWS partners.

2.0 hygIRC and Input for Simulation

The details of hygIRC and input required are similar like those of stucco walls (Chapter A). Siding-clad walls have different construction details and a number of new materials were used in the construction. The following sections describe the additional information that have been used for siding-walls.

2.1 Basic Wall Construction Details

Typical siding-wall construction details are shown in Figures D1 and D2. Figure D1 shows a hardboard siding-wall without a drainage cavity and Figure D2 depicts a wall with vinyl siding. These walls do not have a drainage/ventilation cavity behind the exterior cladding, except 1mm gap between the sheathing membrane and sheathing board. Figures D1a and D2a show the typical hardboard and vinyl-clad walls with a 19mm drainage cavity behind the exterior cladding.

2.2 Material Properties

Apart from the materials used for stucco-wall (Chapter A), following are the additional wall components used for hardboard and vinyl siding-walls were:

- (1) Hardboard siding
- (2) Vinyl siding
- (3) Extruded Polystyrene (XPS)
- (4) Asphalt coated fibre board
- (5) 60 minute building paper

As mentioned in Chapter A, eight distinct sets of material properties are required for *hygIRC*. The material properties for the five materials used to model the siding-wall components are described in the following sections.

2.2.1 Air permeability

The air permeability properties of the five materials, as used for simulations, are shown in Table D1. The values shown in the Table D1 are the product of air permeability and dynamic viscosity of air.

Table D1: Air permeability of materials

Material	Air permeability (m^2)
Hardboard siding	3.30×10^{-16}
Vinyl siding	1.08×10^{-12}
Extruded Polystyrene (XPS)	1.03×10^{-16}
Asphalt coated fibre board	3.20×10^{-12}
60 minute building paper	3.58×10^{-14}

It should be noted that air permeability and water vapour permeability of the vinyl siding units were determined from a specially designed test (Figure D3) sample. Three vinyl siding specimens of size 200mm x 90mm were cut with a longitudinal joint approximately at the middle of the width (Figure D3). The joint was not air or water vapour tight. The vinyl siding specimens (Figure D3) were tested according to the standard air permeability and water vapour permeability test procedures referred in Task 3 report (*Kumaran et al. 2002*). The results obtained from these tests for air permeability or water vapour permeability were used in the simulation. The air permeability and water vapour permeability properties of vinyl siding used in this study are the properties of the composite vinyl siding units with joints.

Hardboard siding was found to be sufficiently air and water vapour tight and therefore no special tests were carried out for hardboard siding joints.

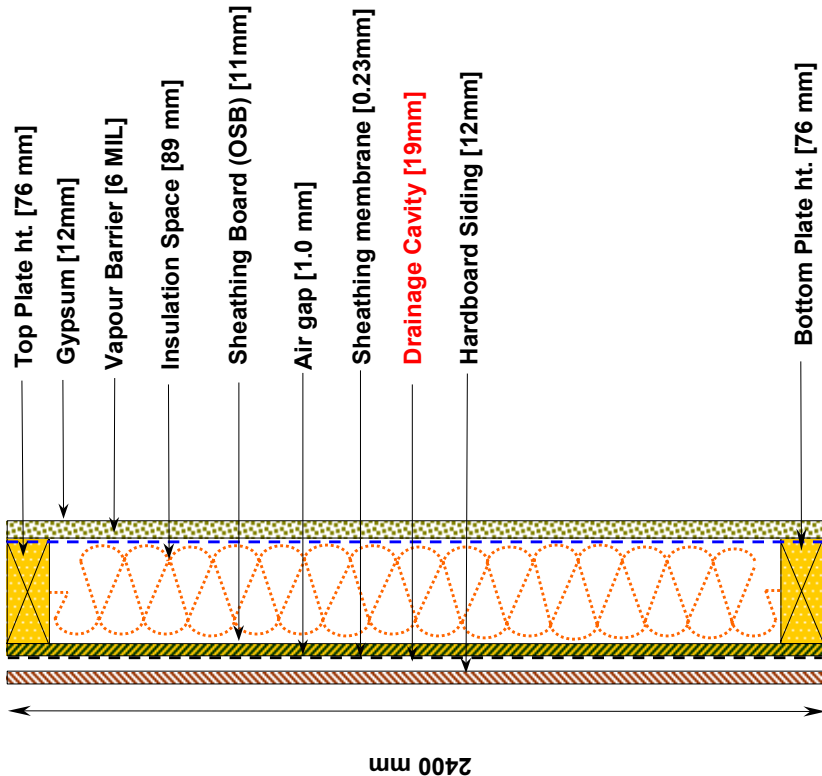


Figure D2: Hardboard siding-wall with a 19mm cavity

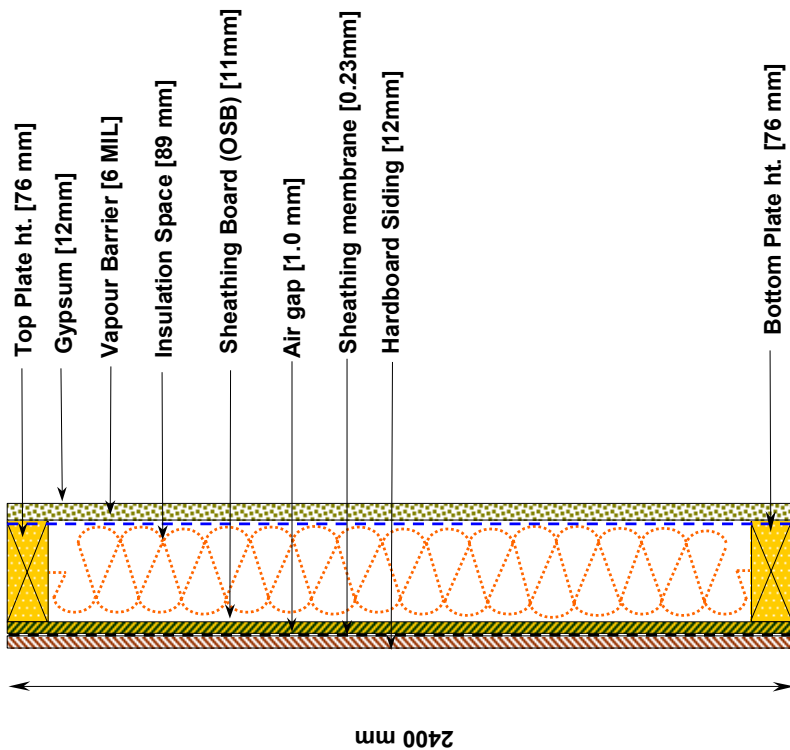


Figure D1: Hardboard siding-wall without a cavity

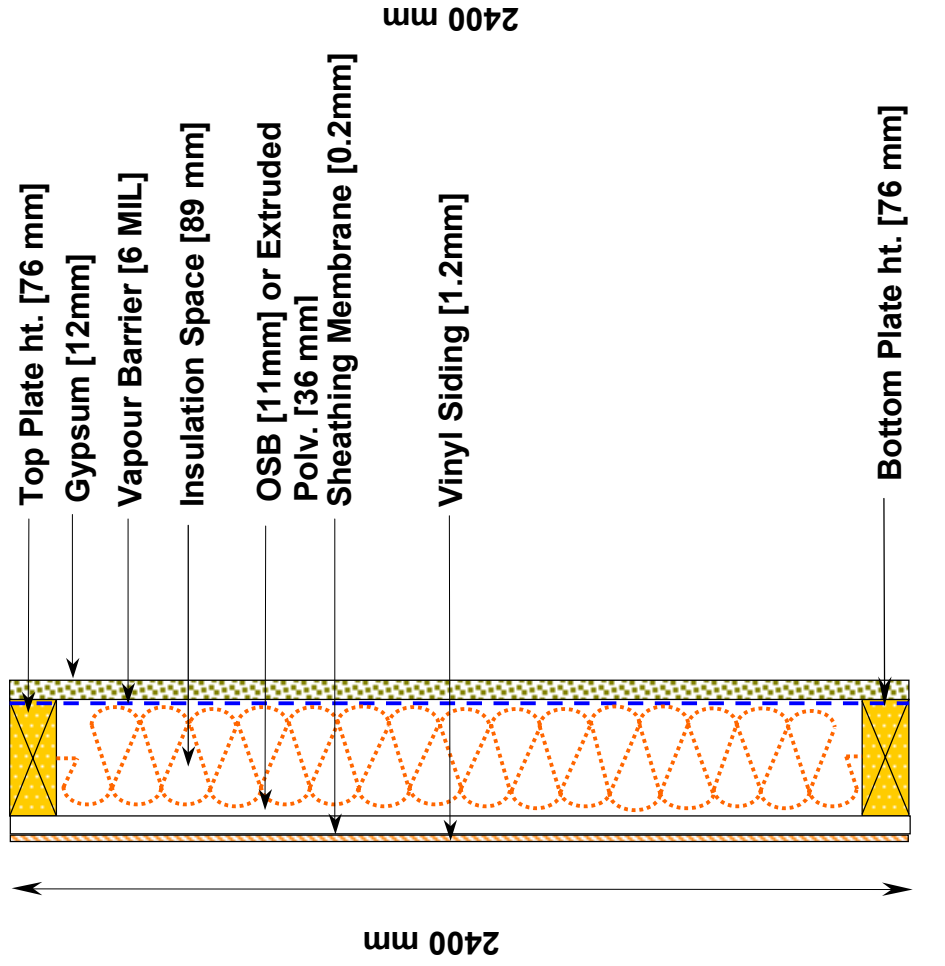


Figure D1a: Vinyl siding-wall without a cavity

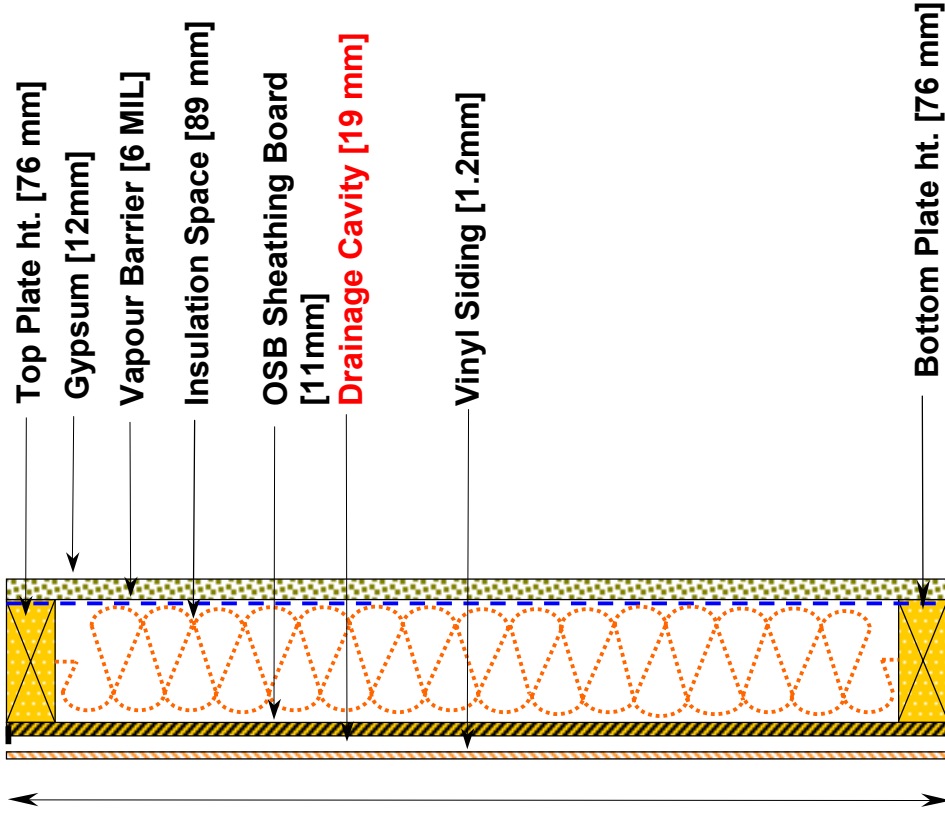


Figure D2a: Vinyl siding-wall with a 19mm

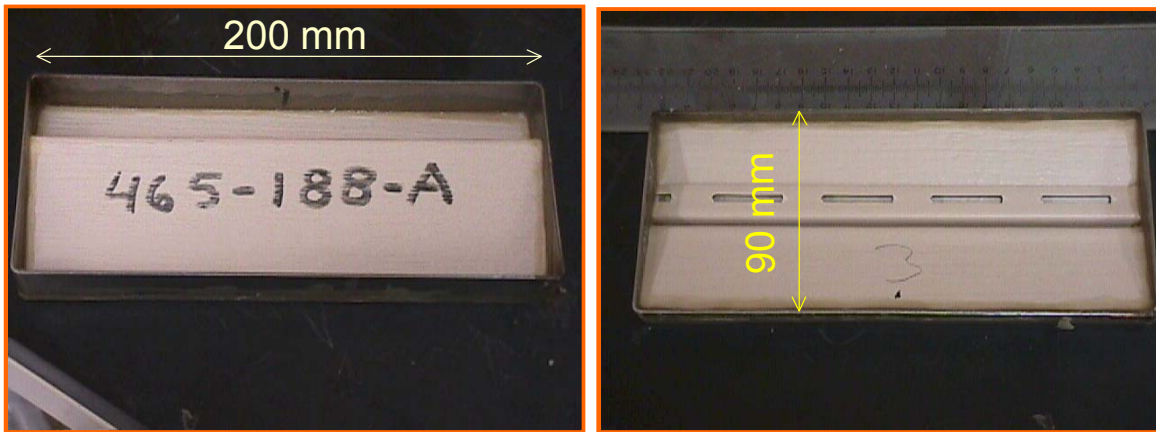


Figure D3: Air and water vapour permeability test specimens for vinyl siding

2.2.2 Thermal conductivity

Measurements were made on dry materials alone. The thermal conductivity of a material changes in relation to the moisture content of the material. Approximate combining rules are used to account for the effect of moisture on thermal conductivity. The thermal conductivity of dry materials is shown in Table D2.

Table D2: Thermal conductivity of materials (dry)

Material	Thermal Conductivity ($\text{W m}^{-1}\text{K}^{-1}$)
Hardboard siding	1.2×10^{-01}
Vinyl siding	1.60×10^{-01}
Extruded Polystyrene (XPS)	2.90×10^{-02}
Asphalt coated fibre board	5.35×10^{-02}
60 minute building paper	1.09×10^{-01}

2.2.3 Dry density

The measured dry density of all the materials are provided in the Table D3.

Table D3: Dry density of materials

Material	Dry Density (kgm^{-3})
Hardboard siding	9.17×10^{02}
Vinyl siding	1.50×10^{03}
Extruded Polystyrene (XPS)	2.83×10^{01}
Asphalt coated fibre board	3.20×10^{02}
60 minute building paper	8.09×10^{02}

2.2.4 Heat capacity

The heat capacity of all the materials are given in the Table D4.

Table D4: Heat capacity of materials

Material	Heat Capacity ($\text{J K}^{-1} \text{kg}^{-1}$)
Hardboard siding	1.88×10^{03}
Vinyl siding	1.26×10^{03}
Extruded Polystyrene (XPS)	1.47×10^{03}
Asphalt coated fibre board	1.88×10^{03}
60 minute building paper	1.88×10^{03}

2.2.5 Sorption isotherm

The relation between relative humidity and moisture content of all the five materials are shown in Figures D4a to D4e.

2.2.6 Suction curve

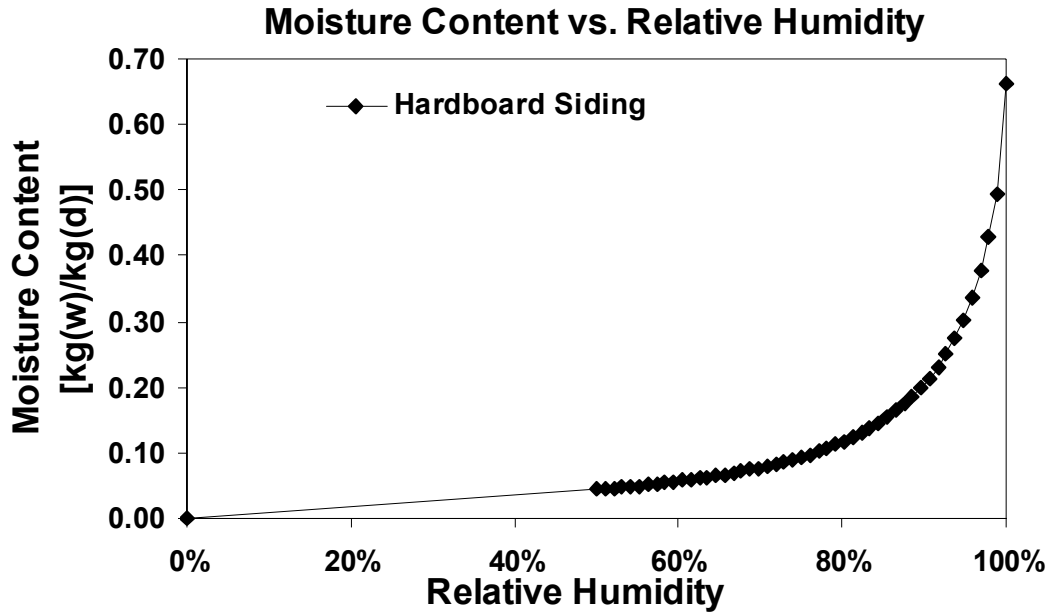
The plots of moisture content as a function of suction pressure are shown in Figures D5a to D5e.

2.2.7 Water vapour permeability

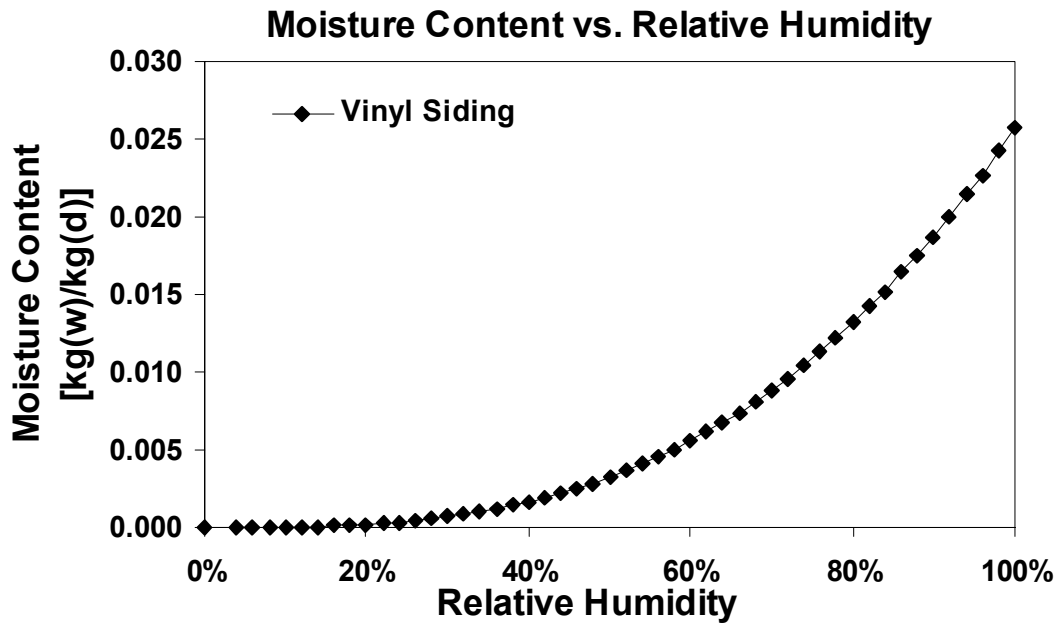
Water vapour permeability of the building material is one of the most critical properties to influence the overall drying characteristics of the wall. The variations of water vapour permeability in relation to relative humidity for all the five materials are shown in Figures D6a to D6e.

2.2.8 Liquid diffusivity

The plots of liquid diffusivity vs. moisture content, for all the five materials are shown in Figures D7a to D7e. The diffusion of liquid through the material takes place when moisture content of the material is close to the corresponding relative humidity of 100% (refer sorption isotherm plots).

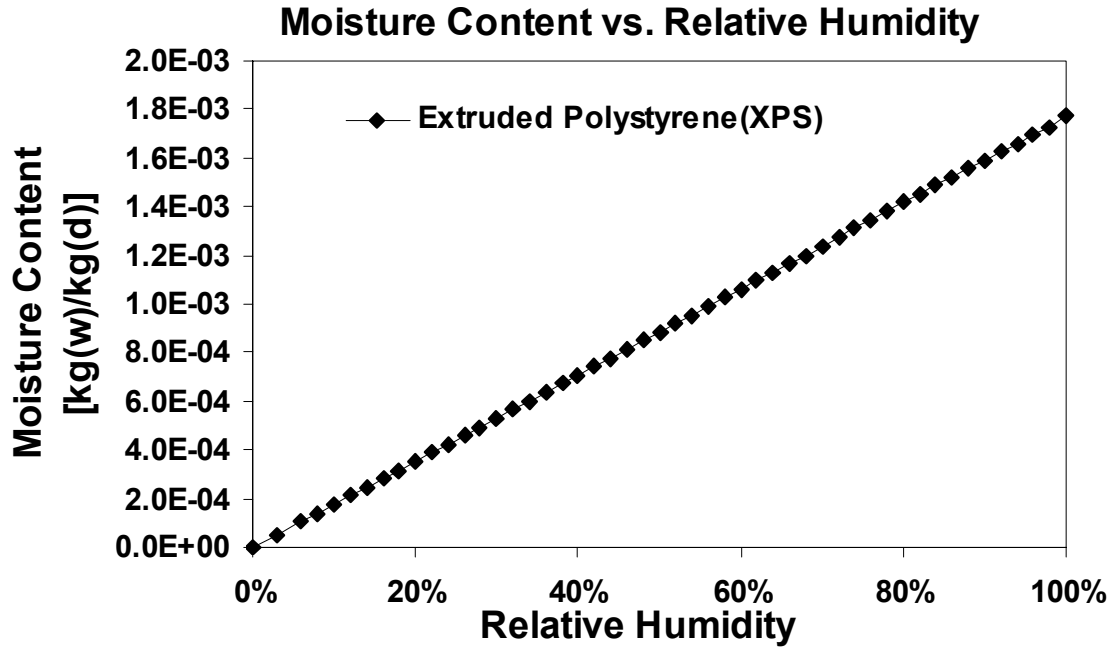


(a) Hardboard siding

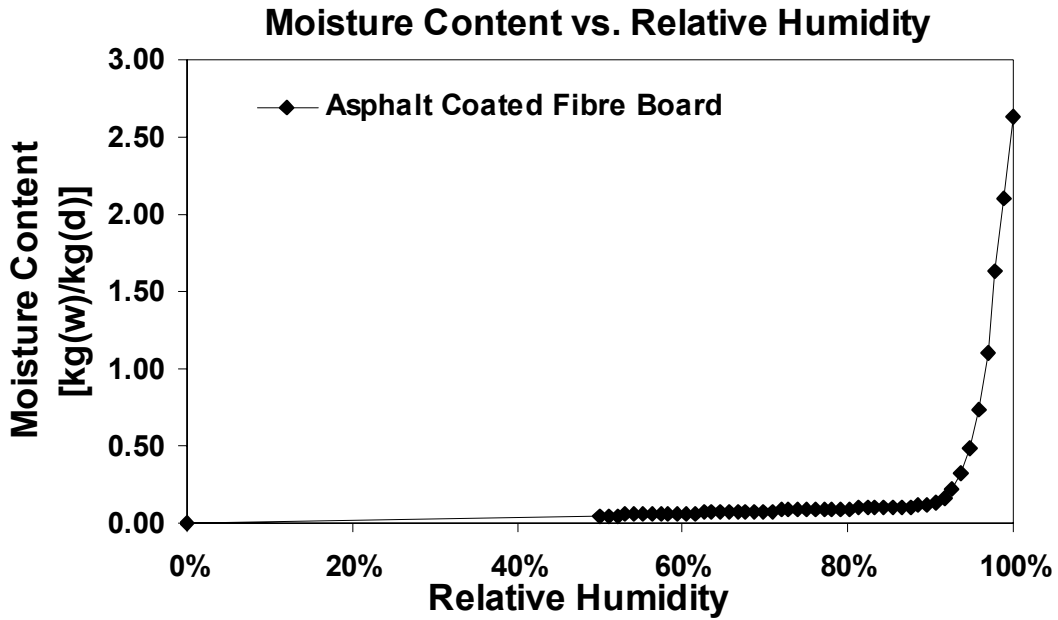


(b) Vinyl siding

Figure D4: Sorption Isotherm

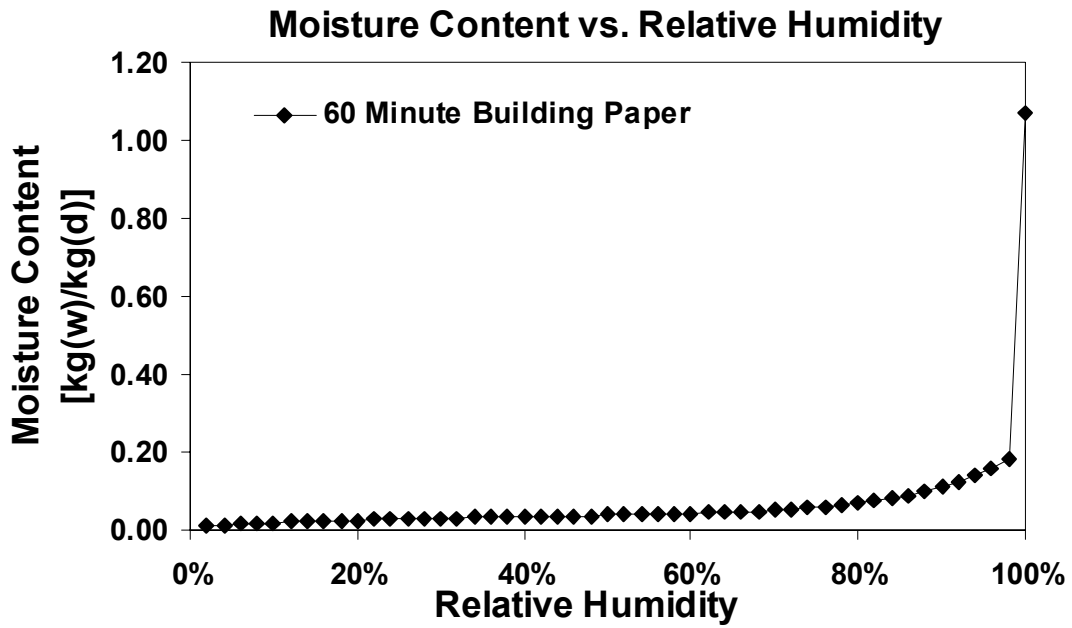


(c) Extruded polystyrene (XPS)



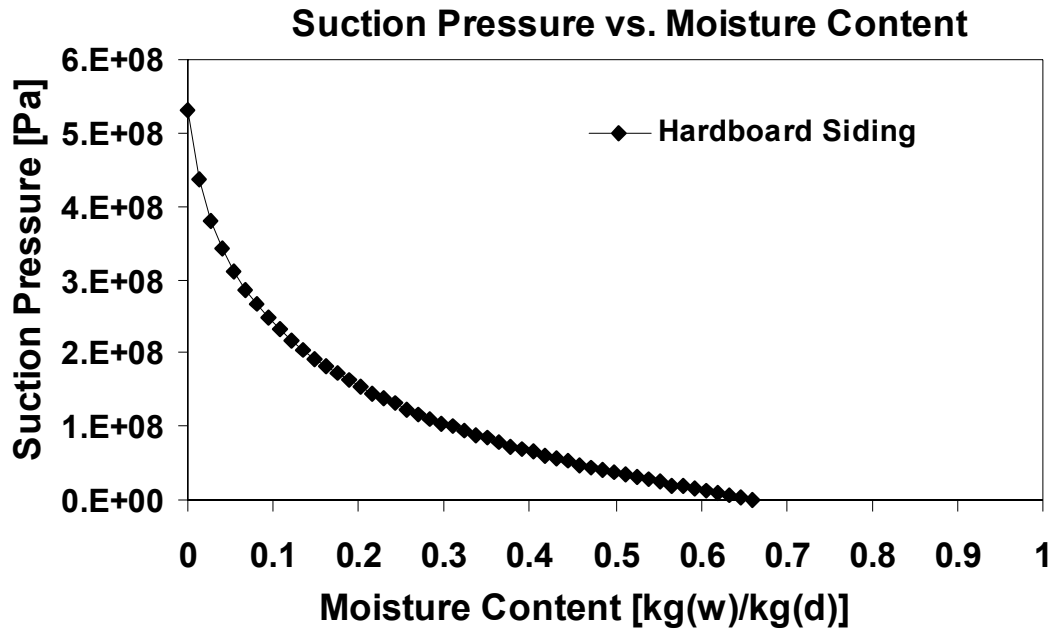
(b) Asphalt coated fibreboard

Figure D4: Sorption Isotherm

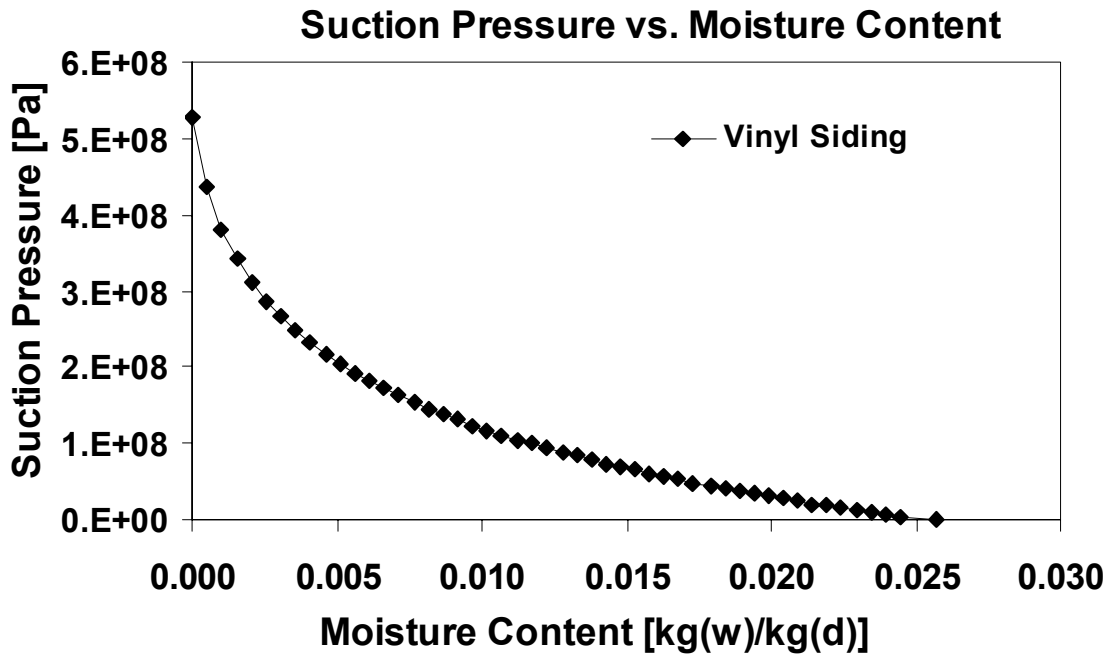


(c) 60 minute building paper

Figure D4: Sorption Isotherm

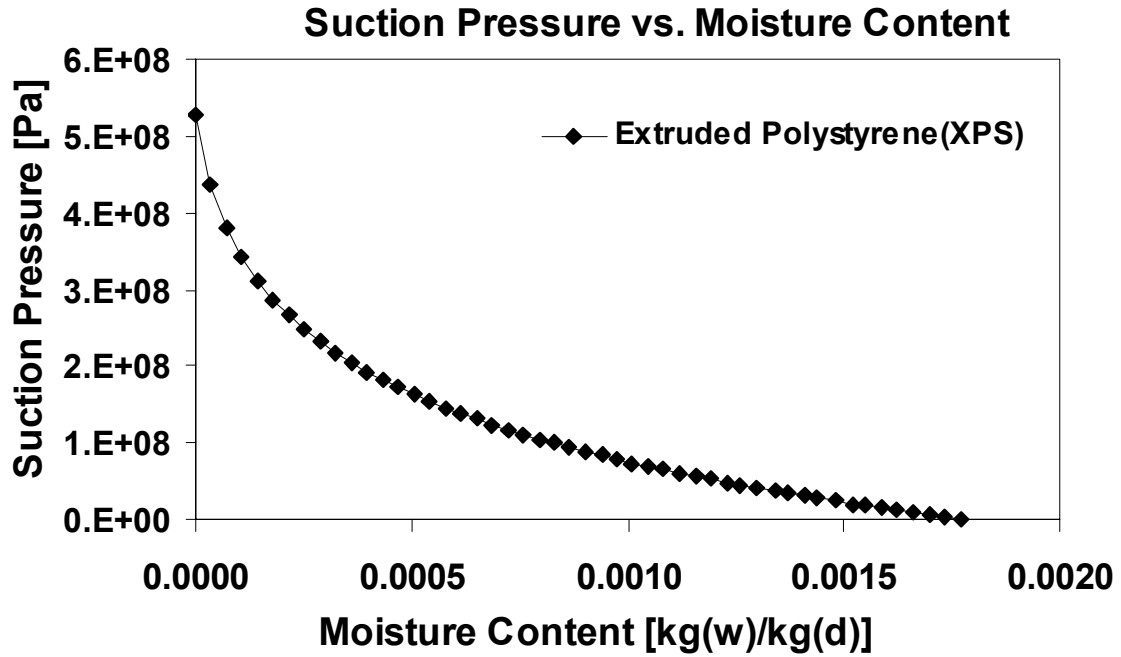


(a) Hardboard siding

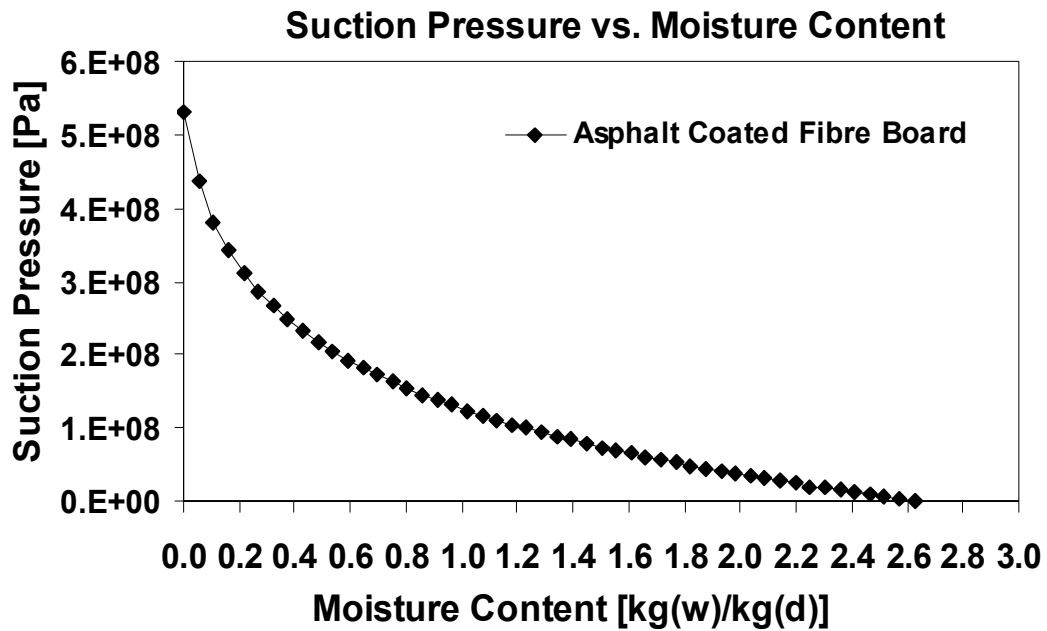


(b) Vinyl siding

Figure D5: Suction Curve

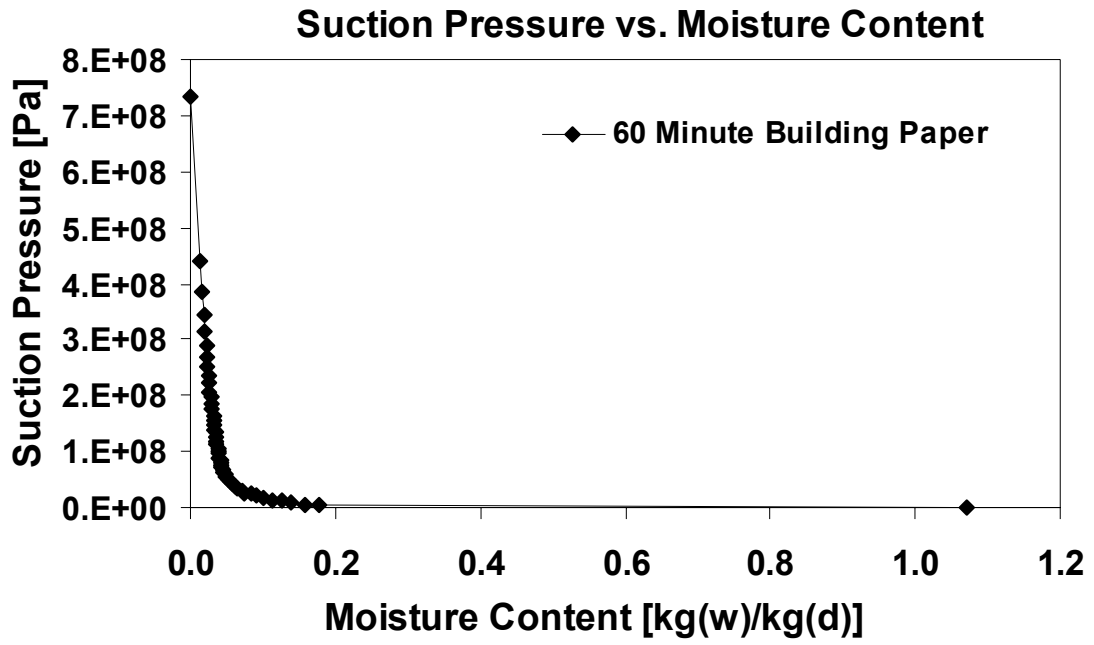


(c) Extruded polystyrene (XPS)



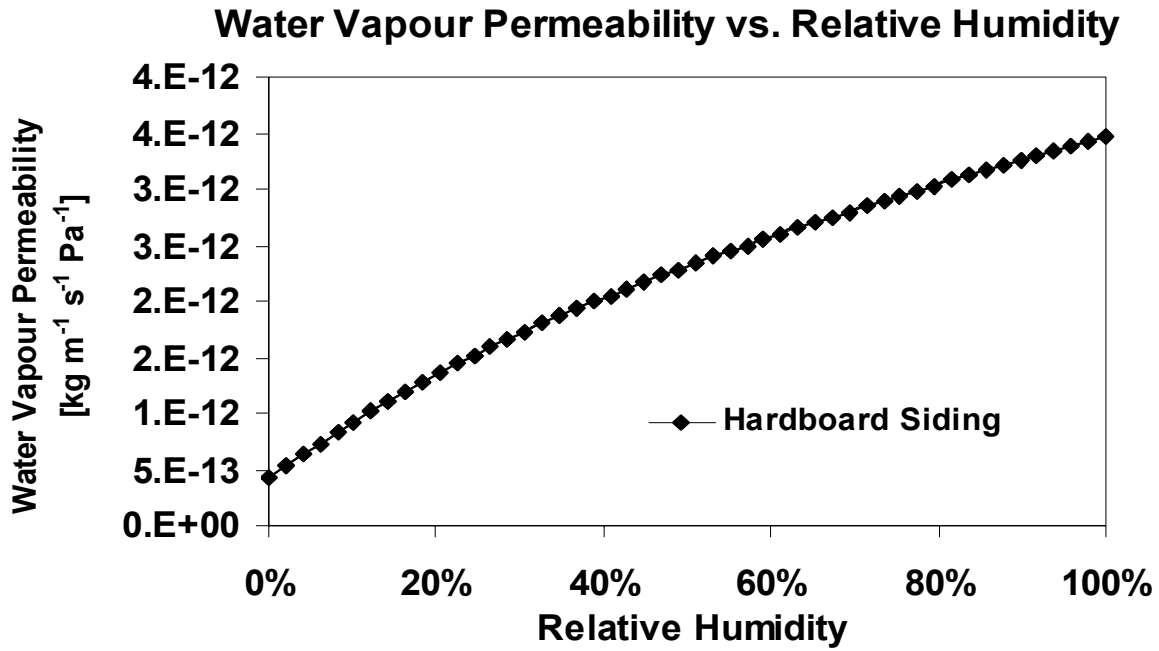
(d) Asphalt coated fibreboard

Figure D5: Suction Curve

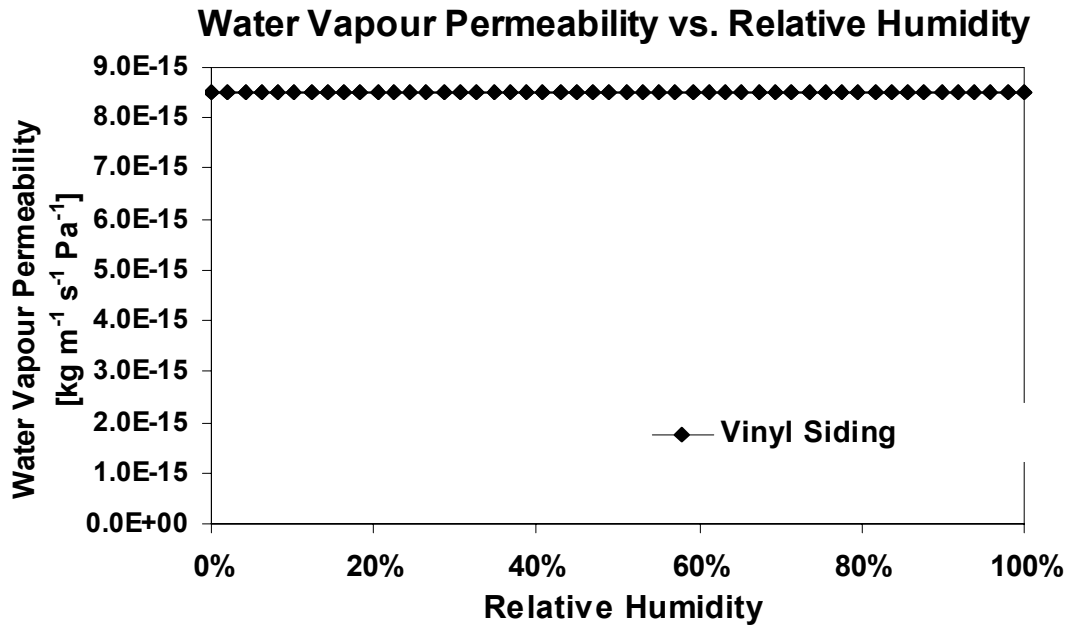


(e) 60 minute building paper

Figure D5: Suction Curve

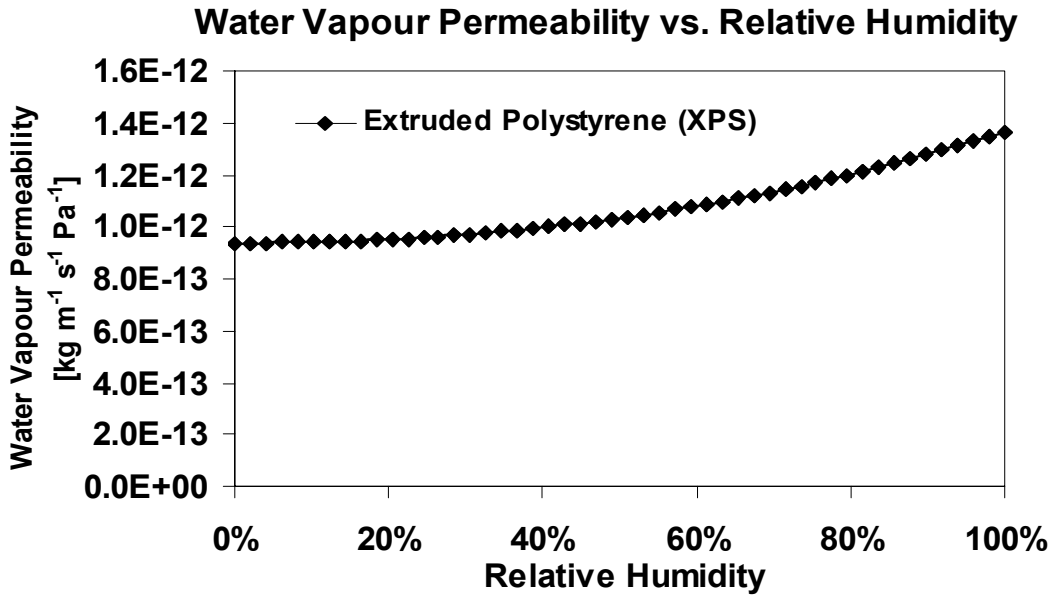


(a) Hardboard siding

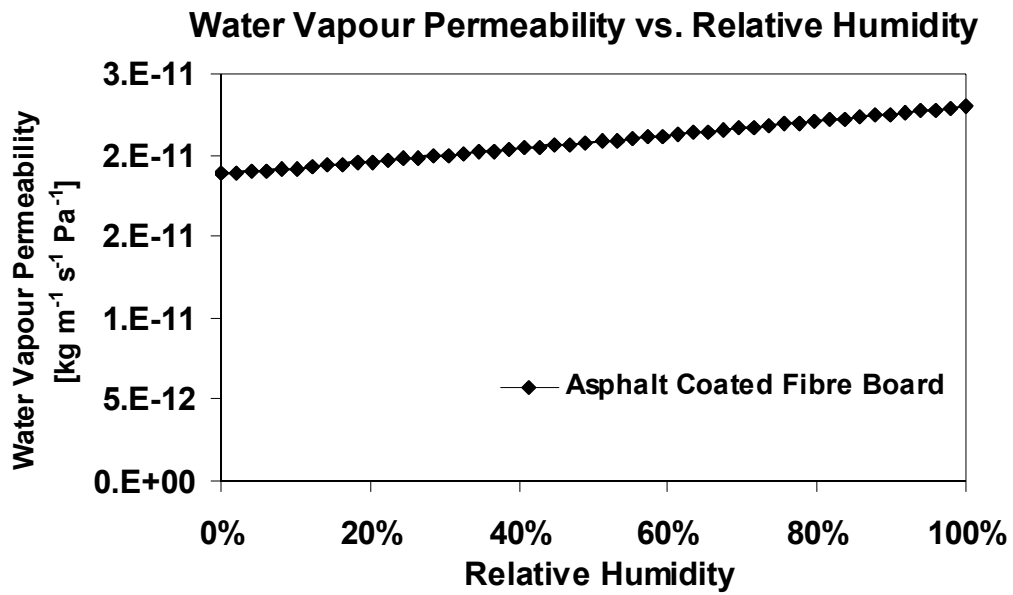


(b) Vinyl siding

Figure D6: Water Vapour Permeability

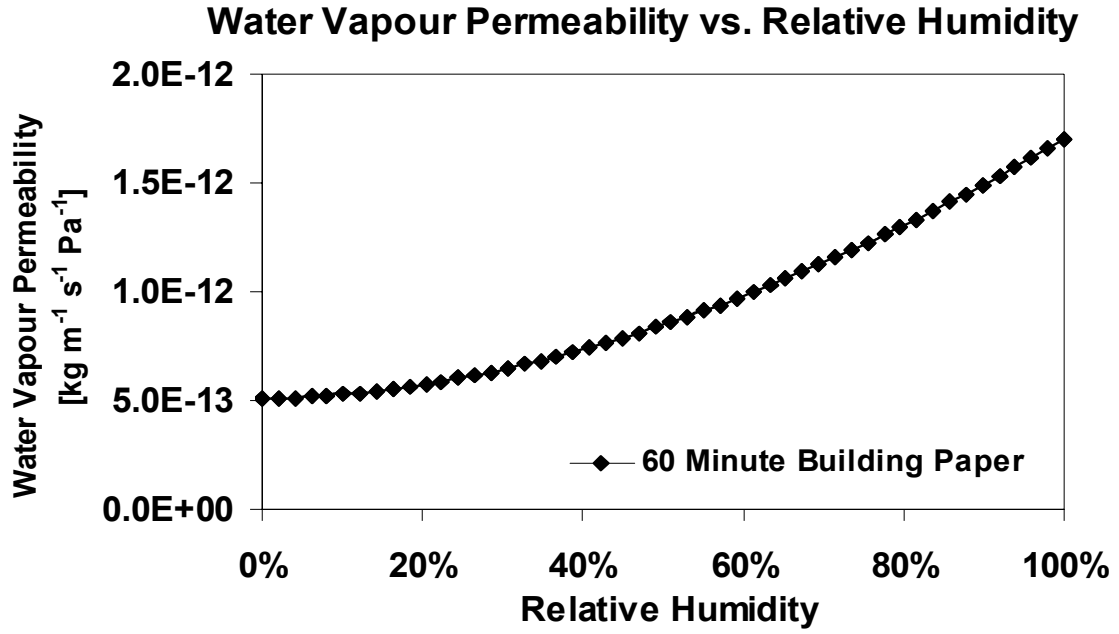


(c) Extruded polystyrene (XPS)



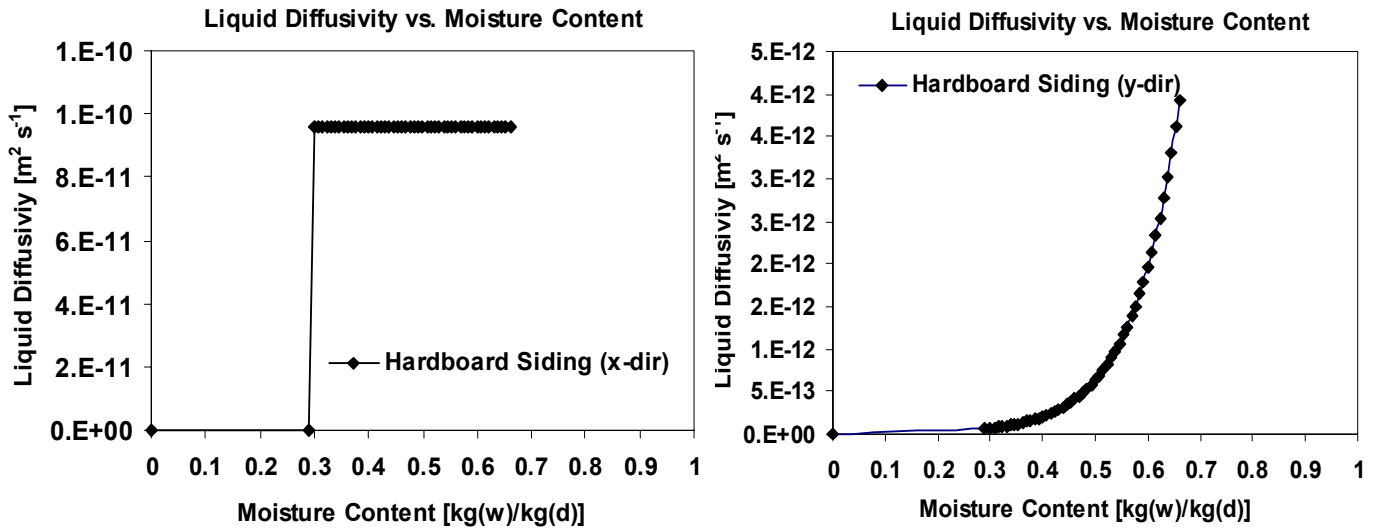
(d) Asphalt coated fibreboard

Figure D6: Water Vapour Permeability

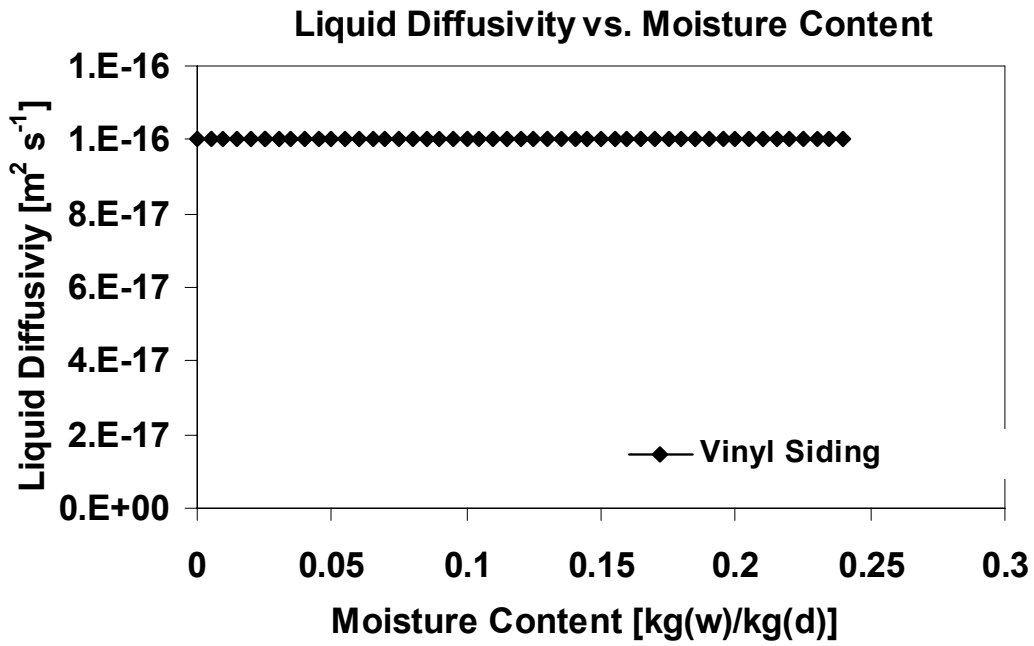


(f) 60 Minute building paper

Figure D6: Water Vapour Permeability

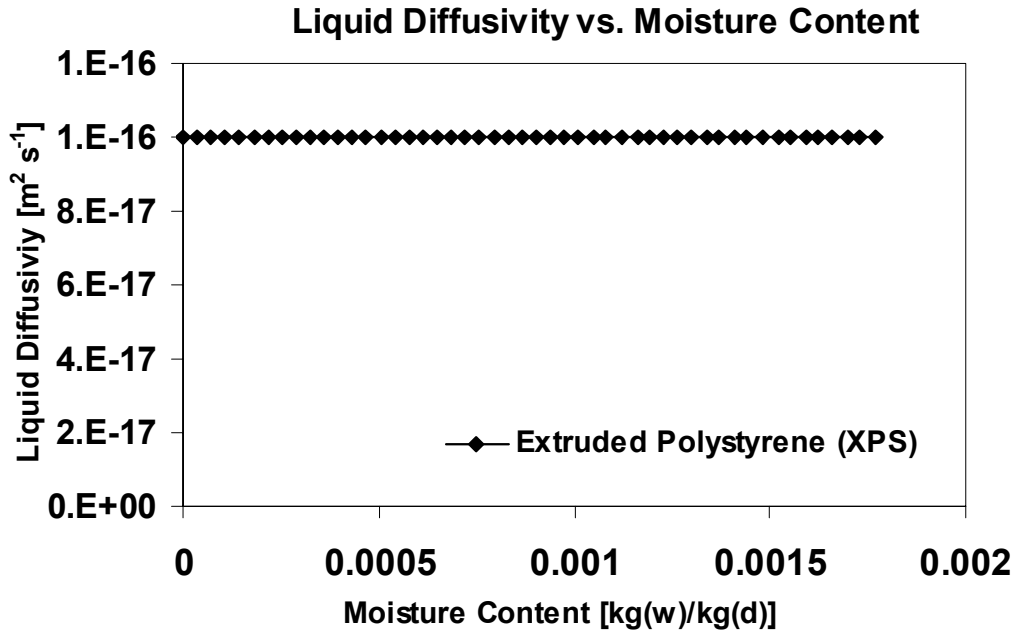


(a) Hardboard siding

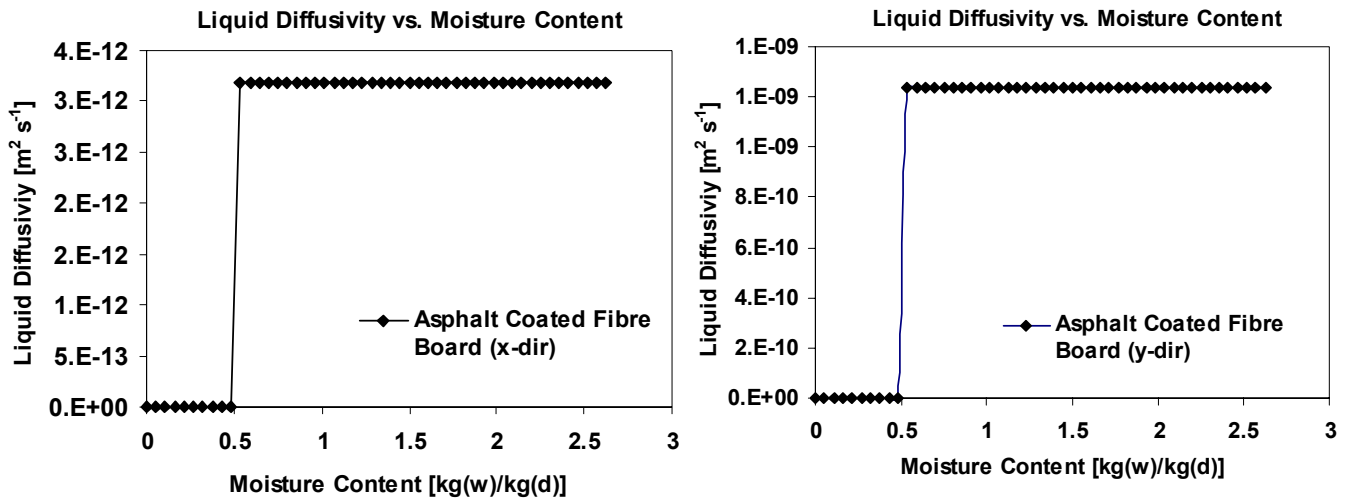


(b) Vinyl siding

Figure D7: Liquid Diffusivity

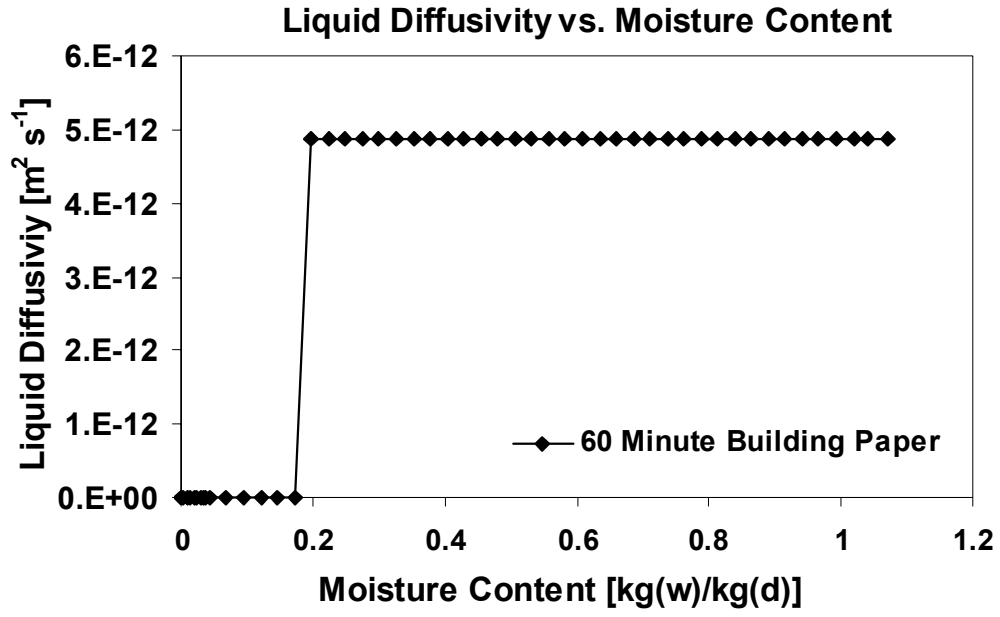


(c) Extruded polystyrene (XPS)



(d) Asphalt coated fibreboard

Figure D7: Liquid Diffusivity



(e) 60 Minute building paper

Figure D7: Liquid Diffusivity

2.3 Boundary Conditions

The indoor and outdoor boundary conditions for siding-walls are same as those for stucco walls and described in Chapter A.

2.4 Exposure Duration

The exposure duration for siding-walls is also the same as that for stucco walls. Readers should refer Chapter A for details.

2.5 Initial Moisture Content and Temperature

Initial conditions (RH and T) for siding-walls are defined in this study were based on the same principles as those described in Chapter A for stucco walls.

2.6 Accidental Moisture Entry - Quantity and Location

hygIRC has the capability to inject any quantity of accidentally entered moisture at any location of the wall and at any time. The quantity of accidentally entered moisture inside the wall and its location were determined from the output of full-scale and small-scale laboratory tests done in MEWS Task 6 (*Lacasse et al. 2002*). Each type of wall has a unique accidentally entered moisture entry function. The function used to determine the amount of accidental moisture entry inside the siding-walls is described below.

Quantity

An equation was derived from the full-scale lab results to estimate the moisture entry rate (Q). This equation depends on the pressure difference across the wall assembly (ΔP) as well as the rate of water dR_p striking the wall. The equation used for both hardboard siding and vinyl siding-clad assemblies is given below:

$$dQ/dR_p = 0.0422 + 1.618E^{-5} \cdot \Delta P - 3.88E^{-8} (\Delta P)^2 + 1.115E^{-10} (\Delta P)^3 \quad [\text{Eqn. D1}]$$

In real-life ΔP is a function of wind pressure and dR_p is representative of wind driven rain. All the parametric studies reported in this report were based on the quantity of moisture entry determined from the use of equation D1.

Location

The location of moisture entry for siding-walls was same, as it was for stucco-walls. The quantity of accidentally entered moisture determined from equation D1 was injected at the bottom of the stud cavity, on the top of the bottom plate at every hourly interval, when applicable.

3.0 Results from *hygIRC* Simulation

More than one hundred simulations were done in this study. An enormous amount of data was generated by *hygIRC* and subsequently post-processed for overall and critical evaluation of the hygrothermal response of the wall. Only selected amount of data are presented in this report for discussion. If required and requested for a stated purpose then any particular aspect of the remaining data could be made available exclusively to the MEWS partners.

The authors feel that the following points about the simulations should be clearly and unambiguously stated to before presenting the results and the related discussions:

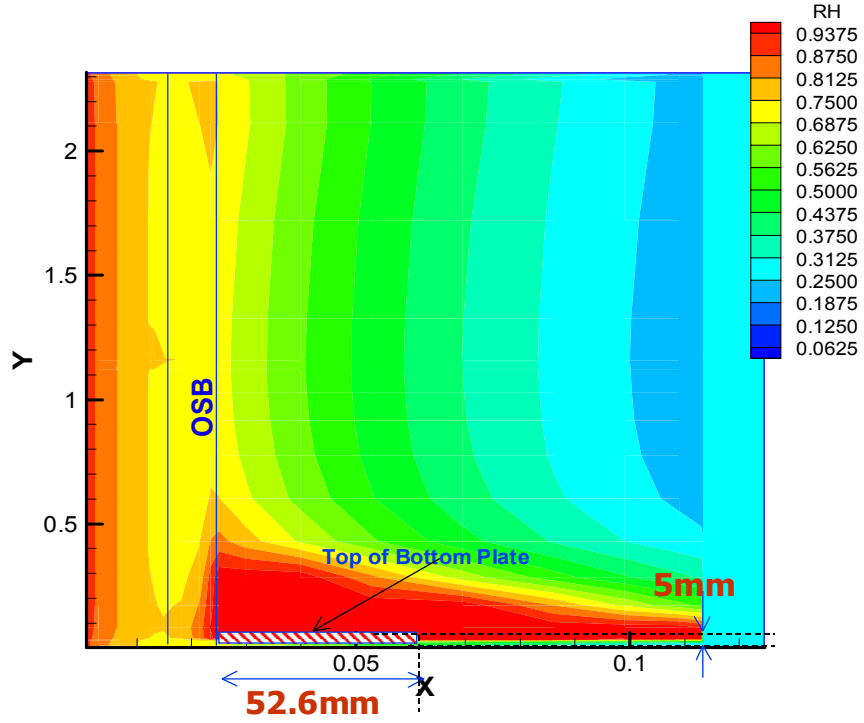
- (1) The main objective of this study is to determine the drying potential and drying characteristics of the wall assembly in case of accidentally entered moisture inside the stud/insulation cavity of the siding-walls assembly.
- (2) The materials used in the simulations are described in section 2.2 of this chapter and the corresponding sections of Chapters A and B.
- (3) Each simulation done in this study has a unique identifier. The identification codes are explained at the end of Tables D6 and D8.
- (4) All the simulations done in this study have accidental moisture entry inside the stud/insulation. One simulation however, with the letters BC appended to the end of the simulation identifier for each location has accidental moisture entry. The accidental moisture was introduced inside the cavity from the beginning of second year till the end of 3rd year.
- (5) It should be noted that all simulations done in this study have the first year (a wet year) without any accidental moisture entry. This was done to generate a realistic moisture distribution inside the wall at the end of first year.
- (6) The wall with accidental moisture entry represents a real wall with deficiency. The wall without accidental moisture entry can be considered as an ideal wall.
- (7) A total of three years simulation is done for each of the case considered in this study. However, all the simulation results are analysed based on the results of second and third year. Hence, all the discussions presented in this chapter are based on the second and third year simulation results and all the graphs represent the data for that period only.
- (8) Drying curves obtained from the simulations, after first year, are shown in Appendix D1. The moisture content in these graphs is expressed with the unit of mass of moisture per unit length (kg/m) of wall or its components entire cross section. These drying curves provide the overall dry characteristics of the whole wall and its major components.
- (9) A detailed study (microanalysis) of the hygrothermal response of the wall assembly was done by analysing relative humidity (RH) and temperature (T) contour plots shown in Figures D8a through d.
- (10) A novel concept called the RHT Index has been introduced by the researchers at IRC/NRC and was used in the parametric study to quantify and compare the localized hygrothermal response of any part of the wall and its components. The RHT index is derived from the RH and T distribution pattern (Figure D8) over a period of time for any specific area of the wall cross-section. The RHT index as defined in this study is:

$$\text{Cumulative 2 year (2}^{nd} \text{ and 3}^{rd} \text{ year) RHT} = \sum (RH - RH_X) \times (T - T_X),$$

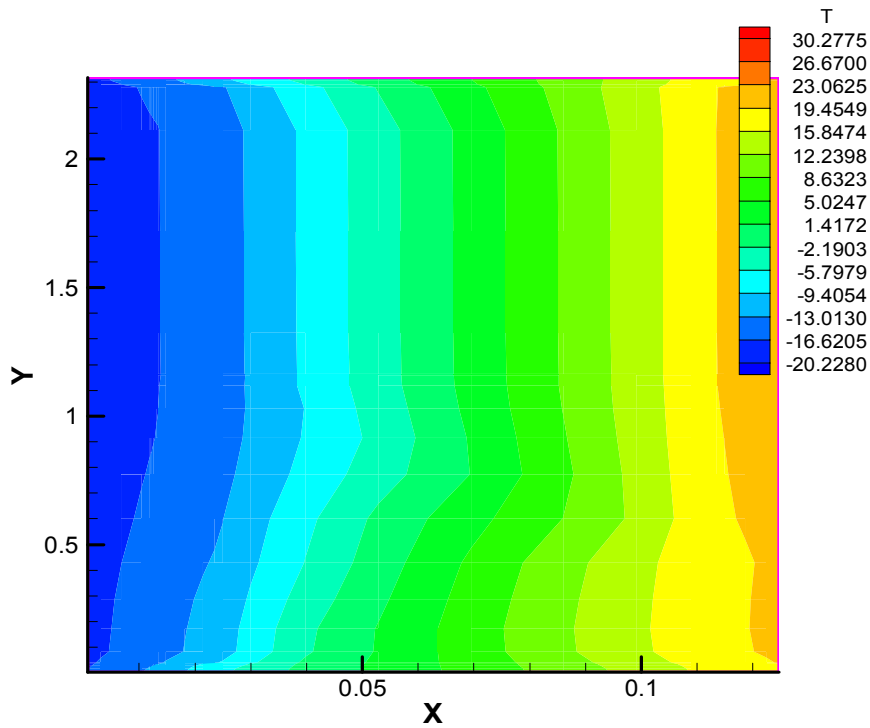
for $RH > RH_X\%$ and $T > T_X^\circ\text{C}$ at every 10 days interval [Eqn. D2]

(During any time step when either or both $RH \leq RH_X\%$ and $T \leq T_X^\circ\text{C}$, the RHT value for that time step is zero.)

Where user-defined threshold values for $RH_X = 95\%$ and $T_X = 5^\circ\text{C}$ have been chosen for this parametric study. RHT values for $RH_X=80\%$ have also been derived and presented in this report. For convenience the RHT values will be referred to as RHT(95) or RHT(80) index according to the threshold RH (i.e. RH_X) level.

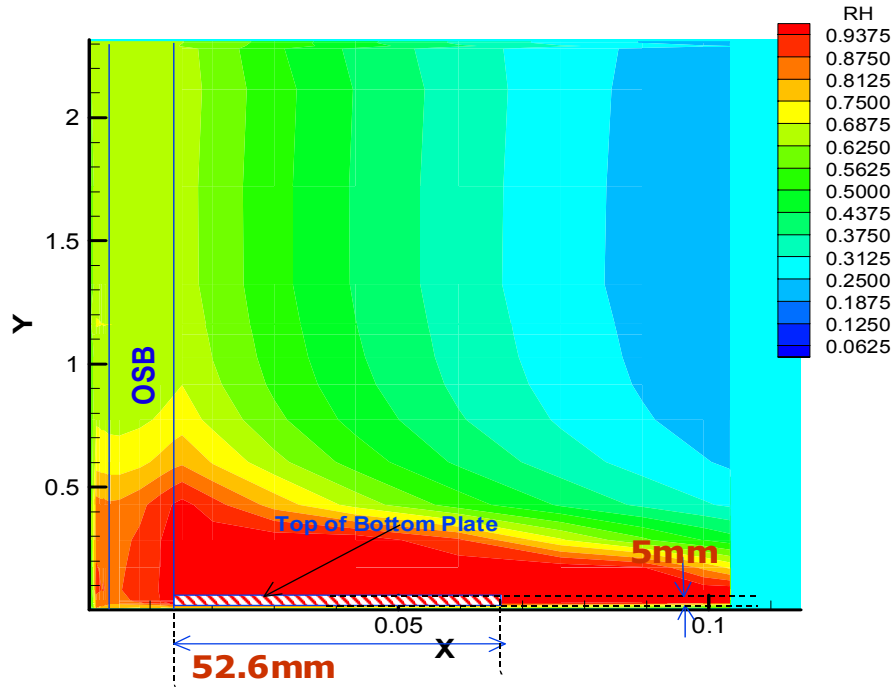


(a) Typical relative humidity contour plot - hardboard siding (width of the wall expanded)

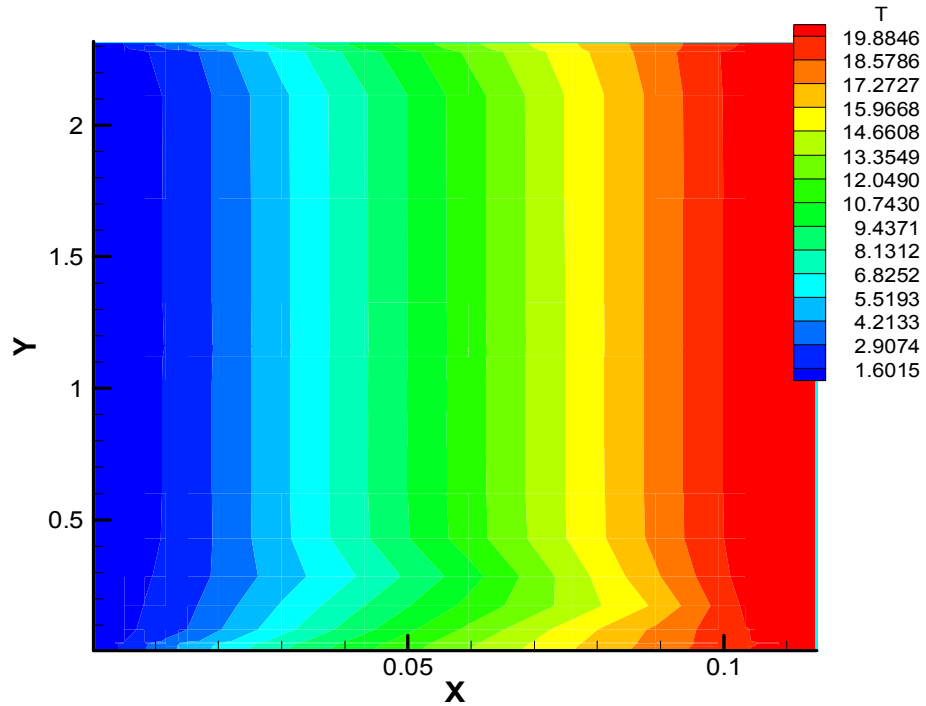


(b) Typical temperature contour plot - hardboard siding (width of the wall expanded)

Figure D8: RH and T Contour Plots



(c) Typical relative humidity contour plot - vinyl siding (width of the wall expanded)



(d) Typical relative humidity contour plot - vinyl siding (width of the wall expanded)

Figure D8: RH and T Contour Plots

- (11) 'Region of focus' is the area for which the RHT index is calculated. This area is the wettest portion of the wall assembly most of the time (see Figures D8a and D8c). For siding-wall simulations, both for hardboard and vinyl, presented in this report for parametric study, the 'region of focus' is a thin slice (5 mm) of the top surface of the bottom plate, extending 53 mm from the sheathing board (see Figure D8a and D8c).
- (12) The RHT index brings out the overall localized combined moisture and temperature response of the selected area of the material or wall assembly. For overall drying and wetting pattern of the siding-walls, at any point of time. Interested readers should look at the drying curves given in Appendix D1.

Table D6: RHT (80) Results for Hardboard-clad Walls
 (Top of the bottom plate - Region of focus; Equation D1)

Simulation ID	RHT (80) Index	Simulation ID	RHT (80) Index	Simulation ID	RHT (80) Index	Simulation ID	RHT (80) Index
(A) OTTAWA							
OTO8HSBC	0	(C) SEATTLE					
OTO8HS	9548	SEO8HSBC	0				
OTSM25HS	9552	SEO8HS	13939				
OTVB7HS	9333	SESM25HS	13943				
OTO8HSCG	6770	SEVB7HS	13373				
OTP18HS	9199	SEO8HSCG	8079			(G) SAN DIEGO	
OTF16HS	9893	SEP18HS	13439			SDO8HSBC	0
OTO8HSW2	9146	SEF16HS	14311			SDO8HS	16579
OTO8HSW4	6648	SEO8HSW2	13349	(E) WINNIPEG		SDP18HS	14431
OTO8HSCB	10223	SEO8HSW4	10217	WPO8HSBC	0	SDF16HS	11682
OTO8HSCBW4	3430	SEO8HSCB	14753	WPO8HS	8377	SDO8HSW2	9033
OTAF26HS	9011	SEO8HSCBW4	7219	WPSM25HS	8380	SDO8HSW4	3719
		SEAF26HS	13212	WPVB7HS	8244	SDVB7HS	10780
				WPO8HSCG	7008		
				WPP18HS	8029		
				WPF16HS	8604		
				WPO8HSW2	8019		
				WPO8HSW4	6706		
		(D) WILMINGTON		WPO8HSCB	8935		
		WIO8HSBC	0	WPO8HSCBW4	5123		
		WIO8HS	18772	WPAF26HS	7793		
		WISM25HS	18766				
		WIVB7HS	18449				
		WIO8HSCG	12837				
		WIP18HS	18365				
		WIF16HS	18971	(F) FRESNO			
		WIO8HSW2	18177	FRO8HSBC	0		
		WIO8HSW4	17209	FRO8HS	9017		
		WIO8HSCB	18458	FRF16HS	7434		
		WIO8HSCBW4	11901	FRO8HSW2	4941		
		WIAF26HS	18158	FRO8HSW4	1758		
				FRVB7HS	6187		
(B) PHOENIX							
PHO8HSBC	0						
PHO8HS	7668						
PHSM25HS	7515						
PHVB7HS	5108						
PHO8HSCG	2104						
PHP18HS	6366						
PHF16HS	5361						
PHO8HSW2	15534						
PHO8HSW4	23994						
PHO8HSCB	8162						
PHO8HSCBW4	21550						
PHAF26HS	5744						

Notation

**O8HSBC :	Base case; No moisture entry; OSB sheathing Board
**O8HS :	Same as **O8HSBC but with moisture entry
**SM25HS :	Same as **O8HS but SBPO polymeric sheathing membrane is replaced by 60 minute building paper
**VB7HS :	Same as **O8HS but Type I vapour barrier is replaced by a vapour barrier that has vapour permeance variable with relative humidity
**O8HSCG :	Same as **O8HS but with no vapour barrier and with painted/coated interior gypsum board.
**P18HS :	Same as **O8HS but with OSB sheathing board is replaced by plywood
**F16HS :	Same as **O8HS but with OSB sheathing board is replaced by fibreboard
**O8HSW2 :	Same as **O8HS but with half of the normal moisture entry (only exception is Phoenix with double moisture entry)
**O8HSW4 :	Same as **O8HS but with quarter of the normal moisture entry (only exception is Phoenix with quadruple moisture entry)
**O8HSCB:	Same as **O8HS but with a 19mm cavity behind the siding

** : PH - Phoenix; FR - Fresno; SD - San Diego; WP - Winnipeg; OT - Ottawa; SE - Seattle;
 WI :- Wilmington

Table D7: RHT (95) Indices for Vinyl-clad Walls
 (Top of the bottom plate - Region of focus; Equation D1)

Simulation ID	RHT (95) Index	Simulation ID	RHT (95) Index	Simulation ID	RHT (95) Index	Simulation ID	RHT (95) Index
(A) OTTAWA						FRX20VSXW4	291
OTO8VSBC	0	(C) SEATTLE				FRSM21VSXW4	268
OTO8VS	1477	SEO8VSBC	0			FRSM0VSXW4	295
OTO8VSW2	1388	SEO8VS	2195				
OTO8VSW4	1118	SEO8VSW2	2046			(G) SAN DIEGO	
OTO8VSW6	254	SEO8VSW4	1494			SDO8VSBC	0
OTO8VSW8	5	SEO8VSW6	829			SDO8VS	3192
OTSM21VSW4	1112	SEO8VSW8	221			SDO8VSW2	2262
OTVB6VSW4	807	SESM21VSW4	1464			SDO8VSW4	247
OTO8VSCGW4	59	SEVB6VSW4	975	(E) WINNIPEG		SDO8VSW6	0
OTSM21VSXW4	2125	SEO8VSCGW4	140	WPO8VSBC	0	SDO8VSW8	0
OTSM0VSXW4	2130	SEX20VSXW4	2761	WPO8VS	1284	SDSM21VSW4	226
		SESM21VSXW4	2712	WPO8VSW2	1168	SDVB6VSW4	176
		SESM0VSXW4	2693	WPO8VSW4	948	SDX20VSXW4	960
				WPO8VSW6	619		
				WPO8VSW8	217		
				WPSM21VSW4	950		
				WPVB6VSW4	898		
		(D) WILMINGTON		WPO8VSCGW4	143		
		WIO8VSBC	0	WPX20VSXW4	1681		
		WIO8VS	3138	WPSM21VSXW4	1690		
		WIO8VSW2	2857				
		WIO8VSW4	2431				
		WIO8VSW6	1869				
		WIO8VSW8	1616	(F) FRESNO			
		WISM21VSW4	2422	FRO8VSBC	0		
		WIVB6VSW4	2134	FRO8VS	1752		
		WIO8VSCGW4	45	FRO8VSW2	534		
		WIO8VSCBW4	1366	FRO8VSW4	47		
		WIX20VSXW4	3477	FRO8VSW6	0		
		WISM21VSXW4	3474	FRO8VSW8	0		
		WISM0VSXW4	3475	FRSM21VSW4	45		
				FRVB6VSW4	31		
(B) PHOENIX							
PHO8VSBC	0						
PHO8VS	1072						
PHO8VSW2	66						
PHO8VSW4	0						
PHO8VSW6	0						
PHO8VSW8	0						
PHSM21VSW4	0						
PHVB6VSW4	0						
PHO8VSCGW4	0						
PHX20VSXW4	0						
PHSM21VSXW4	0						
PHSM0VSXW4	0						

Table D8: RHT (80) Results for Vinyl-clad Walls
 (Top of the bottom plate - Region of focus; Equation D1)

Simulation ID	RHT (80) Index	Simulation ID	RHT (80) Index	Simulation ID	RHT (80) Index	Simulation ID	RHT (80) Index
(A) OTTAWA						FRX20VSXW4	4187
OTO8VSBC	0	(C) SEATTLE				FRSM21VSXW4	4026
OTO8VS	8672	SEO8VSBC	0			FRSM0VSXW4	4146
OTO8VSW2	8438	SEO8VS	12620				
OTO8VSW4	7868	SEO8VSW2	12257			(G) SAN DIEGO	
OTO8VSW6	6246	SEO8VSW4	11314			SDO8VSBC	0
OTO8VSW8	3690	SEO8VSW6	8451			SDO8VS	19197
OTSM21VSW4	7859	SEO8VSW8	5637			SDO8VSW2	17808
OTVB6VSW4	7490	SESM21VSW4	11214			SDO8VSW4	6965
OTO8VSCGW4	2237	SEVB6VSW4	9499	(E) WINNIPEG		SDO8VSW6	1969
OTSM21VSXW4	13764	SEO8VSCGW4	3461	WPO8VSBC	0	SDO8VSW8	483
OTSM0VSXW4	13771	SEX20VSXW4	18251	WPO8VS	7548	SDSM21VSW4	6404
		SESM21VSXW4	18030	WPO8VSW2	7253	SDVB6VSW4	4536
		SESM0VSXW4	17977	WPO8VSW4	6499	SDX20VSXW4	11435
				WPO8VSW6	5619		
				WPO8VSW8	4665		
				WPSM21VSW4	6507		
				WPVB6VSW4	6386		
		(D) WILMINGTON		WPO8VSCGW4	3925		
		WIO8VSBC	0	WPX20VSXW4	11436		
(B) PHOENIX		WIO8VS	17581	WPSM21VSXW4	11412		
PHO8VSBC	0	WIO8VSW2	16995				
PHO8VS	12076	WIO8VSW4	16137				
PHO8VSW2	2280	WIO8VSW6	14091				
PHO8VSW4	0	WIO8VSW8	11876				
PHO8VSW6	0	WISM21VSW4	16145	(F) FRESNO			
PHO8VSW8	0	WIVB6VSW4	15510	FRO8VSBC	0		
PHSM21VSW4	0	WIO8VSCGW4	3376	FRO8VS	13556		
PHVB6VSW4	0	WIO8VSCBW4	12315	FRO8VSW2	5234		
PHO8VSCGW4	96	WIX20VSXW4	21222	FRO8VSW4	1194		
PHX20VSXW4	1403	WISM21VSXW4	21222	FRO8VSW6	218		
PHSM21VSXW4	1303	WISM0VSXW4	21239	FRO8VSW8	0		
PHSM0VSXW4	1329			FRSM21VSW4	1100		
				FRVB6VSW4	934		

Notation

**O8VSBC :	Base case; No moisture entry; OSB sheathing Board
**O8VS :	Same as **O8VSBC but with full moisture load entry
**O8VSW2 :	Same as **O8VSBC but with 1/2 (half) moisture load entry
**O8VSW4 :	Same as **O8VSBC but with 1/4 th (quarter) moisture load entry
**O8VSW6 :	Same as **O8VSBC but with 1/6 th (one sixth) moisture load entry
**O8VSW8 :	Same as **O8VSBC but with 1/8 th (one eighth) moisture load entry
**O8SM21VSW4 :	Same as **O8VSW4 but 30 minute building paper sheathing membrane is replaced by SBPO membrane
**O8VB6VSW4 :	Same as **O8VSW4 but Type I vapour barrier replaced by Type II vapour barrier
**O8VSCGW4 :	Same as **O8VSW4 but with no vapour barrier and with painted/coated interior gypsum board.
**O8VSCBW4 :	Same as **O8VSW4 but 1mm air gap behind the siding is replaced by a 19mm cavity.
**X20VSXW4 :	Same as **O8VSW4 but OSB sheathing board is replaced by XPS foam sheathing.
**SM0VSXW4 :	Same as **X20VSXW4 but 30 minute building paper sheathing membrane is replaced by SBPO membrane
**SM21VSXW4 :	Same as **X20VSXW4 but 30 minute building paper sheathing membrane is removed (i.e. no sheathing membrane)

** : PH - Phoenix; FR - Fresno; SD - San Diego; WP - Winnipeg; OT - Ottawa; SE - Seattle;
 WI :- Wilmington

3.1 Results from Parametric Studies

Results from the parametric studies are to be discussed here primarily with the RHT(95) values from Tables D5 and D7. However, in qualitative sense, the observations would be same if RHT(80) is to be used instead of RHT(95). All the parameters related to hardboard siding-wall are to be discussed first and then the discussion on vinyl siding-wall.

Hardboard Siding:

3.1.1 Sheathing board (hardboard siding-wall)

The three sheathing boards considered in this study were OSB, plywood and uncoated fibreboard. The OSB (OSB I, see section 2.2 in Chapter A) that was chosen has a water vapour permeability value at 100% relative humidity that represents approximately the mean of the other two OSBs (II and III).

The simulation IDs for three sheathing boards are: **O8HS - OSB, **P18HS - Plywood and **F16HS - Uncoated fibreboard.

As can be seen in Table D5 and Figure D9 there was very little difference in moisture response, in terms of RHT(95) index, due to the variation in the type of sheathing board used in hardboard siding-wall.

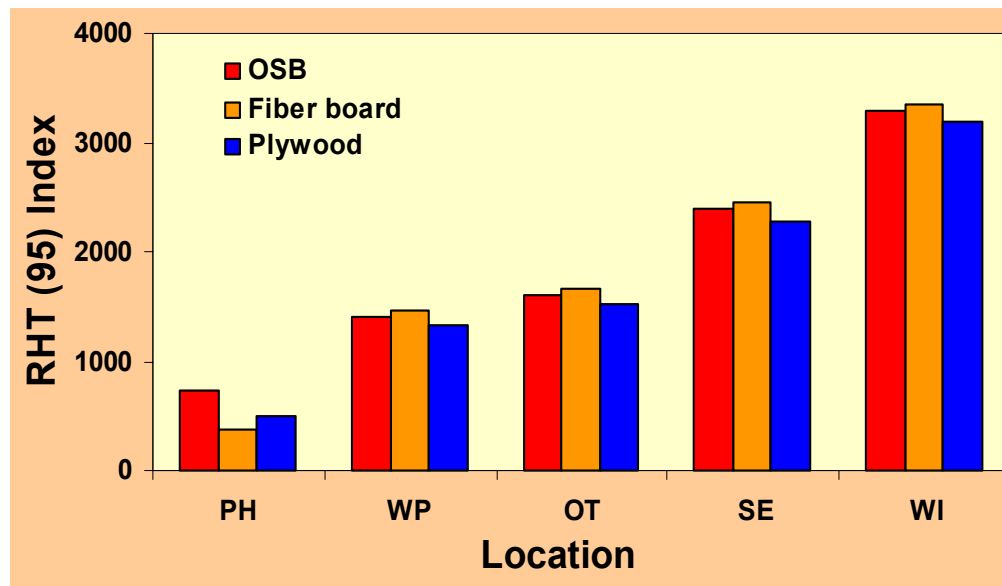


Figure D9: Sheathing boards in hardboard siding

In addition to the three sheathing boards one of the MEWS client members suggested that asphalt coated fibreboard should also be considered as a sheathing board (simulation ID: **AF26HS). The results from the simulation show (Table D5) that the use of asphalt coated fibreboard had no significant influence on the RHT(95) index of hardboard siding-wall, except in dry climates place (e.g. Phoenix).

3.1.2 Sheathing membrane (hardboard siding-wall) (2 types: SBPO polymeric membrane and 60 minute building paper)

The two sheathing membranes considered were SBPO polymeric membrane and 60 minute building paper (simulation IDs: **O8HS and **SM25HS). Properties of these two sheathing membranes are shown in section 2.2. The results, in terms of the RHT(95) index, in Table D5 and Figure D10 show that there was little or no difference in the moisture response due to these two different sheathing membranes.

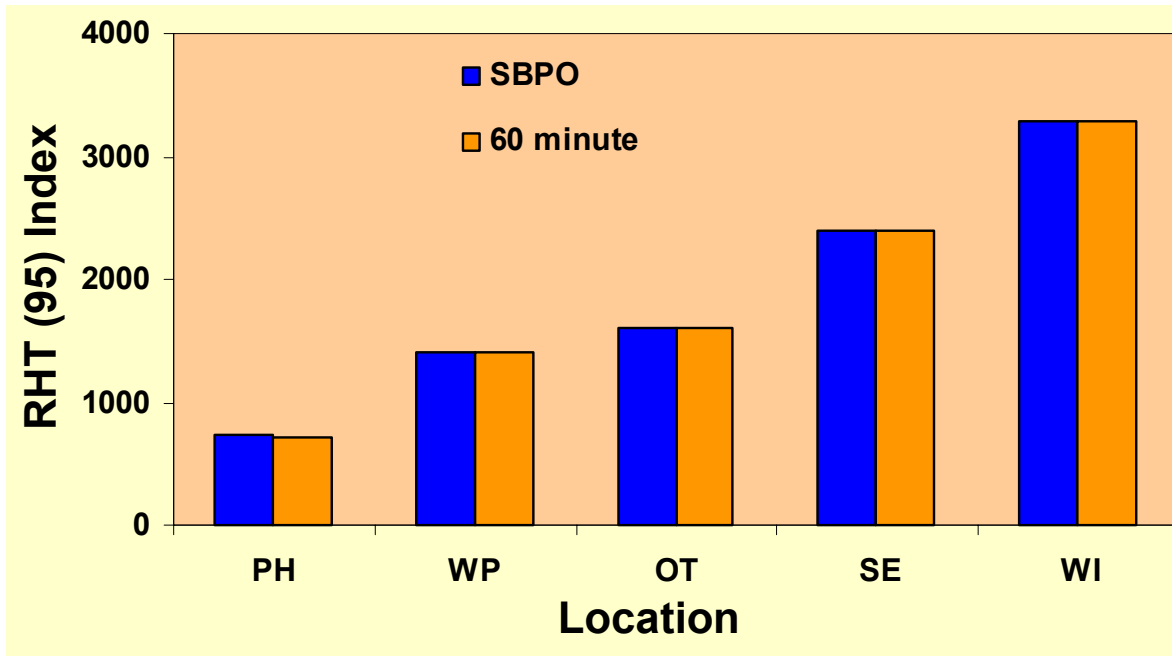


Figure D10: Sheathing membranes in hardboard siding

3.1.3 Vapour barrier (hardboard siding-wall)

Two types of vapour barriers were considered in this study. These two vapour barriers were: (1) Type I, and (2) Variable. A Type I vapour barrier (see Chapter A for details on the material properties) has a constant water vapour permeance of 15 ng/Pa.s.m². The variable type vapour barrier (same as vapour barrier III in Chapter A) is one where the water vapour permeance value is a function of relative humidity and varying between 30 and 320 ng/Pa.s.m². The simulation identifiers are **O8HS for Type I and **VB7HS for variable type. The results shown in Table D5 indicate that higher water vapour permeance value of vapour barrier resulted in lower values of the RHT(95) index. This reduction was small in locations with higher moisture index (MI).

3.1.4 Locations with seven different Moisture Indices (hardboard siding-wall)

The fundamentals behind the moisture index (MI) (see section 3.1.5 of Chapter A) and its values for most of the major locations in North America are given in the report from MEWS Task 4 (Cornick *et al* 2002). Seven locations were chosen for parametric study and the MI values for these cities vary over a wide range as shown below:

<u>Location:</u>	<u>Moisture Index (MI)</u>
Wilmington:	1.13
Seattle:	0.99
Ottawa:	0.93

Winnipeg:	0.86
San Diego:	0.74
Fresno:	0.49
Phoenix:	0.13

The variations of RHT(95) values at different MI with full quantity (Q) of accidental moisture entry inside the stud cavity and also without any accidental moisture entry (i.e. wall without any deficiency) are shown in Figure D11a. Note that with the full quantity (Q) of accidental moisture entry the relationship between RHT(95) and MI does follow a general trend of gradual increase, except the RHT(95) index value for San Diego (Figure D11a). However, if the quantity of accidental moisture entry is halved (i.e. Q/2) then the familiar relationship of a nonlinear increase of the value the RHT(95) index with increasing MI becomes very clear (Figure D11b). Further analysis of the RH and T profile (see Task 8 report for details) over the entire time span reveals that there is an upper and lower limit of the quantity of moisture load for which the gradual incremental relationship between RHT index and MI is valid. The full quantity of accidental moisture entry load (Q) crosses that limit and hence, the 'region of focus' becomes 'too wet' to reflect the RH and T variation effect together on the RHT index. In such a situation RHT index shows only the temperature variation effect and the RHT value will deviate to a higher value. On the other hand if the quantity of accidental moisture entry is too small then also it fails to reflect the RH variation effect and the RHT value will deviate to a lower value. It appears that Q/2 falls in the range of accidental moisture entry that can reflect effects of RH and T together (Figure D11b). Further discussion on this issue can be found in the report from Task 8 (*Beaulieu et al. 2002*).

3.1.5 Accidental moisture entry inside the wall (hardboard siding-wall)

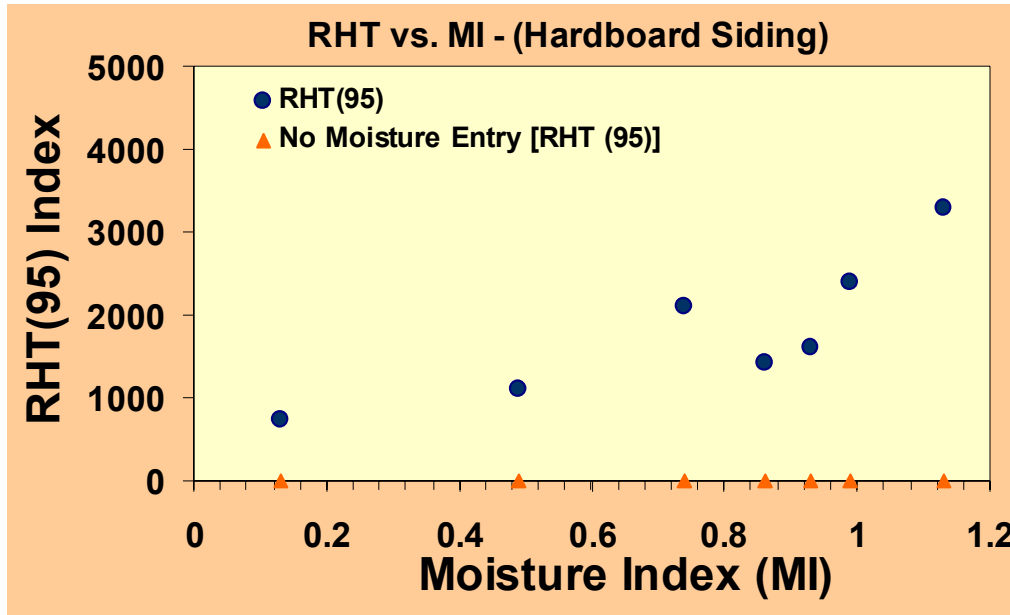
Figure C10a indicates that without accidental moisture entry the RHT(95) index in all the seven locations was zero. However, when accidental moisture entry was considered the RHT(95) index increases with the increase of MI (Table D5).

3.1.6 Quantity of accidental moisture entry (hardboard siding-wall)

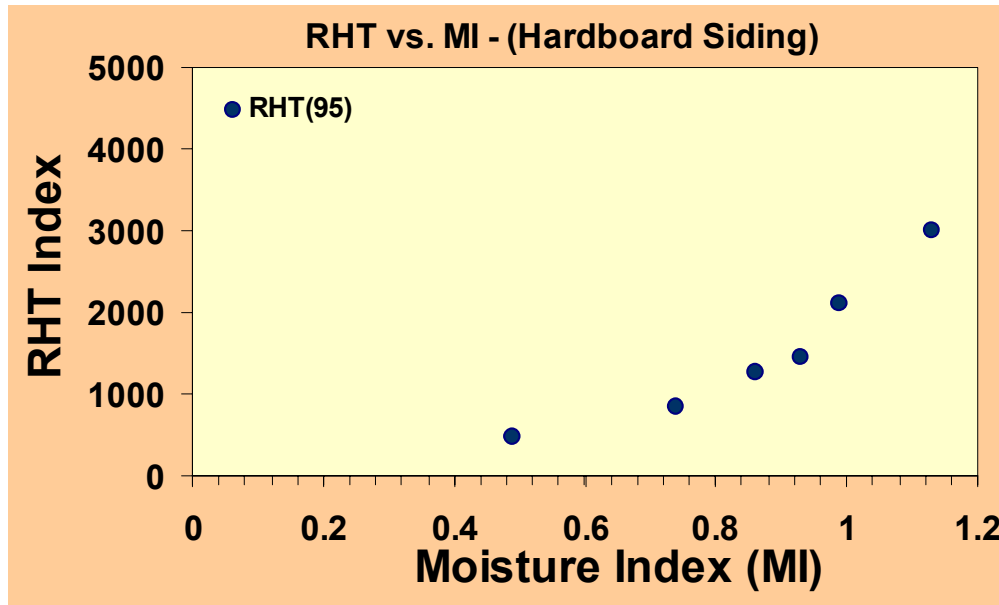
The effect of different amounts of accidental moisture entry inside the wall on the moisture response of the hardboard siding-walls, in terms of RHT(95) index, can be seen in Figure D12. In general it can be said that the severity of the moisture response is a function of quantity of accidental moisture entry inside the wall.

3.1.7 Use of coated gypsum board with no vapour barrier (hardboard siding-wall)

Simulations were done where gypsum board coated with a primer and latex paint has been considered as the vapour control strategy. The hygrothermal properties of such coated gypsum board are given in section 2.2 of Chapter A. The permeance of this coated gypsum board is about 8 times higher than that of the variable type vapour barrier no. III (at 100%RH). The general simulation ID is **O8HSCG (see Table D5). The simulation results show that there were noticeable drops in the RHT(95) values in all the locations. Before any general conclusions can be drawn more cases with different interior RH profiles must be done. Specifically only one interior boundary condition was considered 55% summer RH and 25% winter RH. The interior boundary condition assumption may be too conservative for wetter and more humid climates.



(a) RHT(95) vs. MI plot for the full quantity (Q) and no accidental moisture entry



(b) RHT(95) vs. MI plot for half of the full quantity (Q/2) of accidental moisture entry

Figure D11: Variation of RHT(95) at different locations (hardboard siding)

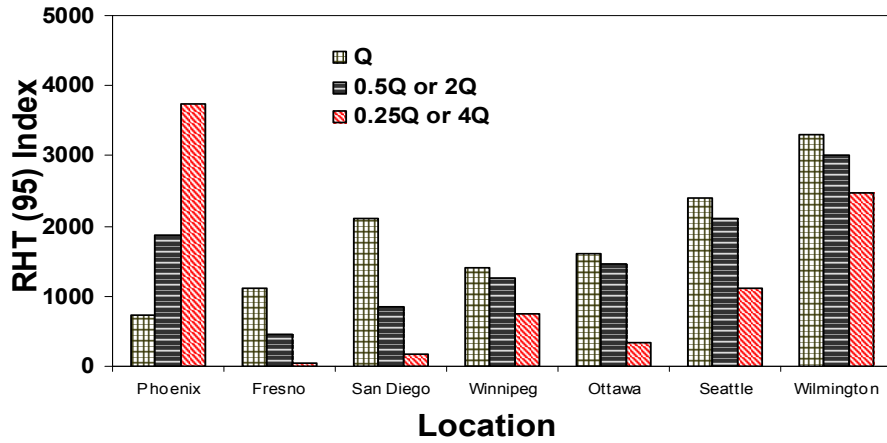
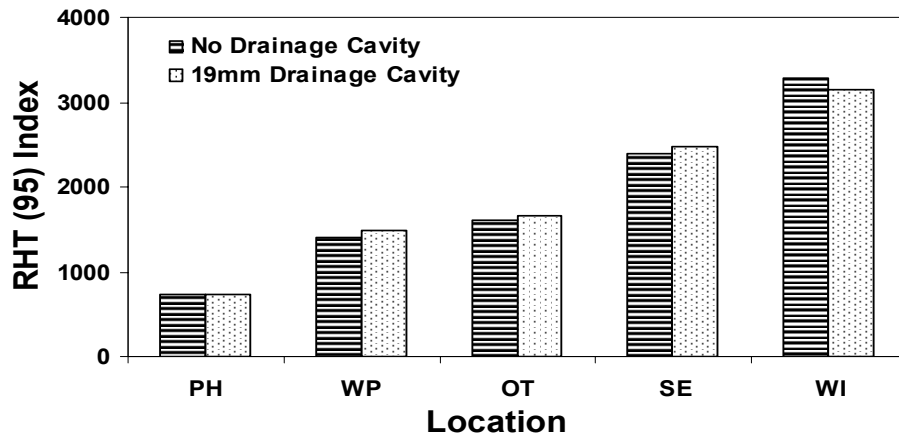
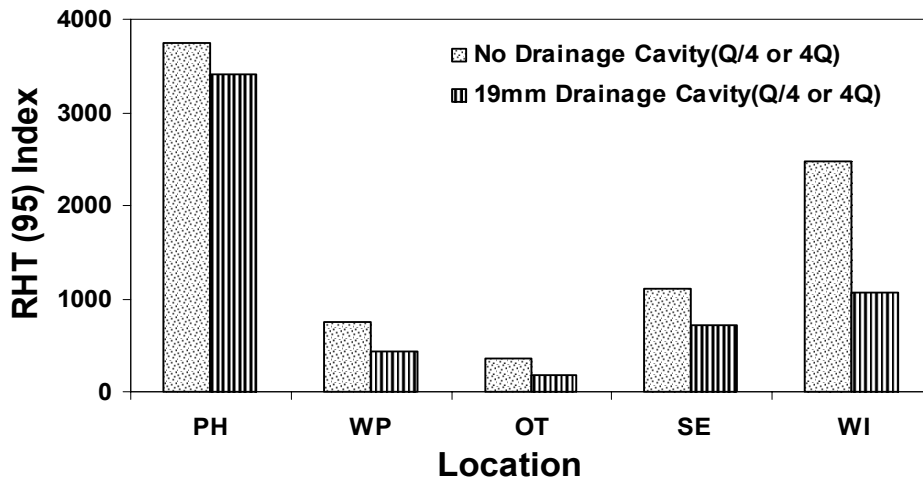


Figure D12: Variation of RHT(95) for different quantity of accidental moisture entry (hardboard siding)



(a) Effect of drainage cavity - Full quantity (Q) of accidental moisture entry



(b) Effect of drainage cavity - 1/4th quantity (Q/4) or 4-times (4Q for Phoenix only) of accidental moisture entry

Figure D13: Effect of drainage cavity (hardboard siding)

3.1.8 Presence of 19mm ventilation cavity inside the wall (i.e. behind the exterior cladding) (hardboard siding-wall)

It was expected that the introduction of an air ventilation cavity behind the exterior cladding would improve the drying characteristics of the wall assembly. Typically a 19-mm wide cavity (Figure D2) was considered in this investigation. The cavity has both bottom (entire 19-mm) and top (3-mm) opening. The simulations were done with the two quantities of accidental moisture entry (Table D5).

The RHT(95) results in Table D6 and Figure D13 show that introduction of cavity behind the stucco helped to reduce the RHT(95) index for the hardboard siding-wall. However, this effect is more significant when quantity of accidental moisture entry was lower (i.e. Q/4 instead of Q). This is evident if the results shown in Figure D13a and Figure D13b are compared.

Vinyl Siding:

3.1.9 Accidental moisture entry inside the wall (vinyl siding-wall)

Results in Table D7 show that without accidental moisture entry, the moisture response of the vinyl siding-wall did not cross the RHT(95) threshold (i.e. RHT(95)=0) in all the seven locations considered. However, when accidental moisture entry is taken into account, the RHT(95) index crossed the zero threshold (i.e. RHT(95)>0) in all the locations considered in this study (Table D7).

3.1.10 Quantity of accidental moisture entry (vinyl siding-wall)

The quantity of accidental moisture, as determined from equation C1, was found to be quite high (more about this in the discussion on the next parameter). Hence, a number of quantities of accidental moisture entry were considered, ranging from full (Q) quantity to 1/8th of the full quantity (Q/8). The results in Table D7 and Figure D14 show that there is a non-linear relationship between RHT(95) index and the quantity of accidental moisture entry inside the stud/insulation cavity of vinyl siding-wall.

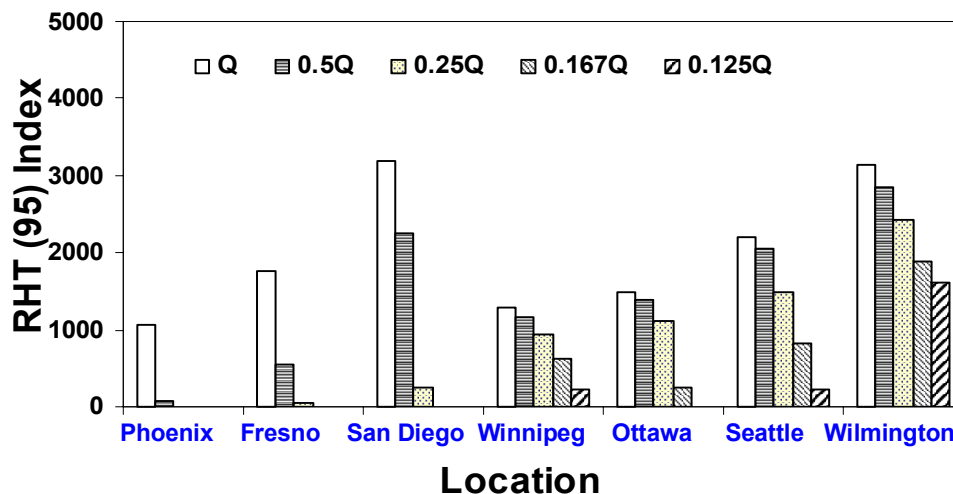


Figure D14: Variation of RHT(95) for different quantity of accidental moisture entry (vinyl siding)

3.1.11 Locations with seven different Moisture Indices (vinyl siding-wall) (MI)

The variations of RHT(95) values at different MI with five different amounts of accidentally entered moisture inside the stud/insulation cavity and also without any accidental moisture entry (i.e. wall without any deficiency) are shown in Figure D15 and in Table D7. It is very evident from Figure D15 that Q/4 was the quantity of accidentally entered quantity of moisture that falls in the range that can reflect effects of RH and T together. Further discussion on this issue can be found in the report from Task 8 (Beaulieu et al. 2002). In this study all other parametric studies were done based on the accidentally entered moisture quantity Q/4.

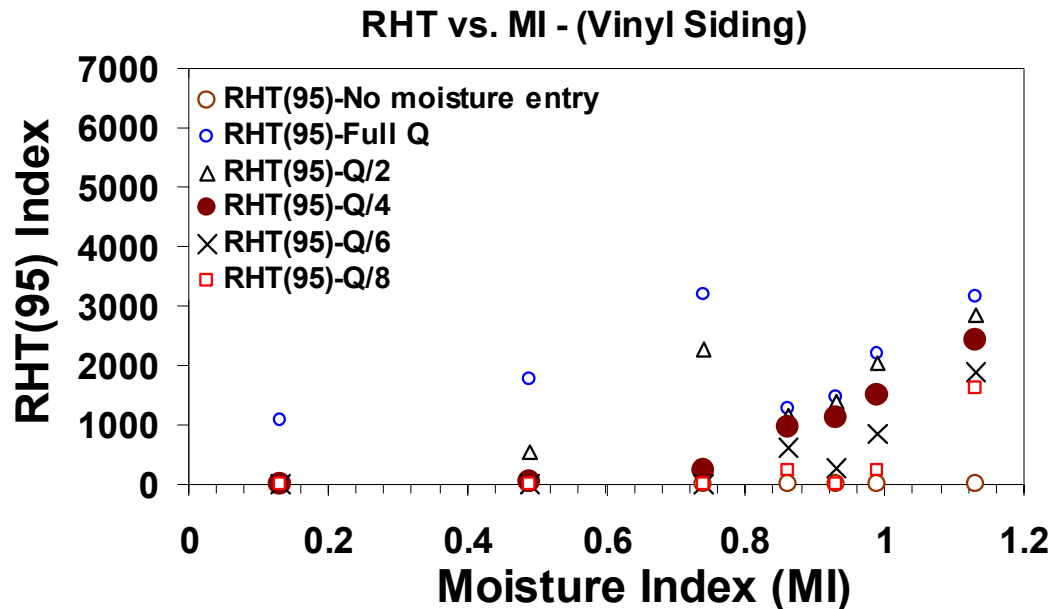


Figure D15: Variation of RHT(95) at different locations (vinyl siding)

3.1.12 Sheathing board (vinyl siding-wall)

Two types of sheathing boards considered in the study were OSB and extruded polystyrene (XPS) foam board. The OSB (OSB I, see section 2.2 in Chapter A) that was chosen has a water vapour permeability value at 100% relative humidity that represents approximately the mean of the other two OSBs (II and III). The vinyl siding-wall with OSB sheathing board (simulation ID: **SM21VSW4) had a SBPO sheathing membrane. The XPS sheathing board thickness was 36mm and the wall had a SBPO sheathing membrane (simulation ID: **SM21VSXW4). The results in Table D7 clearly indicate that XPS sheathing board produced a higher RHT(95) index.

3.1.13 Sheathing membrane (vinyl siding-wall)

SBPO polymeric membrane and 30 minute building paper were the two sheathing membranes that were considered in this study. The general simulation ID for 30 minute building paper is **O8VSW4 and the same for SBPO polymeric membrane is **SM21VSW4. Both these walls were clad with OSB sheathing board. The results from the simulation (Table D7) show that there was no significant difference in moisture response, in terms of RHT(95) index, due to two different sheathing membranes.

The above two simulations are using XPS sheathing board instead of OSB sheathing board (simulation Ids: **X20VSXW4 and **SM21VSXW4). Results (Table D7)

indicated that there was little difference in moisture response due to the use of two different sheathing membranes.

One case study was also been done where XPS sheathing board was used without any sheathing membrane (simulation ID: **SM0VSW4). The simulation results indicated that there was no effect on the RHT(95) index due to the removal of sheathing membrane from a vinyl siding-wall.

3.1.14 Vapour barrier (vinyl siding-wall)

Vapour barriers I and II from the Chapter A were the two vapour barriers considered in this study. Vapour barrier I has a constant water vapour permeance of 15 ng/Pa.s.m² and Vapour barrier II has a constant water vapour permeance of 60 ng/Pa.s.m². The simulation IDs are **O8VSW4 (vapour barrier I) and **VB6VSW4 (vapour barrier II). The results from the simulation (Table D7) indicate that vapour barrier II with higher water vapour permeance produced lower RHT(95) index in all the locations.

3.1.15 Use of coated gypsum board with no vapour barrier (vinyl siding-wall)

Simulations were done where a gypsum board coated with a primer and latex paint was used as the vapour control strategy. The hygrothermal properties of such coated gypsum board are given in section 2.2 of Chapter A. The simulation (ID: **O8VSCGW4) results (Table D7) show that there was a noticeable drop in the RHT(95) values for all the locations due to the use of coated gypsum board with no vapour barrier. Before any general conclusions can be drawn more cases with different interior RH profiles must be done. Specifically only one interior boundary condition was considered 55% summer RH and 25% winter RH. The interior boundary condition assumption may be too conservative for wetter and more humid climates.

3.1.16 Presence of 19mm ventilation cavity inside the wall (i.e. behind the exterior cladding) (vinyl siding-wall)

One simulation (ID: WIO8VSCBW4) was been done where a 19 mm ventilation cavity, with both top (3 mm) and bottom (19 mm) opening, was been introduced behind the vinyl cladding. The result from the simulation (Table D7) indicated that there was a significant reduction in RHT(95) index due to the introduction of vented cavity behind the exterior vinyl cladding.

4.0 Concluding Remarks

The results presented in the aforementioned sections discussed the effect of various environmental and material parameters on the overall moisture response of the hardboard and vinyl siding-wall and its components by primarily examining the local hygrothermal conditions in the wall assembly. A novel concept called RHT index has been successfully developed and used for this purpose. Further discussion and interpretation of the results can be found in MEWS Task 8 reports (*Beaulieu et al. 2002*).

References

1. Beaulieu, P.; Cornick, S.M.; Dalglish, W.A.; Djebbar, R.; Kumaran, M.K.; Lacasse, M.A.; Lackey, J.; Maref, W.; Mukhopadhyaya, P.; Nofal, M.; Normandin, N.; Nicholis, M.; O'Connor, T.; Quirt, J.D.; Rousseau, M.Z.; Said, M.N.; Swinton, M.C.;

- Tariku, F.; van Reenen, D. 2002 "MEWS Task 8 Report", Institute for Research in Construction, National Research Council, Ottawa, Canada.
2. Cornick, S. M., Dalglish, W. A., Said, N. M., Djebbar, R., Tariku, F. and Kumaran, M. K. 2002, "Task 4- Environmental Conditions", Institute for Research in Construction, National Research Council, Ottawa, Canada, (NRCC-45222), pp. 1-106.
 3. Kumaran, K., Lackey, J., Normandin, N., van Reenen, D., and Tariku, F. 2002. "Summary Report from Task 3 of MEWS Project at the Institute for Research in Construction", Institute for Research in Construction, National Research Council, Ottawa, Canada, (NRCC-45369), pp. 1-68.
 4. Lacasse, M. A., Beaulieu, P., O'Connor, T. and Nicholls, M., 2002. "MEWS Final Report from Task 6 - Experimental Assessment of Water Entry into Wood-frame Wall Assemblies", Institute for Research in Construction, National Research Council, Ottawa, Canada.